

**Tribochemistry of Boundary Lubricated
DLC/Steel Interfaces and Their Influence in
Tribological Performance**

Shahriar Kosarieh

Submitted in accordance with the requirements for the degree of

Doctor of Philosophy

The University of Leeds

School of Mechanical Engineering

December 2013

The candidate confirms that the work submitted is his own, except where work which has formed part of jointly-authored publications has been included. The contribution of the candidate and the other authors to this work has been explicitly indicated below. The candidate confirms that appropriate credit has been given within the thesis where reference has been made to the work of others.

In all papers, the primary author completed paper drafting, experimental studies and evaluation of the data. All authors listed on the papers completed proof reading and amendments prior to article submission. Transmission electron microscope sample preparation and operation was undertaken by Dr Michael Ward (Institute for Materials Research, The University of Leeds, UK) and X-ray Photoelectron Spectroscopy sample preparation and operation was carried out by Dr Benjamin Johnson (Faculty of Mathematics and Physical Sciences, The University of Leeds, UK).

This copy has been supplied on the understanding that it is copyright material and that no quotation from the thesis may be published without proper acknowledgement.

© 2013 The University of Leeds and Shahriar Kosarieh

Papers contributing to this thesis

- 1 Kosarieh, S., A. Morina, E. Lainé, J. Flemming, and A. Neville, *Tribological performance and tribochemical processes in a DLC/steel system when lubricated in a fully formulated oil and base oil*. Surface and Coatings Technology, 2013. **217**(0): p. 1-12.
Featured in Chapter 4, 5 and 7

- 2 Kosarieh, S., A. Morina, E. Lainé, J. Flemming, and A. Neville, The effect of MoDTC-type friction modifier on the wear performance of a hydrogenated DLC coating. *Wear*, 2013. 302(1–2): p. 890-898.
Featured in Chapter 4, 6 and 7

Acknowledgements

I would like to express my deepest gratitude to my academic supervisors, Dr Ardian Morina and Professor Anne Neville for their understanding, continued support, enthusiasm, endless encouragement and invaluable advice throughout the project without which this work would not have been possible.

I would like to thank Infineum UK Ltd. and The University of Leeds for funding this PhD study. Many thanks to my industrial supervisors Dr. Emmanuel Laine and Dr Jonathan Flemming at Infineum UK Ltd. for their expertise, technical support and supply of the lubricants tested. I am indebted to Dr Toby Middlemiss of Oerlikon Balzers Coating UK Ltd. for supplying the DLC coatings.

I am grateful to Dr Michael Ward for his great help in operating the Transmission Electron Microscopy and to Dr Benjamin Johnson for undertaking the X-ray Photoelectron Spectroscopy operation.

I would like to thank all my colleagues, technicians and friends of Institute of Engineering Thermofluids, Surfaces and Interfaces (iETSI), In particular, Mrs Jackie Kidd, Mrs Fiona Slade, Dr Michael Bryant, Dr Chun Wang, Dr Thibaut Charpentier, Dr Hongyuan Zhao and all my fellow members of Professor Neville's research group for making a friendly working environment that has been both instructive and enjoyable, and has been a pleasure to be part of.

I am very grateful to my family and friends for all their immense support and encouragement throughout my studies. My special thanks to my dad Ebrahim Kosarieh and my mum Alieh Ahmadi for their unwavering love, patience and encouragement, also I would like to thank my brothers Dr Emad Kosarieh and Dr Amir Homayoon Kosarieh for their endless support and care.

To My Family

Abstract

The application of Diamond-Like Carbon (DLC) coatings for automotive components is becoming a promising strategy to cope with the new challenges faced by automotive industries. DLC coatings simultaneously provide low friction and excellent wear resistance which could potentially improve fuel economy and durability of engine components in contact. The mechanisms by which a non-ferrous material interacts with a variety of lubricant additives is becoming better understood as research efforts in this area increase. However there are still significant gaps in the understanding. A better understanding of DLC wear may lead to lubricant additive solutions being tailored for DLC surfaces to provide excellent durability (wear) as well as similar or increased fuel economy (low friction). In this work, the wear and friction properties of DLC coating under boundary lubrication conditions have been investigated.

In this study, tribological performance of DLC coatings was evaluated using a pin-on-plate tribometer. The experiments were conducted using (High Speed Steel) HSS plates coated with 15 at.% hydrogenated DLC (a-C:15H) sliding against cast iron pins. Oils with different formulations were used in this study and the friction and wear response of the fully formulated oils is discussed in detail.

Using different surface analysis techniques such as optical and scanning electron microscopes (SEM), Energy-Dispersive X-ray analysis (EDX), X-ray Photoelectron Spectroscopy (XPS) analysis, Focused Ion Beam (FIB) and Transmission Electron Microscopy (TEM) were performed on the surfaces to understand physical characterization and the tribochemical interactions between oil additives and the DLC coating. A nano-indentation study was also conducted to observe the changes in the structure of the coating, which can provide a better insight into the wear mode and failure mechanism of such hard coatings.

In light of the physical observations and tribochemical analysis of the wear scar, the tribological performance of a hydrogenated DLC (a-C:15H) coating was found to depend on the oil formulation. The level of Molybdenum Dialkyl Dithiocarbamate (MoDTC) friction modifier (Mo-FM) blended in the oils greatly influenced the friction and the wear performance of the DLC coatings. High concentration of Mo-FM resulted in lower friction but higher wear of a-C:15H DLC coating. However, the addition of Zinc dialkyldithiophosphate (ZDDP) to the oils showed a positive effect in mitigating such high wear. The tribochemical mechanisms, which contribute to this behaviour, are discussed in detail.

Table of Contents

Papers contributing to this thesis	iii
Acknowledgements.....	iv
Abstract.....	vi
Table of Contents	viii
List of Tables	xiii
List of Figures	xv
Nomenclature	xxiv
Chapter 1 Introduction	1
1.1. Global Energy Challenges.....	1
1.2. Rationale and Objectives of this Study.....	3
1.3. Thesis Outline	4
Chapter 2 Tribology.....	6
2.1. Introduction to Tribology.....	6
2.2. Friction	6
2.3. Wear	6
2.4. Hertzian Elastic Contact Analysis and Contact Geometry.....	9
2.5. Lubrication.....	11
2.5.1. Base Oils.....	14
2.5.2. Additives	15
2.5.2.1. Extreme Pressure/Anti-wear	17
2.5.2.2. Friction Modifiers.....	17
2.5.2.3. Detergents	17
2.5.2.4. Dispersants	18
2.5.2.5. Antioxidants	18
2.5.2.6. Viscosity Index (VI) Improvers.....	18
2.5.2.7. Other Additives.....	18
2.6. Surface Coating Deposition.....	19
2.6.1. Physical Vapour Deposition (PVD).....	19
2.6.2. Sputtering/DC Magnetron Sputtering	19
2.6.3. Chemical Vapour Deposition (CVD).....	20

2.6.4.	Plasma Enhanced Chemical Vapour Deposition (PECVD)	21
Chapter 3	Literature Review	23
3.1.	Introduction	23
3.2.	Lubricant Additives and their Interactions with Ferrous Surfaces	23
3.2.1.	Zinc Dialkyldithiophosphate (ZDDP)	24
3.2.2.	Tribological Performance of ZDDP on Ferrous Surfaces	25
3.2.3.	Chemical Properties of ZDDP tribofilm and Mechanisms of Wear Reduction	27
3.2.4.	Mechanical Properties of ZDDP Tribofilm	33
3.2.5.	Molybdenum Dialkyl Dithiocarbamate (MoDTC)	37
3.2.6.	Tribological Performance of MoDTC	42
3.2.7.	Additive-Additive Interactions	43
3.2.7.1.	ZDDP Interactions with MoDTC	44
3.2.7.2.	ZDDP Interaction with Detergents and Dispersants	45
3.2.7.3.	Additive Interactions in Fully Formulated Oils	47
3.3.	Valve Train System	48
3.4.	Diamond-Like Carbon (DLC) Coatings	51
3.4.1.	Application of DLC Coatings	52
3.4.2.	Structure of DLC Coatings	52
3.4.3.	Deposition of DLC Coatings	56
3.4.4.	DLC Performance in Dry Sliding	58
3.4.5.	The Graphitization of Hydrogenated DLC	59
3.4.6.	Chemical Reactivity of DLC	60
3.5.	DLC/lubricant Interactions	62
3.5.1.	Tribochemical Interactions	62
3.5.2.	Effect of DLC Coating Type on DLC/Lubricant Interactions	67
3.5.3.	Super-lubricity of DLC Coating using GMO/PAO	70
3.5.4.	Effect of Hydrogen on DLC/Lubricant Interaction	72
3.5.5.	Adverse Effect of MoDTC on DLC High Wear	75
3.5.6.	Effect of Temperature on the DLC/Lubricant Interaction	77

3.6. Summary.....	80
Chapter 4 Experimental Procedures	83
4.1. Introduction	83
4.2. Test Materials and Coatings.....	83
4.3. Pin-on-Plate Test Rig.....	84
4.3.1. Test Setup.....	84
4.3.2. Test Samples	85
4.3.3. Coating Deposition.....	85
4.4. Lubricants.....	86
4.5. Surface Analysis Techniques	87
4.5.1. Optical Microscope.....	87
4.5.2. WYKO White Light Interferometer.....	88
4.5.3. Scanning Electron Microscope (SEM)/ Energy Dispersive X-Ray (EDX).....	89
4.5.4. Focused Ion Beam (FIB)/ Transmission Electron Microscopy (TEM)	90
4.5.5. Nano-indentation Analysis	92
4.5.6. X-ray Photoelectron Spectroscopy (XPS)	93
4.5.7. Raman Spectroscopy.....	94
Chapter 5 Results: Phase I - Tribological performance and tribochemical processes in a DLC/steel system when lubricated in a fully formulated oil and base oil	96
5.1. Introduction	96
5.2. Tribological Performance of the Steel/CI System.....	98
5.2.1. Friction Results	98
5.2.1.1. Effect of Temperature	99
5.2.1.2. Effect of Time.....	100
5.3. Tribological Performance of the a-C:15H/CI System.....	101
5.3.1. Friction Results	101
5.3.2. Coating Durability and Wear Performance.....	103
5.3.2.1. Optical Microscope/ SEM Images	103
5.3.2.2. EDX Analysis	106
5.4. Overall System.....	107
5.4.1. Friction Performance.....	107
5.4.2. Pin Wear	109

5.4.3.	Effect of Transfer Layer.....	110
5.4.4.	Chemical Analysis of Tribofilms	113
5.5.	Summary.....	123
Chapter 6	Results: Phase II - Effect of Mo-FM on the Tribological performance of a hydrogenated DLC coating.	125
6.1.	Introduction	125
6.2.	Tribological Performance of the Steel/CI System.....	127
6.2.1.	Friction Results	127
6.2.2.	Wear Results.....	128
6.3.	Tribological Performance of the a-C:15H/CI System.....	129
6.3.1.	Friction Results	129
6.3.2.	Coating Durability and Wear Results	131
6.3.3.	Chemical Analysis of Tribofilms	145
6.3.4.	Mechanical Properties of the Coatings.....	148
6.3.5.	Effect of Test Duration	151
6.3.5.1.	Friction Results	152
6.3.5.2.	Wear Results	152
6.3.5.3.	Chemical Analysis of the Tribofilms	157
6.3.5.3.1.	Elemental Composition.....	157
6.3.5.3.2.	Low Friction Film Formation.....	158
6.3.5.3.3.	Anti-wear Film Formation.....	161
6.3.5.4.	Mechanical properties of the coatings.....	164
6.3.6.	Effect of Mo-FM Source	166
6.3.6.1.	Friction Results	166
6.3.6.2.	Wear Results	168
6.3.6.3.	Chemical Analysis of the Tribofilms	171
6.3.6.3.1.	Elemental Composition	171
6.3.6.3.2.	Low Friction Film Formation.....	172
6.3.6.3.3.	Anti-wear Film Formation.....	174
6.3.6.3.4.	Effect of Other Additives	174
6.3.7.	Effect of Counterpart Type	176
6.3.7.1.	Friction Results	177
6.3.7.2.	Wear Results	178
6.3.7.3.	Chemical Analysis of the Tribofilm	179

6.3.7.3.1. Chemical Quantification	179
6.3.7.3.2. Low Friction Film Formation.....	181
6.3.7.3.3. Effect of Other Additives	182
6.4. Summary.....	182
Chapter 7 Discussion	185
7.1. Introduction	185
7.2. Effect of Lubricant Additives on Tribological Performance of the DLC/CI and the Steel/CI System.....	185
7.2.1. Low Friction Film Formation.....	185
7.2.2. Anti-wear Film Formation	189
7.2.3. Effect of ZDDP on Friction Reduction	191
7.2.4. Effect of Other Additives Interaction on Tribofilm Formation	192
7.2.5. Effect of Oil Chemistry on Coating Wear/Delamination.....	193
7.2.5.1. Graphitisation of Hydrogenated DLC Coating....	193
7.2.5.2. Wear Mechanism/DLC Coating Failure.....	196
7.3. Effect of Mo-FM on a-C:15H Coating Durability/Wear.....	198
7.3.1. Mechanisms of MoDTC-induced High Wear on DLC	199
7.3.2. Effect of Mo-FM Source on MoDTC-induced Wear...	205
7.4. Practical Tribochemistry of DLC.....	206
7.4.1. Lubrication Comparison of the a-C:15H/CI and the Steel/CI systems	206
7.4.2. DLC Life Time/Optimum Performance	208
Chapter 8 Conclusions and Future Work	212
8.1. Concluding Remarks.....	212
8.2. Suggestions for Future Work.....	215
List of References	217

List of Tables

Table 2-1 Base oil categories [23].....	14
Table 3-1 Mechanical properties of tribofilmed formed from ZDDP-containing oils.....	35
Table 3-2 Properties of various forms of carbons [150, 155].	55
Table 3-3 Summary of the literature on frictional behaviour of DLC coatings compared to an uncoated steel system	65
Table 3-4 Summary of the literature on wear behaviour of DLC coatings compared to an uncoated steel system	66
Table 3-5 Summary of literature on the effect of MoDTC in promoting high wear of DLC coatings. NM stands for “Not Mentioned”.	76
Table 4-1 Physical properties of plates (substrate/coatings) and counterpart materials.	83
Table 4-2 Oil lubricants-Phase I.....	86
Table 4-3 Oil lubricants Phase II	86
Table 4-4 Summary of the surface analysis techniques which were used in this study.....	87
Table 5-1 Binding energies, concentration of XPS and corresponding chemical in the tribofilms formed on steel plates in steel/CI system by oils FF2+, FF3+ and FF3-.	119
Table 5-2 Binding energies, concentration of XPS and corresponding chemical in the tribofilms formed on CI pins in steel/CI system by oils FF2+, FF3+ and FF3-.....	120
Table 5-3 Binding energies, concentration of XPS and corresponding chemical in the tribofilms formed on a-C:15H coated plates in a-C:15H/CI system by oils FF2+, FF3+ and FF3-.	120
Table 5-4 Binding energies, concentration of XPS and corresponding chemical in the tribofilms formed on CI pins in a-C:15H/CI system by oils FF2+, FF3+ and FF3-.	121
Table 6-1 XPS quantification of tribofilms for a a-C:15H/CI system after 20 h tests.....	145
Table 6-2 Nano-scale mechanical properties of DLC coating after 20 h tests.	149
Table 6-3 Nano-scale mechanical properties of CrN coating interlayer and steel substrate.	150

Table 6-4 XPS quantification of tribofilms for a a-C:15H/CI system after 6 h tests.....	158
Table 6-5 XPS quantification of tribofilms for a a-C:15H/CI system after 12 h tests.....	158
Table 6-6 Nano-scale mechanical properties of DLC coating after 6 h tests.	165
Table 6-7 Nano-scale mechanical properties of DLC coating after 12 h tests.	166
Table 6-8 XPS quantification of tribofilms for a a-C:15H/CI system lubricated in oils with different source of MoDTC.....	172
Table 6-9 XPS quantification of tribofilms on the a-C:15H coating for a-C:15H/CI and a-C:15H/ceramic systems.....	180
Table 7-1 a-C:15H coating thickness loss rate ($\mu\text{m}/\text{h}$) and DLC coating life (h).....	210

List of Figures

Figure 1-1 Breakdown of passenger car energy consumption [1].....	2
Figure 2-1 Advanced stage of abrasive wear and corrosion in inner raceway and rollers of a spherical roller bearing [17].....	7
Figure 2-2 Advanced (a) Fretting grooves worn into the raceways by axial movement of the rollers during transportation. (Courtesy of the Timken Company.) (b) Fretting on the outer diameter of an outer race ring caused by nonuniform seat in housing and Roller Bearing Damage [17].	8
Figure 2-3 Point contact between a sphere and a flat surface [22].....	9
Figure 2-4 Schematic view of (a): boundary lubrication and (b): mixed lubrication [14].	12
Figure 2-5 The modified Stribeck diagram [14].....	14
Figure 2-6 Chronology of development of main classes of lubricant additive [29].	16
Figure 2-7 Schematic diagram of a DC-magnetron sputtering unit.	20
Figure 2-8 Sequence of events during deposition [32].	21
Figure 2-9 Schematic diagram of PECVD system.	22
Figure 3-1 Molecular structure of ZDDP [29].	25
Figure 3-2 ZDDP film structure [71].	28
Figure 3-3 Two-layer model of ZDDP tribofilm [73].	29
Figure 3-4 ZDDP tribofilm profile obtained using Auger Electron Spectroscopy (AES). The top layer contains only zinc polythiophosphate. There is no carbon in the film (except contamination at the outmost surface) [74].	30
Figure 3-5 The MD simulation showing the combined effects of pressure and shear is essential for the digestion of iron oxide embedded in the zinc metaphosphate by MD [74].	31
Figure 3-6 MD simulation of digestion of manganese and chromium oxides nanoparticles embedded in zinc metaphosphate matrix under the effect of (a) pressure and (b) combined pressure and shear. Temperature =353 K. Steps of simulation (1,000,000) [75].	32
Figure 3-7 Schematic diagram of pad structure and composition [29].....	36
Figure 3-8 Schematic picture of the structure and mechanical properties of the full anti-wear film formed by simple ZDTP solution [89].	36

Figure 3-9 MoS ₂ solid state structure [96].....	37
Figure 3-10 MoDTC structure	38
Figure 3-11 Model proposed for MoDTC decomposition [34]	39
Figure 3-12 (a) MD model, (b) behaviour of MoS ₂ layer during simulation from x–z direction, and (c) behaviour of MoS ₂ layer near the upper Fe substrate from x–y direction [109].	39
Figure 3-13 MoS ₂ formation from LI-MoDTC molecule adsorbed on nascent Fe surface [110].	40
Figure 3-14 Molecular structure of Trinuclear MoDTC (Moly Trimer) [111]	41
Figure 3-15 Mechanism of thermal MoS ₂ formation from Moly Trimer [111]	42
Figure 3-16 Schematic structures for films generated by (a) ZDDP and (b) ZDDP+ Detergents+ Dispersant [132].....	47
Figure 3-17 Wear scar width as function of rubbing time [133].	48
Figure 3-18 sp ³ , sp ² and sp hybridised bonding [155].	53
Figure 3-19 Density vs sp ³ fraction for DLC film. The trends are different when comparing ta-C and ta-C:H with a-C:H [166].	54
Figure 3-20 Ternary phase diagram of amorphous carbon coatings [155].	55
Figure 3-21 Schematic representation of hardness and coefficients of friction (COF) of carbon-based and other hard coatings in dry sliding condition [170].....	56
Figure 3-22 Molecular dynamic simulation of the atomic structure of a hydrogenated DLC [170].	57
Figure 3-23 The wear surfaces of the steel pins slid against the PACVD deposited hydrogenated a-C:H film. The tests were carried out unlubricated in room air at 22±2 °C temperature and with 50±5 % relative humidity. The sliding speed was varied in the range 0.1–3.0 ms ⁻¹ and the normal load in the range 5–40 N [181].	58
Figure 3-24 The micro-Raman signal of the steel ball wear surface and wear debris after sliding against a-C:H film for 5000 m in humid air (50±5% relative humidity). The sliding velocity was 2.6 m s ⁻¹ and the normal load 35 N. The diamond and graphite signals are used as reference.....	60
Figure 3-25 Friction coefficients for steel/steel and a-C:H/steel contacts when lubricated in base oil and fully formulated gear oil [229].....	63

Figure 3-26 Composite wear coefficients for steel/steel and a-C:H/steel contacts when lubricated in base oil and fully formulated gear oil [229].	64
Figure 3-27 Influence of coating type on the steady-state friction of boundary-lubricated DLC/DLC contacts tested with mineral oil (M), a mixture of mineral oil and AW/EP additive (M + AW/EP) and a mixture of mineral oil and EP additive (M + EP). DLC-1 and DLC-2 are hydrogenated DLCs with Si-based and Ti-N interlayer ($P_{\max} = 1 \text{ GPa}$, $v = 0.1 \text{ m/s}$, $T = 80^\circ\text{C}$) [209].	67
Figure 3-28 Influence of coating type on the steady-state friction of boundary-lubricated DLC/steel contacts tested with mineral oil (M), a mixture of mineral oil and AW/EP additive (M + AW/EP) and a mixture of mineral oil and EP additive (M + EP). DLC-1 and DLC-2 are hydrogenated DLCs with Si-based and Ti-N interlayer ($P_{\max} = 1 \text{ GPa}$, $v = 0.1 \text{ m/s}$, $T = 80^\circ\text{C}$) [204].	68
Figure 3-29 (a) Wear rates of W-DLC and sulfurized W-DLC coatings and (b) wear rates of balls against W-DLC and sulfurized W-DLC coatings [246].	70
Figure 3-30 Raman spectra of steel counterpart rubbing in pure PAO for DLC/steel tribopair (a) before total wear occurs (b) after partial wear out of coating from the topmost surface [223].	71
Figure 3-31 Schematic illustration of dangling bonds in diamond and weak shear plane between hydrogen-terminated diamond surfaces [250].	72
Figure 3-32 Friction-induced MoS_2 with steel cylinder against DLC-coated flat friction test. XPS Mo3d peak recorded on (a) pure MoO_3 powder; (b) pure cleaved MoS_2 crystal; (c) MoDTC+ZDDP tribofilm on the a-C:H coated flat; (d) MoDTC+ZDDP tribofilm on the a-C coated flat; (e) outside the MoDTC+ZDDP tribofilm on the a-C:H coated flat [206].	74
Figure 3-33 Wear steps of DLC coating in oil containing Mo-DTC [41].	75
Figure 3-34 Effect of operating temperature on steady-state friction of undoped DLC coatings running against uncoated steel ($P_{\max} = 1.5 \text{ GPa}$, $v = 0.02 \text{ m/s}$) [238].	78
Figure 3-35 Effect of operating temperature on wear rate of undoped DLC coatings running against uncoated steel ($P_{\max} = 1.5 \text{ GPa}$, $V = 0.02 \text{ m/s}$) [238].	78
Figure 3-36 Influence of operating temperature on steady-state friction of steel/W-doped DLC combination ($P_{\max} = 1.5 \text{ GPa}$, $V = 0.02 \text{ m/s}$) [238].	79

Figure 3-37 Influence of operating temperature on wear rate of steel/W-doped DLC combination ($P_{max} = 1.5$ GPa, $V = 0.02$ m/s) [238].	80
Figure 4-1 Schematic diagram of the contact in the pin-on-plate tests where the contact is submerged in lubricant.	84
Figure 4-2 Wear measurements of the plates	89
Figure 4-3 Schematic diagram showing the cross section of the a-C:15H coating plate. Concentration of Cr, detected by EDX, is higher inside the wear track compared to outside.	90
Figure 4-4 Typical TEM slide preparation using FIB.	91
Figure 4-5 Typical loading/unloading curve obtained using Nanoindentation on the as-deposited a-C:15H coating.	92
Figure 4-6 Typical survey scan (a) and long scan (b) XPS spectra.	94
Figure 4-7 A typical Raman spectra and Gaussian curve-fitting obtained from as-deposited a-C:15H coating.	95
Figure 5-1 Map of the study which is presented in this chapter.	97
Figure 5-2 Friction coefficient as a function of time for the steel/CI system lubricated in oils.	98
Figure 5-3 Steady state friction coefficients as a function of FF oils for steel/CI system.	99
Figure 5-4 Effect of temperature on coefficient of friction as a function of time in a steel/CI system lubricated in FF3-.	100
Figure 5-5 Effect of time on coefficient of friction as a function of time in a UC steel/CI system lubricated in FF3-.	101
Figure 5-6 Friction coefficient as a function of time for the a-C:15H/CI system lubricated in oils.	102
Figure 5-7 Steady state friction coefficients as a function of FF oils for a-C:15/CI system.	103
Figure 5-8 Optical images of the wear scars formed on the a-C:15H coated plates using (a) PAO, (b) Base oil Group III, (c) FF1+, (d) FF2+, (e) FF3+, (f) FF1- (g) FF2- and (h) FF3-. The arrows on the right side of the images show sliding directions.	104
Figure 5-9 SEM images of the wear scars formed on the a-C:15H coated plates using (a) PAO, (b) Base oil Group III, (c) FF1+, (d) FF2+, (e) FF3+, (f) FF1- (g) FF2- and (h) FF3-. The arrows on the right side of the images show sliding directions.	105
Figure 5-10 Difference between concentrations of Cr inside the wear tracks and outside of the wear tracks using various oils...	107
Figure 5-11 Steady state friction coefficients as a function of lubricants for a-C:15H/CI system versus Steel/CI system.	108

Figure 5-12. Dimensional wear coefficients as a function of lubricants for a-C:15H/CI system.....	109
Figure 5-13 Transfer layer on the pin coming from the wear track of a-C:H coating when (a) PAO, (b) Base oil group III, (c) any of the fully formulated oils were used.....	110
Figure 5-14 Friction response after cleaning transfer material every hour during the test.....	111
Figure 5-15 Effect of cleaning transfer layer on friction and wear.....	111
Figure 5-16 Raman spectroscopic analysis on the samples obtained using PAO. H_d and H_g are the intensity height of D and G peaks, respectively. The coloured boxes on the optical image of the CI pin and the SEM image of a-C:15H coating show the sites where the Raman analyses were carried out.	112
Figure 5-17 XPS survey scan for the tribofilms formed on the steel plates in steel/CI system.	115
Figure 5-18 XPS survey scan for the tribofilms formed on the CI pins in steel/CI system.	116
Figure 5-19 XPS survey scan for the tribofilms formed on the a-C:15H coated plates in a-C:15H/CI system.	117
Figure 5-20 XPS survey scan for the tribofilms formed on the CI pins in a-C:15H/CI system.	118
Figure 5-21 P 2p curve fitting for ZDDP-containing fully formulated oils on a-C:15H plates.....	121
Figure 5-22 Detergent-derived Ca 2p peak (a) and dispersant-derived N 1s peak (b) using fully formulated oils.....	122
Figure 6-1 Map of the study which is presented in this chapter.	126
Figure 6-2 Friction traces as a function of time for the steel/CI system for FF40+, FF40-, FF300+, FF300-, FF600+ and FF600-.....	127
Figure 6-3 Steady state friction coefficients as a function of Mo-FM concentration for steel/CI system.	128
Figure 6-4 Wear coefficient versus Mo-FM concentration for the steel/CI system.....	129
Figure 6-5 Friction traces as a function of time for the a-C:15H/CI system for FF40+, FF40-, FF300+, FF300-, FF600+ and FF600-.....	130
Figure 6-6 Steady state friction coefficients as a function of Mo-FM concentration for a-C:15H/CI system.	130
Figure 6-7 Wear coefficient versus Mo-FM concentration for the a-C:15H/CI system.....	131

Figure 6-8 A typical profile of the wear scar formed on (a): a sample of a-C:15H coating for FF300- fully formulated oil along (b): X direction and (c): Y direction measured by WYKO.....	132
Figure 6-9 A typical profile of the wear scar formed on (a): a sample of a-C:15H coating for FF600+ fully formulated oil along (b): X direction and (c): Y direction measured by WYKO.....	133
Figure 6-10 A typical profile of the wear scar formed on (a): a sample of a-C:15H coating for FF600- fully formulated oil along (b): X direction and (c): Y direction measured by WYKO.....	134
Figure 6-11 Optical images of the wear scars formed on the a-C:15H coated plates using (a) FF40+, (b) FF40-, (c) FF300+, (d) FF300-, (e) FF600+- and (f) Oil600-.The arrows on the images show sliding directions and μ and H_d are the coefficient of friction and the average depth of the wear track, respectively.....	135
Figure 6-12 SEM image of a-C:15H coating along with EDX mapping of the C, Cr and Fe atoms for 20 h tests.....	137
Figure 6-13 TEM image of the unworn a-C:15H coating. The areas circled in red are also presented in higher magnification.....	138
Figure 6-14 TEM image of the worn a-C:15H coating provided by FF600+. The areas circled in red are also presented in higher magnification.....	139
Figure 6-15 TEM image of the worn a-C:15H coating provided by FF600-. The areas circled in red are also presented in higher magnification.....	140
Figure 6-16 EDX mapping of the unworn a-C:15H coating.....	141
Figure 6-17 EDX mapping of the worn a-C:15H coating provided by FF600+.....	142
Figure 6-18 EDX mapping of the worn a-C:15H coating provided by FF600-.....	143
Figure 6-19 Dimensional pin wear coefficients as a function of lubricants for a-C:15H/CI systems.....	144
Figure 6-20 Curve fitting of Mo 3d peaks obtained from tribofilm formed from FF600- on both pin and a-C:15H coating.....	146
Figure 6-21 Carbon species on the wear scar of a-C:15H coating and CI pins for the highest wear giving lubricants (FF600-).	147
Figure 6-22 XPS spectra of ZDDP derived species (a) Zn 2p, (b) P2p formed on the a-C:15H coated plate using different fully formulated oils.....	148

Figure 6-23 Steady state friction coefficients as a function of oils with different Mo-FM concentration at different time intervals for a-C:15H/CI system.....	152
Figure 6-24 Wear coefficient as a function of oils with different Mo-FM level.....	153
Figure 6-25 Optical images of the wear scars formed on the a-C:15H coated plates using (a) FF300+, (b) FF300-, (c) FF600+ and (d) Oil600-.The arrows on the images show sliding directions and μ and H_d are the coefficient of friction and the average depth of the wear track, respectively.....	154
Figure 6-26 SEM image of a-C:15H coating along with EDX mapping of the C, Cr and Fe atoms for 6 h tests.....	155
Figure 6-27 SEM image of a-C:15H coating along with EDX mapping of the C, Cr and Fe atoms for 12 h tests.....	156
Figure 6-28 Curve fitting of Mo 3d peaks obtained from tribofilm formed from oils with different level of MoDTC on the CI pins after (a) 6 h and (b) 12 h.....	159
Figure 6-29 The fitted Mo 3d peaks formed on the CI pins from (a): FF600-, (b):FF300-, (c): FF600+ and (d):FF300+ as a function of test duration.....	160
Figure 6-30 XPS spectra of ZDDP derived species (a) Zn 2p, (b) P2p formed on the a-C:15H coated plate and (c) Zn 2p and (d) P2p formed on the CI pin using FF600+ as a function of test duration.....	162
Figure 6-31 XPS spectra of ZDDP derived species (a) Zn 2p, (b) P2p formed on the a-C:15H coated plate using and (c) Zn 2p and (d) P2p formed on the CI pin using FF300+ as a function of test duration.....	163
Figure 6-32 Friction traces as a function of time for the a-C:15H/CI combination using oils with different Mo-FM source.	167
Figure 6-33 Steady state friction coefficients as a function of oils with different Mo-FM concentration at different time intervals for a-C:15H/CI system.....	167
Figure 6-34 Wear coefficient as a function of oils with different Mo-FM concentration at different time intervals for a-C:15H/CI system.....	168
Figure 6-35 Optical images of the wear scars formed on the a-C:15H coated plates using (a) FF300+ (Mo-FM with oxidation state of +4), (b) FF300- (Mo-FM with oxidation state of +4), (c) FF300+ (Mo-FM with oxidation state of +5) and (d) FF300- (Mo-FM with oxidation state of +5).The arrows on the images show sliding directions and μ and H_d are the coefficient of friction and the average depth of the wear track, respectively...	169

Figure 6-36 SEM image of a-C:15H coating along with EDX mapping of the C, Cr and Fe atoms.....	171
Figure 6-37 Curve fitting of Mo 3d peaks obtained from tribofilm formed from FF300- (Mo-FM with oxidation state of +5) and FF300- (Mo-FM with oxidation state of +4) on the pin.....	173
Figure 6-38 XPS spectra of ZDDP derived species (a) Zn 2p, (b) P2p formed on the a-C:15H coated plate using Mo-FM with oxidation state of +5-containing fully formulated oils.	174
Figure 6-39 Detergent-derived Ca 2p peak formed on a-C:15H plate (a) and CI pin (b) using oils with different MoDTC.....	175
Figure 6-40 Dispersant-derived N 1s peak formed on a-C:15H plate (a) and CI pin (b) using oils with different MoDTC.	176
Figure 6-41 Friction traces as a function of time using different counterpart on a-C:15H coated plate lubricated in FF600-.....	177
Figure 6-42 Steady state friction coefficients as a function of FF600- using different counterpart on a-C:15H coated plate.	177
Figure 6-43 Optical images of the wear scars formed on the a-C:15H coated plates using (a) FF600- (ceramic ball) and (b) FF600- (CI pin). The arrows on the images show sliding directions and μ and H_d are the coefficient of friction and the average depth of the wear track, respectively.....	178
Figure 6-44 SEM image of a-C:15H coating along with EDX mapping of the C, Cr and Fe atoms.....	179
Figure 6-45 Survey scan obtained from inside a-C:15H coating wear scar when rubbed against CI (top) and ceramic (bottom).	180
Figure 6-46 Curve fitting of Mo 3d peaks obtained from tribofilm formed from FF600- on the a-C:15H coating using the CI pin (top) and the ceramic ball (bottom).	181
Figure 6-47 Detergent-derived Ca 2p peak (a) and dispersant-derived N 2p peak (b) using FF600- oil using the CI pin(top) and the ceramic ball (bottom).	182
Figure 7-1 Average coefficient of friction as a function of Mo-sulphide/Mo-oxide ratio for a-C:15H/CI system using oils with different concentration of Mo-FM after 20 h tests.....	187
Figure 7-2 Mo-sulphide/Mo-oxide ratio for a-C:15H coating as a function of test duration using oils with different level of Mo-FM.....	188
Figure 7-3 Schematic diagram of low friction film present at the interface in (a):steel/CI [253] and (b): a-C:15H/CI systems.....	189
Figure 7-4 The phase transformation temperature of DLC coating as a function of contact pressure [278].	195

Figure 7-5 Schematic of the effect of iron particles and positive edges of the scratches on pressure induced graphitisation of DLC coating when lubricated in base oils.	196
Figure 7-6 Schematic of the effect of tribochemical protective layer in suppressing graphitisation of DLC coating when lubricated in conventional fully formulated oils (low concentration of Mo-FM).	198
Figure 7-7 Raman spectra of carbon powder after heating with MoO₃ [41].	200
Figure 7-8 Wear and harness variation with time using DLC/CI and DLC/ceramic systems.	203
Figure 7-9 Schematic diagram showing the MoDTC-induced wear mechanisms. (1) and (2) represent the first and the second stage of the proposed wear mechanisms.	204
Figure 7-10 The comparison between the wear depth of the CI pins when rubbed against a-C:15H coating and uncoated steel plates with average cam nose wear in 4D55T/C diesel engine [286].	208
Figure 7-11 Friction and wear response of a-C:15H coating in the a-C:15H/CI system lubricated with oils formulated with different Mo-FM level (20 h tests).	209
Figure 7-12 Average wear depth on a-C:15H coating as a function of FF oils formulated with different Mo-FM level.	210

Nomenclature

DLC	Diamond-Like Carbon
HSS	High Speed Steel
a-C:15H	15 at.% hydrogenated DLC
CI	Cast Iron
SEM	Scanning Electron Microscopy
EDX	Energy Dispersive X-ray
XPS	X-ray Photoelectron Spectroscopy
FIB	Focused Ion Beam
TEM	Transmission Electron Microscopy
Mo-FM	MoDTC-type Friction Modifier
MoDTC	Molybdenum Dithiocarbamate
ZDDP	Zinc dialkyldithiophosphate
μ	Friction coefficient
F	Friction force (N)
W	Normal load (N)
V	Wear volume (m ³)
K	Dimensionless wear coefficient
A _r	Real area of contact (m ²)
L	Sliding distance (m)
H	Hardness (Pa)
k	Dimensional wear coefficient (m ³ N ⁻¹ m ⁻¹)
E	Young's modulus (Pa)
E'	Reduced Young's modulus (Pa)
ν	Poisson's ratio
R'	Reduced radius of curvature (m)
R	Radius of curvature (m)
P	Hertzian contact pressure (Pa)
a	Radius of the contact area (m)
δ	Maximum deflection (m)
τ	Shear stress (Pa)
λ	Lambda ratio
h_{\min}	Minimum film thickness (m)
RMS	Root Mean Square
R _q	RMS roughness of the two surfaces
U	Entrainment speed (ms ⁻¹)
η_0	Dynamic viscosity at atmospheric pressure of the lubricant (Pas)
α	Viscosity-pressure coefficient (m ² N ⁻¹)
PAO	Polyalphaolefin
PVD	Physical Vapour Deposition
CVD	Chemical Vapour Deposition
PECVD	Plasma Enhanced Chemical Vapour Deposition
XANES	X-ray Absorption Near Edge Structure
AFM	Atomic Force Microscopy

IFM	Infinite Focus Microscopy
MD	Molecular Dynamics
FF	Fully Formulated oil
RF	Radio Frequency
FTIR	Fourier Transform Infrared Spectroscopy
GMO	Glycerol Mono-Oleate
HSAB	Hard and Soft Acids and Bases
UHV	Ultra High Vacuum
V_L	Volume loss of pin material (m^3)
h	Height of the sphere of pin worn after the wear test (m)
r	Radius of the wear scar (m)
T	Operating Temperature ($^{\circ}C$)
v	Specific volume (m^3kg^{-1})
K_{DLC}	Thermal conductivity of the DLC coating ($Wm^{-1}K^{-1}$)
K_{CI}	Thermal conductivity of the Cast Iron Pin ($Wm^{-1}K^{-1}$)
u	Sliding Velocity (ms^{-1})
T_c	Critical phase transformation temperature ($^{\circ}C$)
L	Phase transition energy of diamond (Jkg^{-1})

Chapter 1 Introduction

1.1. Global Energy Challenges

Friction, lubrication and wear have always been a challenge for human beings throughout history. They have a great impact on the efficiency and lifetime of the driveline in contact, and thus on the global economy. A substantial amount of energy is being dissipated to overcome friction, particularly in the transportation, industrial, and power-generation sectors whereas the wear of the products and components and their replacement causes a considerable loss to the economy [1, 2].

In addition, increasingly stricter emission legislation has made industry to devote a huge effort to produce energy-efficient vehicles. This provides benefits both economically and environmentally. In certain countries, financial penalties are imposed on companies which do not meet the CO₂ requirements. In 2009, the European Union imposed a new average CO₂ emissions reduction target and made it to 130 g/km, until 2015 [3, 4].

Furthermore, application of mineral oils as lubricants is another issue to be considered as the global oil resources are limited and the disposal of the oil waste in nature would be environmentally problematic. About 1% of the crude oil accounts for formulating the lubricants while between 13% (in EU countries) and 32% (in the US) of these oils finds its way to the nature after being used almost with different properties and appearance. Although, base oils are biodegradable, finished lubricants contain additives which makes them poorly compatible with the ecosystem [5, 6].

Transportation consumes about 20% of the global primary energy which leads to about 18% of the total anthropogenic greenhouse gas emissions [3, 7]. Passenger cars are responsible for 45% of the total energy consumption in transportation. It has been reported that friction and wear reduction in engine and drive train components could save an enormous 120 billion US dollars annually [8].

In a passenger car, fuel energy is consumed in the exhaust system, the cooling system and to generate mechanical power (see Figure 1-1). Mechanical power is responsible for about 38% of the fuel energy used in a passenger car and only about 21.5% of the variable available energy in the fuel find its way to move a passenger car, with some 33% being dissipated mainly as frictional losses [1]. A significant proportion of the mechanical power losses of the engine arises at the sub-mechanisms of the internal combustion engine. 10% reduction in mechanical losses would lead to 1.5% reduction in fuel consumption [9]. Friction losses take place primarily at the pistons, piston rings, bearings and valve mechanism. Applying new friction modifiers as well as implementing novel coatings for some of the engine components such as valve train and piston rings/liner, can lead to reduction in the losses and improvement in fuel efficiency which is obviously desirable.

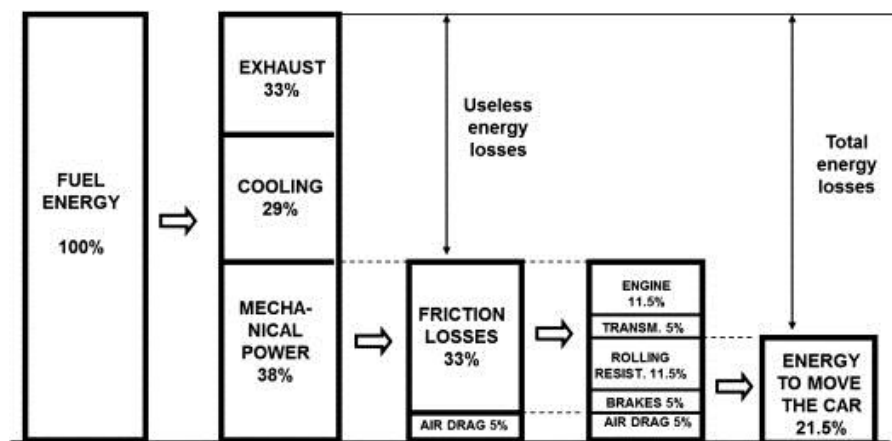


Figure 1-1 Breakdown of passenger car energy consumption [1].

Tribologically loaded surfaces in power train and drive-line components must operate under high loading conditions. Design changes and the use of conventional technologies can, to a certain extent, cope with this demand, however, alternative surface engineering solutions are required to deal with these changes. In addition, lubricant additives (e.g. ZDDP) contain P- and S- which can be harmful to catalytic convertors and to the environment subsequently. Reduction in the losses and improvement in fuel efficiency can be achieved to some extent by using low viscosity oils and new friction modifiers as well as implementing novel coatings for engine components.

Moreover, reducing the wear and frictional losses to extend the life time and improve the efficiency of the engine components is a need. Thus, it is crucial to optimise coating and lubricant compatibility for achieving a system with better performance in terms of fuel economy and durability.

The use of DLC coatings has increased over the last decade, particularly in high value racing engines, primarily due to their ability to provide good wear resistance with low friction. Commonly used friction modifiers and anti-wear additives are optimised to work on ferrous surfaces. Thus, researchers have started to consider how conventional lubricant additives interact with DLC surfaces but the results so far have been non-conclusive.

DLC itself is not an appropriate description for a type of coating. It can have variable levels of hydrogenation, different application methods, different layered structures and different levels of doping. Thus, a systematic study is required to accurately define how the characteristics of DLC affect the interactions with the lubricant additives and conversely how the structural changes of the lubricant additive affect the interaction with the DLC surface. The tribochemistry of DLC is essentially an area which needs more systematic attention and this research project has aimed to address this for a specific type of DLC coating and subset of lubricants.

1.2. Rationale and Objectives of this Study

In this work, the tribological performance and tribochemical interactions of a hydrogenated DLC coating under boundary lubrication conditions have been investigated. It should be borne in mind that entire replacement of the conventional ferrous components with those of novel coatings may not take place soon enough and therefore the conventional lubricants, initially optimised to work on the Fe-base surface, should still lubricate the coated parts. Therefore, it is important to know how the conventional lubricants would interact with the new coatings. The overall aim of the project was to improve the understanding of DLC lubrication to enable additive solutions to be tailored to DLC surfaces. The specific objectives are:

- To assess how the nature of the fully formulated oils affects the tribochemical reactions at DLC interfaces in a hydrogenated DLC. This would provide a map of the overall performance of the fully formulated oils on the tribological performance of DLC in comparison to uncoated steel.
- To study the effect of a MoDTC-type friction modifier (Mo-FM) concentration on the tribological performance of hydrogenated DLC coating under boundary lubrication conditions using fully formulated oils. This could elucidate whether or not additive solutions can be tailored for an optimum performance of DLC/lubricant.

The performance of a commercial DLC coating lubricated with different fully formulated oils was investigated in this study. Oils were blended based on the formulations which are used in different regions of the world. The tests were performed in a reciprocating pin-on-plate tribotester and the test conditions were chosen to be representative to a valve-train system.

1.3. Thesis Outline

The outline of this thesis is as follows:

In Chapter 2 the basic concept of tribology which is absolutely crucial to understanding lubricant/DLC interaction is presented. In addition, different deposition techniques by which novel coatings are being produced are explained in detail.

The literature around the lubricant/DLC interaction has been reviewed extensively in Chapter 3. Moreover, the nature of the tribofilm formed from known friction modifier and anti-wear additives is presented and the current understanding of the effect of different additives on the tribological performance of the ferrous surfaces as well as DLC coatings has been discussed.

Experimental details and the descriptions of the materials which have been used in this study are provided in Chapter 4. In addition, surface analysis techniques which were conducted in this study have been explained in detail.

In Chapter 5, the overall performance of DLC coating using a range of commercial fully formulated oils was investigated followed by surface analysis which explained the obtained results. The tribological performance and the tribochemical interactions were compared with that of an uncoated steel system.

Following the obtained results presented in Chapter 5, one fully formulated oil was chosen and the effect of Mo-FM concentration in that particular oil was investigated in Chapter 6. The idea was to see any deviation in terms of tribological performance which was observed in the previous chapter. In addition, the effect of test duration was studied for a better comparison of wear mechanisms between different oils. The effect of MoDTC type and counterpart type was also examined and the results are presented in this chapter.

In Chapter 7, a comprehensive discussion of the important obtained observations has been provided in relation with the published literature. In addition, the contributions made in this work are also highlighted.

Chapter 8 summarises the main conclusions obtained from this work and proposes potential future work.

Chapter 2 Tribology

2.1. Introduction to Tribology

Amidst the developments in engineering science and technology at an ever-increasing rate and its tendency towards high efficiency and less energy loss, new aspects of science is introduced. Tribology is relatively a new word in engineering and most of the knowledge has been achieved after the second world war [10] and was defined in the United Kingdom in 1966 [11]. However, it may be considered as gathering previous known subjects of friction, wear and lubrication.

Tribology is derived from the Greek word 'tribos' meaning rubbing or sliding [10]. Therefore, it can be thought of as the science of rubbing or, if stated more formally, "science of interactive surfaces in relative motions". The scientific studies of tribology go back to the studies of friction carried out by Leonardo da Vinci (1452-1519) and lubrication science, as it is known today it all started with theory of Sir Isaac Newton (1642-1727), that fluid resistance to shear depended on the velocity gradient while, considerable studies of wear just appeared in the middle of the twentieth century [12].

2.2. Friction

Friction is a resistance which occurs when one body is forced to move tangentially over another [13]. It occurs in dry as well as lubricated contacts. In many applications, low friction is desirable as it results in less energy loss and a better efficiency. It should be mentioned, however, that high friction is desirable in particular applications (e.g. brakes, clutches. etc.) [14]. The coefficient of friction is defined by $\mu = \frac{F}{w}$ where F is friction force and w is the normal load applied.

2.3. Wear

Wear is a progressive damage of the surface along with material loss which happens on the surface of a body due to its motion over another under load.

As a consequence of plastic deformation or/and material loss, there will be inefficiency in performance of industrial machines [15], it will limit the useful life of engineering components and it has a significant effect on reliability and consequently upcoming maintenance. Therefore researchers around the world have investigated wear and mechanisms by which it may occur. In addition, investigations have been made towards finding new ways of reducing and/or controlling the process of wear. Generally, there are five basic wear mechanisms.

- Adhesive wear is almost the worst form of wear and least preventable one which occurs due to cold welding at asperity junctions.
- Abrasive wear (see Figure 2-1) comes from cutting grooves from a softer surface when a harder surface moves over it either by asperities on a harder body (two-body abrasion) or by hard particles brought into the interface [16].
- Fatigue wear is removal of material from a body by fatigue over a long period of time due to cyclic stress changes [13].
- Corrosive wear (see Figure 2-1) occurs when chemical reaction and rubbing comes together at the same time (e.g. formation of chemical oxide layers on metal surfaces and following removal by rubbing).
- Erosive wear is impact of hard particles carried by a fluid on the surface which results in damage on that surface and its rate depends upon the kinetic energy of the particles.

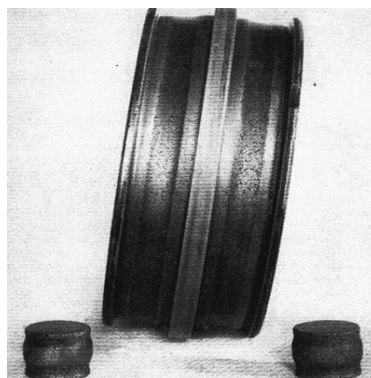


Figure 2-1 Advanced stage of abrasive wear and corrosion in inner raceway and rollers of a spherical roller bearing [17].

Wear is a complex process since sometime more than one mechanism involves in its appearance. Galling and scuffing occur due to severe

adhesive wear and results in a catastrophic damage and roughened surface. High temperature is a consequence of friction heating occurred due to this kind of wear. In lubricated interface it is called scuffing and in non-lubricated interface it is called galling [14]. Scoring is an abrasive kind of wear which produces pattern of scratches on the surface and can cause severe failure in some cases [13]. Polishing is a phenomenon which appears by mild abrasive wear [16] sometimes combined with corrosive wear which will give a very smooth, often mirror-like, surface texture. It can lead to a catastrophic failure in lubricated components due to the fact that polished surface is unable to retain enough lubricant and will be starved of sufficient lubricant [14]. Fretting (shown in Figure 2-2) is phenomenon which is as a result of synergy between adhesive, corrosive and abrasive wear and usually happens between metal surfaces where the degree of relative motion is relatively small (e.g. splined flange) [14]. Pitting is a consequence of fatigue wear. Pits and craters can be seen on the surface as a result of this wear and it is a common damage in rolling element bearings where it operates under high vibration and noise [14].

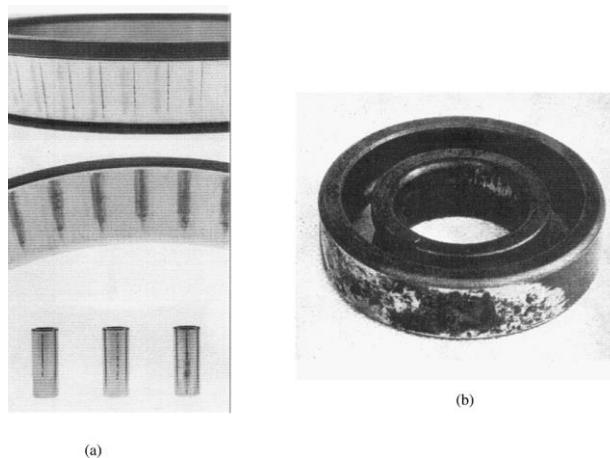


Figure 2-2 Advanced (a) Fretting grooves worn into the raceways by axial movement of the rollers during transportation. (Courtesy of the Timken Company.) (b) Fretting on the outer diameter of an outer race ring caused by nonuniform seat in housing and Roller Bearing Damage [17].

It has been postulated by Archard that the total wear volume is proportional to the real contact area multiplied by the sliding distance [18] and is defined as:

$$V = KA_rL = KL\frac{W}{H} = kLW \quad \text{Equation 2-1}$$

Where V is the wear volume (m^3), K is the dimensionless wear coefficient, A_r is the real area of the contact (m^2), L is the sliding distance (m), W is the load (N) and H is the hardness of the softer surface (Pa) [11]. Since defining a precise H is difficult, a rather more useful quantity than the value of " K " alone is the ratio of K and H which is called dimensional wear coefficient " k " and is defined as:

$$k = \frac{V}{LW} \quad \text{Equation 2-2}$$

The unit of the dimensional wear coefficient is generally expressed as $\text{m}^3\text{N}^{-1}\text{m}^{-1}$ or $\text{mm}^3\text{N}^{-1}\text{mm}^{-1}$. It should be considered that Archard law does not reflect the influence of lubricant chemistry and it is usually valid when mechanical mechanisms, adhesive wear in particular, are dominant [15].

2.4. Hertzian Elastic Contact Analysis and Contact Geometry

In many tribological applications, including rolling contact bearings, gears, cams and tappets, seals, etc., the contacting surfaces have low conformity resulting in very small contact areas and very high pressures, as a result. These stresses can be defined from the analytical formulae, based on the theory of elasticity, developed by Hertz in 1881 [19-21]. Hertz formulated the concept of a geometrically equivalent solid loaded against a perfectly rigid plane (Figure 2-3).

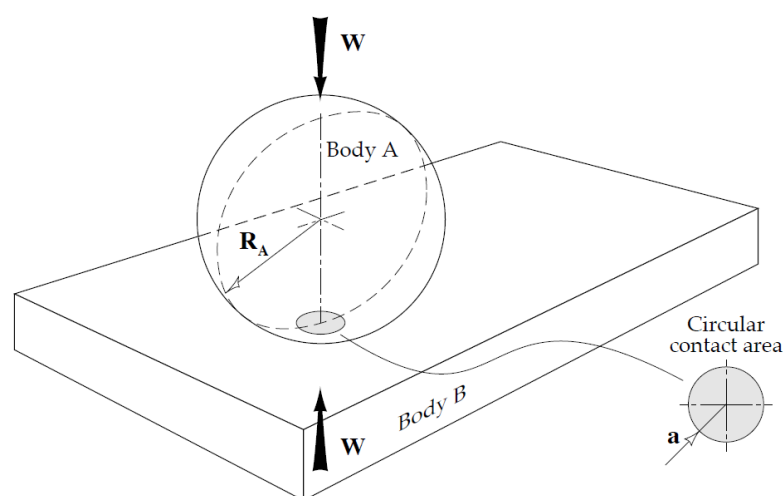


Figure 2-3 Point contact between a sphere and a flat surface [22].

Where reduced Young's modulus is defined as:

$$\frac{1}{E'} = \frac{1}{2} \left[\frac{1 - \nu_A^2}{E_A} + \frac{1 - \nu_B^2}{E_B} \right] \quad \text{Equation 2-3}$$

Where:

ν_A and ν_B are the Poisson's ratios of the contacting bodies "A" and "B", respectively;

E_A and E_B are the Young's moduli of the contacting bodies "A" and "B", respectively.

The radii of curvature of a plane surface are infinite and symmetry of the sphere applies so that $R_{Bx} = R_{By} = \infty$ and $R_{Ax} = R_{Ay} = R_A$. The reduced radius of curvature (R') is defined as:

$$\frac{1}{R'} = \frac{1}{R_x} + \frac{1}{R_y} \quad \text{Equation 2-4}$$

Where:

$$\begin{aligned} \frac{1}{R_x} &= \frac{1}{R_{Ax}} + \frac{1}{R_{Bx}} = \frac{1}{R_A} + \frac{1}{\infty} = \frac{1}{R_A} \\ \frac{1}{R_y} &= \frac{1}{R_{By}} + \frac{1}{R_{By}} = \frac{1}{R_A} + \frac{1}{\infty} = \frac{1}{R_A} \end{aligned}$$

Thus:

$$\frac{1}{R'} = \frac{1}{R_x} + \frac{1}{R_y} = \frac{1}{R_A} + \frac{1}{R_A} = \frac{2}{R_A}$$

Maximum contact pressure (Hertzian stress) (P_a) is defined as:

$$P_{\max} = \frac{3W}{2\pi a^2} \quad \text{Equation 2-5}$$

Where:

W is the normal load (N) and a is the radius of the contact area (m) and is defined as:

$$a = \left(\frac{3WR'}{E'}\right)^{\frac{1}{3}} \quad \text{Equation 2-6}$$

Average contact pressure (Pa) is defined as:

$$P_{\text{average}} = \frac{2}{3} P_{\text{max}} = \frac{W}{\pi a^2} \quad \text{Equation 2-7}$$

Maximum deflection (m) is defined as:

$$\delta = 1.0397 \left(\frac{W^2}{E'^2 R'}\right)^{\frac{1}{3}} \quad \text{Equation 2-8}$$

Maximum shear stress (Pa) is located at :

$$Z = 0.638a \quad (\text{i.e. beneath the surface}) \quad \text{Equation 2-9}$$

And is defined as:

$$\tau_{\text{max}} = \frac{1}{3} P_{\text{max}} \quad \text{Equation 2-10}$$

2.5. Lubrication

Lubrication is defined by effective application of solid, liquid or gas between two bodies with the purpose of reducing friction and/or wear as one body moves over the other. The lubricant is a substance used to decrease friction

and wear and by means of that to provide smooth running and better life of tribological components [14]. The term lubricant is predominantly related to oils and greases but it comprises a wide range of materials including mineral oil, synthetic oil, grease, vegetable oil, water, air, process fluid, solid, etc.

The form of lubrication involved in a tribological interface is dependant of materials of the surfaces, surface conformity and texture, lubricant properties and operating conditions (e.g. load, speed, temperature, environment and etc.). An easy way to classify the form of lubrication in a tribological interface is through lubrication regimes. They enable us to have an idea about the overall performance of the tribological system usually in terms of friction and wear. There are four lubrication regimes:

- **Hydrodynamic Lubrication:** the surfaces are prevented to come into contact by a fluid lubricant film separation which is thick enough.
- **Boundary lubrication:** (shown in Figure 2-4a) fluid film does not separate the surfaces and contact will occur over an area similar to the one in dry contact.
- **Mixed Lubrication:** (shown in Figure 2-4b) a mixture of hydrodynamic and boundary lubrication is encountered.
- **Elastohydrodynamic:** Lubrication: occurs under high pressure generated by low conformity and highly loaded interface [14].

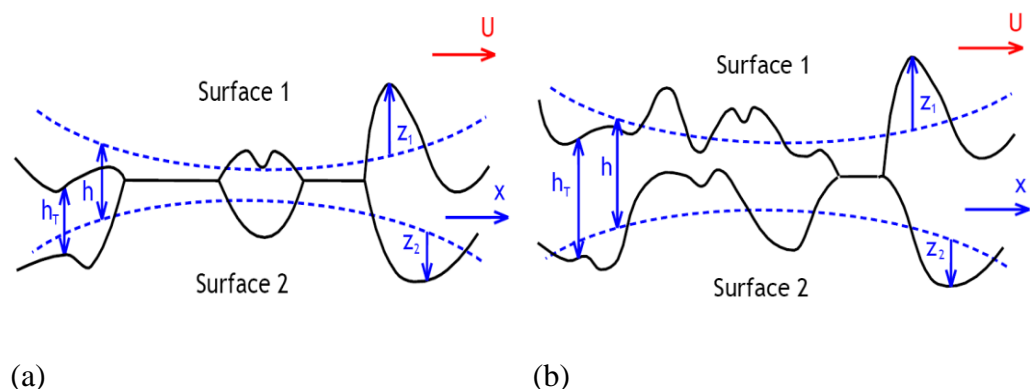


Figure 2-4 Schematic view of (a): boundary lubrication and (b): mixed lubrication [14].

Illustrated in Figure 2-5 is a modified Stribeck diagram where λ is defined by:

$$\lambda = \frac{h_{\min}}{R_q} \quad \text{Equation 2-11}$$

Where, R_q is the Root Mean Square (RMS) roughness of the two surfaces in contact and is defined by:

$$R_q = \sqrt{R_{q1}^2 + R_{q2}^2} \quad \text{Equation 2-12}$$

R_{q1} and R_{q2} are the respective RMS surface roughness of the two solid surfaces and h_{\min} , minimum film thickness for a point contact, is numerically defined as [21, 22]:

$$\frac{h_{\min}}{R'} = 3.63 \left(\frac{U\eta_0}{E'R'} \right)^{0.68} (\alpha E')^{0.49} \left(\frac{W}{E'R'^2} \right)^{-0.073} (1 - e^{-0.68k}) \quad \text{Equation 2-13}$$

Where:

h_{\min}	is the minimum film thickness (m);
U	is the entraining surface velocity (m/s), i.e. $U = (U_A + U_B)/2$, where the subscripts 'A' and 'B' refer to the velocities of bodies 'A' and 'B' respectively;
η_0	is the dynamic viscosity at atmospheric pressure of the lubricant (Pas);
E'	is the reduced Young's modulus (Pa) ;
R'	is the reduced radius of curvature (m);
α	is the viscosity-pressure coefficient (m^2/N) ;
W	is the contact load (N);
k	is the ellipticity parameter defined as: k $= a/b$, where 'a' is the semiaxis of the contact ellipse in the transverse direction (m) and 'b' is the semiaxis in the direction of motion (m). For point contact $k=1$.

Lambda ratio (λ) is used in the modified version of Stribeck diagram due to the direct relation between lubrication regimes and the nature of the surface texture. In most of the cases in automotive applications, the lubrication regime is of boundary lubrication nature [15].

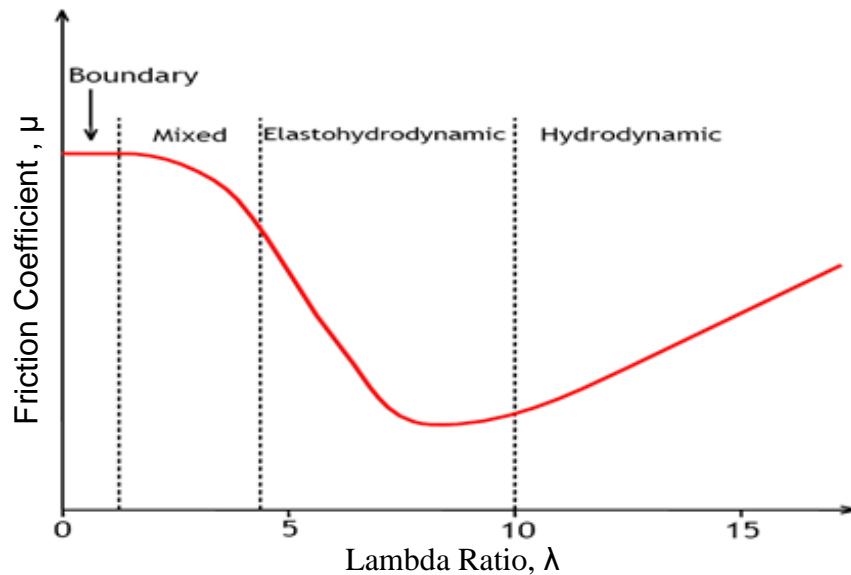


Figure 2-5 The modified Stribeck diagram [14].

2.5.1. Base Oils

Different base oils are being used in the lubricants such as mineral oils, vegetable oils, synthetic oils and re-refined oils. American Petroleum Institute (API-1509) has classified them into five different categories based on the saturate content, sulphur content and viscosity index. In Table 2-1 the API classification of base oils is shown. Physical and chemical properties of base oils will influence the effectiveness of the additives blended in the automotive lubricants [23].

Table 2-1 Base oil categories [23].

Base oil	Description	Sulphur (%)	Saturates (%)	Viscosity index
Group - I	Solvent refined oils	> 0.03%	≤90	> 80 to <120
Group - II	mineral oils	< 0.03%	≥90	> 80 to <120
Group - III	mineral oils	< 0.03%	≥90	> 120
Group - IV	All Polyalphaolefins (PAOs)			
Group - V	All base oil not in Group I –IV.			

Base oils can be mineral or synthetic oils. Mineral oils are usually consisted of hydrocarbons together with nitrogen, oxygen and sulphur and are produced from natural crude oil. They start to degrade at temperatures above 80°C and therefore their oxidation stability is not as good as synthetic oils. Mineral oils are relatively cheap and used in applications with low loads, pressures and operating temperatures [23, 24].

Synthetic lubricants are hydrocarbons with a fully controlled chemical structure, commonly used as base oil. They have a better thermal stability, oxidative stability, viscosity and flow characteristics over a wide range of operating conditions which made them quite popular to be used as base oils. Polyalphaolefins (PAO's) are among the most popular synthetic oils and are derived from ethylene and esters [23, 24].

Depending on the application of the lubricant, an appropriate base oil should be selected. PAO's are free of the impurities or waxes which are usually found in conventional mineral oils. This will offer longer service life, good stability and good overall performance of the lubricant at both low and high temperatures. However, some useful elements such as sulphur and nitrogen that naturally exist in crude oil are absent in their composition, which should be taken into account when selecting the additive package for the lubricant [23, 24] .

2.5.2. Additives

Chemical additives are oil soluble chemicals or mixture of several chemicals introduced to the base oil to modify or improve the existing properties of the lubricant or add completely new properties to the base oil. This will increase useful life of operation of the lubricant and the component in contact. This will particularly affect the applications in which high temperature, pressure, and environment are involved [23, 25]. Based on their functionality, lubricant additives are either to protect the metal surfaces in the engines, such as anti-wear, anti-rust and anti-corrosion additives or to reinforce base stock

performance, such as antioxidants, dispersants, viscosity modifiers and pour point dispersants.

Friction reduction in marine engines was first achieved using oiliness additives which was introduced in 1918 [26]. Later on, between 1930 and 1940, a large group of additive classes, including pour point depressants, extreme pressure (EP) additives, viscosity modifiers, antioxidants, corrosion inhibitors and detergents, were discovered. Antiwear additives were first developed mainly to cope with problems arising in aviation applications at the time [27, 28] but, soon became a key component of engine motor oils [29]. Although the most important types of lubricant additives had been identified by the mid-1940s, much remains to be done in developing new chemistries. In Figure 2-6, chronology of development of main classes of lubricant additive is given [29].

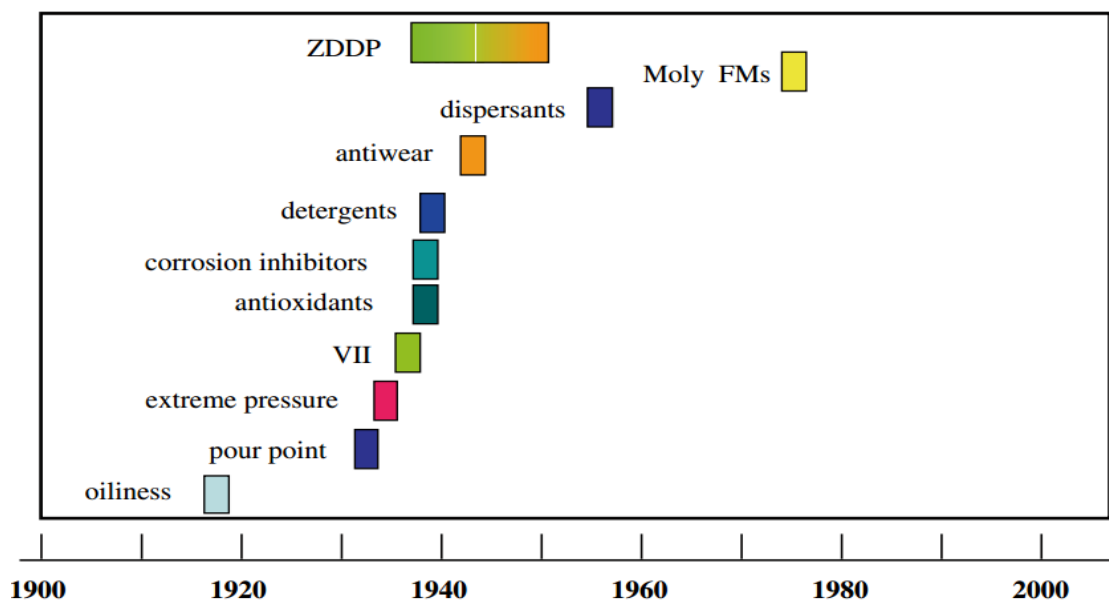


Figure 2-6 Chronology of development of main classes of lubricant additive [29].

The most common additives which are being used in lubricants are described as follows.

2.5.2.1. Extreme Pressure/Anti-wear

Generally adding extreme pressure/anti wear (EP/AW) mixtures to the lubricant leads to increase in the boundary lubrication abilities of the lubricant to decrease friction and prevent scuffing and scoring wear. EP additives, generally made from sulphur or phosphorus, chemically interact with the surface to make a lubricious protective layer on the surface. On the other hand, AW additives with long chain polar molecules of fatty oils, acids, or esters, create sacrificial lubricious adsorbed layers on the surface [25]. Zinc dialkyldithiophosphates (ZDDPs) are by far one of the most common EP/AW additives which can generate boundary lubrication films by chemical reactions with the surface and provide the greatest film strength which can be applied in most severe operating conditions [14, 30].

2.5.2.2. Friction Modifiers

Friction modifiers are employed to reduce friction, increase oil film strength and to prevent oil film rupture by forming surface films [23]. Laboratory tests have shown that a variety of esters, amides and metal soaps decrease up to 30% of friction. Modern engine oils often embody a friction modifier [14]. These additives fall into two categories; the physically absorbed fatty acids and amides, and chemically reactive species such as Molybdenum dithiocarbamate (MoDTC). The latter is commonly being used as a friction modifier in modern engine oils [14, 30].

2.5.2.3. Detergents

Detergents are used in the lubricants to reduce or prevent deposits in engines operated at high temperatures. They control build-up of varnish and sludge by reacting with oxidation products to form oil soluble material which remains suspended. They also neutralize acids and clean deposits [23]. The common detergents which are being used today are organic soaps and salts of alkaline earth metals such as calcium, magnesium, sodium. Some of the most common metal-containing detergents used in the oil formulations include but not limited to calcium and magnesium sulphonates and calcium phenates [23, 30].

2.5.2.4. Dispersants

Dispersants are to disperse or suspend fine particles of soot, potential sludge and varnish material into the oil particularly those formed at low temperature operation. They act as surface active compounds by adsorbing at the surface of the soot and prevent them from forming bigger particles [23]. Dispersants do not contain any metal and therefore are ashless. Typical dispersants are polymeric succinimides, succinic esters of polyols and Manich base [23, 30].

2.5.2.5. Antioxidants

Antioxidants can minimize the formation of resins, varnish, acids, sludge and increase the life of the oil, as a result. Their mode of action is to react with organic peroxides, terminating the oxidation chain. They reduce formation of acids by decreasing oxygen take up in the oil. In addition they prevent catalytic reactions [23].

2.5.2.6. Viscosity Index (VI) Improvers

VI property is usually dependent upon the type of base oil chosen. However, polymeric additives are used to increase the VI. These long chain polymers are the key to the success of multi-grade mineral, engine oils (e.g. SAE 10W-30) to gain adequate viscosity for high and low temperature performances. However, the polymers are just capable of improving VI under minimal shear stress and at high shear stresses, related to those in rolling bearings; are unable to stop the flow to increase viscosity. Furthermore, under specific operating conditions (e.g. high shear), the polymers break down earlier than the lubricant, therefore acting as the limiting factor in the lubricant lifetime [25].

2.5.2.7. Other Additives

Apart from the mentioned additives which are the main lubricant additives, there are many other important additive groups such as pour point depressants, antifoaming agents, corrosion inhibitors, rust inhibitors, demulsifiers, emulsifiers, etc. , each of which has a different mode of action by which they protect the surface and enhance the properties of the base oil [25]. These additives are usually present in the finished lubricant and play a great role with regards to the lubricant performance in the lubricated system.

2.6. Surface Coating Deposition

2.6.1. Physical Vapour Deposition (PVD)

PVD is a deposition technique in which material is vaporized from a solid or liquid source in the form of atoms or molecules, transported in the form of a vapour through a vacuum or low pressure gaseous (or plasma) environment to the substrate where it condenses. PVD is usually used to deposit very thin films in the range of a few nanometres to about ten micrometres; however they can also be applied to produce multilayer coatings, graded composition deposits, very thick deposits and freestanding structures. Using PVD, the substrates with different sizes from very small to very large (e.g. 10' x 12' glass panels) and almost any shapes can be coated. PVD processes typically have deposition rate of 1–10 nanometres per second. They can deposit films of elements and alloys as well as compounds. Compounds can be formed by the reaction of depositing material with the ambient gas environment such as nitrogen or with a co-depositing material (e.g. titanium carbide, TiC). Typical process temperatures in PVD are in the range of 200–300°C. In a PVD process, prior to coating deposition, the substrate is bombarded with argon ions for cleaning purposes. One of the main disadvantages of PVD process is that it is a line-of-sight technique leading to poor surface coverage, and thus makes coating of complex shapes almost impossible [31].

2.6.2. Sputtering/DC Magnetron Sputtering

The term sputtering can be described as the removal of material from a solid target by the bombardment of high energy ion particles. The ejected atoms will be then deposited on the substrate and form the desired thin film of the target material onto the substrate surface.

DC magnetron sputtering is one of different types of sputtering in which sputtering occurs in a vacuum chamber where the path of the generated atoms are controlled by magnetrons. An array of high voltage magnetron cathodes are placed beneath the target. A low pressure gas, commonly argon, will be introduced into the deposition chamber while applying an electric field between the target (cathode) and the substrate (anode). This will cause ionisation of the gas (argon) atoms and generation of a high flow between the target and the substrate. The generated high energy plasma

hits the target and results in ejection of atoms from the target material and the atoms bond with the substrate.

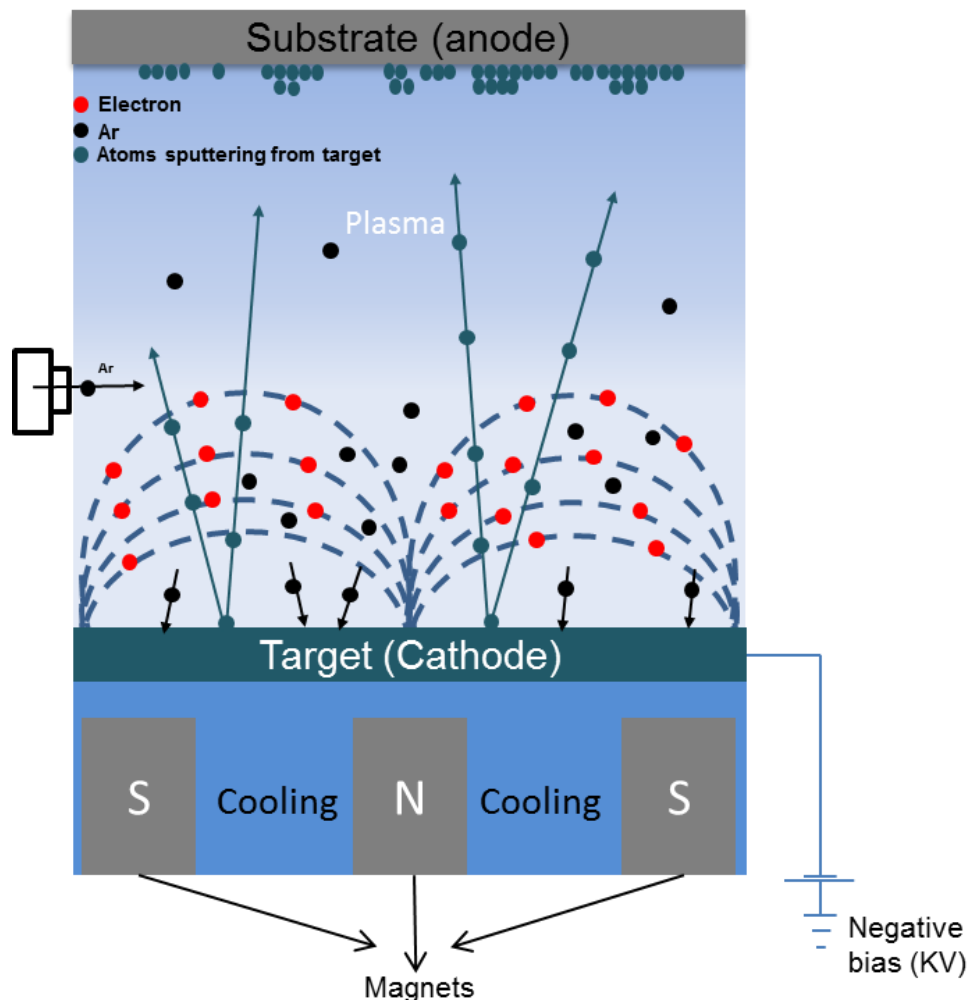
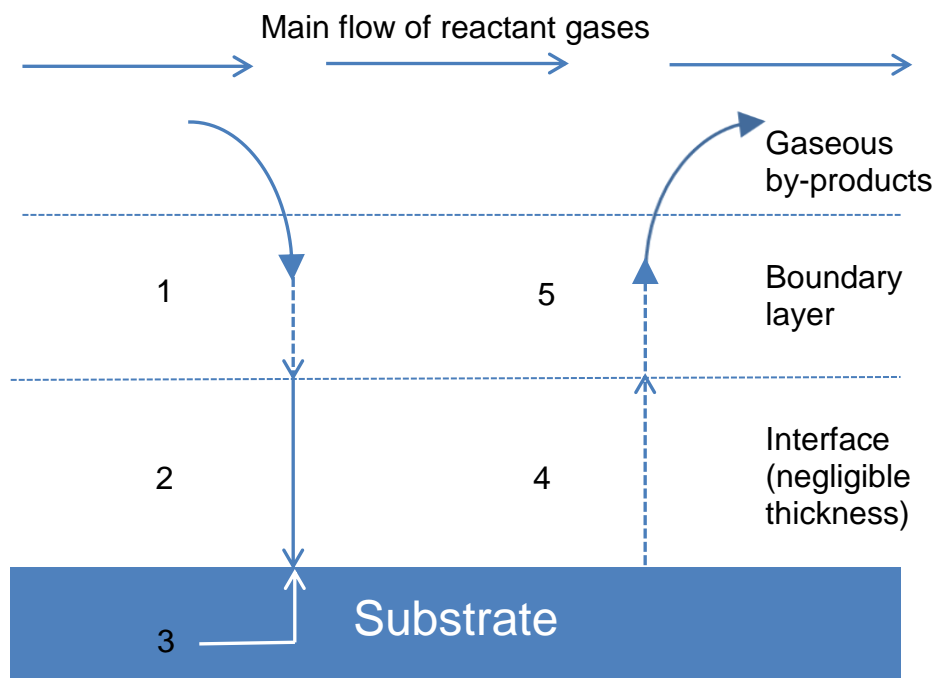


Figure 2-7 Schematic diagram of a DC-magnetron sputtering unit.

2.6.3. Chemical Vapour Deposition (CVD)

CVD refers to “the deposition of a solid on a heated surface from a chemical reaction in the vapour phase”. CVD are among vapour-transfer processes which is atomistic in nature. In other words, the deposition species are atoms or molecules or a combination of these. In many respects, CVD will be followed by PVD or a combination of both will be applied to deposit a coating onto the substrate, especially, in the newer processes such as plasma enhanced CVD which will be explained as follows [32].



- 1- Diffusion in of reactants through boundary layer.
- 2- Absorption of reactants on substrate.
- 3- Chemical reaction takes place.
- 4- Desorption of absorbed species.
- 5- Diffusion out of by-products.

Figure 2-8 Sequence of events during deposition [32].

2.6.4. Plasma Enhanced Chemical Vapour Deposition (PECVD)

The PECVD is a process of depositing thin films from a gas phase to solid state on a substrate. It can be considered as combination of PVD and CVD systems where the glow discharge of PVD facilitates plasma creation of the reacting gases. The main advantage of PECVD is the lower deposition temperature compared to that of thermally driven CVD while maintaining a good deposition rates and high quality product. More recently, the PECVD of diamond films has captivated a large amount of interest [33]. The schematic diagram of the PECVD process is shown in Figure 2-9.

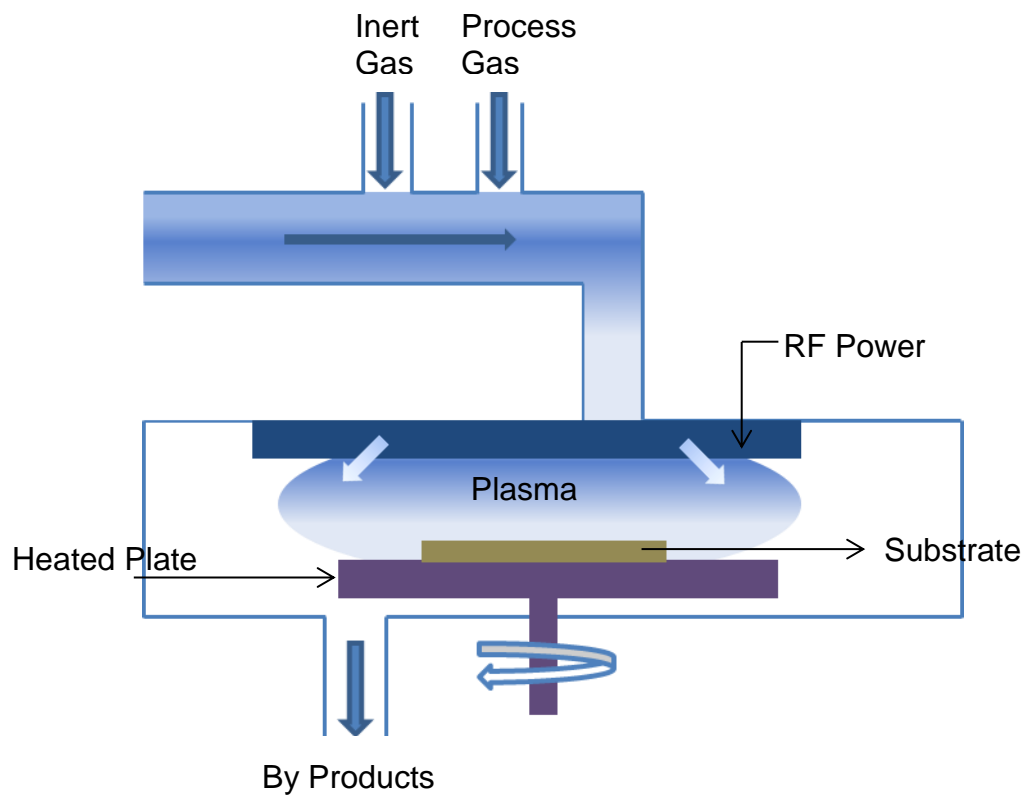


Figure 2-9 Schematic diagram of PECVD system.

Chapter 3 Literature Review

3.1. Introduction

With the application of non-ferrous hard coatings, lubricant/surface interactions, particularly when the components experience the boundary/mixed lubrication regime, have become a new challenge for both researchers and industry. In this chapter, a comprehensive review of the current understanding of the lubricant additives and their interactions with ferrous surfaces, which are key to understanding lubricant/coating interactions, has been provided. Furthermore, Diamond-like carbon (DLC) coatings and their properties have been described. This review will aim to cover the current understanding of lubricant/DLC interactions and the effect of conventional lubricant additives on the tribological performance of DLC coatings has been shown.

3.2. Lubricant Additives and their Interactions with Ferrous Surfaces

Commonly-used friction modifiers and anti-wear additives are optimized to form tribofilms on ferrous surfaces. Molybdenum dithiocarbamate (MoDTC) and Zinc dialkyldithiophosphates (ZDDP) are well-known friction modifier and anti-wear additives respectively, used for ferrous surfaces. MoS₂ low friction sheets, derived from MoDTC decomposition, provide low friction at tribological contacts [34-36]. ZDDP offers anti-wear properties by forming sulphide and phosphate containing tribofilms at the ferrous surfaces [35-37]. In addition, MoDTC has been found to improve the wear resistance of the ferrous surfaces by forming N-containing species in the tribofilm [35]. With the emergence of new non-ferrous coatings, researchers have started to consider how different lubricant additives interact with various types of hard coatings such as DLC coatings under boundary lubrication. However, in order to understand how the current lubricant additives would interact with this novel surfaces (non-ferrous), there is a need to understand and review how these additives will behave on ferrous materials and the mechanisms by which they form tribofilms on the surface.

3.2.1. Zinc Dialkyldithiophosphate (ZDDP)

Zinc dialkyldithiophosphate (generally referred to as ZDDP) additive is one of the most common anti-wear additives which are being used in engine oils. It offers a wide range of properties which provide the lubricant with the required characteristics such as anti-wear, extreme pressure (EP) and anti-oxidant action [29].

Following the applications of phosphorous and sulphur containing additives which started in the 1930s, ZDDP was first introduced by Lubrizol in 1941 as antioxidant additive; however, its ability as anti-wear additive, by forming reaction films on rubbing metal surfaces, was noticed in 1955 and was mainly used in engines to prevent excessive wear in the cam and follower contact [29, 38, 39].

With the introduction of exhaust after treatment system catalysts in 1990s, ZDDP was found to have a detrimental effect on the catalytic converters as ZDDP-derived phosphorus and sulphur oxidised the exhaust catalysts which in turn could reduce the life of the exhaust treatment system [29]. In order to cope with this issue and due to the fact that ZDDP is the only source of P in the engine lubricant, restrictions on the ZDDP concentration have been considered. However, ZDDP has been the most effective anti-wear additive used in the lubricants and limitations on its concentration can result in ineffectiveness of the lubricant in terms of wear performance [38]. This is where the surface engineering comes into equation by providing an alternative solution which could reduce the dependence on ZDDP additive. One of the potential solutions is to apply hard coatings such as Diamond-Like Carbon (DLC).

ZDDP's molecular structure is rather complex and is shown in Figure 3-1. The radical group can be alkyl or aryl and its task is to help to increase the solubility additive in the base oil.

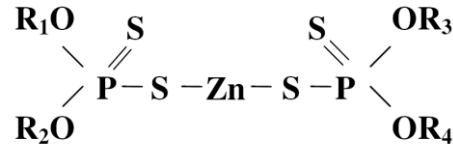


Figure 3-1 Molecular structure of ZDDP [29].

ZDDP is the product of reaction between alcohols, phosphorus pentasulphide and zinc salts. Depending on the type of organic alcohol used to synthesize ZDDP, it will fall into three different types namely, aryl ZDDP, primary ZDDP ($\text{CH}_3\text{CH}_2\text{CH}_2\text{CH}_2\text{O}-$), secondary ZDDP ($\text{CH}_3\text{CH}_2\text{CH}(\text{CH}_3)\text{O}-$) [40]. The ranking of anti-wear effectiveness of different type of ZDDPs are as follows [29]:

Secondary alkyl > primary alkyl > aryl

Aryl ZDDPs which are more thermally stable are preferably used in diesel engine whereas more reactive primary and secondary ZDDPs are widely used in gasoline engines [41, 42]. It has been reported that primary ZDDP gives more wear than secondary ZDDP which was mainly related to the thermal stability of the additives, molecular weight and/or concentration of unreacted acids used in the production of ZDDP [43].

The effectiveness of ZDDP is correlated to the formation of a tribofilm on the surface followed by its chemical activation with the surface. ZDDP is mainly efficient in non-conforming surfaces where elastohydrodynamic lubrication breaks down such as cam and follower in valve train system [44].

3.2.2. Tribological Performance of ZDDP on Ferrous Surfaces

Different factors have been found to influence tribological performance of ZDDP such as temperature, contact pressure and the surface properties [45-47].

ZDDP was shown to be more effective in wear reduction when it was used in oils lubricating fully hardened metals [45]. It was shown that formation and depletion of the ZDDP tribofilm resulted in loss of materials and higher wear as a result [45]. The hardness values of two materials rubbing against each other was suggested to be as close as possible for ZDDP to be effective in film formation on the surface. This would in turn lead to a shorter running-in period, easier growth of surface film and less cutting and ploughing action [46, 47]. Also, roughness of two interacting surfaces was suggested to be similar in order to have a better wear protection by ZDDP [46].

Another factor which affects the ZDDP effectiveness in wear reduction is contact load. ZDDP was shown to reduce wear at low loads while increased the wear rate when the load was high. This was attributed to the lower sulphur content of the formed tribofilm at high loads. Sulphides are much harder than polyphosphates and reduction in sulphite content in the film would lead to lower mechanical strength and higher wear, as a result [48]. ZDDP-derived hard sulphides enhance the load bearing capability which in turn protect the surface from extreme pressure [48, 49]. Sliding speed was also found to affect the film formation from ZDDP [46, 50].

ZDDP starts to form a physisorbed film at around 50°C and a chemisorbed film at temperatures above 80°C [46]. It was suggested that higher sliding speed would increase the chemisorbed film formation from ZDDP [51]. The thickness of the tribofilm formed from ZDDP was shown to be 5-50 nm and on the wear scar [52]. This film thickness was reported to vary depending on the temperature and the ZDDP concentration in the lubricant [53, 54].

Therefore, it seems that operating conditions play a great role in providing the improved anti-wear performance by ZDDP and sufficient supply of the additive in the oil to replenish the tribofilm is crucial.

Reports that have been published about the effect of ZDDP on the friction performance have been contradictory and quite complicated. In the literature, the presence of ZDDP in the lubricants have been reported to increase the friction [48, 55-58]. It was shown that ZDDP has a detrimental

effect on the effectiveness of friction modifiers. The increase in friction in the presence of ZDDP was attributed to the anti-wear film formation [56]. It was suggested that increase in roughness due to the film formation could promote boundary lubrication which in turn increased the friction values [58]. The highest impact of ZDDP on increasing the friction was seen mainly in mixed lubrication regime and to some extent in boundary lubrication. However, friction change was not observed in EHL lubrication [59]. Besides the effect of higher roughness of ZDDP tribofilm, ZDDP was shown to inhibit the lubricant entrainment into the contact resulting in a reduced EHL film thickness compared to ZDDP-free lubricants [60, 61]. In contrast, in some other literature, addition of ZDDP to the lubricant was found to have either neutral effect [62] or a decrease on friction [63].

The difference in the reported results could be related to different test parameters (i.e. additive mixture, material, temperature, etc.) which was used in each study.

3.2.3. Chemical Properties of ZDDP tribofilm and Mechanisms of Wear Reduction

In order to understand the mechanisms by which ZDDP could facilitate low wear, it is crucial to know the chemical species as well as the elements which are present in the formed tribofilm. ZDDP tribofilm is made up of inorganic polymer materials containing zinc, phosphorus, oxygen and sulphur [64-66].

Different mechanisms have been proposed for the ZDDP decomposition such as, surface adsorption [67, 68], thermal degradation [69, 70], thermo oxidation and hydrolysis [64, 65]. It was shown that increasing temperature resulted in higher ZDDP decomposition rate which indicates that ZDDP decomposition has a thermal nature [69]. In another literature, the chemical reactivity of ZDDP with iron was shown to be key for anti-wear property of ZDDP. Hydrolytic mechanism of ZDDP was proposed by Spedding and Watkins [64, 65]. They concluded that ZDDP breakdown is water-catalysed and elimination of water from the reaction would suppress the ZDDP decomposition.

A layered film structure has been proposed by Bell *et al.* [71] and is given in Figure 3-2. Based on this model, the top layer of the ZDDP tribofilm composed of glassy phosphate films whereas the layer near the surface was rich in iron sulphide and iron oxides.

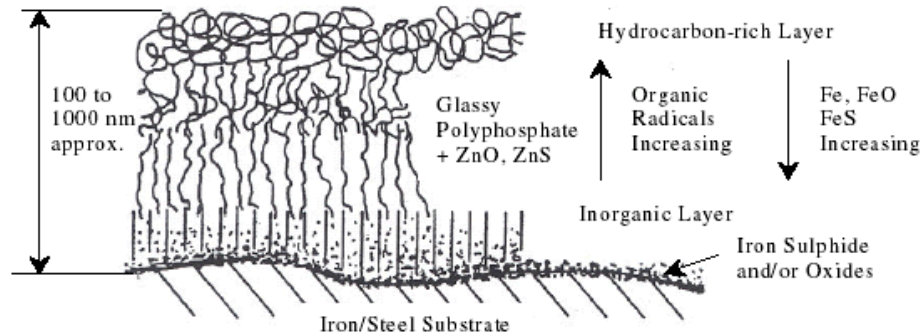


Figure 3-2 ZDDP film structure [71].

Using surface sensitive analytical techniques such as X-ray photoelectron spectroscopy (XPS) and X-ray Absorption Near Edge Structure (XANES), Yin *et al.* [72] showed that increasing the test duration, enhanced the long chain polyphosphate formation on the topmost surface. XPS analysis revealed that the thickness of film after 12 h tests was much thicker than that of 30 min test. They also concluded that the rate of ZDDP decomposition would increase with increase in temperature and load. In addition, more ZDDP was detected on the tribofilm when concentration of ZDDP was higher in the lubricant.

In Figure 3-3, a simple model for ZDDP tribofilm proposed by Martin *et al.* [73] is shown. Based on the proposed model, the top layer is rich in long chain zinc poly(thio)phosphate polymer-like material with the thickness of about 10 nm. A mixed iron and zinc short chain polyphosphate with a gradient concentration of about 100 nm thick was formed in the bulk containing metal sulphide precipitates which was likely to be ZnS and ZnO. Interestingly, no oxide/sulphide layer was found at the interface between the phosphate and the steel surface[73].

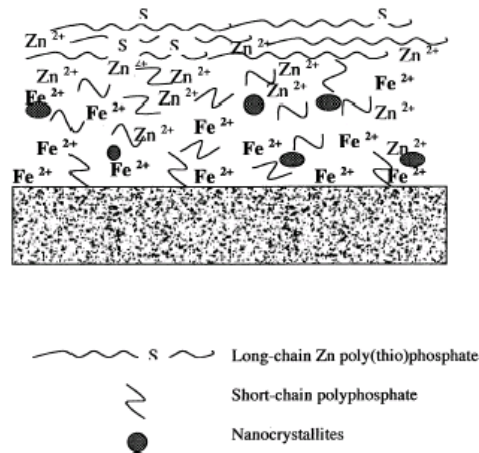
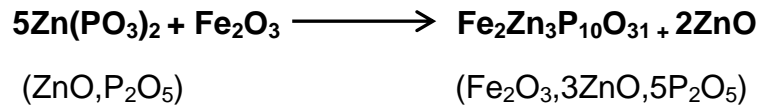


Figure 3-3 Two-layer model of ZDDP tribofilm [73].

No carbon was evident in the bulk of the ZDDP tribofilm (Figure 3-4) [74]. It was proposed that sulphur might partly substitute for oxygen in the polymer chain backbone (O–P–S instead of O–P–O). Thermo-oxidative decomposition of ZDDP results in the formation of phosphate film on a steel surface. It will be followed by a reaction between the phosphate and the iron oxide native layer. The reaction between the phosphate and Fe_2O_3 , provides an inter-grown layer based on the acid–base chemical reaction (HSAB). Iron oxide particles can be formed during the wear process, when the thermal film is disrupted and dissolved oxygen from the lubricant reacts with the nascent surface. Iron oxide particles could also originate from other parts of the mechanical system. Iron oxide particles, Fe_2O_3 in particular, can cause severe damage by abrasive wear of the film. This is mainly correlated to the high hardness of the crystallized oxide as well as its high melting point ($>1200^\circ\text{C}$) [74].

An important aspect of the anti-wear mechanism of ZDDP, which has been identified, is the ability of polyphosphate glasses to eliminate abrasive particles of metal oxides through tribochemical reactions [73, 75]. The proposed model by Martin et al. [73] illustrates that the third body abrasive iron oxide particles can be eliminated by the formation of short-chain mixed iron/zinc phosphate glasses as a result of classical acid–base chemical reactions (HSAB). Fe^{+3} is harder Lewis acid compared to Zn^{2+} and the cation exchange is more favourable based on the HSAB principle [76]. On the other hand, phosphates are hard bases and will react with the harder acid leading

to reaction of iron and the phosphate which in turn results in elimination of the iron oxide. Starting from the polymer-like zinc metaphosphate for example, a possible route for the elimination of 1 mole of Fe_2O_3 was suggested to be as follows [73, 74, 77]:



The above reaction illustrates the cation exchange process between iron oxide (as Fe_2O_3 in this case) and zinc (as ZnO) [74].

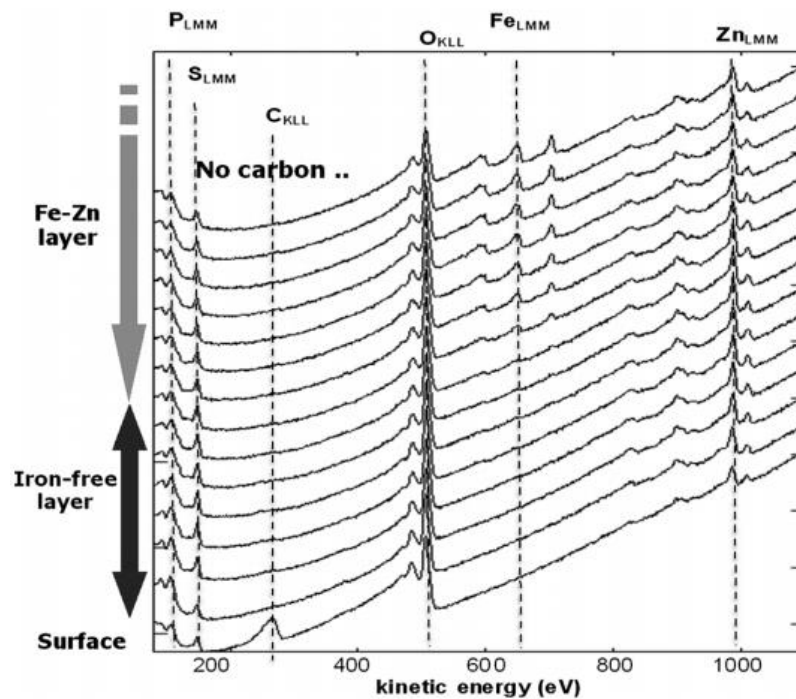


Figure 3-4 ZDDP tribofilm profile obtained using Auger Electron Spectroscopy (AES). The top layer contains only zinc polythiophosphate. There is no carbon in the film (except contamination at the outmost surface) [74].

Molecular Dynamics (MD) simulation has been used by authors [74, 75, 78] to study very basic and important tribochemical reactions occurring during sliding between the glassy zinc phosphates and the nano-oxide particle. Martin *et al.* [74] have recently developed a classical molecular dynamics

approach to study the HSAB reactions occurring in the anti-wear chemistry of ZDDP. They have proposed that the combined effects of pressure and shear in the confined interface region is crucial for the tribochemical reaction of ZDDP and that the particle cannot be eliminated only by pressure (Figure 3-5).

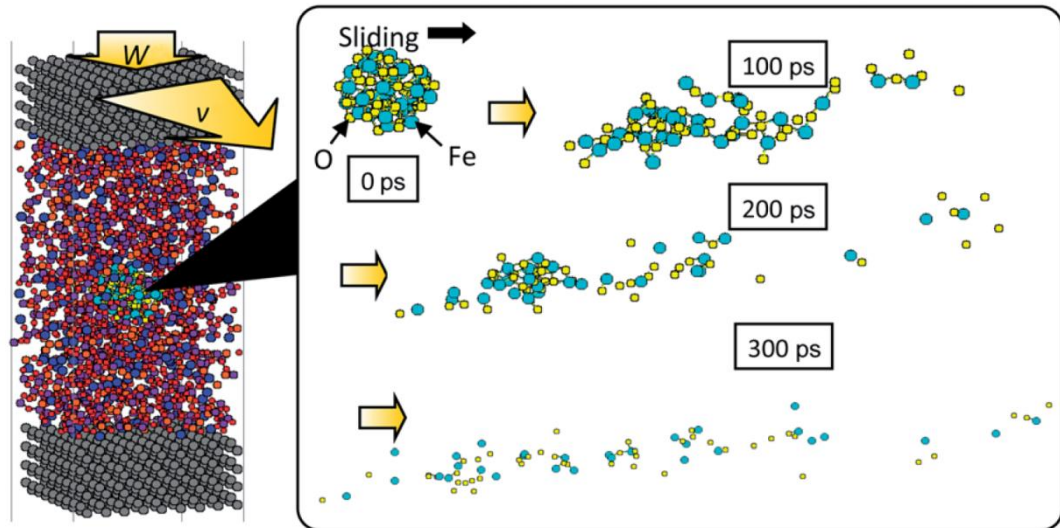


Figure 3-5 The MD simulation showing the combined effects of pressure and shear is essential for the digestion of iron oxide embedded in the zinc metaphosphate by MD [74].

In another study on MD calculation coupled with finite element (FM) method, the mixing of zinc phosphate and native iron oxide on ferrous substrate was found to be responsible for both increasing mechanical hardness of the tribofilm material and its adhesion to the iron oxide substrate [79].

The role of the nature of manganese oxide and chromium oxide, which are generally found in chemical composition of steel substrate, in achieving anti-wear effect of ZDDP has also been investigated using MD. It was found that, in spite of having higher melting point and hardness compared to iron oxides, manganese oxide and chromium oxide are eliminated from the

system by zinc phosphate under the combined effects of pressure and shear, in a similar manner to digestion of iron oxides Figure 3-6 [75].

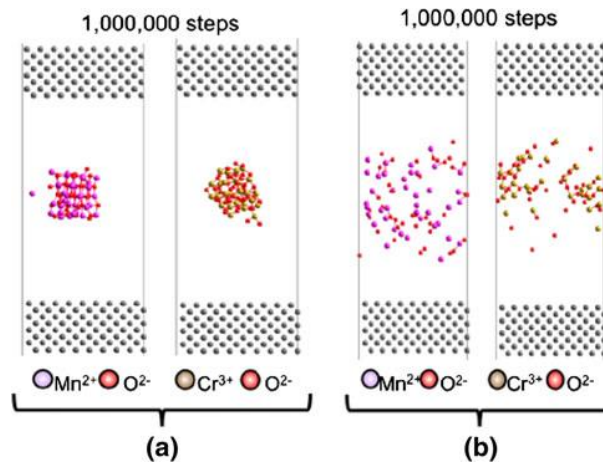
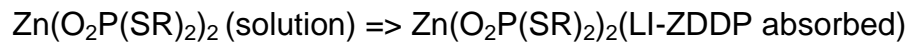


Figure 3-6 MD simulation of digestion of manganese and chromium oxides nanoparticles embedded in zinc metaphosphate matrix under the effect of (a) pressure and (b) combined pressure and shear. Temperature =353 K. Steps of simulation (1,000,000) [75].

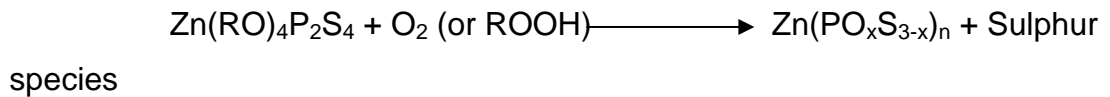
Another layer structure model for the ZDDP film formation has been proposed by Fuller *et al.* [80]. In this model, the presence of Fe_2O_3 was not found to be essential for the anti-wear film formation. It was shown that hydrolysis of polyphosphates is involved in the formation of short chain polyphosphates. The presence of a linkage isomer of ZDDP (LI-ZDDP) was found to be important for the ZDDP film formation. The proposed ZDDP film formation processes are as follows:

1. ZDDP is adsorbed onto metal surface:
 $\text{Zn}((\text{RO})_2\text{PS}_2)_2 (\text{solution}) \Rightarrow \text{Zn}((\text{RO})_2\text{PS}_2)_2 (\text{ZDDP absorbed})$
2. ZDDP in solution is converted into a linkage isomer of ZDDP:
 $\text{Zn}((\text{RO})_2\text{PS}_2)_2 (\text{solution}) \Rightarrow \text{Zn}(\text{O}_2\text{P}(\text{SR})_2)_2 (\text{LI-ZDDP in solution})$

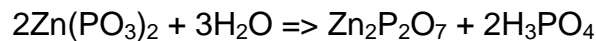
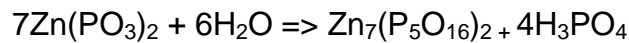
3. The linkage isomer of ZDDP in the solution is adsorbed onto the metal surface:



4. Thermal degradation of the adsorbed linkage isomer of ZDDP by O_2 or ROOH to form long chain polyphosphate $\text{Zn}(\text{PO}_3)_2$:



5. Hydrolysis of polyphosphate by the water present in the base oil to form short chain polyphosphates:



Another hypothesis regarding the mechanism by which ZDDP can protect the surface from further wear is the action of ZDDP phosphate film as a viscous lubricant in boundary lubrication [81]. Although, temperature and shear would affect the viscosity of the glass. Formation of ZDDP-derived glassy phosphate could also passivate the surface against further thermo-oxidative reactions (e.g. corrosion wear). In another work by Williams [82], the effectiveness of ZDDP in reducing wear was related to the formation of a tribofilm which is softer than the substrate and could reduce the asperities in contact.

3.2.4. Mechanical Properties of ZDDP Tribofilm

Many researchers have studied and evaluated mechanical properties of ZDDP tribofilms [83-91]. They have used different techniques (mainly nanoindentation) to evaluate the thickness and mechanical properties of the films formed from ZDDP-containing oils. Bec and Tonck [84] used nanoindentation analysis along with imaging procedures in order to measure the hardness and Young's modulus of the tribofilm. They found that the

ZDDP film is heterogeneous and that mechanical properties of the film showed reduction in their values. Ye *et al.* [92] measured the mechanical properties of ZDDP and ZDDP/MoDTC tribofilms and did not find any difference with regards to the mechanical properties of the films. They reported that the values of hardness and the reduced Young's modulus gradually increased with increase in depth. In another study by Pidduck and Smith [85], the thickness of the ZDDP tribofilm was found to be dependent on the oil formulation. They found that the film thickness was in the range of 100-140 nm when base oil was formulated with ZDDP, detergent and dispersant. Bec *et al.* [93] used combination of nanoindentation experiments with continuous stiffness measurements and a specific developed rheological model to determine the nanomechanical properties of the films formed from ZDDP-containing oils. They found that tribofilm formed from ZDDP + MoDTC was heterogeneous whereas its thickness and mechanical properties varied depending on the test location. The films were found to be mono layer at some locations and bilayered structure in other places. In contrast, the film formed from ZDDP+ MoDTC + detergent/dispersant was found to be homogeneous. Only its thickness was found to vary, depending on the test area. Table 3-1 summarises some of the obtained results by authors [84, 85, 92, 93]. The variation in mechanical properties of ZDDP could be due to numerous factors. These include different test parameters, different type of blends, different concentration of ZDDP and different measurement techniques.

In addition, Graham *et al.* [87] used Atomic Force Microscopy (AFM) and Infinite Focus Microscopy (IFM) to provide high resolution topographic images and to measure quantitative nanomechanical properties of the films derived from alkyl and aryl ZDDP. They found different distinct regions within alkyl films with respect to topography and mechanical properties. The values obtained for indentation modulus of alkyl was in the range of 37 ± 7.3 to 209 ± 38 GPa whereas the maximum value of the indentation modulus for aryl

films was found to be 50 ± 10 GPa. This could explain the better wear protection provided by alkyl ZDDPs compared to aryl ZDDPs.

Table 3-1 Mechanical properties of tribofilm formed from ZDDP-containing oils.

Author(s)		[84]		[92]		[93]		[85]
Technique(s)		Nanoindentation/ Imaging procedures		Nanoindentation/ AFM		Nanoindentation/ rheological film model		AFM
						Unwashed film	Solvent washed	
Penetration Depth (nm)		3	30	5	30	-	-	-
ZDDP film	E (GPa)	78-115	127-156	150	215	-		
	H (GPa)	2-4.5	8.4-11	6	10			
	Film thickness (nm)	-	-	≤ 100				
ZDDP+ MoDTC film	E (GPa)	-		150	215	5-80	8-110	
	H (GPa)			6	10	0.2-4.8	0.3-3	
	Film thickness (nm)			≤ 100		60-120	3-175	
ZDDP+ FM+ detergent, dispersant	E (GPa)	-		-		10-80	15-120	100-140
	H (GPa)					1-4	0.3-3.5	
	Film thickness (nm)					2-147	5-125	

Aktary *et al.* [88] used Scanning Electron Microscopy (SEM) and infrared spectroscopy and showed that precipitation of ZDDP products resulted in formation and growth of islands containing long chain polyphosphates. These islands were found to be surrounded by shorter chain polyphosphates which were formed beneath the top layer. Some other studies [92, 94] showed that ZDDP anti-wear tribofilm is a mixture of white patches and dark strips formed along sliding direction [92, 94]. Nicholls *et al.* [95] suggested that the raised white patches are long chain polyphosphates and the dark areas are mainly consisted of short chain polyphosphates and undecomposed ZDDP. Figure 3-7 shows a schematic diagram of the ZDDP tribofilm pad structure.

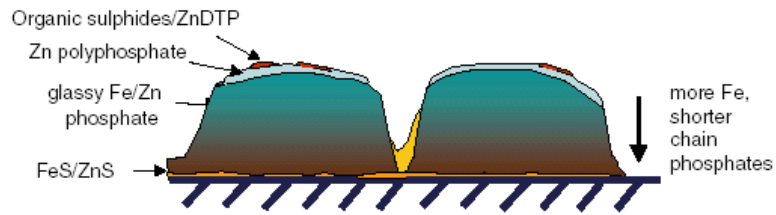


Figure 3-7 Schematic diagram of pad structure and composition [29].

In Figure 3-8, the schematic picture of the most likely ZDDP tribofilm layers structure and their mechanical properties is given [89].

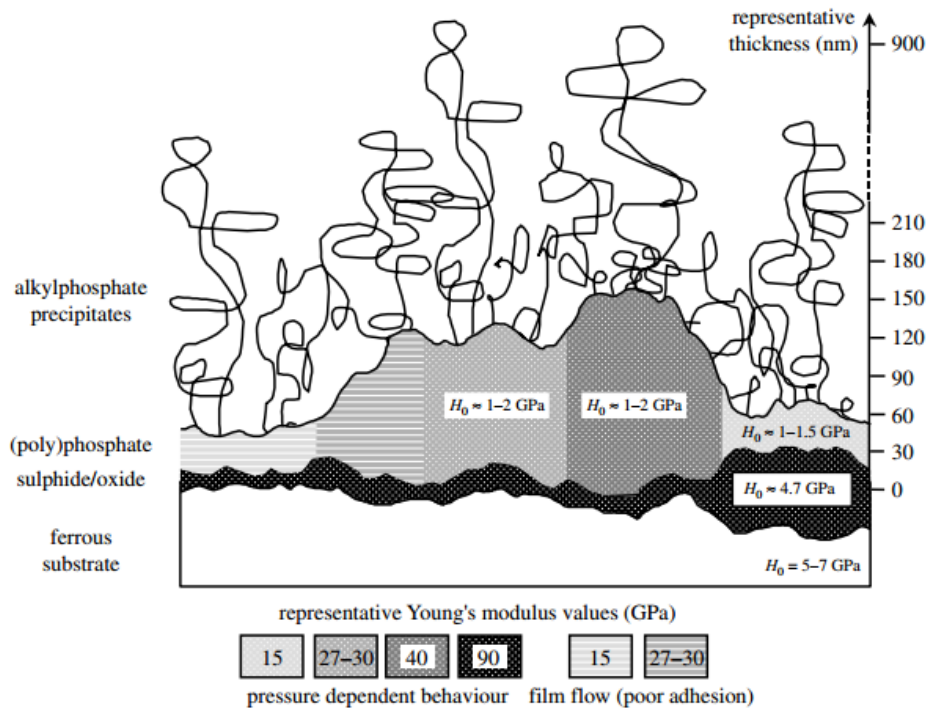


Figure 3-8 Schematic picture of the structure and mechanical properties of the full anti-wear film formed by simple ZDTP solution [89].

Nevertheless, based on the published literature, the anti-wear tribofilms have been found to be patchy and inhomogeneous and different mechanical properties (i.e. hardness and elastic modulus), have been reported for ZDDP tribofilm. This controversy could be related to different test methods, measurement techniques and surface preparation used. However, it is

apparent that the obtained values for hardness and modulus of the film formed from ZDDP are generally smaller than the substrate.

3.2.5. Molybdenum Dialkyl Dithiocarbamate (MoDTC)

One of the most important types of friction modifier are molybdenum-sulphur containing compounds. They were shown to reduce friction by forming a layer-lattice structure of MoS_2 film on ferrous surfaces [96-105]. The bonding between atom species in MoS_2 molecules are strong covalent whereas between the layers weak Van der Waals attraction exist. This weak Van der Waals forces between the layers facilitates low friction by maintaining easy shear within the molecule. The MoS_2 solid state structure is shown in Figure 3-9 [96].

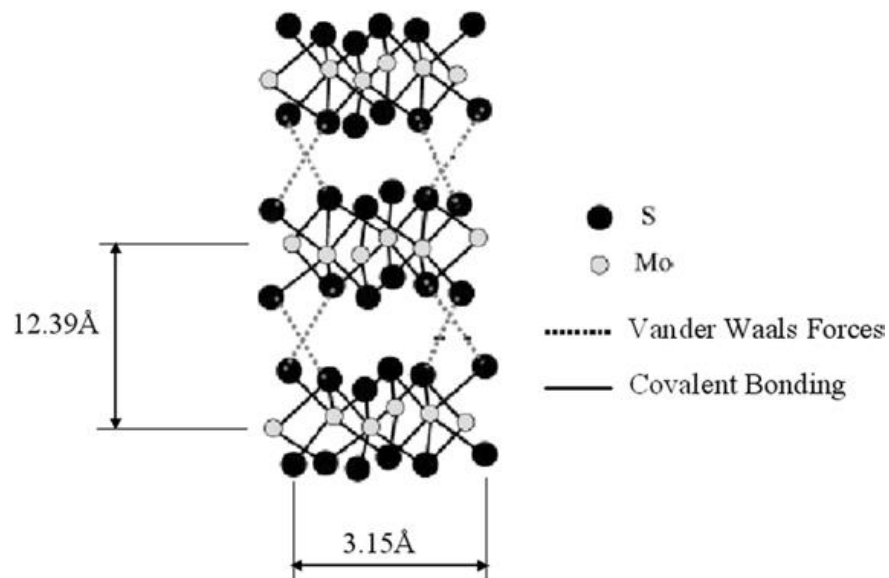


Figure 3-9 MoS_2 solid state structure [96].

Molybdenum disulphide adheres freely to most of the substrates. Mo-S complexes are not only able to provide low friction but also enhance the load bearing capability [106, 107]. They are reported to provide EP and anti-wear properties as well as friction reduction.

One of the most commonly used Mo-S compound friction modifier additives is molybdenum dialkyl dithiocarbamate (MoDTC) [97, 98]. Two Mo atoms are present in the centre of the molecule and for that reason this compound is also called Moly Dimer. The structure of MoDTC is shown in Figure 3-10.

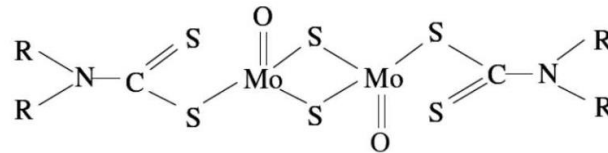


Figure 3-10 MoDTC structure

High temperature ($> 200^{\circ}\text{C}$) and rubbing is required for the formation of low friction MoS_2 from MoDTC. The MoDTC effectiveness in giving low friction depends on its concentration in the oil, the MoDTC type, type of contact, load and surface roughness and varies with the operating temperature [97, 100, 101]. The surface analysis provided inside the wear scar showed the formation of MoS_2 and MoO_3 whereas only MoO_3 was detected outside of the wear scar [97, 108]. Furthermore, *Grossiord et al.* [34] detected undecomposed MoDTC in the tribofilm. They proposed MoDTC decomposition in a two-stage model. According to their model, first stage of the MoDTC decomposition is electron transfer at the Mo-S chemical bond in MoDTC (Figure 3-11a), resulting in the formation of three free radicals (Figure 3-11a b): one relates to the core of MoDTC and the other two to the chain ends. The third step is the formation of MoS_2 and MoO_2 from core radical decomposition (Figure 3-11c) which can oxidise in the presence of O_2 .

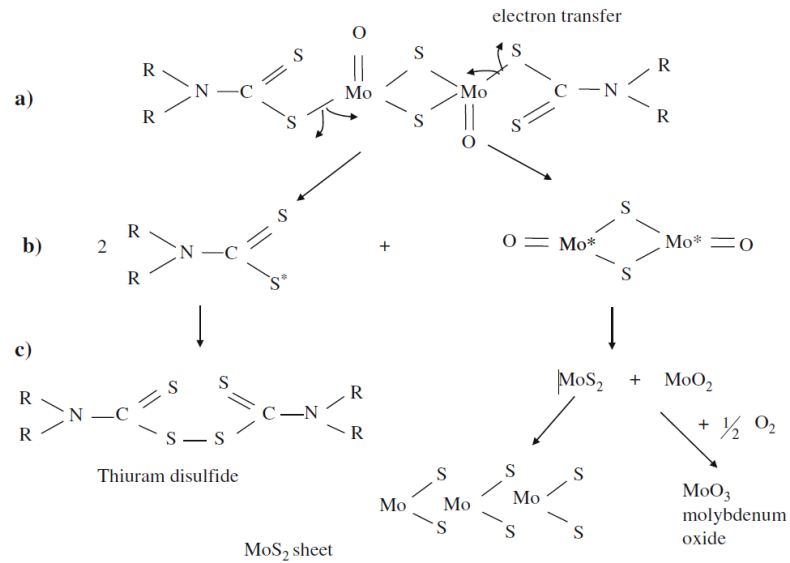


Figure 3-11 Model proposed for MoDTC decomposition [34] .

MD modelling was used to study the dynamics of MoS₂ tribofilm formation on Fe substrate. It was shown that, as a result of the tribochemical reactions, MoS₂ layer which was initially amorphous, self-organized its structure and formed layered MoS₂ tribofilm. MoS₂ layer was initially generated on the Fe surface, followed by the formation of an intermediate MoS₂ layer (Figure 3-12) [109].

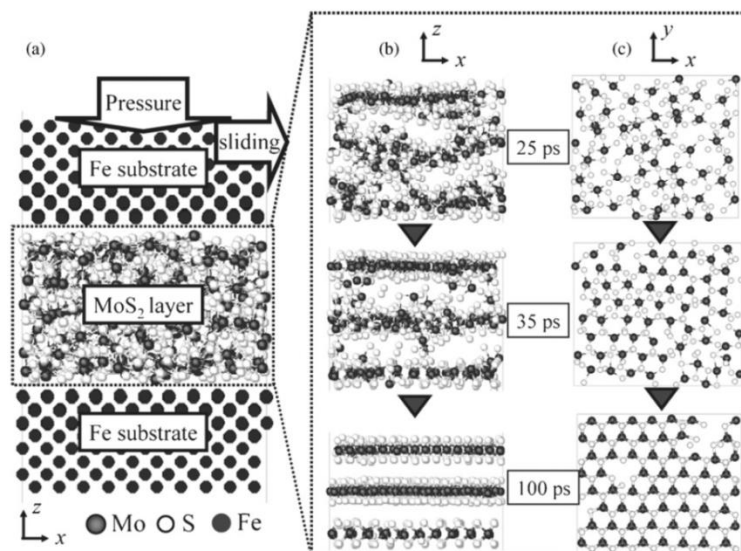


Figure 3-12 (a) MD model, (b) behaviour of MoS₂ layer during simulation from x-z direction, and (c) behaviour of MoS₂ layer near the upper Fe substrate from x-y direction [109].

The chemical reaction dynamics of the MoDTC molecule in the heated engine oil phase and on the nascent iron surface were investigated by Onodera *et al.* [110]. It was suggested that, in the heated oil phase, the MoDTC molecule produced its linkage isomer and, subsequently, a weak bonding intermediate. They have demonstrated that the adsorbed molecule decomposed into molecular MoS₂ on the rubbing nascent iron surface. This indicated the initiation of MoS₂ solid film formation. In addition, they suggested that this dissociation reaction dynamics were initiated by electron donation from the nascent surface and promoted by mechanical force during dynamic friction [110].

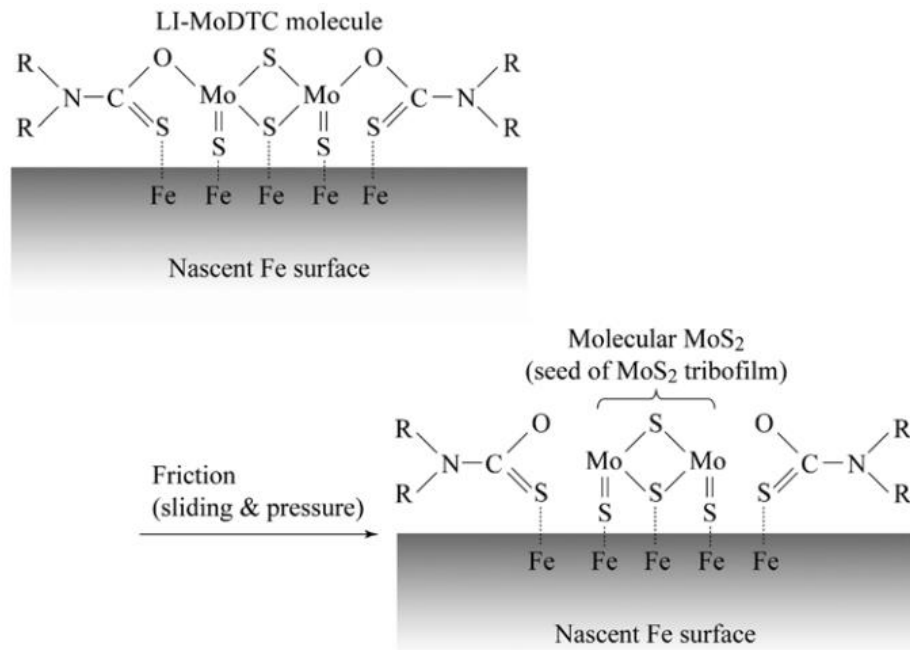


Figure 3-13 MoS₂ formation from LI-MoDTC molecule adsorbed on nascent Fe surface [110].

During rubbing of the two surfaces over each other in tribological contacts, metal layer will be exposed after mechanical removal of the iron oxide which will form a nascent iron surface. Morina *et al.* [35] suggested that, the MoDTC-derived thiuram disulphide further decomposes and reacts with the

nascent iron surface leading to formation of iron sulphide. According to the HSAB principle, S^{2-} are soft base and Fe atoms are hard acids resulting in reaction of iron and sulphide which in turn forms FeS_x , leaving the N part to deposit on the surface. Iron sulphide could reduce wear by acting as a protective layer and by that enhance the formation of a friction-reducing layer of MoS_2 from the other radical.

Moly Trimer is a term referred to one type of MoDTC with trinuclear structure and composed of three Mo atoms around a central core, as shown in Figure 3-14. In the molecular structure of Moly Trimer, unlike Moly Dimer (see Figure 3-10), no oxygen atom is present in the trinuclear core. Oxygen in the Moly Dimer contributes significantly to the formation of MoO_3 which is detrimental to both wear and friction performance.

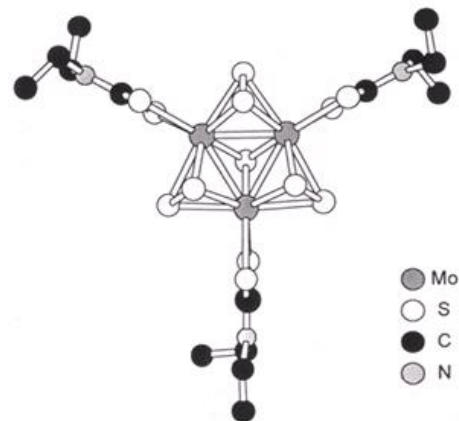


Figure 3-14 Molecular structure of Trinuclear MoDTC (Moly Trimer) [111]

The mechanisms by which Moly Trimer is decomposed thermally is shown in Figure 3-15 [111]. The trinuclear additive molecular structure is composed of three Mo atoms that are linked by three disulfide ligands. The remaining coordination sphere of each Mo atom is filled with a dithiocarbamate ligand. The oxidation state of Mo in Moly Dimer is +5 and requires a reduction to

oxidation state of +4 before it can form low-friction MoS_2 . In addition, the presence of oxygen in the Moly Dimer structure is detrimental to the friction performance as it leads to the formation of molybdenum oxide. In contrast, the oxidation state of Moly Trimer is +4 and it can readily react to form MoS_2 which in turn can facilitate friction reduction. Besides, the molecular structure of the trinuclear core resembles the hexagonal units found in lamellar MoS_2 . Therefore, for the formation of MoS_2 , the loss of the apical sulphur atom and dithiocarbamate is required which is then followed by the aggregation of MoS_2 . Although, the thermal decomposition of Moly Trimer to form MoS_2 has been verified, the tribochemical contribution has not been explored [111].

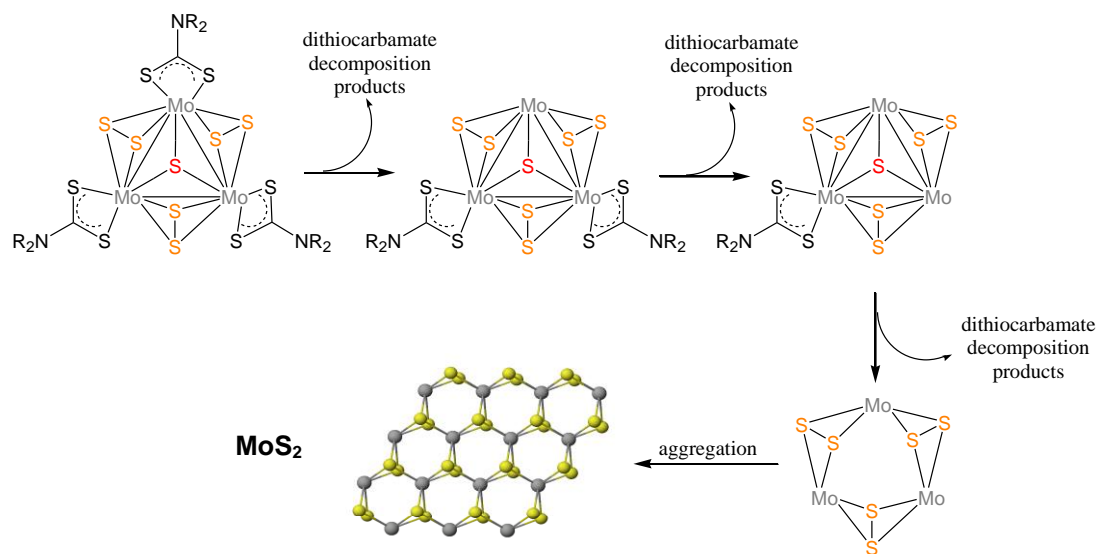


Figure 3-15 Mechanism of thermal MoS_2 formation from Moly Trimer [111]

3.2.6. Tribological Performance of MoDTC

MoDTC was shown to provide a very low friction values of around 0.05 in the mixed to boundary lubrication [100, 112]. However, the effectiveness of MoDTC in giving low friction depends on different factors such as, MoDTC concentration, MoDTC type, operating load, operating temperature, type of contact, roughness, etc [100].

The friction traces given by MoDTC-containing oil shows two distinct regions. The initial region is called the induction phase which is followed by the reduced steady state friction. Yamamoto and Gando [97] claimed that

the concentration of MoDTC in the solution only affects the first region of the friction response and the final friction value was independent of the MoDTC concentration used. In contrast, Sorab *et al.* [113] showed that the level of MoDTC in the oil must be more than 500 ppm for an efficient friction reduction. In another work, in order to have a reduction in friction, the level of MoDTC was suggested to be at least 180 ppm but was found to be temperature sensitive [101]. Nevertheless, these results suggest the important role of concentration and the operating temperature on the effectiveness of MoDTC.

It was also found that combination of high additive concentration with high temperature provided the most effective friction reduction by MoDTC [100]. Increasing the temperature resulted in a lower induction time; whereas, this reduction failed to continue and the friction increased [101]. In contrast, Yamamoto *et al.* [114] showed that increasing temperature above 100°C, resulted in higher induction time but that the steady state friction values were lower than tests with lower temperatures. They realized that the optimum temperature for the best performance of MoDTC was achieved with 80°C.

Graham *et al.* [100] showed that the type of contact is also important in effectiveness of MoDTC in reducing the friction. They reported that MoDTC is only effective in boundary lubrication where direct solid-solid contacts occur. They observed that in the sliding/rolling contact MoS₂ formation is hindered by the micro-elastohydrodynamic lubrication which exists at such contacts.

3.2.7. Additive-Additive Interactions

Interactions of two or more additives may lead to either synergistic or antagonistic effects on the tribological performance of component in contact. It was reported by Rounds [115] that ZDDP in combination with metallic dithiocarbamate oxidation inhibitors, primary alkyl amine friction modifiers, sulphur and chlorine containing EP agents showed a detrimental effect on the wear performance; whereas, addition of detergents, dispersants, oxidation inhibitors, VI improvers and EP agents to ZDDP showed little or no effect on the wear performance. The literature on the interactions of

additives and the related tribological performance will be reviewed in this section.

3.2.7.1. ZDDP Interactions with MoDTC

In general, the performance of engine oil additives, such as; ZDDP may be influenced when used in conjunction with other additives. This effect could be synergistic or antagonistic and therefore a great deal of research has carried out to study the possible effects [116] from which a considerable amount was focused on the ZDDP interaction with MoDTC.

In the literature several reports showed that MoDTC in combination with ZDDP was more effective in friction reduction [117-119]. Muraki *et al.* [119] showed that under rolling-sliding conditions, combination of ZDDP with MoDTC resulted in both lower friction and better wear performance suggesting a synergistic effect of ZDDP on frictional behaviour of MoDTC. However, mechanism by which ZDDP could promote MoS₂ formation was not provided. ZDDP tribofilm formation was shown to be responsible for more effective friction reduction by MoDTC. It was shown that friction started to drop as soon as the ZDDP tribofilm was formed [120].

Martin *et al.* [121] reported a synergistic effect on both friction and wear when ZDDP was used together with MoDTC compared to individual ZDDP or MoDTC. They suggested that the wear is reduced due to the reaction of MoO₃ and possible iron oxides with zinc polyphosphate leading to their elimination. This would also preserve the pure MoS₂ from oxidation which in turn could improve the friction performance. In contrast, Morina *et al.* [35] found that ZDDP showed an improved wear performance than ZDDP/MoDTC. On the other hand, Kasrai *et al.* [117] showed that almost the same wear was given by ZDDP and ZDDP/MoDTC whereas the friction was reduced for ZDDP/MoDTC compared to MoDTC or ZDDP alone.

Sogawa *et al.* [122] studied the contribution of MoDTC and ZDDP in providing sulphur for MoS₂ formation in a ZDDP/MoDTC-containing solution. They realized that about 40% of the required sulphur for MoS₂ formation is

derived from ZDDP which clearly shows the interaction between ZDDP and MoDTC to form MoS₂.

MoDTC has been shown to have a detrimental effect on the structure of ZDDP tribofilm. It was shown that a thick patchy pad-like tribofilm which was formed by ZDDP alone became much thinner and the patchy structure was vanished [123]. In another work, MoDTC/ZDDP tribofilm was found to be rougher than ZDDP alone which could elucidate any relation between lower observed friction and the transformation to elastohydrodynamic lubrication [92].

3.2.7.2. ZDDP Interaction with Detergents and Dispersants

Detergents and dispersants are key additives in oil formulation as they will keep the insoluble products in suspension which would later be removed by filters. Detergents have also been shown to offer anti-wear properties by forming carbonates in the wear scar [115, 124, 125]. Metallic detergents were seen to have an antagonistic effect on the wear performance of ZDDP [124, 126, 127].

ZDDP effectiveness was deteriorated due to the interaction with overbased metallic detergents. This behaviour was attributed to the competition between these two additives for surface sites. It was shown that Ca²⁺ ions took over the Zn²⁺ in the polyphosphate structure of tribofilms, leading to the formation of short chain polyphosphate [124]. This was in agreement with a previous work by Willermet *et al.* [125] who showed the formation of ortho- and pyro-phosphates with lower molecular weight than phosphates when Zn partially replaced with Ca.

In agreement with other works, Kasrai *et al.* [127, 128] reported ineffectiveness of ZDDP in combination with detergents. They investigated the effect of overbased calcium sulphonates in formation of sulphur and phosphorous species. Surface analysis of the tribofilms showed that the presence of detergent along with ZDDP resulted in the formation of calcium phosphate instead of long chain polyphosphates. The higher wear given was

thought to be related to the higher hardness of calcium phosphate formed from detergent in the solution compared to the wear given ZDDP only.

Yin *et al.* [72] showed that calcium phenate detergents have an adverse effect on the ZDDP film formation even at low temperatures whereas calcium sulphates interaction with the absorbed ZDDP occurred only at high detergent concentrations.

Rounds [115] reported that succinimide dispersants increased wear when added to ZDDP solutions in 4-ball wear tests. Similarly, Shiomi *et al.* reported the same effect when used in valve train tests [129]. However, this adverse effect was diminished by borating the succinimide. Formation of a borate component in the anti-wear film was responsible for this improvement [130]. The antagonistic effect of dispersants on wear reduction was attributed to the reduction in the amount of ZDDP available for film formation by forming a complex. The degree of their impact on wear, however, depends on the strength of the complexes formed with various dispersants and with amines [125]. However, no evidence was found for such behaviour by adsorption studies [131]. Borated dispersants, for instance, could contribute to this behaviour by formation of a borate component in the anti-wear film [130]. Succinimide together with other additives increases the decomposition temperature of ZDDP. This will promote scuffing wear at lower oil temperatures when using a succinimide and other additives with ZDDP [130].

Smith *et al.* [132] showed that with a simple ZDDP mineral oil solution, the film is mainly composed of phosphate which is bonded to the ferrous substrate. When both detergent and dispersant are used in the ZDDP solution, the film thickness was increased but in a more patchy shape which has no clear underlying sulphide layer. This was attributed to the competition for surface sites between the wider range of surface-active additives present in the formulation. Dispersant only formed a thin layer of nitrogen-containing material on the outer surface [132] and did not mainly contribute in the film structure. The schematic structure for the film formed with ZDDP-containing lubricant and ZDDP/detergents/dispersant solution is shown in Figure 3-16.

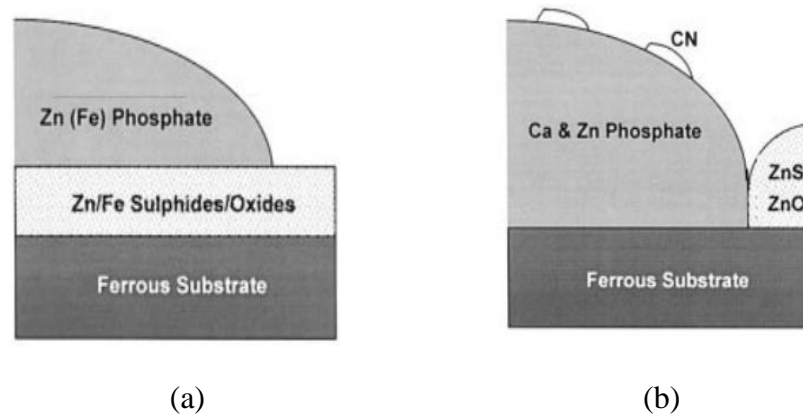


Figure 3-16 Schematic structures for films generated by (a) ZDDP and (b) ZDDP+ Detergents+ Dispersant [132].

It was also found that the mechanical properties of the tribofilm formed from ZDDP varied with the addition of the detergent to the oil formulation. The indentation modulus was measured to be lower for the film formed from ZDDP/detergent compared to ZDDP tribofilm. Contribution of CaCO_3 in the tribofilm was thought to be the main reason for such measured values [91].

3.2.7.3. Additive Interactions in Fully Formulated Oils

Engine oil formulations contain different types of additives including anti-wear, extreme pressure, antioxidants, dispersant, detergents, corrosion inhibitors, etc. The physical and/or chemical properties of the base oil, or the (ferrous) surface might be affected by individual additives present in the lubricant formulation. However, the mechanisms by which each additive contributes to the overall performance of the surface/lubricant is complex and, thus studies on the tribofilms formed from fully formulated oils are limited.

Using a fully formulated oil (FF) which is commercially available, wear of 52100 steel was reported to increase substantially compared to ZDDP alone. Figure 3-17 shows the time dependent wear scar widths (WSWs) for the films formed from FF oils compared to ZDDP alone. Using X-ray Absorption Near Edge Structure (XANES), it was shown that tribofilm formed

from the fully formulated oil was rich in medium chain Ca phosphate. It was concluded that ZDDP does not play its role fully as an anti-wear agent (by forming Zn-phosphate) in FF oils, and only initiate the film formation. After the initial film formation, ZnS and Ca phosphate film grow. ZDDP-derived tribofilm was found to be mainly consisted of ZnS (78%) whereas the remaining 22% Zn was identified as Zn Phosphate. In addition, MoS₂ formation was also evidenced in the tribofilm whereas no Mo-oxide was present in the film [133].

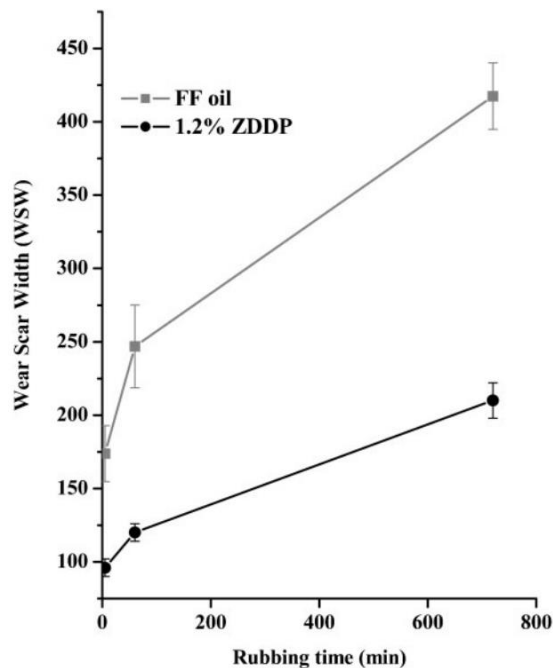


Figure 3-17 Wear scar width as function of rubbing time [133].

3.3. Valve Train System

Increased power for internal combustion engines by means of the enhancement in engine breathing has been realized since 100 years ago [134]. Valve train system is one of the most important components in an internal combustion engine which is responsible for introducing air into the combustion chamber and for exhausting the burnt gases. The lubrication of cam and follower in a valve train system has been always a challenge for manufacturers and a great deal of research has been carried out to investigate the engineering background to this issue [135, 136].

Although, it has been demonstrated that elastohydrodynamic lubrication plays a role in valve train, the modern cam and follower is traditionally operating under boundary lubrication regime where chemical reactions between the lubricant and the surfaces dominate the tribological performance of the component by forming thin films on the surfaces in contact [134]. The severe operating conditions (i.e. high temperature and high pressure) which exist in boundary lubrication regime imply that cam and follower experience high wear. Polishing, scuffing and pitting were suggested to be the main modes of failure in cam and follower [9, 134]. The mode of failure depends significantly on the combination of materials in contact, lubricant additive package, design and operating condition under which valve train system operates.

Different types of cast iron such as grey [137], nodular, chilled and hardened [138] have been used to make camshafts. Although steel and composite materials have been recently used as an alternative to cast iron, cast iron remains the cheaper option and is still being used for large volume production of camshafts [139].

Offering outstanding anti-wear properties, ferrous powder sintered metal with high chromium, high chromium cast iron or silicon nitride ceramics are conventionally used as follower materials also called shims [140]. Recently, steel or light weight forged aluminium have been used as shim materials as the use of ceramics has not been economically feasible [141]. Around 40% reduction of friction torque has been reported when steel tappets were replaced with aluminium ones along with an aluminium retainer [142]. The limiting factor, however, was the requirement of coating on the side wall of the aluminium tappet to prevent galling effect.

Different surface treatments are conducted to improve the running-in and prevent early stage failures. One of the treatments of the cam surfaces is deposition of different coatings such as phosphate coatings, oxide coatings, carbon bearing epsilon FeN layers, etc. This would enhance the wettability of the surface, and thus offers improved running-in performance [143]. Chemical conversion method such as phosphating, oxidizing, sulfidizing, tufftriding, etc. are among surface modification techniques which are

traditionally being used to improve running-in properties of metallic shims. [135, 138]. In addition, depending on the type of materials used, several other surface modification methods including induction hardening or flame hardening of cast iron, carburizing of low carbon steel, induction hardening of medium carbon steel, electroplating and depositing PVD or CVD coated hard coatings etc., are applied on cam and shim surfaces [144].

Of particular interest is the application of Diamond-Like Carbon (DLC) coatings of different types in engine valve train as it offers excellent running-in, low friction and anti-wear properties [145-148]. In several attempts, shims in gasoline engines have been coated with DLC coatings [145-148]. In addition, other parts of valve train reported to be coated by DLC are camshaft, valve stem and rocker arm [146].

Slight improvements in friction torque was reported by Gangopadhyay *et al.* [147] when production shim was replaced with a 10 at.% Si doped hydrogenated DLC coated shim. This improvement was only seen when the lubricant was free of friction modifier. Friction modifier containing lubricants did not show any improvement in friction comparing production shims with those of DLC coated. Yasuda *et al.* [145], using fully formulated oils, reported a significant 45% reduction of friction reduction when they coated steel shims with ion-plated PVD-DLC compared to conventional phosphate coated shim. However, no substantial difference in friction was observed using tungsten doped DLC and undoped hydrogenated DLC compared to conventional steel shims [146]. In fact, pitting wear and spallation of DLC coatings was evident after the test.

Nissan has claimed that they managed to reduce friction by approximately 40% between engine parts by combination of a hydrogen-free DLC and an optimized lubricant. They correlated the friction reduction to formation of ultra-low friction film of nanometer scale on top of the hydrogen-free DLC coating. Nissan stated that applying this technology would lead to 25% reduction in overall engine friction [149].

Nevertheless, the performance of DLC coatings is greatly influenced by the type of DLC coatings as well as selection of lubricant additives which will be reviewed extensively in the following sections. The focus of this study is to investigate the lubricant/surface interaction at cam/follower contact, and so, the material selection and operating condition was chosen to replicate the tribological situation which is experienced in a valve train of an internal combustion engine (see Chapter 4).

3.4. Diamond-Like Carbon (DLC) Coatings

The hardest known material is diamond which has unique mechanical properties such as high elastic limit and yield stress, high thermal conductivity, chemical inertness, excellent electrical insulation characteristics, high dielectric constant, low coefficient of thermal expansion and the lowest compressibility of any material [150]. Diamond can also be doped with different doping elements to become semiconductor. It is also very transparent to the light from visible to the infrared part of the spectrum [151]. Moreover, diamond demonstrates a good tribological properties when polished [152]. The properties and high density of diamond implies that it is formed and crystallized under high pressure which in nature can happen at about 150 kilometres in depth within the earth. The very first synthetic diamond was made in 1950s using high pressure and high temperature techniques. Later in 1980s, CVD deposition technique was employed to make diamond in lower pressures in the form of polycrystalline coating [151, 153].

Diamond-like carbon is a carbon coating which has similar mechanical, optical, electrical and chemical properties to diamond but do not have a crystalline lattice structure, rather is an amorphous carbon coating having a network of sp^2 (graphite-like) and sp^3 (diamond-like) and hydrogen bonds. Diamond like carbon is a term referred to a wide range of carbon base materials with interesting properties, like low coefficient of friction, high wear resistance, high hardness, chemical inertness, a relatively high optical gap and high electrical resistance. Its properties are dependent on the ratio of sp^2/ sp^3 bonds. DLC may contain as high as 50 % hydrogen (a-C:H) and as low as 1-2 % hydrogen (a-C). Several doping elements such as metals,

nano-particles, etc. are incorporated to reduce the internal stress as well as enhancing the adhesion strength of the coatings [154, 155].

3.4.1. Application of DLC Coatings

Excellent physical, mechanical and tribological properties of DLC films make them a good candidate for variety of applications. In industrial applications, DLC coatings can be classified in two main categories, namely undoped single layer DLC and doped DLC films. The former is applied when the contact pressure is comparatively low as well as the shear stresses and/or heat generation is not significant. Knives used in textile industry to cut many layers of synthetic fibres, are good examples of the application of unoped single layer DLC film. On the other hand, for high shear stress application, DLC coatings with interfacial bonding layers and alloyed and layered coating structures are typically used. Ball bearing cages and cages, journal bearings, gears from aircraft landing-flap controls, compressor screws and extrusion dies in cutting tools for aluminium are examples of such DLC coatings (doped) applications [156]. Furthermore, some of the moving components in the engine, such as diesel engine injection system, were coated with DLC and the wear rates have been shown to be decreased successfully [157]. Recently, DLC coatings are widely used in more than thirty components in an automotive engine [158]. In addition, DLC coatings have a role to play in medical applications such as orthopaedic pins and screws and for bearing surfaces of artificial joints. They are also applied as anti-reflection coatings on germanium and silicon optics and solar cells or as the protective coatings on zinc sulphide IR windows. DLC coatings improve the scratching resistance of the metal components [159]. DLC coatings have a wide application as a protection of the hard disk drives and other magnetic recording media [160]. Providing low friction and wear, DLC coatings are able to reduce the dependency on lubricant friction modifiers and anti-wear additives which contain sulphur and phosphorous and are harmful to catalytic converters.

3.4.2. Structure of DLC Coatings

Carbon is made up of three different types of bonding configuration, namely sp^3 , sp^2 and sp (Figure 3-18). In diamond, four sp^3 hybridized orbitals forms four equal C-C bonds with adjacent atoms which is responsible for the

tetrahedral structure of the diamond. Superior properties of diamond, like high hardness and high thermal conductivity, originate from these strong covalent bonded atoms in the tetrahedral structure. In graphite, three trigonally sp^2 hybrid orbitals lie in a plane in which each carbon is bonded to three other carbon atoms with strong covalent bonds. The layers of carbon atoms are then attached to each other by weak Van der Waals forces which accounts for the layered structure of graphite which in turn is responsible for the low friction behaviour of graphite [150, 161, 162]. DLC films have a mixed structure of sp^3/sp^2 and the proportions of sp^3/sp^2 are dependent on the deposition technique and deposition parameters used. Depending on the deposition technique used, DLC films can be formed on the substrate at rather low temperatures, in the range of below 200°C [163] to 325°C [164], and overheating the substrate would have a detrimental effect on the film properties. Furthermore, the substrate material does not play an important role on the film growth and the film properties [150, 165].

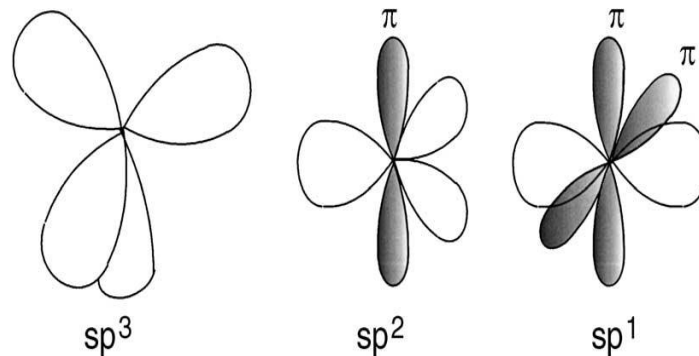


Figure 3-18 sp^3 , sp^2 and sp hybridised bonding [155].

In terms of hydrogen content, DLC coatings can be divided into two different categories namely hydrogenated amorphous carbon, a-C:H, coatings and hydrogen-free carbon, a-C, coatings. The hydrogen content of the film in a-C:H can vary significantly depending on the deposition method, hydrocarbon source and deposition parameters. The role of hydrogen in a hydrogenated DLC film is mainly to gain a wide optical gap and high electrical resistivity. In addition hydrogen can help to stabilize the diamond structure by maintaining the sp^3 hybridization configuration [164]. It should be mentioned that too

much hydrogen content would cause the molecular interconnection not to be formed and the higher the hydrogen content the lower the hardness.

In Figure 3-19, the relation between density and sp^3 content for ta-C, ta-C:H and a-C:H which is proposed by Ferrari *et al.* [166] is given. They suggested that in ta-C, properties, such as Young's modulus, hardness, density and smoothness correlate directly with the C-C sp^3 fraction. In a-C films, hydrogen is considered as an impurity. Tetrahedral amorphous carbon, ta-C, is a highly sp^3 bonded which is also referred to as amorphous diamond because of its tetrahedral structure that is similar to diamond [150].

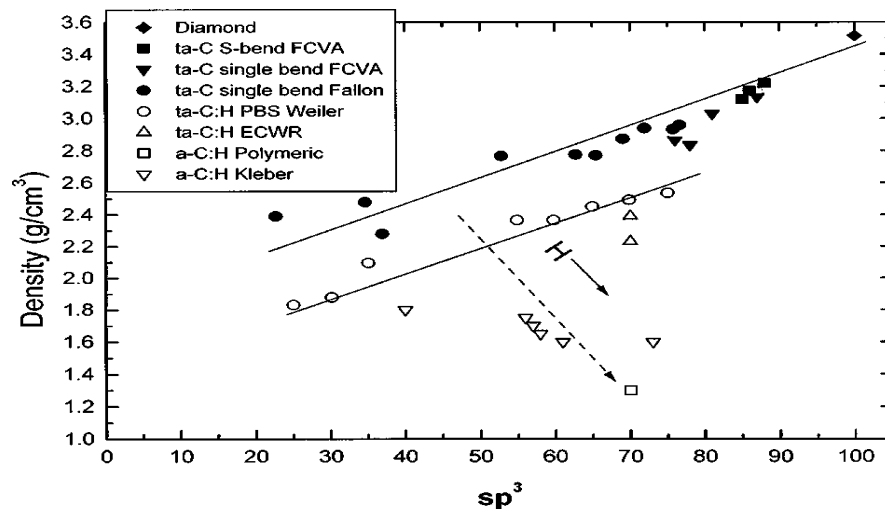


Figure 3-19 Density vs sp^3 fraction for DLC film. The trends are different when comparing ta-C and ta-C:H with a-C:H [166].

Various forms of DLCs are shown by the phase ternary diagram as in Figure 3-20. This diagram was proposed by Ferrari and Robertson [167], who have contributed significantly in understanding the chemical and structural properties of DLC films using different spectroscopic techniques. Most of the a-C:H coatings remain in the middle of the diagram showing a varying ratio of sp^3/sp^2 bonding and hydrogen content while a-C coatings are placed at the left side and depending on the ratio of sp^3/sp^2 the mechanical properties of the coatings would be different. The sp^2 bonded graphitic carbon lies in the lower left-hand corner. The ta-C coatings lie on the left side of the diagram depending on the ratio of sp^3/sp^2 . Phases that have high

content of hydrogen are not able to form an interconnected molecular structure, rather form gas or liquid molecules and lie at the lower right-hand corner of the diagram [168].

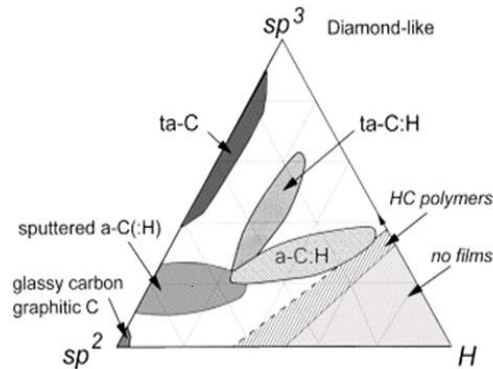


Figure 3-20 Ternary phase diagram of amorphous carbon coatings [155].

The hardness and density variation of DLC films with respect to their sp^2 , sp^3 and H content have been summarised in Table 3-2 and are compared with those of diamond and graphite.

Table 3-2 Properties of various forms of carbons [150, 155].

	Density (gcm^{-3})	Hardness (GPa)	at.% sp^3	at.% H
Diamond	3.2	100	100	0
Graphite	2.3	-	0	0
a-C	1.9-2.4	11-15	2-5	1-2
a-C:H, hard	1.6-2.2	10-25	30-60	10-40
a-C:H, soft	0.9-1.6	<5	50-80	40-65
ta-C	3.0	55-65	65-85	<1

DLC films can offer the broadest range of hardness and friction values, whereas some of the recently developed nanocomposite coatings are capable of providing super hardness but lack lubricity or low friction [169, 170]. Figure 3-21 shows classification of different coatings with regards to their hardness and friction performance implying the fact that most carbon coatings and in particular, DLC coatings can provide not only low friction but also high hardness.

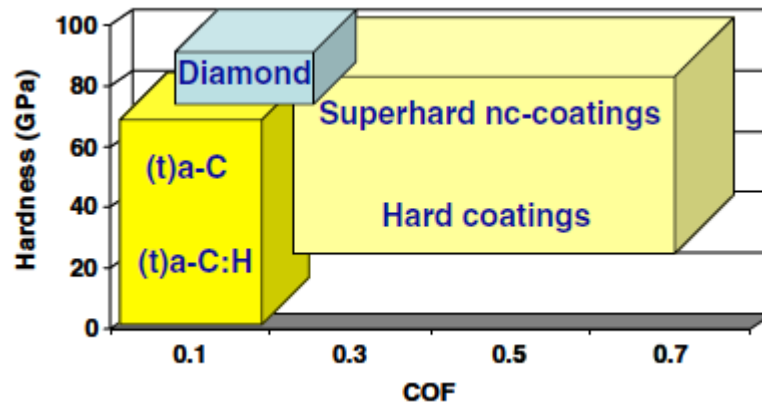


Figure 3-21 Schematic representation of hardness and coefficients of friction (COF) of carbon-based and other hard coatings in dry sliding condition [170].

3.4.3. Deposition of DLC Coatings

DLC coatings are formed when ionized and decomposed hydrocarbon or carbon species hit the surface with energies ranging from several tens of eV to 200 eV [150, 171]. All deposition methods are considered to be non-equilibrium processes as described by the interaction of energetic ions with the surface of the growing films. Deposition pressure, bias voltage, etc. may be different depending on the deposition method which is being used to make DLC coatings [155]. DLC coatings can be deposited on the substrate at temperature in the range of 200°C [163] to 325°C [164]. This property makes deposition of DLC coatings possible on most engineering materials including polymers [150]. However, the chemical nature of these substrate could play a great role in formation of a strong bonding and adhesion of the DLC film to the substrate. In most tribological applications where the surface is under high normal and/or shear forces, poor adhesion of DLC film to the substrate, may result in permanent fracture and delamination of the DLC coating from the substrate [170, 172].

Carbide- and silicide-forming substrates (such as Si, Ti, W and Cr) can promote a strong interfacial bonding to the substrate which is not the case for other metallic and ceramic substrates. However, deposition of an initial bond layer on these substrate prior to DLC deposition could enhance the adhesion of the DLC film to the substrate. These interlayers, which are

chosen from strong carbide- and silicide-formers, make a chemical reaction with the substrate and provide a strong bonding. The deposition of these interlayers are typically done in the same chamber prior to the actual DLC deposition [170].

As mentioned in the previous chapter, deposition methods can be classified into two major categories, namely, chemical vapour deposition (CVD) techniques and physical vapour deposition (PVD) techniques. CVD techniques, like DC plasma and radio frequency (RF) plasma assisted chemical vapour deposition, and PVD techniques, such as sputter deposition, ion-plating techniques and ion beam techniques can be applied to make hydrogenated DLC films. Molecular Dynamics (MD) simulation of the atomic structure of a hydrogenated DLC is shown in Figure 3-22 [170].

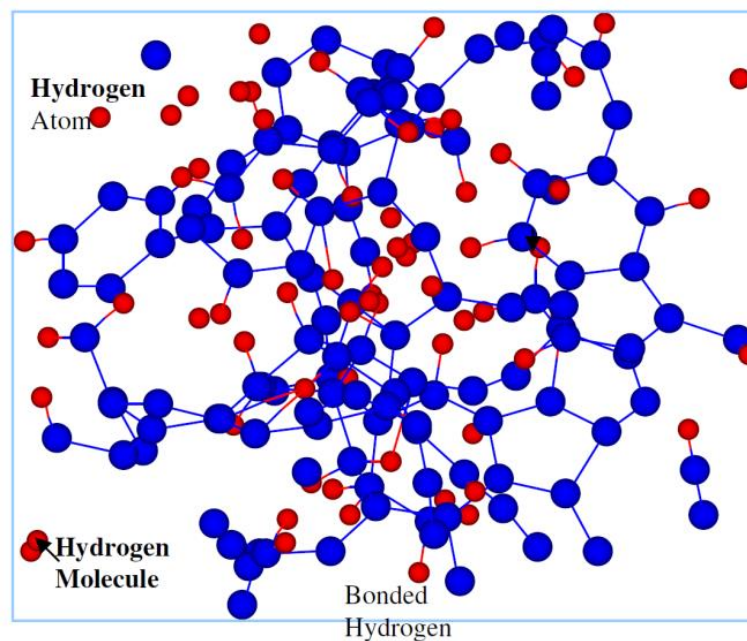


Figure 3-22 Molecular dynamic simulation of the atomic structure of a hydrogenated DLC [170].

PVD techniques such as magnetron sputtering, mass selected ion beam (MSIB), cathodic arc and laser plasma deposition are typically employed to form hydrogen-free a-C and ta-C coatings [150, 173-175].

3.4.4. DLC Performance in Dry Sliding

Formation of a transfer layer has been observed frequently in tribological testing of DLC coatings and initially has been reported by authors [176-178]. This carbonous transfer layer was seen to be formed on the sliding surfaces and reduce the friction drastically [177] whereas in another study the generation of the transfer of hydrocarbons with a specific orientation to the ball surface was reported to be responsible for friction reduction [178]. Increasing the sliding distance (from 20-25 km) has been seen to improve the formation of transfer layer, in ambient air, resulting in lower friction values (from 0.16 to 0.05-0.07) [179, 180]. In addition, as shown in Figure 3-23, the sliding speed has a positive effect on the transfer film formation, where the high load and high sliding speed provided the largest and most compact transfer layer on the steel counterparts. Furthermore, the thick transfer layer was also seen to decrease wear rate of the hydrogenated DLC coating and the steel pin counterpart [181]. Although formation of transfer layer is typically reported in the tests conducted in ambient air, it was also seen in experiments carried out in Ultra High Vacuum (UHV) when DLC was rubbing against steel [182].

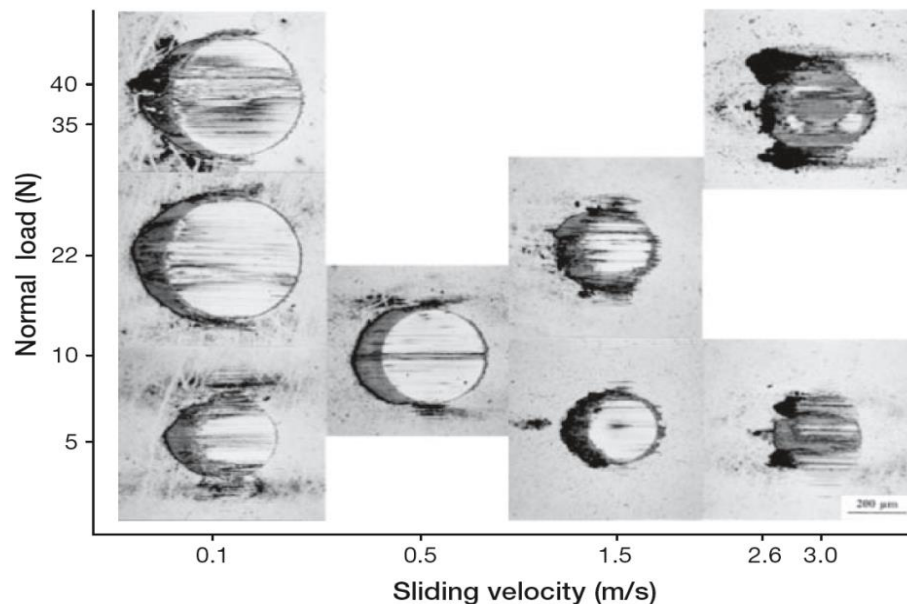


Figure 3-23 The wear surfaces of the steel pins slid against the PACVD deposited hydrogenated a-C:H film. The tests were carried out unlubricated in room air at 22 ± 2 °C temperature and with 50 ± 5 % relative humidity. The sliding speed was varied in the range 0.1–3.0 ms^{-1} and the normal load in the range 5–40 N [181].

3.4.5. The Graphitization of Hydrogenated DLC

At high temperatures, hydrogen in the a-C:15H coating starts to diffuse out of the coating matrix, giving rise to collapse of the tetrahedral sp^3 structure to a graphite-like sp^2 structure, often referred to as “graphitization” [183]. The graphitization of DLC is strongly dependent on the thermal and/or straining effects, as was widely reported by researchers [184-186]. The graphitization process has reported to start at temperature between 200°C to 300°C but is more pronounced at temperature above 300°C or 400°C and the transformation process completes at a high temperature of 700°C or more [187]. However, the hydrogenated DLC has reported to have a lower transition temperature due to having higher strain [170, 183, 188, 189].

The graphitization of DLC plays an important role in friction reduction under dry sliding conditions [185, 190, 191]. Under tribological conditions, usually, the softer of the two materials will be worn while this is not the case for DLC. Wear products from DLC, which can have a graphite nature [192], can be transferred to the counter body forming a so-called transfer layer on the softer surface. The softer surface will then be protected from being worn off while the DLC slides over the transfer layer. The wear rate of DLC will also be extremely low after the transfer layer is formed. In addition the transfer layer also behaves as a solid lubricant [185, 193]. The formation and adhesion properties of this transfer layer depend strongly on the tribological and environmental conditions as well as the chemical properties of the counterpart [194].

The detection of graphitization has been carried out using different surface analysis techniques. Among which, Raman spectroscopy (Figure 3-24) has been widely used by different authors to characterize carbonous transfer layer or the debris particles at the sliding interfaces to find any sign of carbon with disordered graphitic structure [186, 195, 196].

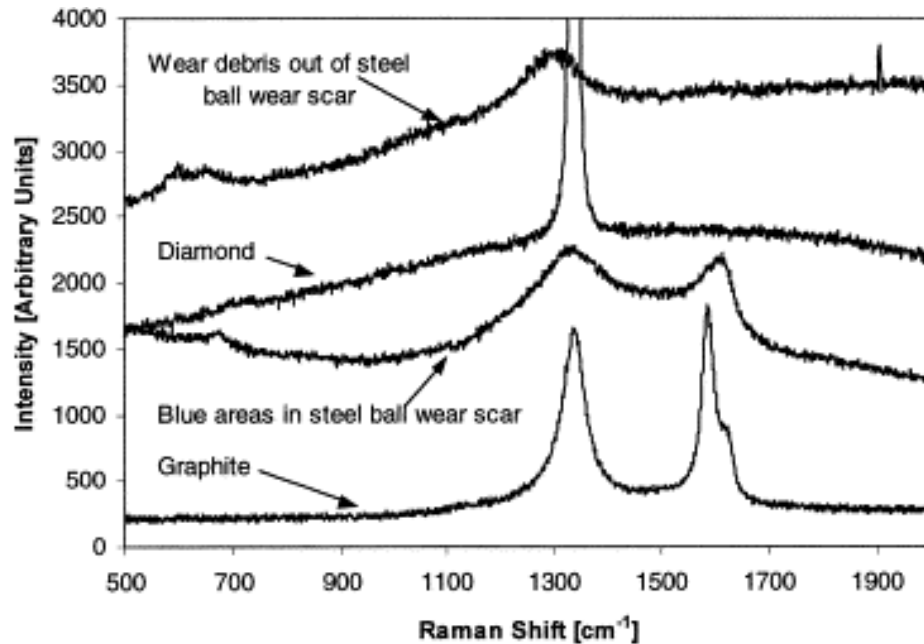


Figure 3-24 The micro-Raman signal of the steel ball wear surface and wear debris after sliding against a-C:H film for 5000 m in humid air ($50\pm 5\%$ relative humidity). The sliding velocity was 2.6 m s^{-1} and the normal load 35 N. The diamond and graphite signals are used as reference.

In addition to Raman analysis, the electron diffraction pattern analysis, Fourier Transform Infrared Spectroscopy (FTIR) and bright field-dark-field imaging has also been used to investigate the graphitization of hydrogenated DLC coatings [186, 194, 197, 198]. Using nanoindentation analysis, the transfer layer with graphitic nature has been found to have lower Young's modulus (E) and hardness (H) compared to bare coating [199].

3.4.6. Chemical Reactivity of DLC

DLC coatings have the potential to be tailored for desirable properties such as low friction, high wear resistance and anti-sticking properties, to be best suited for different engineering applications under dry and lubricated conditions [200]. In particular, lubrication of DLC has attracted interest in automotive industry for their more general and wider range of applications in mechanical components. However, the properties of DLC under lubricated condition is totally different from those which were extensively studied under dry or different gas atmosphere [184, 201, 202]. Their well-known low friction and anti-sticking properties are attributable to their inertness and low surface

energy in non-lubricated conditions whereas one of the requirements for an efficient boundary lubrication regime is the chemical reactivity of the surface with lubricant additives. In addition, low friction values observed for DLC in dry conditions were not usually seen in lubricated condition. Therefore, improvements of DLC boundary lubrication is required by means of using different additives and optimising the additives/coatings which in turn requires the reactivity of DLC.

The improvement of the tribological behaviour of DLC has been reported by using additive-containing oils in DLC/steel systems. Tribochemical reaction between the DLC and steel counterpart has been reported but the tribofilm was only found on the steel counterpart rather than the actual DLC coating [203]. It is reasonable to expect that the presence of steel in the DLC/steel system can promote DLC/lubricant interaction. This could be mainly due to the interaction between the steel counterpart and the lubricant additives in conventional manner; thus, they would react with oils and additives, which are originally designed to form tribofilms on metal surfaces. Moreover, these reaction products can in turn transfer to the DLC coating or/and interact with DLC surfaces and affect the tribochemical and tribological interactions at the interface [204].

Furthermore, self-mated DLC/DLC contacts were observed to be inactive in comparison to DLC/steel [200]. In contrast, in many other studies, additives were found to significantly affect the tribological performance of self-mated DLC/DLC contacts [204-209] which clearly suggest the interaction between DLC and the additives and elucidate the interference of the steel from the system. In general, the tribological performance, especially wear, of the DLC was improved in the presence of lubricant additives [204-209]. However, direct evidence of such interaction was not provided for different reasons [209]. For doped-DLC coatings, the improved tribological behaviour was correlated to the presence of doping elements in DLC matrix which could replicate “metal-like” behaviour [204, 209] and simulate well-understood conventional additives reaction mechanisms [210]. In addition, in some recent studies, direct reaction between DLC coatings and additives were evidenced [211-214] and elucidate any doubt about the DLC/additive interactions.

3.5. DLC/lubricant Interactions

As mentioned earlier, conventional lubricant additives are designed to work on ferrous surfaces. However, many engine DLC coated components are lubricated by conventional additive-containing lubricants. Different researchers have started to evaluate interactions between lubricant additives with various types of non-ferrous DLC coatings under boundary lubrication.

In this section a review of the current understanding of the DLC/lubricant interactions and the important factors which could affect this interaction is provided.

3.5.1. Tribochemical Interactions

The tribochemistry of DLC is complex and has been a matter of interest to different research activities in recent years. The sliding contact surfaces of DLCs are chemically very stable. Therefore, in static condition, they do not normally take part in the chemical interactions with solid materials and/or liquids when brought into direct contact [170]. However, they may interact with counterfaces and their surroundings such as water molecules, oxygen and hydrocarbons under influence of dynamic sliding contacts. DLC coatings have been reported to be chemically inert using a steel pin sliding against DLC-coated disks lubricated in oil containing MoDTC and/or ZDDP [215]. In contrast, molybdenum-based friction modifiers and ZDDP anti-wear have been shown to form low friction MoS₂ sheets and/or ZDDP-derived compounds respectively, on the DLC coating providing low friction and better wear performance under boundary lubrication conditions [4, 206, 216-220].

Extensive research has been carried out on DLC/lubricant interaction and the friction and wear mechanisms of DLC coatings. Previous works are mainly focused on tribological performance of DLC coatings using model oils containing one or combination of additives. These include anti-wear additive zinc dialkyl-dithiophosphate (ZDDP) [212, 213, 218, 221, 222], glycerol mono-oleate (GMO) [207, 212, 223] molybdenum dialkyl-dithiocarbamate (MoDTC) [41, 224], combination of ZDDP and MoDTC [206, 215] and EP additives [225-228].

In the literature, studies on the more realistic DLC/fully formulated oil systems, are limited [229-233]. An improved friction and wear performance of a-C:H coatings compared to the uncoated steel surfaces (Figure 3-25 and Figure 3-26) was reported under fully formulated oil lubrication [229, 230]. Using fully formulated oils, no additive reactions on the DLC-coating surface was detected, while on the uncoated steel counterpart, typical S and P tribofilms was formed [230]. In contrast, Vengudusamy *et al.* [229] showed that a mixture of a-C:15H- and additive-derived products were present in the tribofilm formed in a-C:15H/steel contact compared to those present in the steel/steel contact under fully formulated oil lubrication. Forsberg *et al.* [231] investigated the performance of DLC coatings with varying doping types and layer structures lubricated with two different commercially available engine oils. They performed reciprocating ball-on-flat tests (coated flat specimen rubbed against steel balls). It was revealed that silicon doped coating enhanced formation of protective tribofilms by means of activating the additives and showed the best overall wear performance. In addition, doubling the initial contact pressure resulted in approximately 20% friction reduction for all coating/lubricant combinations, while the wear rates were reduced with over 50% for some combinations.

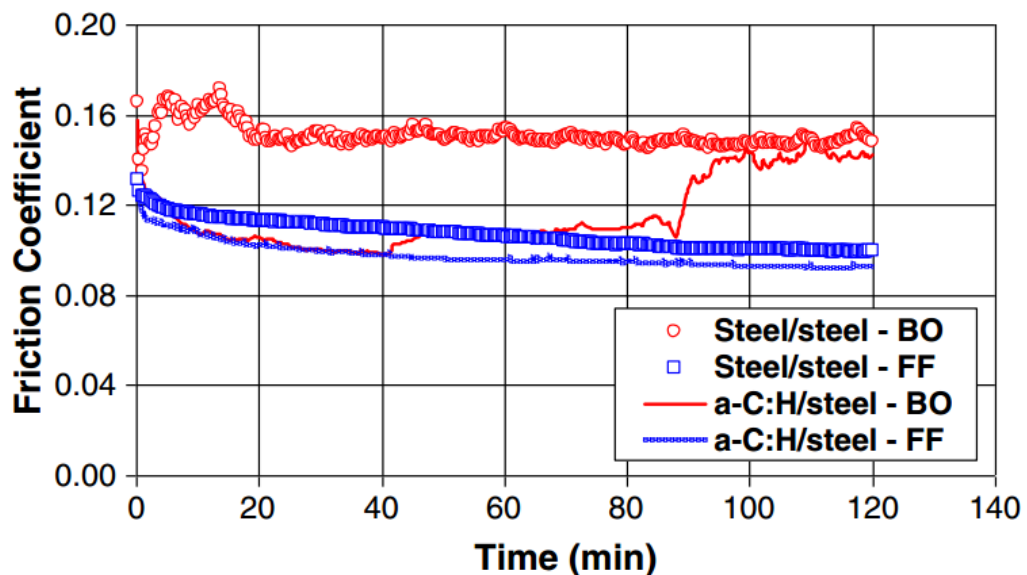


Figure 3-25 Friction coefficients for steel/steel and a-C:H/steel contacts when lubricated in base oil and fully formulated gear oil [229]

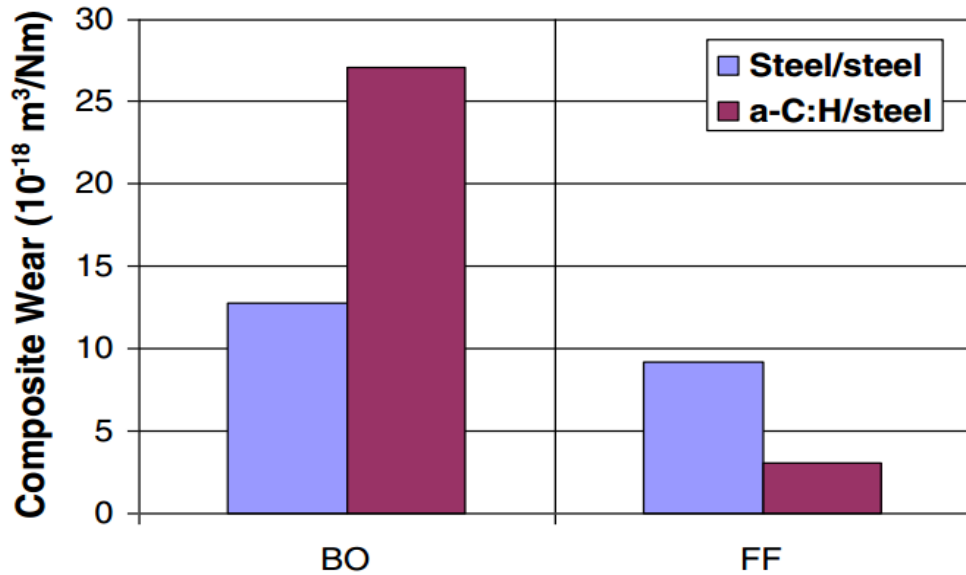


Figure 3-26 Composite wear coefficients for steel/steel and a-C:H/steel contacts when lubricated in base oil and fully formulated gear oil [229].

In the automotive components, either the DLC coating is deposited on one part and the other part remains uncoated or both parts are coated [144]. Selection of additives could affect the friction and wear response of both DLC/steel and DLC/DLC combinations.

In most of the literature, the wear data of the ferrous counterparts are given rather than the wear of DLC coatings. This could be mainly due to the short tests duration which gave insignificant wear of DLC coating whereas wear on the softer ferrous counterbodies was measurable. Ronkainen *et al.* [234] reported a lower pin wear when rubbed against a-C:15H coating in the a-C:H/steel system compared to a-C/steel combination when extreme pressure additive was used (see Table 3-4). However, the response was opposite when pure mineral base oil was used. In addition, no measurable wear was reported for a-C and a-C:15H coatings. Similar observations were reported by Barros'Bouchet *et al.* [206] and Stallard *et al.* [235]. The higher hardness of a-C coating compared to a-C:H coatings, was responsible for such higher wear given by a-C coatings to the steel counterbodies. Stallard *et al.* [235] also reported higher wear of a-C:H coating than a-C coating indicating that higher hardness of a-C coatings govern not only the wear of the counterpart but also the wear of the coating itself. Table 3-3 and

Table 3-4 summarise some of the literature on the tribological performance and DLC/lubricant interactions.

Table 3-3 Summary of the literature on frictional behaviour of DLC coatings compared to an uncoated steel system

Source	Lubricants	Test/Duration	Material/Coatings Combinations		COF
[206, 236]	PAO+ MoDTC+ ZDDP	Reciprocating cylinder-on-flat/ 1 h	a-C	Steel	~0.08
			a-C:H	a-C:H	~0.04
			a-C:H	Steel	~0.05
			Ti-C:H	Ti-C:H	~0.06
			Ti-C:H	Steel	~0.05
			Steel	Steel	~0.06
[233]	PAO	pin-on-disk/ 2 h	WC-C:H	WC-C:H	~0.078
			WC-C:H	Steel	~0.082
			Steel	Steel	~0.075
	GL-4 Fully formulated oil		WC-C:H	WC-C:H	~0.07
			WC-C:H	Steel	~0.06
			Steel	Steel	~0.08
[207]	PAO+ GMO	pin-on-disk/ 1 h	a-C	a-C	~0.03
			a-C	Steel	~0.02
			a-C:H	a-C:H	~0.12
			a-C:H	Steel	~0.09
			Steel	Steel	~0.1
[237]	PAO	HFRR High Frequency Reciprocating Rig(ball-on-disk) /1 h	a-C:H	a-C:H	~0.02
			Steel	Steel	~0.12
	PAO+ ZDDP		a-C:H	a-C:H	~0.07
			Steel	Steel	~0.08
[234]	Mineral Base oil + EP additive	Reciprocating pin-on-disk/ 21 h	Steel	Steel	~0.12
			a-C	Steel	~0.08
			a-C:H	Steel	~0.13
			a-C:H (Ti)	Steel	~0.12
[214, 220]	PAO + secondary ZDDP	pin-on-plate/ 6 h	a-C:30H	Cl	~0.10
			Steel	Cl	~0.12
	PAO + Moly Dimer		a-C:30H	Cl	~0.12
			Steel	Cl	~0.12
	PAO + Moly Dimer + secondary ZDDP		a-C:30H	Cl	~0.07
			Steel	Cl	~0.09
	PAO + Moly Trimer		a-C:30H	Cl	~0.05
			Steel	Cl	~0.07
PAO + Moly Trimer + secondary ZDDP	a-C:30H	Cl	~0.04		
	Steel	Cl	~0.07		
[223]	PAO	Pin-on-disc/1 h	ta-C	Steel	~0.09
			ta-C	ta-C	~0.025
	PAO+ GMO		ta-C	Steel	~0.025
			ta-C	ta-C	~0.025
[229]	PAO	Ball-on-disc/ 2 h	a-C:15H	Steel	~0.15
			Steel	Steel	~0.15
	GL-5, SAE 75W-85 Fully formulated oil		a-C:15H	Steel	~0.09
			Steel	Steel	~0.10

*Superlow friction coefficient

Based on the published results, the effectiveness of the lubricant in providing low friction and wear greatly depends on the type of DLC coating, type of tests, tests parameters, additive package, and type of contact. The obtained results were different and even contradictory in some cases. Some of the governing factors which could influence the tribological behaviour of the DLC coating will be discussed in more detail in the following sections.

Table 3-4 Summary of the literature on wear behaviour of DLC coatings compared to an uncoated steel system

Source	Lubricants	Test/Duration	Material Combination	Total Wear	
				Plate/Cylinder $\times 10^{-18} \text{ m}^3/\text{Nm}$	Counterbody $\times 10^{-18} \text{ m}^3/\text{Nm}$
[234]	Mineral Base oil + EP additive	Reciprocating pin-on-disk/ 21 h	a-C/Steel	No Wear	300
			a-C:H/Steel	No Wear	80
			a-C:H (Ti)/Steel	No Wear	50
			Steel/Steel	No Wear	90
[235]	Semi-synthetic oil (10W40)	pin-on-disk/ 10 h	a-C/Steel	0.03	4.3
			a-C:H/Steel	0.12	0.6
			Steel/Steel	0.35	7.4
[206]	PAO+ MoDTC+ ZDDP	Reciprocating cylinder-on-flat/ 1 h	a-C/Steel	Not Mentioned	50
			a-C:H/Steel	Not Mentioned	2
			Ti-C:H/Steel	Not Mentioned	2
			Steel/Steel	Not Mentioned	6
			a-C:H/ a-C:H	Not Mentioned	0.06
			Ti-C:H/ Ti-C:H	Not Mentioned	0.2
[214, 220]	PAO + secondary ZDDP	pin-on-plate/ 6 h	a-C:30H/Cl	Delaminated	0.442
			Steel/Cl	71.2	47
	PAO + Moly Dimer		a-C:30H/Cl	Delaminated	11.4
			Steel/Cl	6.95	18.7
	PAO + Moly Dimer + secondary ZDDP		a-C:30H/Cl	Delaminated	4.93
			Steel/Cl	78.7	50.1
	PAO + Moly Trimer		a-C:30H/Cl	0.918	0.945
			Steel/Cl	2.76	7.63
	PAO + Moly Trimer + secondary ZDDP		a-C:30H/Cl	0.879	0.476
			Steel/Cl	2.47	1.59
[229]	PAO	Ball-on-disc/ 2 h	Steel/steel	6.3	6.5
			a-C:15H/steel	22.7	4.4
	GL-5, SAE 75W-85 Fully formulated oil		Steel/steel	6.5	5.0
			a-C:15H/steel	4.4	0.2

3.5.2. Effect of DLC Coating Type on DLC/Lubricant Interactions

The tribological behaviour of DLC under boundary lubrication, depends significantly on the coating type [209, 226, 230, 238, 239], as illustrated in Figure 3-27. For self-mated DLC/DLC contacts the obtained friction and wear was lower for non-doped DLCs than for doped ones. When additives were blended into the base oil, a soft amorphous layer was formed on some of the non-doped DLCs but not doped ones. However, no direct evidence of DLC/lubricant interaction was found for DLC/DLC contacts [209]. In contrast, MoDTC and ZDDP were shown to interact directly with some hydrogenated DLCs and form tribofilms on the coating surface, and thus improved the friction and wear performance of these contacts [206, 217]. Therefore, it is clear that the DLC/lubricant interaction strongly depends on the type of DLC as well as lubricant composition, particularly when these coatings are rubbed against uncoated steel surfaces [170].

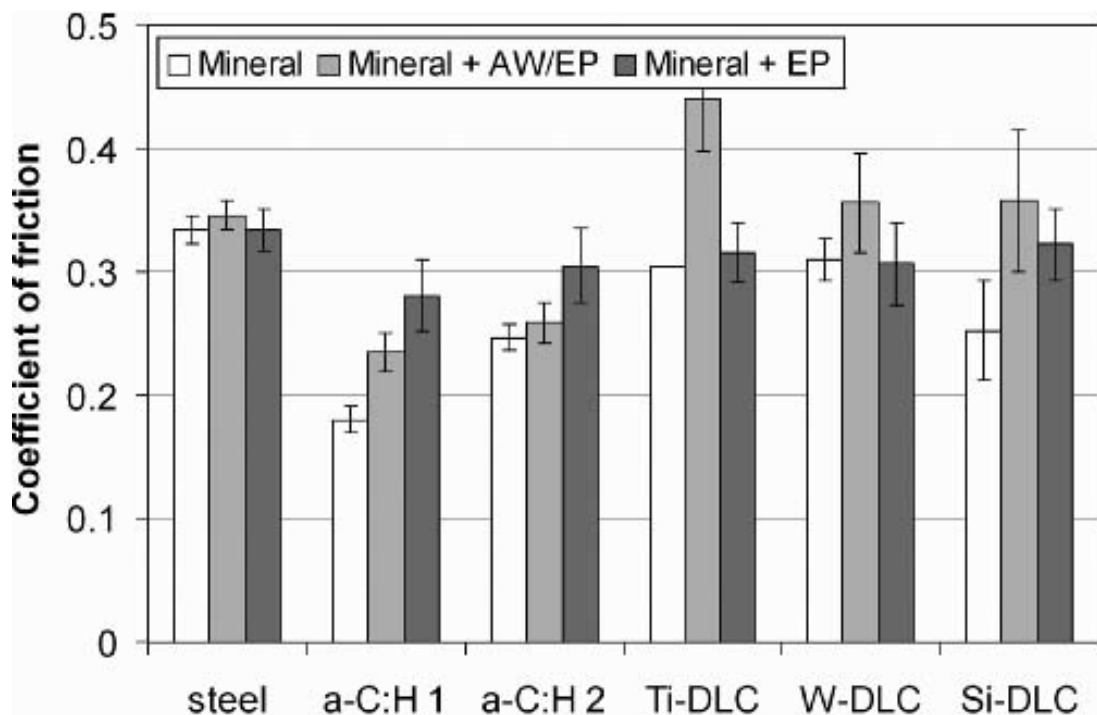


Figure 3-27 Influence of coating type on the steady-state friction of boundary-lubricated DLC/DLC contacts tested with mineral oil (M), a mixture of mineral oil and AW/EP additive (M + AW/EP) and a mixture of mineral oil and EP additive (M + EP). DLC-1 and DLC-2 are hydrogenated DLCs with Si-based and Ti-N interlayer ($P_{\max} = 1$ GPa, $v = 0.1$ m/s, $T = 80^{\circ}\text{C}$) [209].

Low wear and friction similar to boundary-lubricated steel surfaces (~ 0.15) was obtained using non-doped DLC coatings rubbed against uncoated steel when lubricated in pure PAO oil. In addition, EP (a mixture of amine phosphates, having 4.8% and 2.7% of P and N, respectively) and AW (dialkyl dithiophosphate, containing 9.3% of P and 19.8% of S) additives as well as fully formulated oils were found to have insignificant effect on friction and wear of non-doped DLC coatings [240], particularly at lower additive concentrations. On the other hand, for self-mated DLC/DLC contacts, no indication of reaction products or tribofilm formation on the DLC-coated surface was found [225, 233, 241, 242]. For DLC/steel system, however, friction reduction and good wear performance was related to the formation of a carbon transfer layer on steel counter surfaces after sliding [164]. In addition, in the DLC/steel system, high additive concentrations resulted in the interaction between lubricant additives and the steel counterface in a similar way to steel/steel system [243]. For DLC/steel contacts, the lowest steady state friction was observed in the steel/W-DLC system when lubricated with the EP additive. However, this steady-state friction was observed with the cost of DLC coating removal and reaching to Cr-interlayer (Figure 3-28) [204].

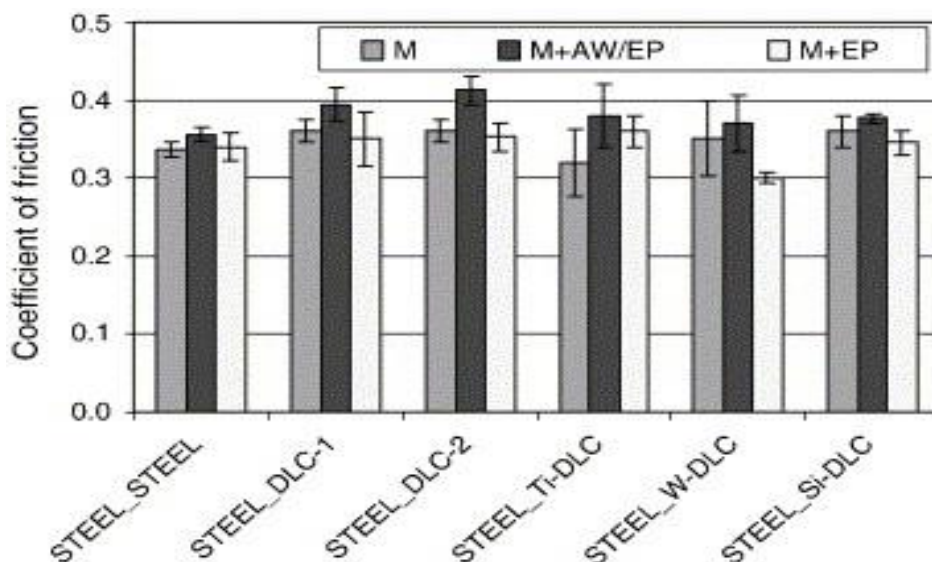


Figure 3-28 Influence of coating type on the steady-state friction of boundary-lubricated DLC/steel contacts tested with mineral oil (M), a mixture of mineral oil and AW/EP additive (M + AW/EP) and a mixture of mineral oil and EP additive (M + EP). DLC-1 and DLC-2 are hydrogenated DLCs with Si-based and Ti-N interlayer ($P_{\max} = 1$ GPa, $v = 0.1$ m/s, $T = 80^{\circ}\text{C}$) [204].

Friction and wear performance of doped DLC coatings was seen to be better than uncoated steel surfaces, but generally give about two times higher wear rates than non-doped DLC coatings. However, additive interaction with doped DLC coatings was found to be much more pronounced than pure DLCs, especially metal-doped DLC coatings (Me-C:H) [217]. The improvement of the boundary lubricating effect of DLC coatings, in a metal-doped DLC, was related to the “metal-like” behaviour of the doping element which was present in the DLC matrix [209, 217]. For metal-doped DLC coatings, tribofilms were usually formed on the steel counterpart or on the exposed steel substrate, but not on the DLC coating itself [43,44,46,47]. However, for some Mo-based additives MoS₂ containing layers were also found on the coated surface [206, 217, 241].

It was shown that, W-doped DLC coatings gave a friction of about 0.15 when rubbed against uncoated steel lubricated in pure PAO oil. Similar friction values were obtained using low AW additive concentrations, whereas high AW additive concentrations resulted in similar friction as seen in steel/steel system in boundary lubrication. EP additive concentration, however, greatly influence the tribology of W-doped DLC coatings, with optimum EP additive concentration resulting in considerable improved friction and wear of the contact [230, 243]. In another work, ZDDP+ MoDTC mixture was reported to provide overall beneficial performance in W-DLC/CI lubrication compared to single MoDTC or ZDDP model oils. Friction reduction, however, was more attributed to the formation of MoS₂ rather than WS₂-containing tribofilm in W-DLC/CI tribocouple [244].

More recently, the effect of tungsten content on the tribological performance of W-doped DLC under PAO lubrication condition was investigated by Fu *et al.* [245]. It was revealed that increasing W content in the coatings resulted in friction reduction. In addition, the mechanical properties of the coatings (hardness and elastic modulus) was not significantly influenced by W content. However, the influence of W content on the wear rates of the DLC-coated sample was less pronounced when W content was less than 10.73 at.%.

In another study, Yue *et al.* [246] showed that sulfurized W-DLC coating showed better friction and wear (Figure 3-29) performance than W-DLC when lubricated by PAO+ MoDTC. The improved tribological properties were related to the formation of WS_x as well as the higher ratios of Mo sulphide/Mo oxide and sp^2/sp^3 .

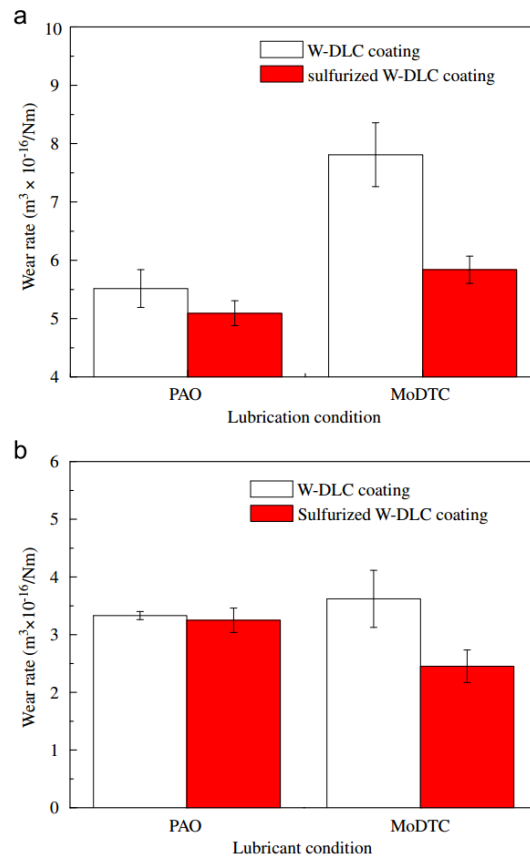


Figure 3-29 (a) Wear rates of W-DLC and sulfurized W-DLC coatings and (b) wear rates of balls against W-DLC and sulfurized W-DLC coatings [246].

3.5.3. Super-lubricity of DLC Coating using GMO/PAO

Super low friction was obtained using PAO+ GMO in the ta-C/steel and the ta-C/ta-C system [207, 223]. Kano *et al.* [207] showed that using PAO+GMO model oil, super low friction of 0.02 was obtained in a ta-C/ta-C system. The thickness of the tribofilm formed using PAO+GMO was reported to be less than 2 nm. They suggested that the tribochemical reaction of lubricant alcohol function groups with the hydroxilated carbon atoms resulted in the formation of OH-terminated layer on the ta-C surface. They related the

obtained super-low friction to the low van der Waals forces between the OH-terminated surfaces. Similarly, Minami *et al.* [247], reported that the addition of GMO to PAO improved the friction performance of the DLC/steel contact to 0.02-0.03 from 0.12 without GMO. They suggested that GMO interacted with DLC in the ester form and the hydroxyl groups in the molecule was mainly responsible for such interaction. Tasdemir *et al.* [223] reported ultra-low friction for ta-C/steel and ta-C/ta-C combination in PAO and PAO+GMO. Using PAO alone, however, ultra-low friction behaviour did not last long in the ta-C/steel system mainly due to the total wear of coating (steady state friction was almost equal to 0.09). Interaction between nascent ta-C surface and base oil or graphitization of very thin topmost surfaces of ta-C DLC was thought to be responsible for the observed ultra-low friction (Figure 3-30). In addition, Equey *et al.* [237] reported a similar response of friction by using PAO alone in a-C:H/a-C:H system. In contrast, Podgornik *et al.* [233] did not observe such a friction drop using PAO in WC-C:H/WC-C:H system. Furthermore, recently Vengudusamy *et al.* [229] reported that with PAO, a-C:H/steel contact exhibited lower friction than steel/steel contact (0.15) for the first 90 min of the tests. However, this value gradually increased to the value of steel/steel contact (0.15) probably due to the high wear of a-C:15H coating and reaching to the substrate. Based on the published literatures, the effectiveness of PAO seems to be greatly influenced by the type of DLC used.

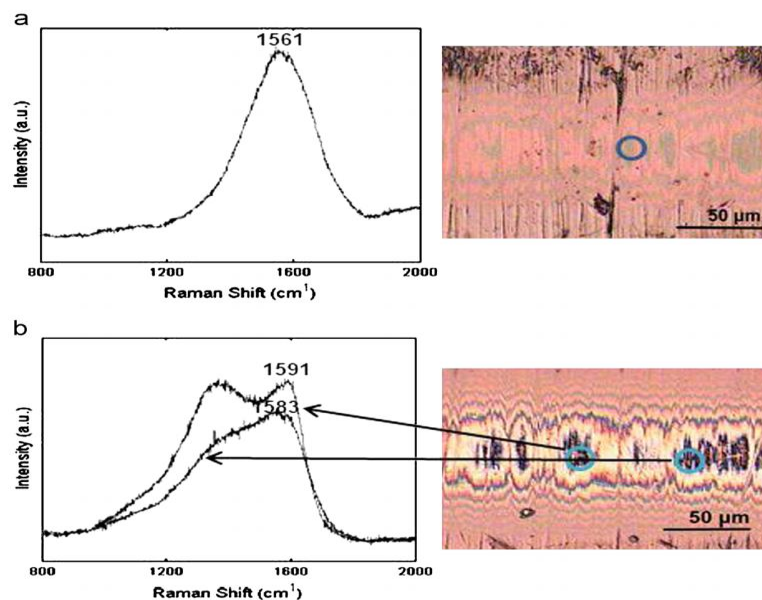


Figure 3-30 Raman spectra of steel counterpart rubbing in pure PAO for DLC/steel tribopair (a) before total wear occurs (b) after partial wear out of coating from the topmost surface [223].

3.5.4. Effect of Hydrogen on DLC/Lubricant Interaction

It looks quite obvious that the presence of hydrogen in DLC matrix is playing a great role for their interactions with lubricant additives. Although this significant role has already been investigated extensively [184, 210, 248-250], the published results are different and, thus the exact mechanisms by which hydrogen could take part in the DLC/lubricant interaction has been poorly understood. In diamond, carbon atoms can form three covalent bonds whereas the fourth bond remains open and dangling out of the surface. These dangling bonds can be passivated by chemisorbed species from the environment such as O and H to form water molecules, and so the initial high friction would drop [250, 251] (Figure 3-31).

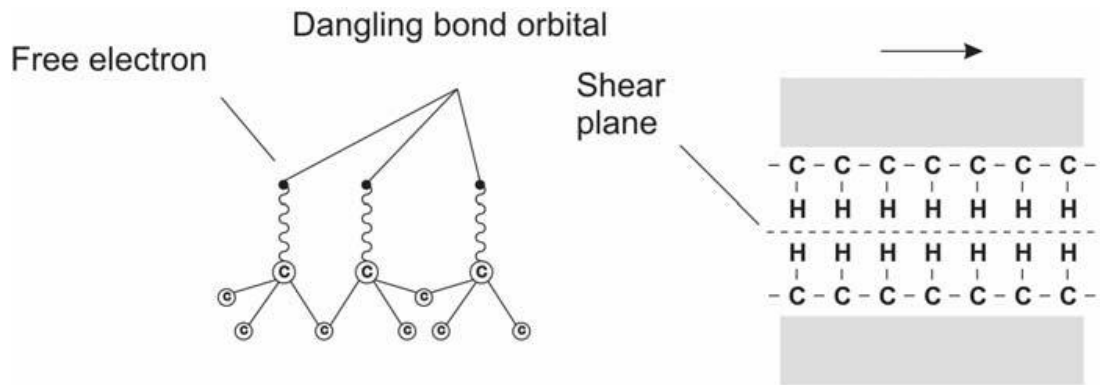


Figure 3-31 Schematic illustration of dangling bonds in diamond and weak shear plane between hydrogen-terminated diamond surfaces [250]

It was suggested that similar mechanisms could participate in DLC/lubricant interaction and the lubricant additives could interact with the dangling bonds of DLC [251]. Hydrogen in hydrogenated DLC terminated the dangling bonds, implying that different species are responsible for DLC/lubricant interaction and adsorption of lubricant additives. That could explain the different behaviour of non-hydrogenated and hydrogenated DLC when lubricated with different additive package.

The effect of hydrogen content on the friction performance of DLC has been reported by Yasuda *et al.* [145] and Mabuchi *et al.* [252]. It was shown that the friction coefficient decreased with a lower hydrogen content of the film.

They claimed that higher hydrogen content in the DLC film resulted in poor wettability of the surface which in turn affected the interaction between the engine oil and the DLC surface. Therefore, the higher obtained friction was due to the loss of additive adsorption on the DLC surface.

In contrast, Barros' Bouchet *et al.* [206] reported the positive effect of hydrogen in the tribofilm formation on the DLC coating. They found that hydrogenated DLC provided lower friction compared to hydrogen-free DLC. Performing XPS analysis, they showed the presence of additive-derived tribofilm on both a-C:H and a-C coating when rubbed against AISI 52100 steel (Figure 3-32). However, the ratio of $\text{MoS}_2/\text{MoO}_3$ for a-C:H was five times higher than that observed with hydrogen-free DLC. The lower friction obtained by hydrogenated DLC was attributed to this higher ratio. They argued that, during friction process, DLC dangling bonds form hydrogen-terminated surfaces reacted with the oil additives. They made assumptions on the basis of the chemical hardness approach (HSAB principle). Based on their argument, from the chemical hardness point of view, hydrogenated carbon materials are soft bases and favourably interacts with soft acids, like Mo^{4+} , involved in the formation of MoS_2 . On the other hand, hydrogen-free carbon materials could be considered as 'intermediate bases' which reacts with Mo^{6+} and promotes the formation of MoO_3 high friction species. This could explain why hydrogen-containing carbon materials gave a higher ratio of $\text{MoS}_2/\text{MoO}_3$ and lower friction, as a result. They also reported the positive effect of ZDDP when used in combination with MoDTC. They claimed that ZDDP could facilitate the formation of low friction MoS_2 by supplying more sulphur. Kano *et al.* [215] performed similar tests and found out that ZDDP/MoDTC solution provided lower friction than ZDDP alone. However, after conducting XPS analysis, no evidence of tribofilm formation on the DLC surface was found. Instead, the tribofilm was observed on the steel counterpart.

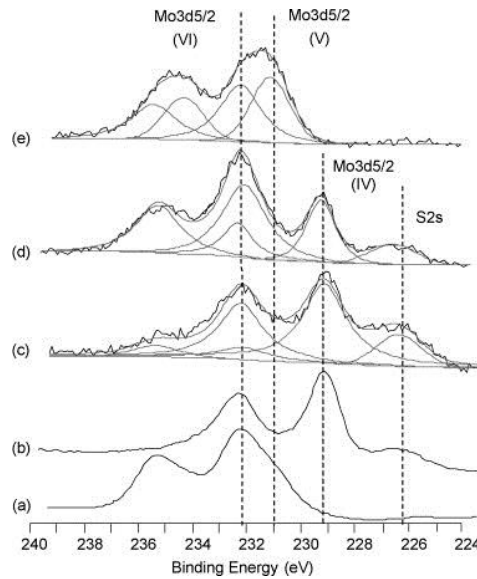


Figure 3-32 Friction-induced MoS_2 with steel cylinder against DLC-coated flat friction test. XPS Mo3d peak recorded on (a) pure MoO_3 powder; (b) pure cleaved MoS_2 crystal; (c) MoDTC+ZDDP tribofilm on the a-C:H coated flat; (d) MoDTC+ZDDP tribofilm on the a-C coated flat; (e) outside the MoDTC+ZDDP tribofilm on the a-C:H coated flat [206].

In addition, role of hydrogen in the DLC matrix on the wear performance of the DLC/steel contact, when lubricated in ZDDP, has been reported by Barros' Bouchet *et al.* [206]. The wear of steel counterpart was seen to be higher when rubbed against hydrogen-free DLC than that of hydrogenated one. The XPS analysis revealed that P and Fe were depleted in the tribofilm formed on both DLC surfaces suggesting that iron did not take part in the ZDDP film formation and that no transfer of iron to DLC counterface was occurred. ZDDP-derived ZnO/ZnS was detected in the tribofilm formed from ZDDP on both surfaces but the presence of Zn was more pronounced on the hydrogenated DLC.

Equey *et al.* [213] observed the formation of ZDDP tribofilm on the hydrogenated DLC coating in a self-mated DLC/DLC contact. The tribofilm was easily removed after the samples were cleaned in an ultrasonic bath with cyclohexane suggesting that the adhesion of the ZDDP tribofilm to hydrogenated DLC was weaker than uncoated ferrous surface. In addition, Fe was not detected in the tribofilm formed on the DLC coating implying that no delamination of the coating occurred and that ZDDP formed a tribofilm on the DLC without the presence of Fe.

3.5.5. Adverse Effect of MoDTC on DLC High Wear

Recently, the effect of MoDTC in increasing wear of a DLC coating in a DLC/steel contact has been reported [41, 214, 220, 253-256]. Shinyoshi *et al.* [41] performed block-on-ring tests to evaluate the friction and wear properties of DLC coatings in the MoDTC-containing oil. The results suggested that MoO_3 which is the decomposition product of MoDTC reacted with DLC and promoted the wear of DLC coating. The wear mechanism by which MoDTC is giving high wear to DLC is summarised in Figure 3-33.

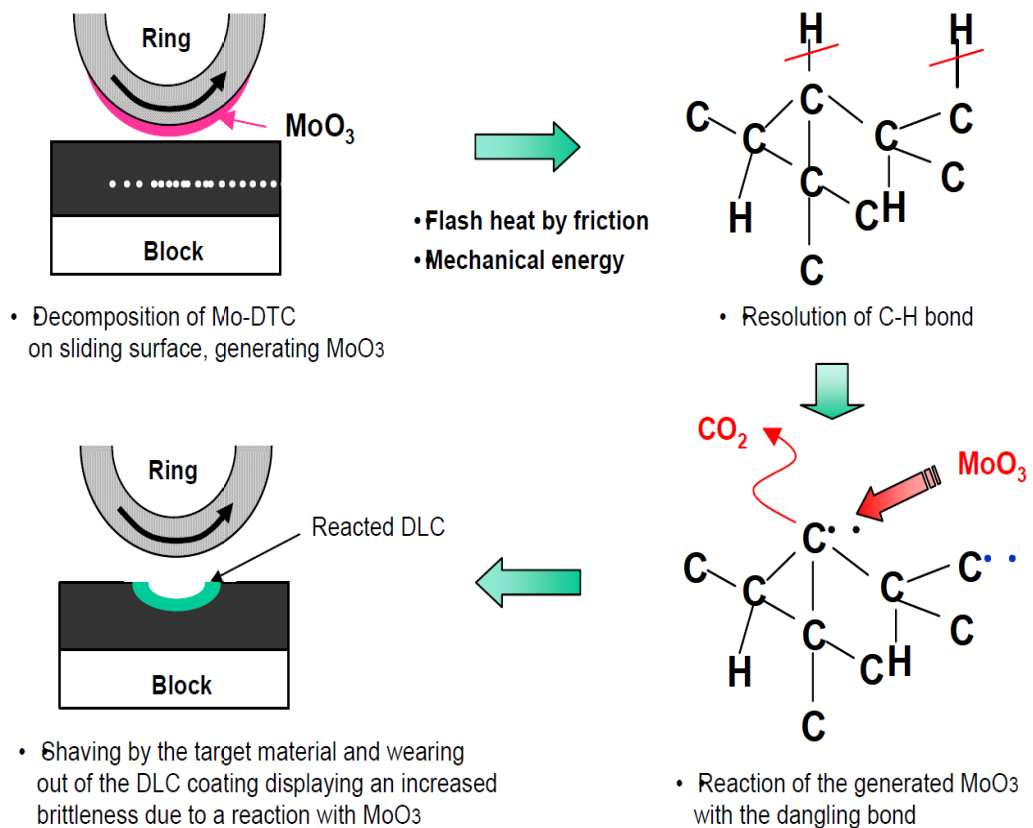


Figure 3-33 Wear steps of DLC coating in oil containing Mo-DTC [41].

Haque *et al.* [220] showed that DLCs rubbed against steel in the presence of a MoDTC-containing base oil gave extremely high wear but that the addition of the anti-wear additive ZDDP terminated this effect. Sugimoto [254] also reported the higher wear of DLC in a DLC/steel system when lubricated in MoDTC-containing fully formulated oil. However, the wear process was reported to be almost entirely independent of the presence or absence of

MoO₃. In contrast, Tung *et al.* [232] showed that MoDTC can reduce the wear of a DLC coating lubricated in fully formulated engine oil which could be due to the fact that ZDDP was present in his oil and could suppress the effect of MoDTC on promoting wear of DLC coatings reported by others. Vengudusamy *et al.* [255] studied the tribological behaviour of several types (a-C, a-C:H, WC-DLC, Si-DLC, etc.) of DLC coatings for MoDTC-containing oil in the DLC/steel system. The wear rates of DLC coatings lubricated with MoDTC were shown to be even higher than those with PAO. This was correlated to the formation of large amounts of abrasive MoO₃ which in turn will enhance removal of tribofilms from DLC coatings and thus high wear. Recent literature on the harmful effect of Mo-containing friction modifier in promoting high wear of DLC is summarised in Table 3-5.

Table 3-5 Summary of literature on the effect of MoDTC in promoting high wear of DLC coatings. NM stands for “Not Mentioned”.

Author(s)	System	Type of DLC	High wear for DLC coating observed with:			Wear Mechanism
			Model oils		Fully formulated oils	
			MoDTC	ZDDP +MODTC		
[232]	DLC/CI	NM	-	-	No	A protective tribofilm produced by MoDTC with ZDDP, which acts to reduce wear.
[41]	DLC/steel	NM	Yes	-	-	Oxidative wear due to reaction of MoO ₃ with the DLC active sites.
[220, 253]	DLC/CI	a-C a-C:15H	Yes (Multiple sources)	No	-	In the absence of ZDDP, high pressure exerted by small third body particles could go beyond the endurance limit of the coating.
[255]	DLC/steel	a-C a-C:H Si-DLC WC-DLC	Yes	-	-	“Pro-wear process must involve the presence of the steel counterface”
	DLC/DLC		No	-	-	
[254]	DLC/steel	a-C:H	-	-	Yes	Graphitization of the DLC followed by the formation of hard Mo compounds on the steel counterpace accelerating the wear on the DLC plate.

The origin of “MoDTC induced wear” on DLC is not fully understood and previous studies mainly used single additive solutions rather than realistic fully formulated oils. Furthermore, the addition of ZDDP to the lubricant has been shown to cancel or reduce the effect of MoDTC in promoting wear on DLC coatings, but it has not been reported whether other surface active additives in the oil could provide similar protection. Therefore, a comprehensive understanding of the DLC/MoDTC interaction, especially on the wear performance of DLC coating, is still to be clearly produced.

3.5.6. Effect of Temperature on the DLC/Lubricant Interaction

Although many researches have been carried out on the boundary lubrication of DLC coatings, the actual boundary lubrication mechanisms, the DLC/lubricant additives interaction and the parameters involved are still poorly understood. Operating temperature of contact surfaces in boundary lubrication may vary with changes in contact pressure and sliding speed. Contact temperature is an important factor which can have a detrimental effect on the reactivity of different additives with metals [210, 257]. The tribological properties of DLC surfaces can be changed when the coated surfaces will be exposed to different operating temperatures, particularly when lubricated by formulated oils [238].

For non-doped DLC coatings, regardless of operating temperature, no significant difference in friction and wear was observed using both base oils and formulated lubricants, as shown in Figure 3-34 and Figure 3-35 [238]. However, when temperature exceeds 200°C, decomposition of DLC starts occurring [188, 238], leading to reduced friction but with the cost of increased coating wear rate [238].

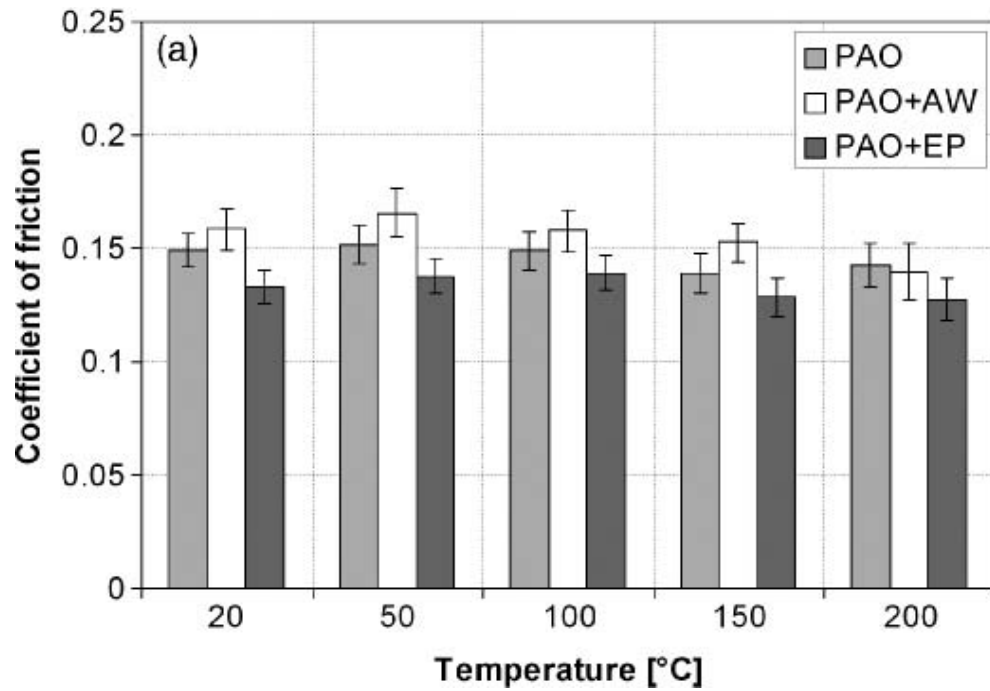


Figure 3-34 Effect of operating temperature on steady-state friction of undoped DLC coatings running against uncoated steel ($P_{\max} = 1.5$ GPa, $v = 0.02$ m/s) [238].

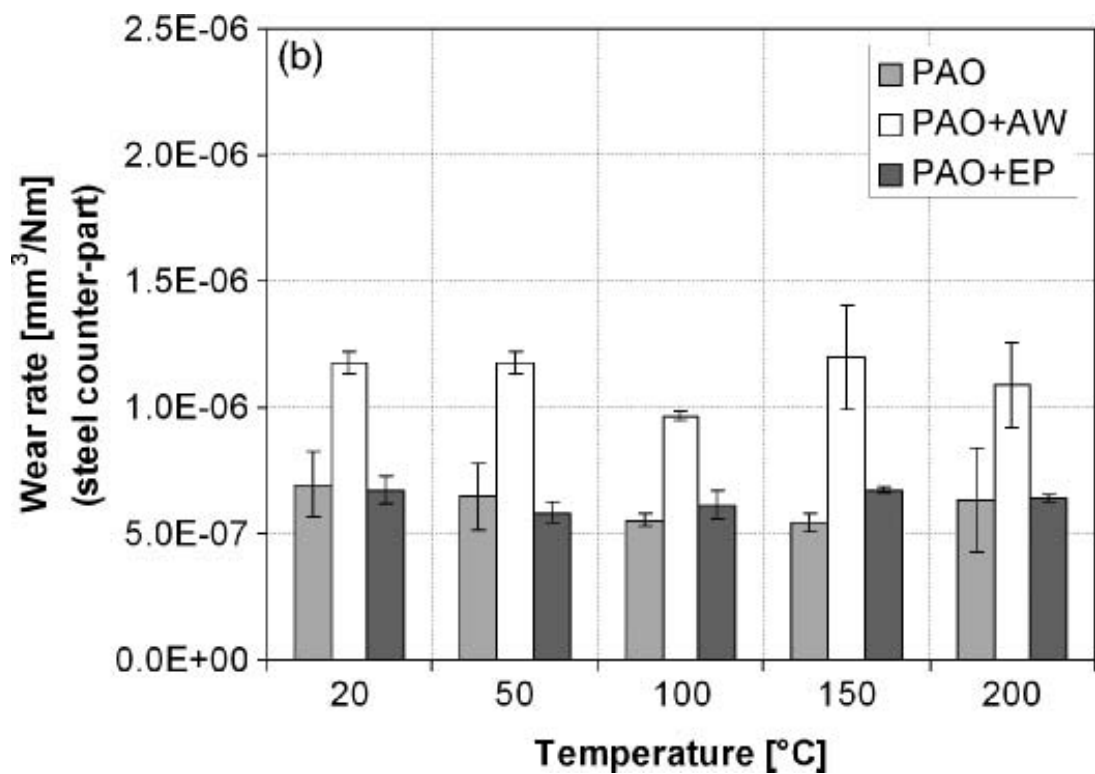


Figure 3-35 Effect of operating temperature on wear rate of undoped DLC coatings running against uncoated steel ($P_{\max} = 1.5$ GPa, $v = 0.02$ m/s) [238].

On the other hand, tribological performance of metal-doped DLC coatings was found to be much more sensitive to the operating temperature. The effect of test temperature on the tribological behaviour of W-doped DLC coatings in boundary lubricated condition, is shown in Figure 3-36 and Figure 3-37. Similar to non-doped DLC coatings, for additive-free PAO oil, friction and wear rates were observed to be almost independent of the operating temperature up to 200°C. Apart from coefficient of friction at 200°C, the same behaviour was also observed when PAO+ AW additives was used [238]. However, using PAO+ EP additive, increase in temperature was found to affect both friction and wear. When the temperature exceeded 100°C, up to 40% reduction in friction was observed (Figure 3-36). The low friction observed was related to the formation of WS₂-containing tribofilms. W–S reaction kinetics was accelerated in higher temperatures and activation energy was increased [258], thus promoted faster tribofilm formation and friction reduction as a result.

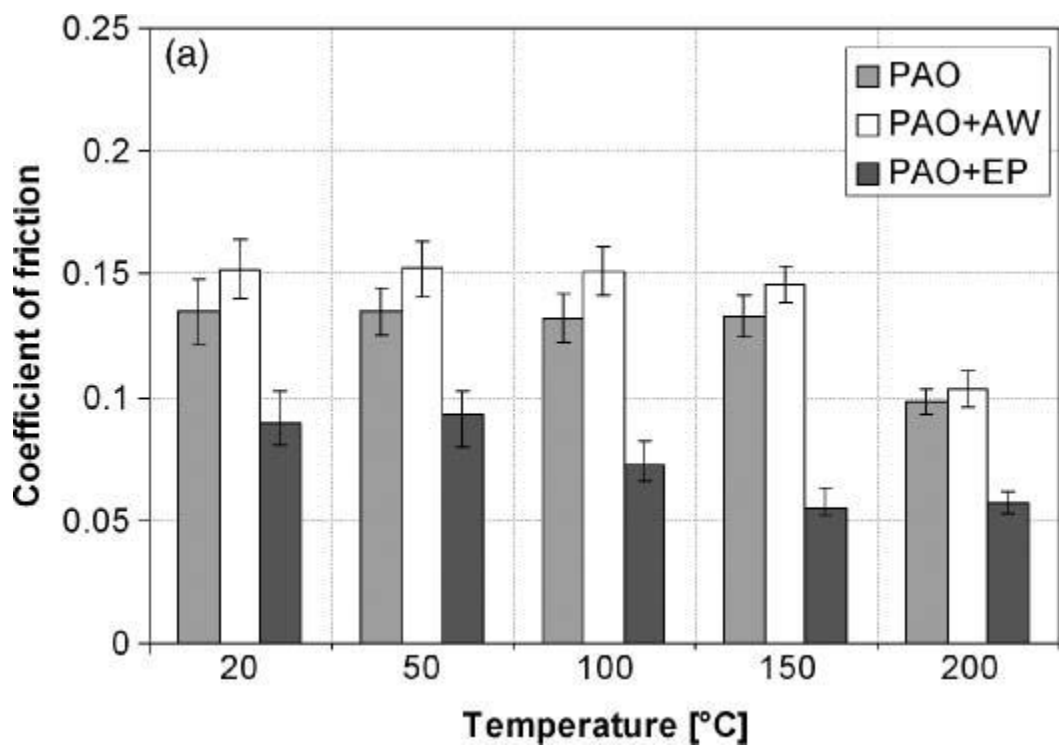


Figure 3-36 Influence of operating temperature on steady-state friction of steel/W-doped DLC combination ($P_{\max} = 1.5$ GPa, $V = 0.02$ m/s) [238].

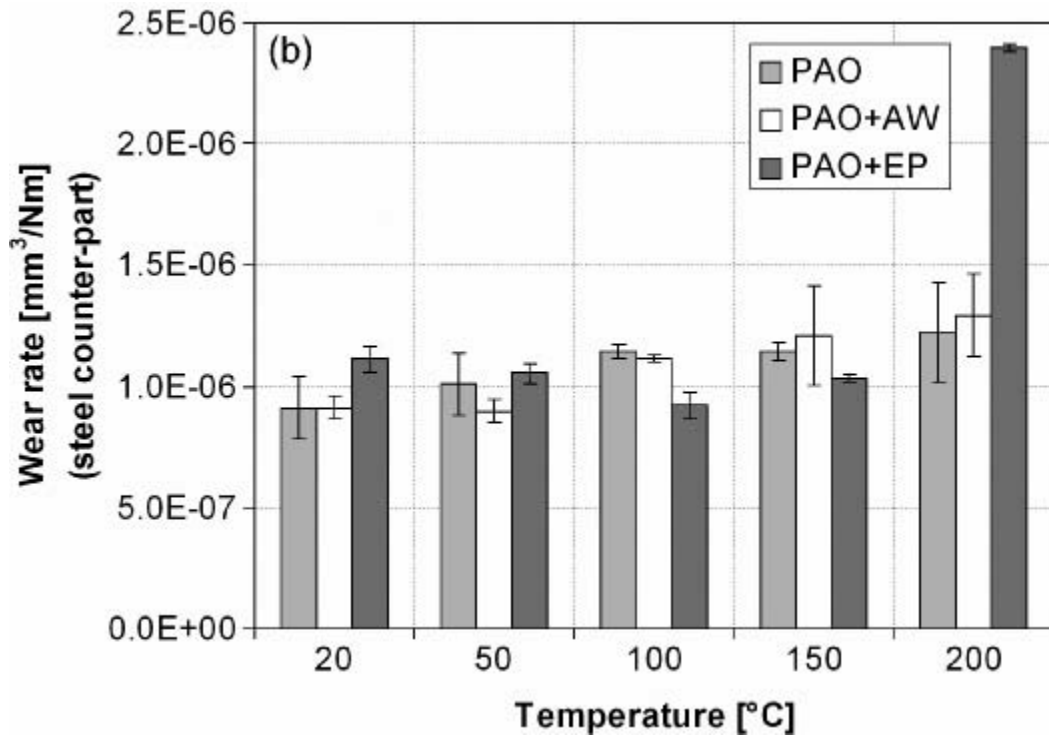


Figure 3-37 Influence of operating temperature on wear rate of steel/W-doped DLC combination ($P_{\max} = 1.5$ GPa, $V = 0.02$ m/s) [238].

Nevertheless, based on the published literature, it is obvious that the effect of temperature on boundary lubricated DLC coatings is greatly influenced by the type of DLC coatings as well as the lubricant additive package used.

3.6. Summary

This review provided a summary of the current understanding of the lubricant additives and their interactions with ferrous surfaces. Furthermore, Diamond-like carbon (DLC) coatings and their properties have been described. The state of the art in lubricant/DLC interaction and the effect of different parameters on the tribological performance of DLC coatings has been shown.

Molybdenum Dithiocarbamates (MoDTC) and Zinc Dialkyldithiophosphates (ZDDP) are well-known friction modifier and anti-wear additives respectively, used for ferrous surfaces. Having low shear strength, MoS_2 low friction crystals, derived from MoDTC decomposition, provide low friction at the

tribological contacts in boundary lubrication conditions [34-36]. ZDDP offers anti-wear properties by forming sulphide- and phosphate-containing tribofilms at ferrous surfaces [35-37]. It has also been suggested that the presence of ZDDP could promote MoS₂ formation and that ZDDP may enhance durability of the MoS₂ sheets [259, 260]. In addition, MoDTC has been found to improve the wear resistance of the ferrous surfaces by forming N-containing species in the tribofilm [35].

Diamond-Like Carbon (DLC) coatings have become an attractive surface engineering solution in the automotive industry as they offer excellent tribological performance including low coefficient of friction, high wear resistance [234, 261] and outstanding running-in properties [234]. Diamond like carbon coatings have similar properties to diamond but are amorphous carbon coating consisting network of sp² (graphite-like), sp³ (diamond-like) and hydrogen bonds.

Commonly used lubricant additives are designed to form tribofilms on ferrous-base surfaces. It is therefore essential to optimize coating and lubricant compatibility to enable additive solutions to be tailored to DLC surfaces. The properties of DLC coatings depend extensively on the sp²/sp³ ratio as well as hydrogen content, which in turn depends on the deposition process and applied parameters [262]. Thus, the interaction between lubricant additives and DLC depends significantly on the type of DLC used.

Different researchers have started to evaluate interactions between lubricant additives with various types of non-ferrous DLC coatings under boundary lubrication. DLC coatings have been reported to be chemically inert using a steel pin sliding against DLC-coated disks lubricated in oil containing MoDTC and/or ZDDP [215]. In contrast, molybdenum-based friction modifiers and ZDDP anti-wear have been reported to form low friction MoS₂ sheets and/or ZDDP-derived compounds respectively, on the DLC coating providing low friction and better wear performance under boundary lubrication conditions [4, 206, 216, 217, 219, 220, 263]. Based on the published literature, researchers mostly used model oils containing one or combination of additives rather than more realistic fully formulated oils. Obviously, interaction between different additives could result in antagonistic

or synergistic effects which influence the tribological behaviour of the contacts in a real engine when lubricated with a fully formulated oil.

Based on the literature presented in this chapter, DLC/lubricant interaction depends significantly on numerous factors such as contact conditions, test parameters, the physical and mechanical properties of the DLC coatings, lubricant type, etc. Therefore, a comprehensive understanding of the DLC/lubricant interaction is still to be clearly produced. The main objective of this study is to evaluate how the nature of the fully formulated oils affects the tribochemical reactions at DLC interfaces in a hydrogenated DLC. This could provide information regarding the feasibility of modifying additive solutions for increased performance of DLC/lubricant.

Chapter 4 Experimental Procedures

4.1. Introduction

In this chapter, the details of test materials and coatings, test lubricants, sample preparation techniques, coating deposition techniques, experimental rigs are presented along with the surface analysis techniques used to test and characterise lubricant/surface interactions.

4.2. Test Materials and Coatings

In this study, tests were performed in a pin-on-plate rig where the HSS M2 Grade steel samples were coated by 15 at.% hydrogen containing DLC (a-C:15H) coatings. The concentration of hydrogen in DLC coating was provided by the supplier. BALINIT® DLC STAR, a commercial low hydrogenated DLC coating, was supplied by Oerlikon Balzers Coating (UK). This coating is popular because of its high hardness, excellent load bearing capability, excellent fatigue resistance and corrosion resistance. The coated samples were pure sliding against BS 1452 cast iron (CI) pins. The properties of materials and coatings are given in Table 4-1. Steel/CI, a-C:15H/CI and a-C:15H/ceramic were the material combinations which were used in this study.

Table 4-1 Physical properties of plates (substrate/coatings) and counterpart materials.

Properties of coating and other related materials	Ferrous Material		Ceramic Ball	DLC Coating
Specification	HSS M2 Grade	Cast iron BS1452	Si ₃ N ₄	a-C:15H ^a
Hardness	8.0 GPa	4.0 – 4.5 GPa	14-17 Gpa	17.0 GPa
Reduced Young's modulus	218 GPa	134 GPa	300-320 Gpa	190 GPa
Roughness, R _q	0.04-0.06 μm	0.07-0.09 μm	0.02-.0025 μm	0.04-0.06 μm
Composition/ Coating thickness	C 0.64%, Si 0.55%, Cr 1.57%, and Mn 0.49%	C 3.0%, Si 2.0%, Mn 0.4%, Cr 0.1%, Cu 0.3%	90% Si ₃ N ₄	2-4 μm coating

^aCommercial coatings obtained from Oerlikon Balzers Ltd., UK.

4.3. Pin-on-Plate Test Rig

4.3.1. Test Setup

A reciprocating pin-on-plate tribometer under boundary lubrication conditions was used to simulate the severe conditions that occur at the cam/follower contact [134] in the valve train of an internal combustion engine. The lubricant is heated using a heater and the temperature is maintained at a set value (mainly 100°C in this study) using the feedback controller where a thermocouple is used to detect the temperature of the reservoir. The contact point of the plate and the pin was lubricated under a static volume of oil (3 ml). The speed can be adjusted by a built-in speed controller. The stroke length and average speed were 10 mm and 0.020 m/s respectively (stroke frequency of 1 Hz) and the contact between the plate and the pin was pure sliding in a lubricated condition as given in Table 4-1.

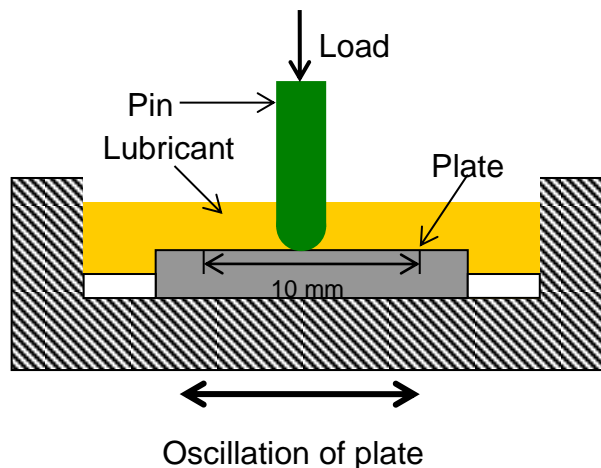


Figure 4-1 Schematic diagram of the contact in the pin-on-plate tests where the contact is submerged in lubricant.

Considering the radius of curvature on the CI pin, the load was used such that the initial Hertzian contact pressure was 700-800 MPa, similar to the pressure range of cam/follower contact in a passenger gasoline engine. In the DLC/CI system the actual load was about 390 N and in the DLC/ceramic the actual load was 13 N. Hertzian contact pressure was calculated using Equation 2-5 and Equation 2-6. Considering load, material and lubricant properties and using Equation 2-11, Equation 2-12 and Equation 2-13, the

calculated lambda ratios were well below unity (≈ 0.004) meaning that lubrication occurred in the boundary lubrication regime. To evaluate friction performance, each type of test was repeated three times and average repeatability was seen to be less than 0.03 for the friction coefficient in the steady state region (i.e. last hour of the test). The friction force was measured using a bi-directional load cell of the range of 58.8 N with a combined error of -0.0037 N. The combined error is considered to be the combination of non-linearity, temperature effect, load cell sensitivity and hysteresis. The data collected from the load cell is converted to digital signal in an analogue to digital converter and finally processed by Labview software in a computer. The friction force data was measured continuously and periodically averaged every minute. The duration of the tests varied between 6, 12 and 20 h.

4.3.2. Test Samples

The dimensions of the CI pins which were used in pin-on-plate tests were 20 mm in length, diameter 6 mm and the ends of the pins had a 40 mm radius of curvature. The geometry of the plate was 15 mm \times 6 mm \times 3mm. The radius of silicon nitride ball was 6 mm. All sample preparations, heat treatment, etc. have been conducted by external provider and the properties of the CI pin, the silicon nitride ceramic ball, High Speed Steel (HSS) plates and the DLC coating are given in Table 4-1. Prior to the tests, samples were cleaned using acetone in an ultrasonic bath for 15 minutes.

4.3.3. Coating Deposition

A hybrid unbalanced magnetron sputter ion plating/PECVD deposition system was used to deposit the a-C:15H coating on the steel plate. First the substrates were cleaned by Ar⁺ plasma ion etching using pulsed DC bias followed by deposition of a thin adhesion promoting Cr layer by DC magnetron sputtering with a pulsed DC bias. A CrN intermediate layer was then deposited by introducing nitrogen gas into the chamber. Finally, by adding a hydrocarbon gas, a layer of the a-C:15H coating was deposited using a plasma enhanced chemical vapour deposition (PECVD) technique, where a pulsed DC bias was applied on the substrate and a discharge enhancing electrode with a 13.56-MHz RF generator was used.

4.4. Lubricants

In phase I, six fully formulated oils were used as given in Table 4-2. All the oils are supplied by Infineum UK limited and the key additive components of each oil are shown in Table 4-3. In addition to the information provided, the fluid contains detergent, dispersant as well as antioxidants.

Table 4-2 Oil lubricants-Phase I

Lubricants	Annotations	Base stock	P from ZDDP (ppm)	Mo (ppm)	Other Additives	Detergent Dispersant Antioxidant
PAO	PAO	Group IV	N/A	N/A	N/A	Y
Base	Base oil	Group III	N/A	N/A	N/A	Y
Fully formulated oil 1	FF1+	Group III	750	40	GMO	Y
Fully formulated oil 2	FF2+	Group III	750	-	-	Y
Fully formulated oil 3	FF3+	Group III	750	60	GMO	Y
Fully formulated oil 4	FF1-	Group III	-	40	GMO	Y
Fully formulated oil 5	FF2-	Group III	-	-	-	Y
Fully formulated oil 6	FF3-	Group III	-	60	GMO	Y

In phase II, ZDDP-containing (FF1+) and ZDDP-free (FF1-) oil with three levels of a MoDTC type friction modifier (Mo-FM) were used. In this phase of the study, FF1+ and FF1- oils are annotated FF40+ and FF40- , respectively (40 is the Mo concentration in the oil). This relabeling was done for an easier comparison between oils with different MoDTC level. The key additive components in each oil are shown in Table 4-3.

Table 4-3 Oil lubricants Phase II

Lubricants	Annotations	P (ppm)	Mo (ppm)*
Fully Formulated Oil	FF40+ (FF1+)	750	40
	FF300+	750	300
	FF600+	750	600
	FF40- (FF1-)	-	40
	FF300-	-	300
	FF600-	-	600

*All FF oils contain organic friction modifier (OFM), detergent, dispersant and antioxidant.

4.5. Surface Analysis Techniques

Different surface analysis techniques were used in this study to provide better understanding of the mechanisms involved in the lubricant additive interaction. The description of each technique will be explained in detail. The summary of the techniques which are used in this study is given in Table 4-4.

Table 4-4 Summary of the surface analysis techniques which were used in this study.

Surface analysis technique	The application
Optical Microscope	Physical observation of the surface features
WYKO white Light Interferometer	Roughness evaluations, wear scar depth, cross sectional area and wear volume measurements of samples.
Scanning Electron Microscope (SEM)/ Energy Dispersive X-Ray (EDX)	Visual evaluation of the sample surfaces and to provide information about wear mechanisms and durability of the DLC coatings.
Focused Ion Beam (FIB)/ Transmission Electron Microscopy (TEM)	Coating characterization before and after the tests.
Nano-indentation	To provide mechanical properties of the samples.
X-Ray Photoelectron Spectroscopy (XPS)	Chemical analysis of the tribofilms formed on the samples.
Raman Spectroscopy	To characterize DLC for structural modification.

4.5.1. Optical Microscope

A Leica DM6000M Microscope was used for physical observation of surface features providing information on wear mechanisms. This microscope is capable of recording high quality 2D and 3D Images using LAS V3.8 software. In this study the optical microscope was used along with other techniques to investigate the durability of coatings as well as to measure the diameter of the wear scars formed on the counterpart pins. The diameters of the pins were used to measure the lost segment of the sphere on the pins using Equation 4-1.

$$V_L = \frac{1}{6} \pi h [3r^2 + h^2] \quad \text{Equation 4-1}$$

Where $h = R - \sqrt{R^2 - r^2}$

R = Radius of the curvature for the pin

$r = \frac{d}{2}$ = Radius of the wear scar measured by the optical microscope

V_L = Volume loss of pin material (m^3)

h = Height of sphere of pin worn after the test (m)

Finally, the specific wear coefficients have been calculated using the Archard wear equation (see Equation 2-2).

4.5.2. WYKO White Light Interferometer

Wear of the plates (where measurable) was measured using a Veeco WYKO white light interferometer (NT3300S model) which had the capability to measure wear scar depth, cross sectional area and wear volume. In this study, the cross sectional areas of the wear scars were measured at least in three different positions across the wear track. The average value of the cross sectional area was multiplied by the stroke length which gave the wear loss volume of the plate. The typical data of the cross sectional area of the wear scar, obtained from the Vision64 software, is given in Figure 4-2. The software was also capable to provide the wear volume directly but levelling the surface made it difficult to get the correct wear volume. Measuring the wear volume, the specific wear coefficients were calculated using the Archard wear equation (see Equation 2-2).

Wear measurement of the plates in phase I was a challenge as the wear rate was extremely low and there was no roughness variations comparing different samples and therefore the wear evaluation was done semi-qualitatively using SEM/EDX analysis of the wear scar on the plates.

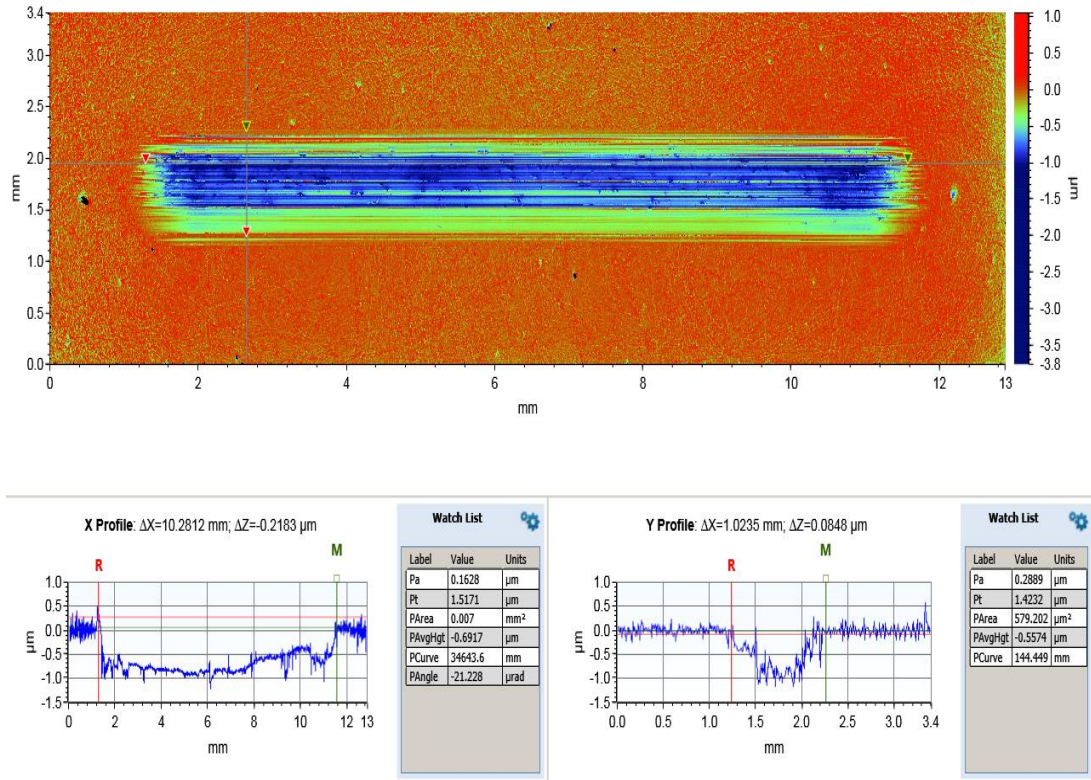


Figure 4-2 Wear measurements of the plates

4.5.3. Scanning Electron Microscope (SEM)/ Energy Dispersive X-Ray (EDX)

In this study, a Zeiss EVO MA15 Variable Pressure SEM was used to investigate the mechanism of wear and the durability of the coatings. This SEM is integrated with an Oxford Instruments Energy Dispersive X-ray (EDX) analysis system. In this study, the EDX analysis was used to provide information about the durability of the coating. EDX mapping obtained within the wear tracks showed the presence of C and Cr. Cr comes from the underlying CrN/Cr intermediate layer and so could be used as a qualitative analysis of the extent of the coating wear. The higher the Cr intensity in the EDX maps, the higher removal of coating thickness due to wear (Figure 4-3).

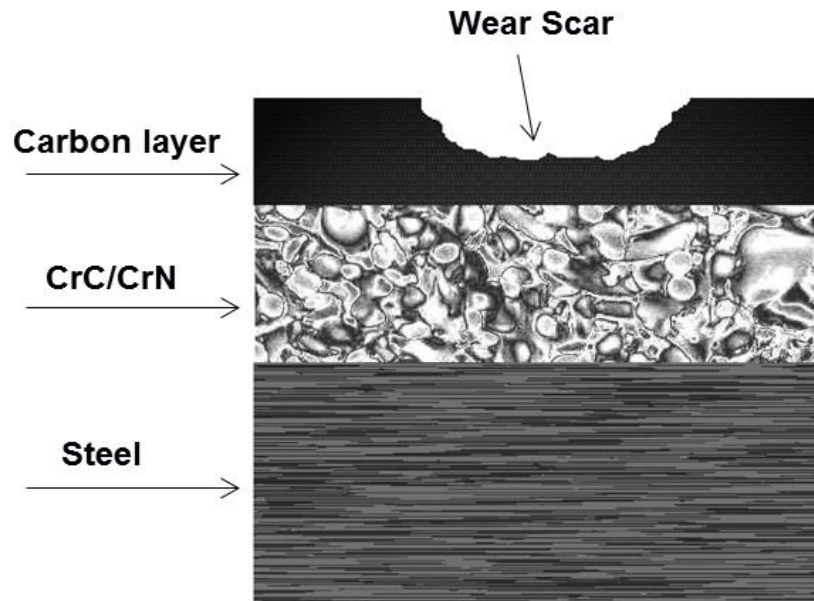


Figure 4-3 Schematic diagram showing the cross section of the a-C:15H coating plate. Concentration of Cr, detected by EDX, is higher inside the wear track compared to outside.

4.5.4. Focused Ion Beam (FIB)/ Transmission Electron Microscopy (TEM)

FEI Nova200 NanoLab high resolution Field Emission Gun Scanning Electron Microscope (FEGSEM) with precise Focused Ion Beam (FIB) was used to expose cross-sections of the DLC samples. Milling was performed at 30 kV and at beam currents between 5 and 0.1 nA. A final cleaning step was performed at 5 kV and with a beam current of 29 pA. Cross-sections were then removed in-situ using a Kleindiek micromanipulator and attached to a TEM support grid ready for analysis. Sputter coating was applied to the surface before a thicker 1 μm Pt layer was applied by a gaseous injection system. This was done in order to protect the surface from the ion beam. To get a high resolution view of the provided cross-sectional areas of the DLC coatings, Transmission Electron Microscopy (TEM) analyses were performed. TEM characterisation was carried out using a Philips CM200 FEGTEM operated at 197 kV and fitted with a Gatan GIF200 imaging filter. The TEM high resolution images were taken to characterise the DLC coatings before the tribo-test and to provide quantitative and qualitative information about the thickness of the DLC coatings post tribo-tests. Prior to the analysis, DLC samples were cleaned in an ultrasonic acetone bath for 15

4: Experimental Procedures

minutes. Figure 4-4 shows the different steps involved in FIB sample preparation to be used for TEM analysis of the cross-sections.

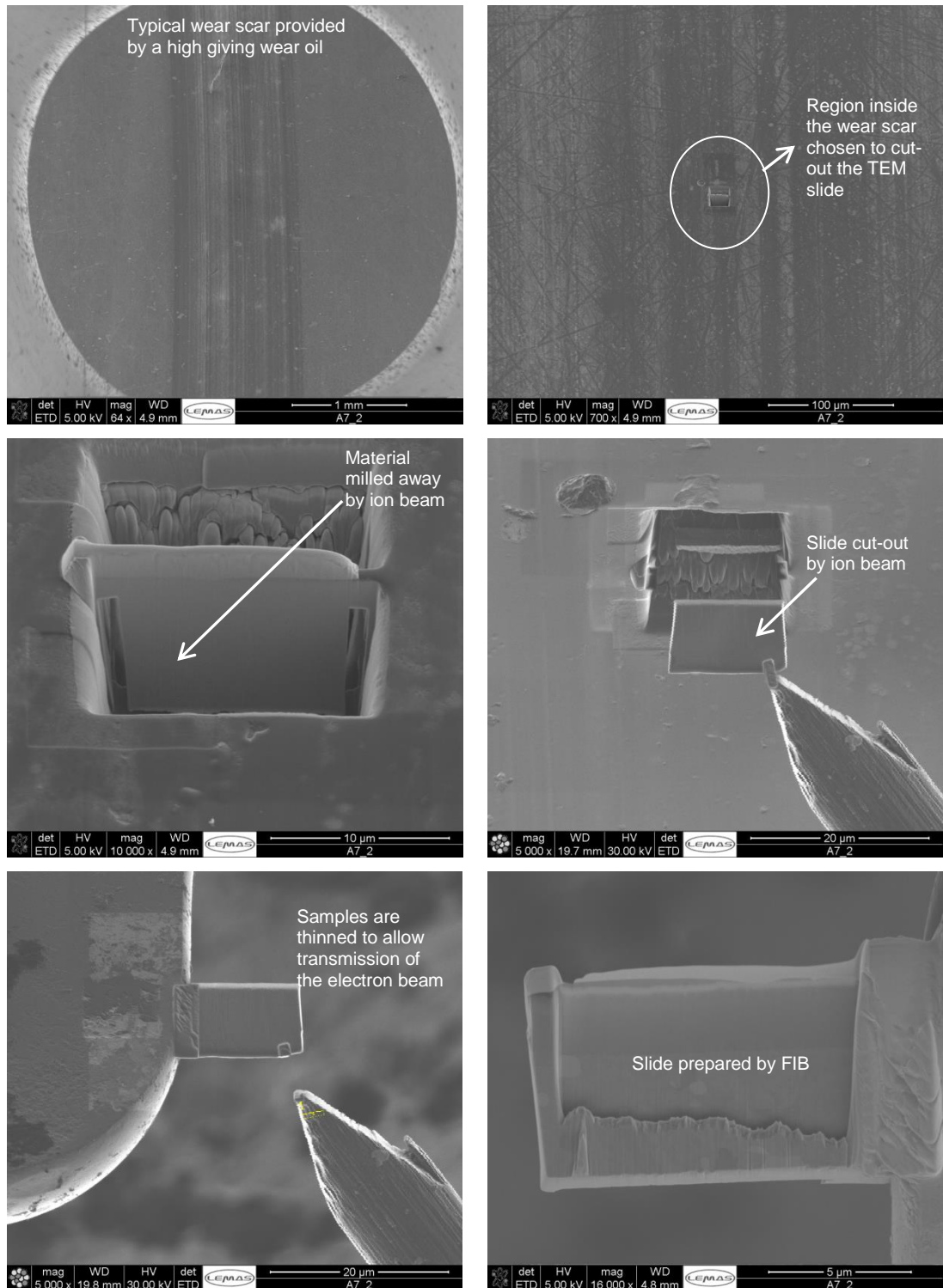


Figure 4-4 Typical TEM slide preparation using FIB.

4.5.5. Nano-indentation Analysis

Mechanical properties of the coatings were obtained by nano-scale indentation using a Micro Materials Limited NanoTest™ Platform One device. The indentations were performed in a controlled environment temperature of 25°C, using a Berkovich-type indenter. The Berkovich indenter used in this study had a three faced pyramid and a typical tip radius of 100-500 nm. As a result of the measurement, the force–displacement curve was produced. A typical loading/unloading curve obtained using nanoindentation on the as-deposited a-C:15H coating is given in Figure 4-5. By analysing the recorded results, the mechanical properties such as hardness and modulus of elasticity were obtained. Nano-indentation analysis in this study was performed to check the modification/graphitisation of the DLC coatings, not to characterize tribofilms. Therefore, prior to the tests, all samples were left in an ultrasonic acetone bath for at least 15 minutes. This would most probably lead to the removal of the tribofilm which is weakly bonded to the DLC coatings.

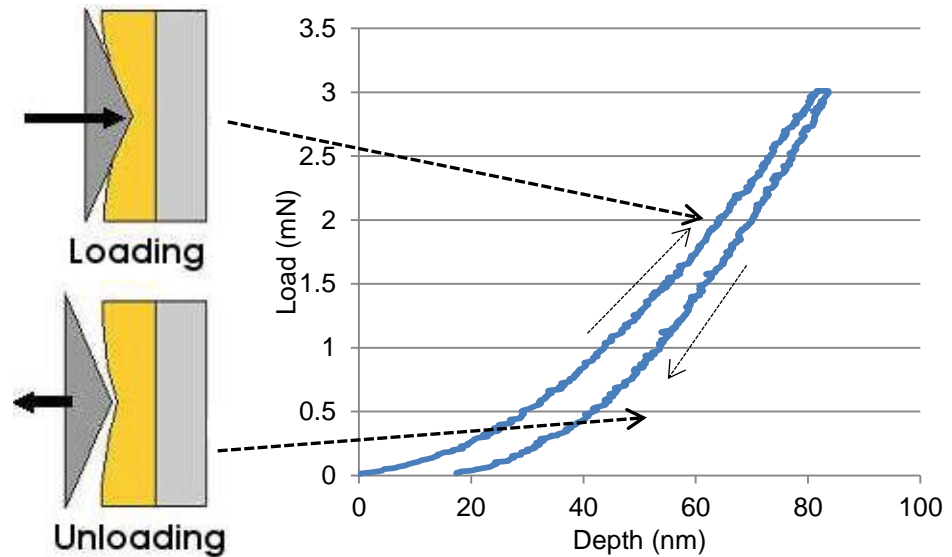


Figure 4-5 Typical loading/unloading curve obtained using Nanoindentation on the as-deposited a-C:15H coating.

A commonly used rule of thumb is to limit the indentation depth to less than 10% of the thickness of the coating to eliminate the “substrate effects” [264, 265]. Therefore, in this study, the indentation load was set at 5 mN, resulting

in a maximum indentation depth of 80-120 nm in the coating (In this study the thickness of as-deposited DLC coating was about 2.5 μm). Loading and unloading was performed for 30 s with a 5 s hold at pick load. A thermal drift correction of 60 s at 90% unloading was used so that the material could settle within temperature variations caused by the indentation process. A standard indentation grid of four rows by three columns (50 μm spacing) was chosen arbitrarily and was applied to all samples. The indenter was tested regularly for accuracy using a standard silicon plate that has known hardness values.

4.5.6. X-ray Photoelectron Spectroscopy (XPS)

XPS analysis measurements were made on the tribofilm formed on the plate surfaces. This surface sensitive technique can analyse very top layer of the surface (5 nm depth). Any residual oil and/or contaminants were removed by soaking the samples in N-heptane for 10 seconds prior to the XPS analysis. An area of 500 μm \times 500 μm in the wear scar of the plates has been analysed using a monochromatized Al K $[\alpha]$ source in the XPS. Spatial mode was chosen to acquire all the spectra. The XPS survey scan was used to determine the type of elements present in the tribofilms (Figure 4-6a) The curves on the XPS peaks obtained from long scans (Figure 4-6b) were fitted using CasaXPS software [266] and the quantitative analyses of the peaks were performed using peak area sensitivity factors. The chemical species corresponding to each binding energy have been found using a handbook of XPS [267]. The position of C1s peak (284.8 eV) was considered as the reference for charge correction. The peak area ratio, difference between binding energies of the doublets, and full-width at half-maximum (FWHM) were constrained to provide the most appropriate chemical meaning. A linear background approximation was used to process the data in this study.

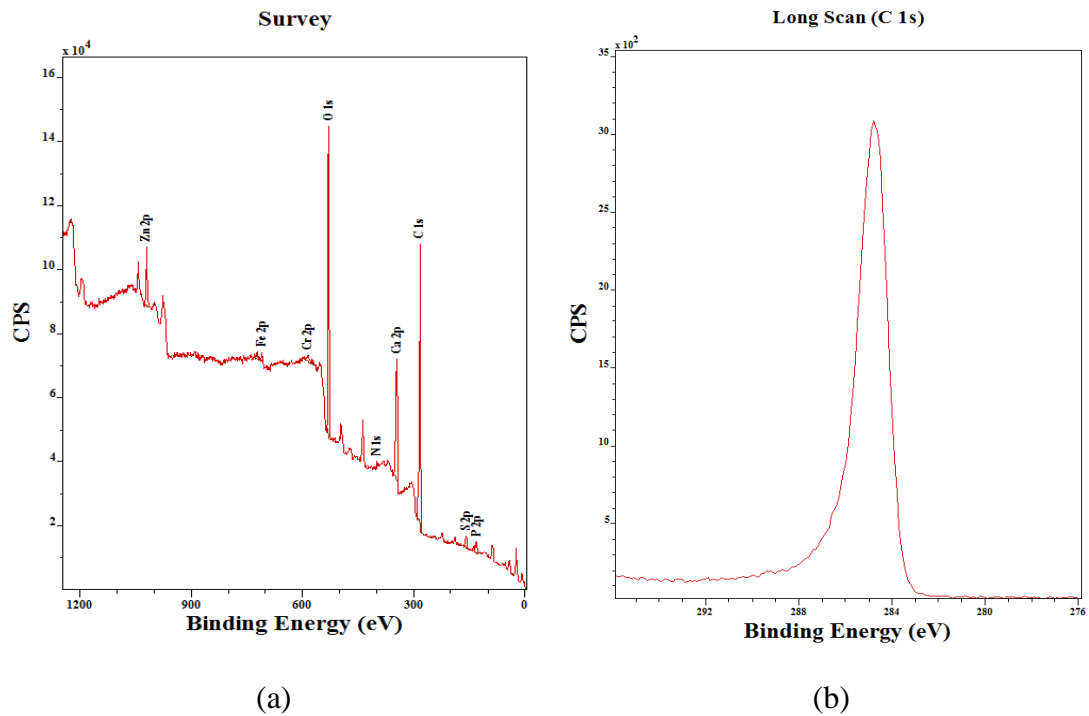


Figure 4-6 Typical survey scan (a) and long scan (b) XPS spectra.

4.5.7. Raman Spectroscopy

Raman Spectroscopy has been used as a technique to characterize DLC coatings, and their wear debris in the literature [198, 268, 269]. Renishaw inVia Raman microscope was used to analyse the structural modifications of the a-C:15H coating and nature of the layer transferred to the CI pin. The excitation wavelength used was 325.02 nm and the spectra were acquired with 10% power filter. The current intensity was controlled in order to achieve probing depth within 1 μm . The acquired Raman spectra usually comprised of distinct carbon peaks. In the Raman spectra recorded outside of the wear track, the G peak around 1580 cm^{-1} represents the graphite and D peak 1380 cm^{-1} represents the disorder-condensed benzene rings in amorphous carbon [198, 269]. The spectra were fitted with Lorentzian-Gaussian distributions associated with the peaks commonly found in amorphous hydrogenated carbon (Figure 4-7).

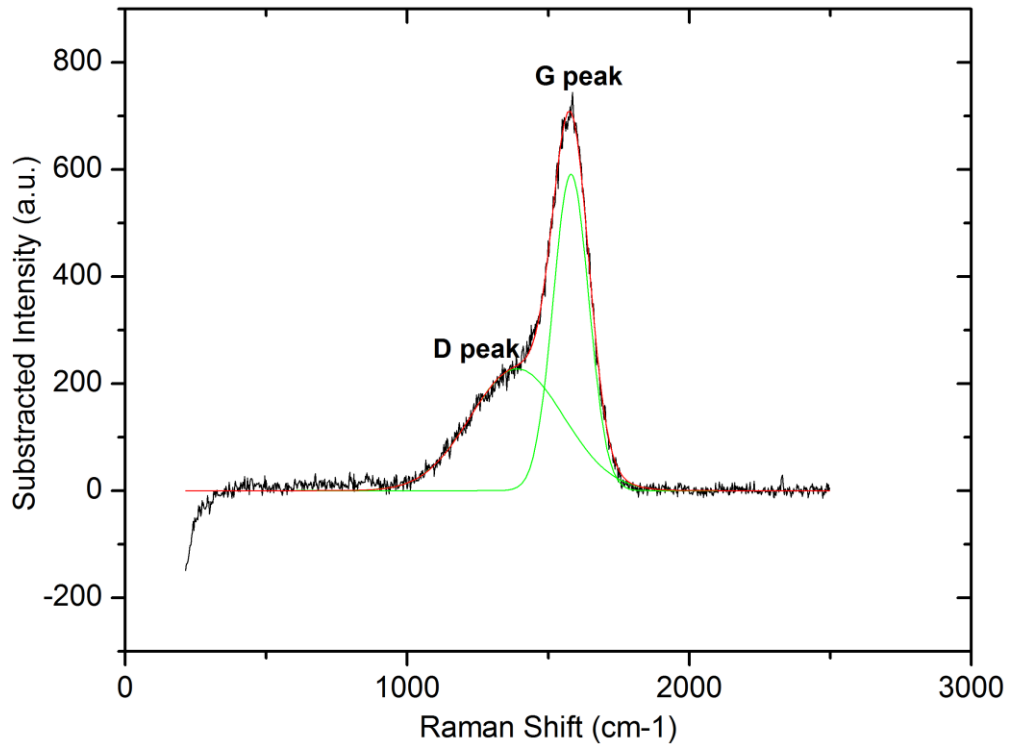


Figure 4-7 A typical Raman spectra and Gaussian curve-fitting obtained from as-deposited a-C:15H coating.

In Figure 4-7, a Raman spectra and Gaussian curve-fitting obtained from as-deposited a-C:15H coating is shown. In the actual analysis, the ratio of the intensity between the D and G peaks is considered to characterise the structure of the a-C:15H coating, rather than considering the overall intensity taken from one location to another. It is reported that the relative intensity height of the D peak is related to the microcrystalline size of the graphitic cluster, where less-graphitic amorphous films have a lower H_D/H_G value [167, 270-272]. Therefore, higher values of the H_D/H_G ratio imply transformation of the a-C:15H coating into graphite in the a-C:15H matrix under the present boundary-lubricated conditions [198].

Chapter 5 Results: Phase I - Tribological performance and tribochemical processes in a DLC/steel system when lubricated in a fully formulated oil and base oil

5.1. Introduction

In phase I of the study, the overall view of the tribological performance of the a-C:15H coating/commercial fully formulated oil system in terms of friction, wear and coating durability under boundary lubrication conditions has been investigated and the tribological performance compared with that of an uncoated steel system. In this chapter, results obtained from pin-on-plate tests performed using a-C:15H coating and uncoated steel system lubricated with various fully formulated oils are presented.

Based on the published literature, most authors have used model oils (containing one or combination of additives) rather than more realistic fully formulated oils. Obviously, the interaction between different additives in a fully formulated oil could result in antagonistic or synergistic effects which affects the tribological behaviour of the contacts in a real engine. For the above reason, in this study, fully formulated oils were used which could provide a more realistic evaluation of DLC/lubricant interaction.

Two material systems namely steel/CI, a-C:15H/CI were used for the pin-on-plate tests. Eight oils designated as Base, PAO, FF1+, FF2+, FF3+, FF1-, FF2- and FF3- were used in this study. The properties of materials and coatings, geometry of the samples, coating deposition techniques, and oil compositions are described in Chapter 4 and the test duration was 6 h in Phase I of the study. All tests have been conducted at least three times and the results were observed to be repeatable. The map of the study which is conducted and presented in this chapter is shown in Figure 5-1.

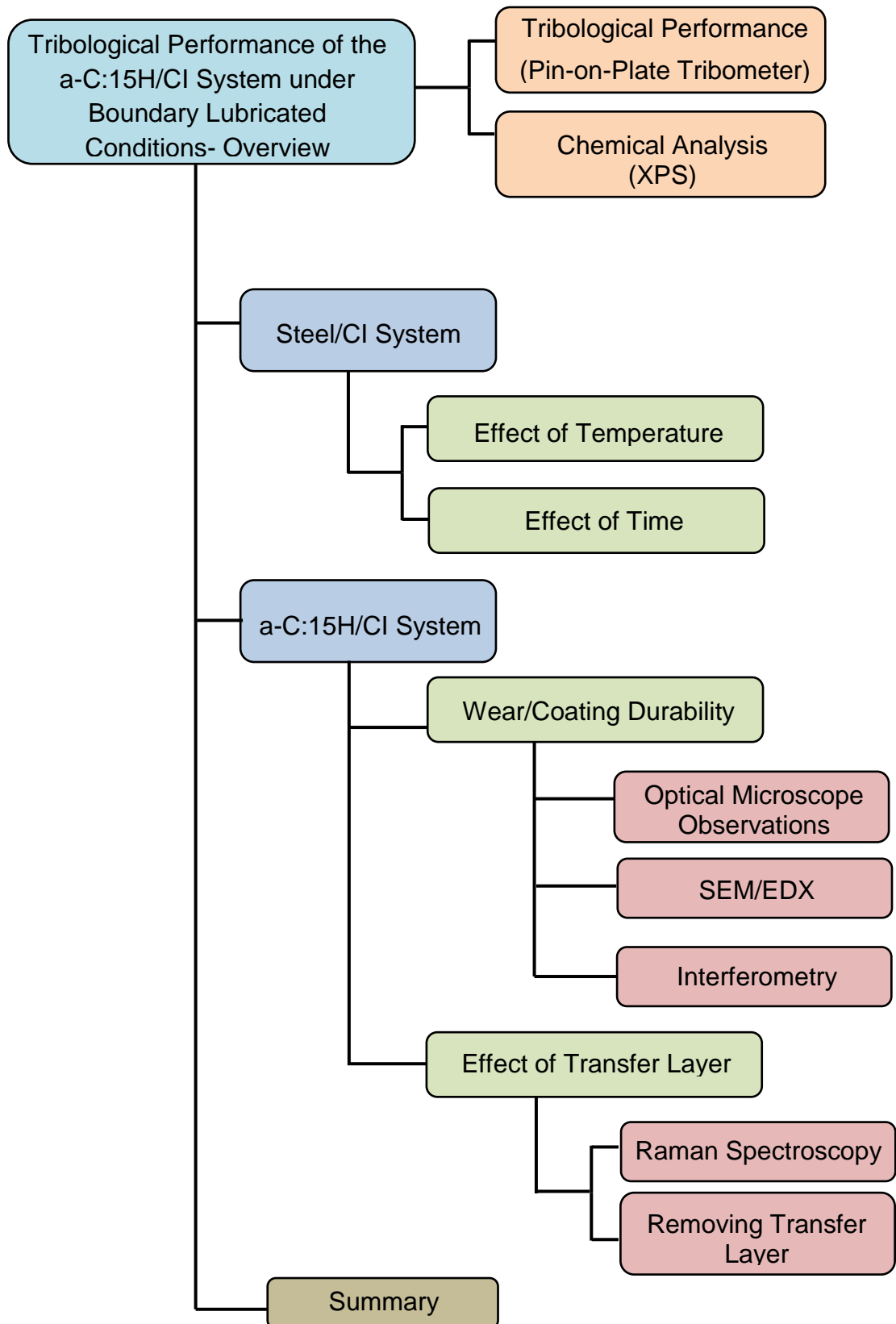


Figure 5-1 Map of the study which is presented in this chapter.

5.2. Tribological Performance of the Steel/CI System

5.2.1. Friction Results

In Figure 5-2, the friction results of the steel/CI system as a function of time using eight different fully formulated oils are presented. Based on the friction traces, it can be seen that all the fully formulated oils followed a similar trend with time. However, Base oil (Base group III) showed an increase in friction with regards to time. Generally, all oils exhibited a high friction coefficient of above 0.1.

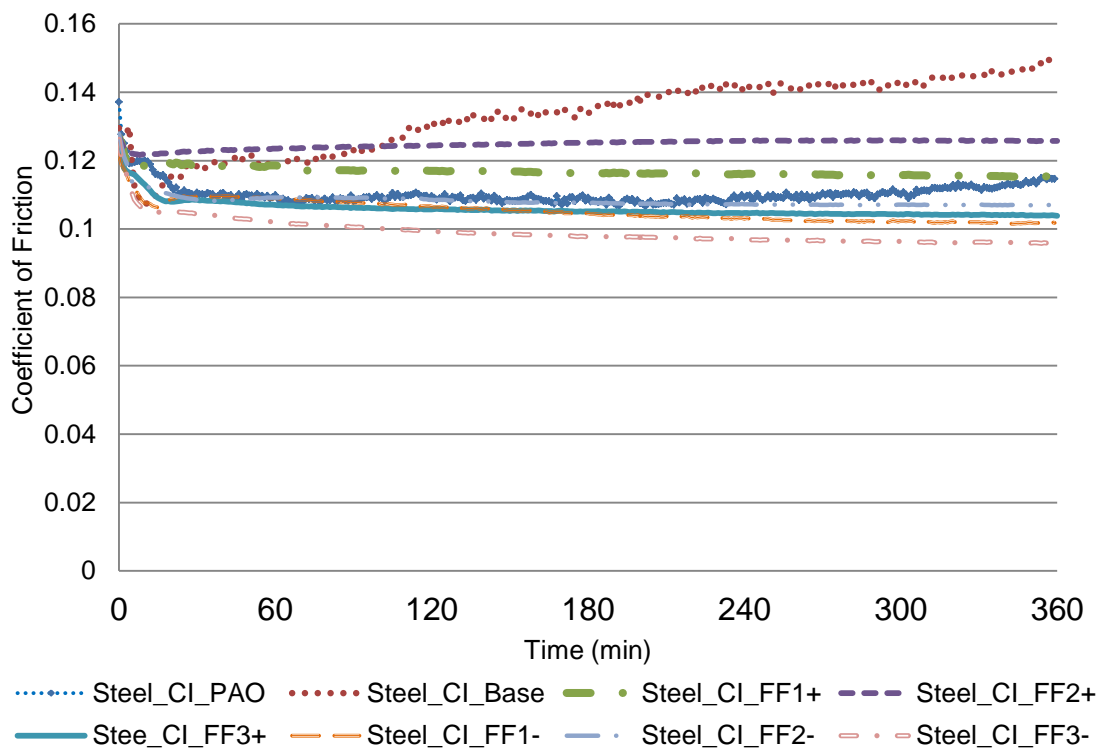


Figure 5-2 Friction coefficient as a function of time for the steel/CI system lubricated in oils.

In addition, the steady state coefficients of friction (i.e. last hour of the tests) as a function of different fully formulated oils for steel/CI system are shown in Figure 5-3. Based on the obtained results, ZDDP increased friction and FM decreased friction for most of the cases. However, despite the presence of FM in the oils (except for FF2+ and FF2-), none of the oils showed any significant friction drop with time and all fully formulated oils gave relatively

high friction in the range of 0.1 to 0.12. Among ZDDP-containing FF oils, FF2+ showed higher friction compared to FF1+ and FF3+ oils. It was also the case for ZDDP-free oils where FF2- showed higher friction value compared to FF1- and FF3- oils. This was not surprising as there was no Friction Modifier (FM) in FF2+ and FF2- oils formulation. In fact, ZDDP-containing FF2+ showed high friction values in the range of PAO and Base oil group III. Based on the friction results for steel/CI system, it was also seen that the presence of ZDDP in the formulated oils increased friction values in comparison to ZDDP-free oils as has been widely reported for steel systems [48, 55-58].

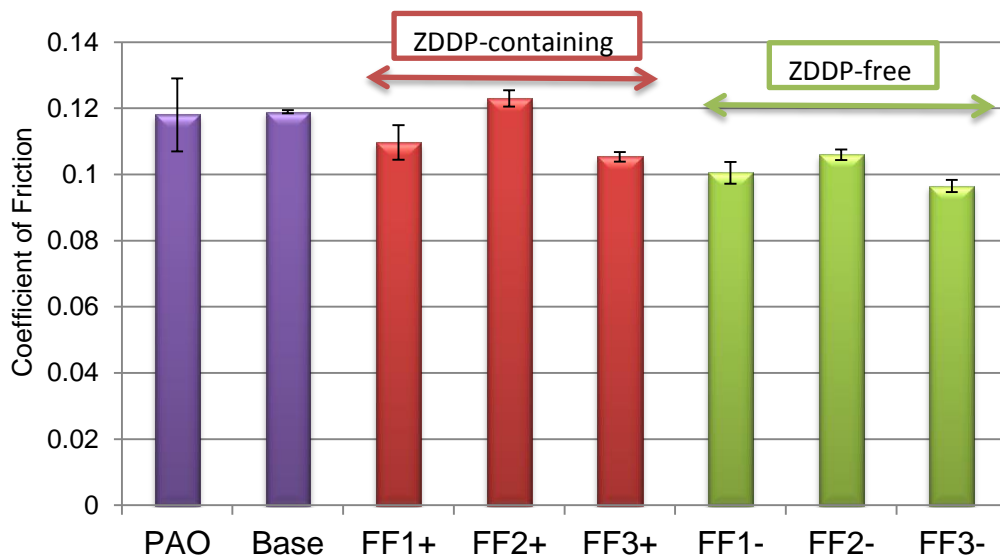


Figure 5-3 Steady state friction coefficients as a function of FF oils for steel/CI system.

5.2.1.1. Effect of Temperature

All fully formulated oils showed relatively high friction in the range of 0.1 to 0.12 and the presence of FM did not offer any significant improvement in friction behaviour of steel/CI system. It could be argued that friction modifiers were not functioning at the given experimental conditions. It was shown that, in the steel/lubricant system, increasing temperature above 100°C, resulted in lower steady state friction values than tests with lower temperatures [97, 114]. To prove this supposition, tests were performed using FF3- oil at

100°C and 140°C. Tests performed using FF3- at 140°C showed almost the same friction as that obtained at 100°C (Figure 5-4). This was in contrast with the findings of Yamamoto *et al.* [97] where with the oil containing MoDTC, increasing the temperature from 100°C to 120°C resulted in friction reduction from 0.07 to below 0.05.

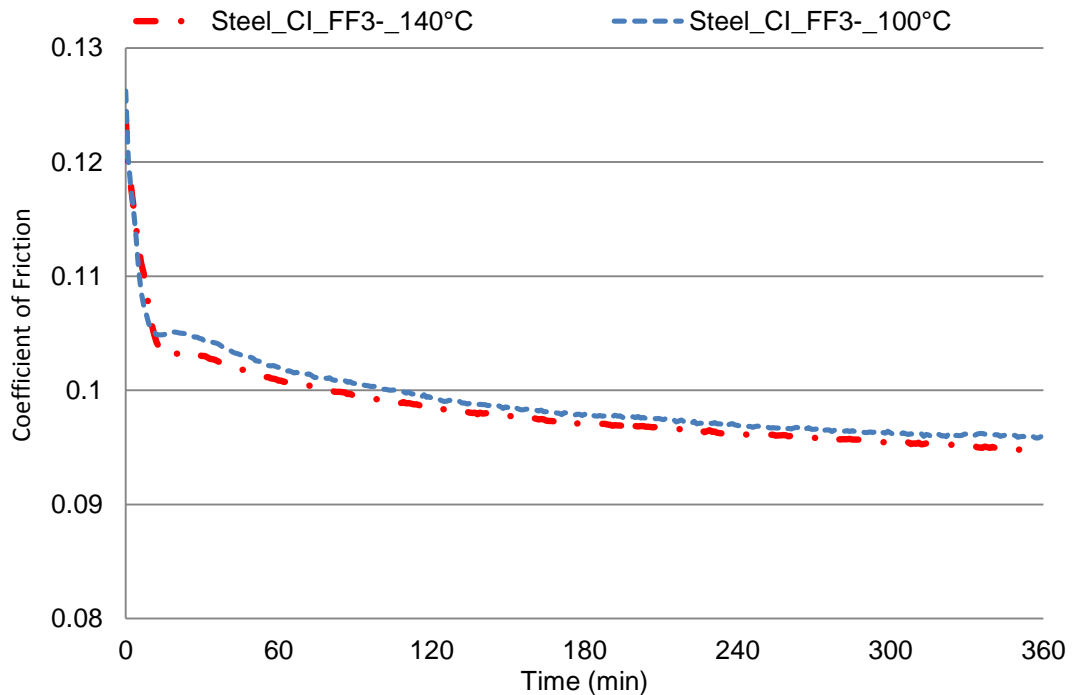


Figure 5-4 Effect of temperature on coefficient of friction as a function of time in a steel/CI system lubricated in FF3-.

5.2.1.2. Effect of Time

In this phase of the study, the tribo-tests were performed for 6 h and no drop in friction was observed using any of the fully formulated oils. Therefore, in order to find out the potential effect of the test duration on the friction performance of different oils, tests for FF3- (FM containing but ZDDP-free) which provided comparatively lower friction than other oils after 6 h tests, were continued longer (20 h). This was carried out to elucidate whether or not increasing the test duration facilitates the formation of a low friction tribofilm on the surface and lower friction as a result. Figure 5-5 shows the friction response with respect to time. Based on the obtained results, no significant difference in terms of friction was observed even after 20 h tests.

It could be argued that the low concentration of the FM additive in the oils and the presence of other additives could potentially affect the low friction film formation on the surface. Chemical analysis of the surfaces post tribo-tests could support the observed friction behaviour which will be discussed later in this chapter.

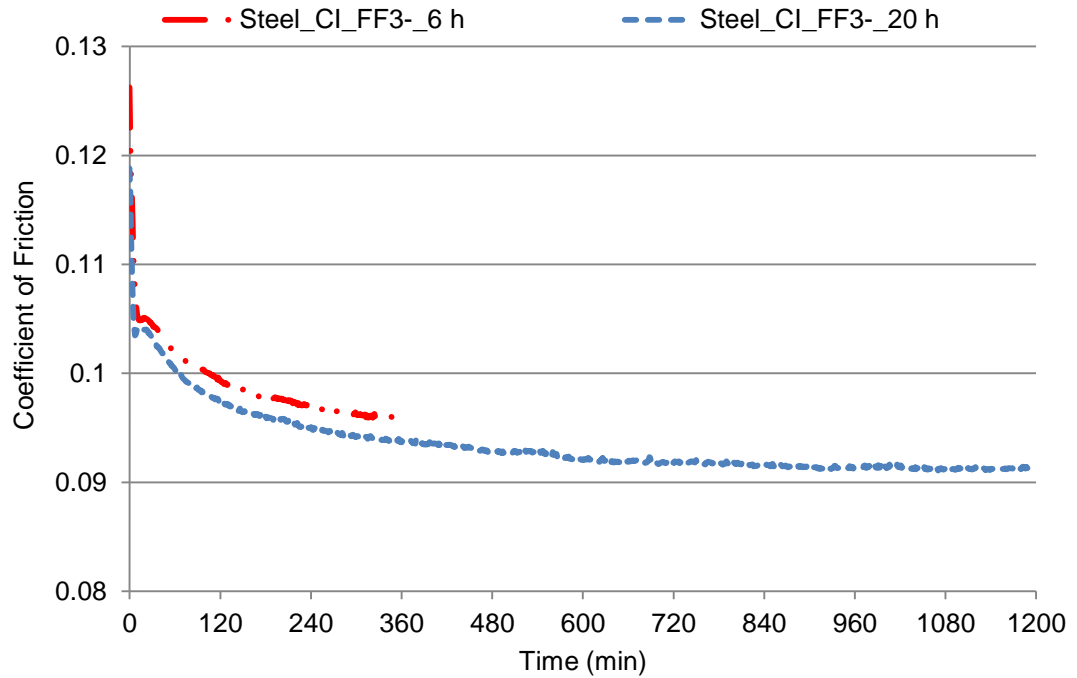


Figure 5-5 Effect of time on coefficient of friction as a function of time in a UC steel/CI system lubricated in FF3-.

5.3. Tribological Performance of the a-C:15H/CI System

5.3.1. Friction Results

The friction coefficient as a function of time for the a-C:15H/CI combination using eight different oils is given in Figure 5-6. All fully formulated oils followed the same trend with regards to time and no friction variation was seen with time whereas, interestingly, a drop in friction was observed when PAO and Base oil (group III) with no additives were used. Additive-free PAO showed a drop in friction 2 h after the start of the tests giving the lowest steady state coefficient of friction of all the oils in the a-C:15H/CI system.

Although this low friction was obtained at the cost of high wear which will be explained in detail later in the section 5.3.2 and 5.4.3 .

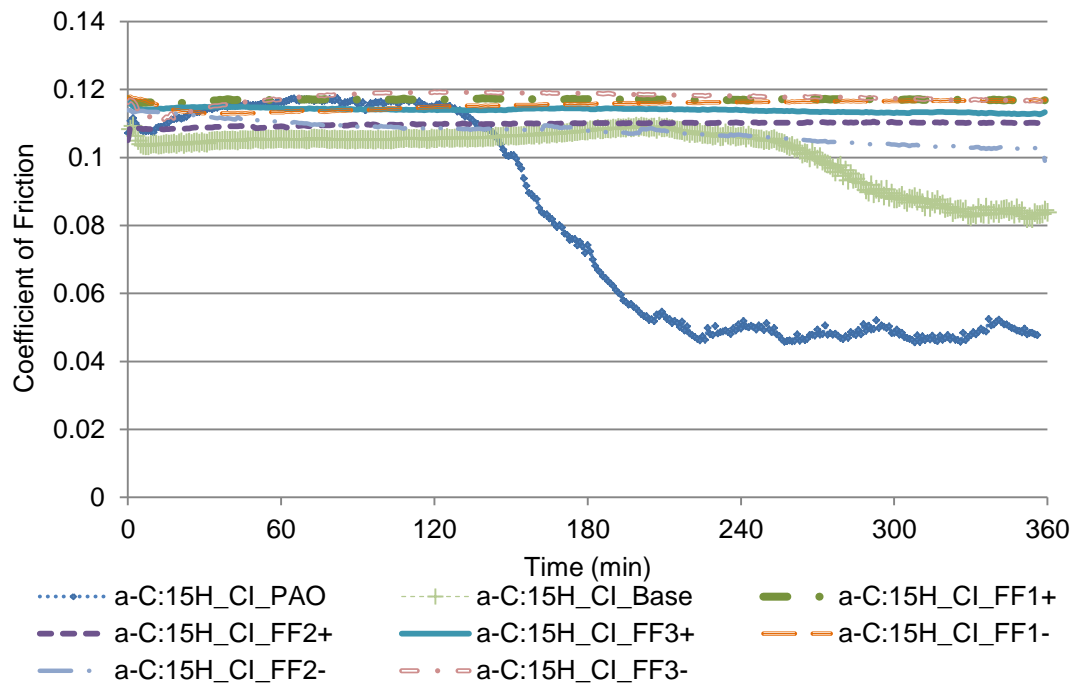


Figure 5-6 Friction coefficient as a function of time for the a-C:15H/CI system lubricated in oils.

In addition, the average steady state friction (i.e. the last hour of the tests) as a function of different oils for a-C:15H/CI system are presented in Figure 5-7. Overall, base oils and additive-containing fully formulated oils behave in a completely different manner to the a-C:15H/CI system. In general, additive-free base oils gave lower friction than fully formulated oils. PAO, in particular, provided the lowest friction when used in a-C:15H/CI system. Using fully formulated oils, FF2+ and FF2- showed lower friction than other fully formulated oils which is opposite to what was seen in steel/CI system and the friction values obtained using FF2- oil was lower than FF2+ whereas for other fully formulated oils and considering the error bars the presence of ZDDP in the oils did not significantly affect the friction values. Nevertheless, it is evident that Mo-FM was not effective in friction reduction of a-C:15H/CI as oils containing FM showed even higher friction than FM-free oils. However, it should be borne in mind that the Mo-FM concentration in FF1+/FF1- and FF3+/FF3- was only 40 and 60 ppm, respectively. This could

be the main reason for the obtained friction values which were quite high for both DLC and steel systems compared to typical friction values reported in the literature and will be discussed in the discussion (Chapter 7) in detail.

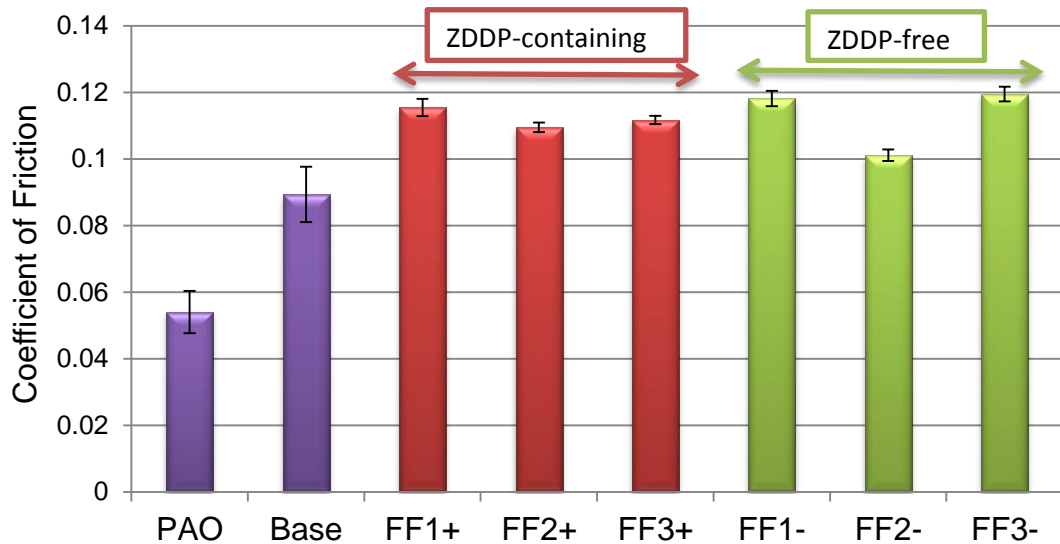


Figure 5-7 Steady state friction coefficients as a function of FF oils for a-C:15/CI system.

5.3.2. Coating Durability and Wear Performance

5.3.2.1. Optical Microscope/ SEM Images

The wear of the plates on both a-C:15H/CI and steel/CI systems using fully formulated oils was observed to be very low making the wear measurements extremely difficult. Figure 5-8 shows typical images of the wear scar; it is evident that the extent and mechanisms of wear is dependent on the type of lubricant and additive-containing oils showed improved wear performance of DLC coatings.

Obviously, PAO (Figure 5-8a) and Group III base oil (Figure 5-8b) showed much higher wear of the a-C:15H coatings with some evidence of delamination across the wear scar whereas using fully formulated oils (Figure 5-8c-f) there was no delamination; rather, the wear of the coatings was dominated by gradual polishing wear.

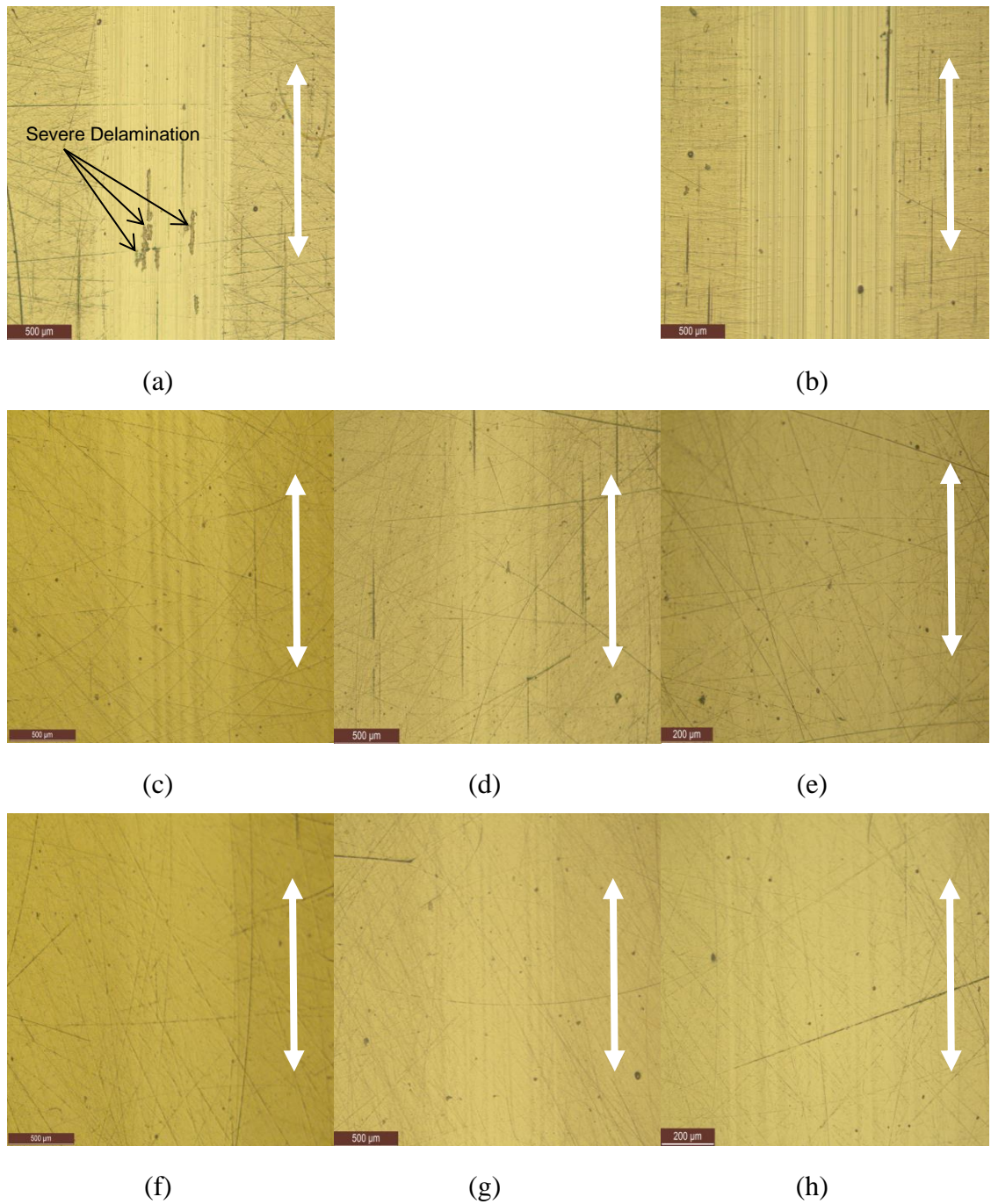


Figure 5-8 Optical images of the wear scars formed on the a-C:15H coated plates using (a) PAO, (b) Base oil Group III, (c) FF1+, (d) FF2+, (e) FF3+, (f) FF1-, (g) FF2- and (h) FF3-. The arrows on the right side of the images show sliding directions.

In addition, SEM analysis was carried out in the wear scars of the a-C:15H coated plate to investigate coating durability (Figure 5-9).

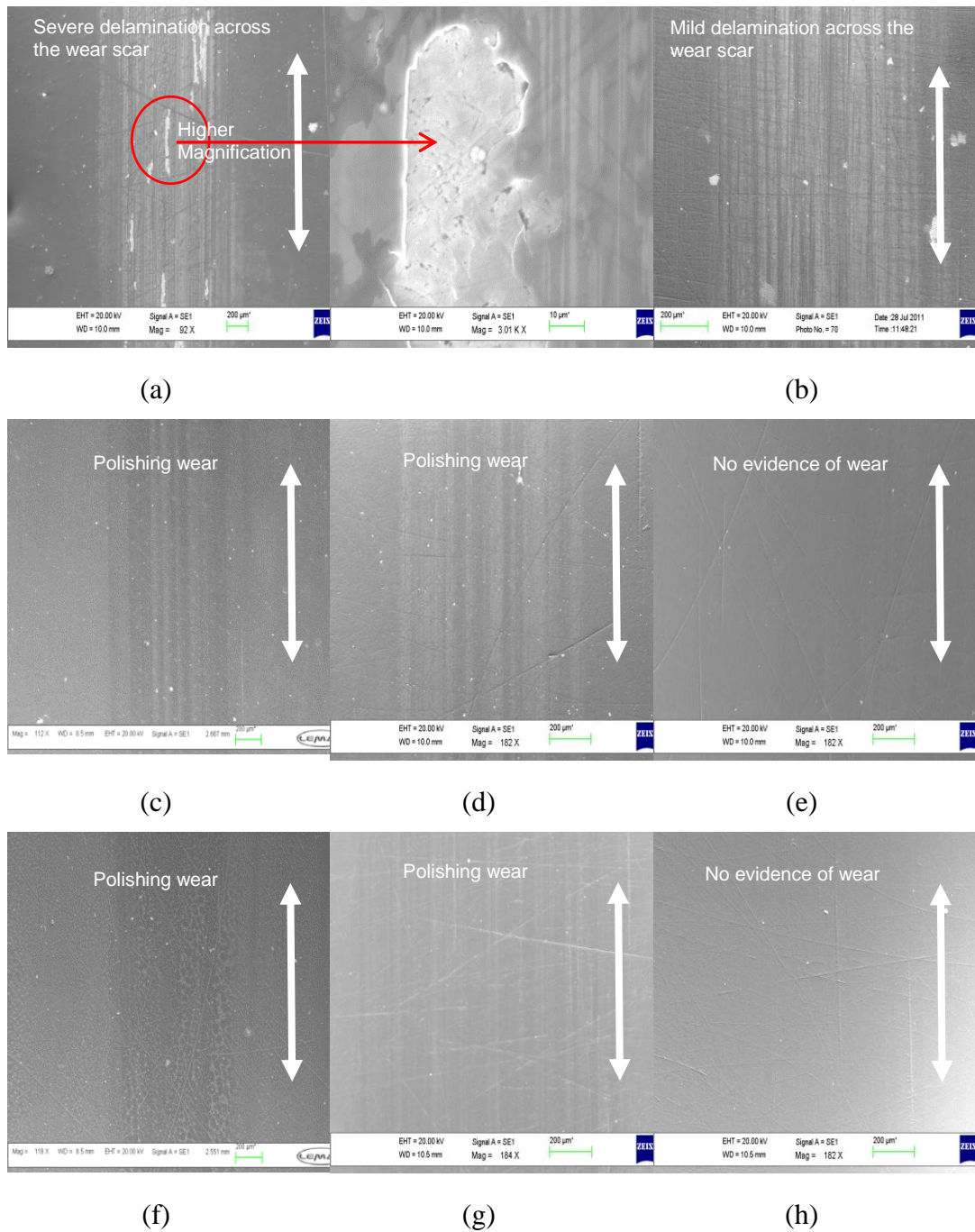


Figure 5-9 SEM images of the wear scars formed on the a-C:15H coated plates using (a) PAO, (b) Base oil Group III, (c) FF1+, (d) FF2+, (e) FF3+, (f) FF1-, (g) FF2- and (h) FF3-. The arrows on the right side of the images show sliding directions.

Observations from SEM images showed good agreement with the optical microscope images and wear results. Based on the optical microscope images and SEM images, severe delamination of the a-C:15H coating at

multiple regions was seen when lubricated in PAO (Figure 5-8a and Figure 5-9a) while Group III base oil (Figure 5-8b and Figure 5-9) gave limited delamination at some regions on the a-C:15H coated plate. In contrast in fully formulated oils (Figure 5-9c-f) no delamination was observed and the main wear mechanism involved was polishing.

As shown earlier, using fully formulated oils, the wear of the a-C:15H plates was not measurable and there was almost no variation in the roughness measurements suggesting that all fully formulated oils showed a good wear performance, and thus the wear rates of the DLC coated plates could not be compared after 6 h tests. However, it turns out that oils with 60 ppm of Mo-FM showed virtually no wear suggesting the positive effect of Mo-FM in the oil with low concentration and that for coatings lubricated with the ZDDP-containing oil wear was even lower (see Figure 5-8e and Figure 5-9e) as reported elsewhere [253]. FF1+, FF2+, FF1- and FF2- provided microscratches on the wear scar of the coating. The colour of the wear tracks was brighter than outside of the wear track suggesting an insignificant polishing wear of the DLC coating.

5.3.2.2. EDX Analysis

To verify the observations from SEM results and optical microscope images, EDX was carried out in the wear scar. It is important to note that, the SEM/EDX analysis in this study was performed to check the durability of coating, not to characterize tribofilms. Therefore tribofilm on the plates were removed using acetone prior to the SEM/EDX analysis.

EDX spectra obtained from inside the wear tracks showed presence of C and Cr. The difference between concentration of Cr in the wear tracks and outside of the wear tracks was used to identify the wear performance of various oils which are shown in Figure 5-10. The repeatability of the results for the coating durability was considered obtaining spectra in three different places across the wear tracks for tests using the same oil. Due to the fact that PAO showed severe delamination on the a-C:15H-coated sample plate, EDX analysis was performed outside the delaminated regions.

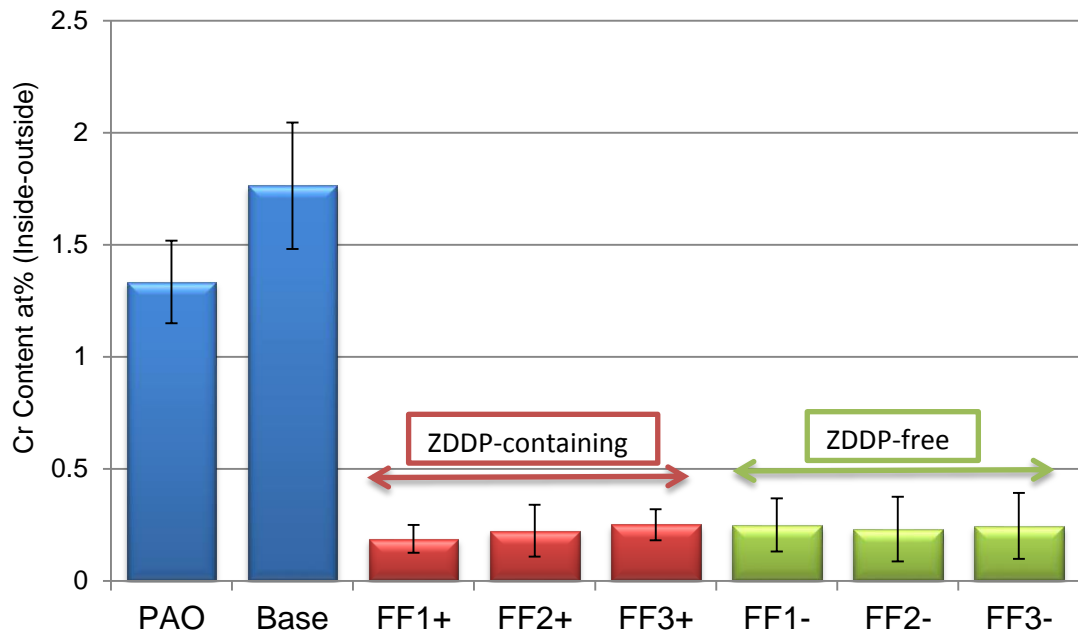


Figure 5-10 Difference between concentrations of Cr inside the wear tracks and outside of the wear tracks using various oils.

Based on the results, it is apparent that fully formulated oils showed very little difference in concentration of Cr implying very low wear on the coated plates which is in line with the initial observation and Optical/SEM images and explains why the wear on the plates were immeasurable using interferometer. Highest gradual wear was observed for additive-free base oil oils.

5.4. Overall System

As explained in previous section, tribological performance of the chosen oils on both steel and DLC system have been examined and reported. In this section, friction and wear and the tribochemistry involved in the obtained results are presented. In addition, an overall comparison between the performance of the oils on a-C:15H are made with that of steel system.

5.4.1. Friction Performance

The average friction coefficient values for the last hour of the test as a function of lubricant for a-C:15H/CI system versus steel/CI system are

plotted in Figure 5-11. This graph will facilitate a direct comparison between steel system with DLC system as a function of coefficient of friction. Shown in Figure 5-11, the friction values for steel/CI system and a-C:15H/CI system does not lie on the 45° line which means that the friction performance of all the oils are different for the steel/CI in comparison with the a-C:15H/CI system.

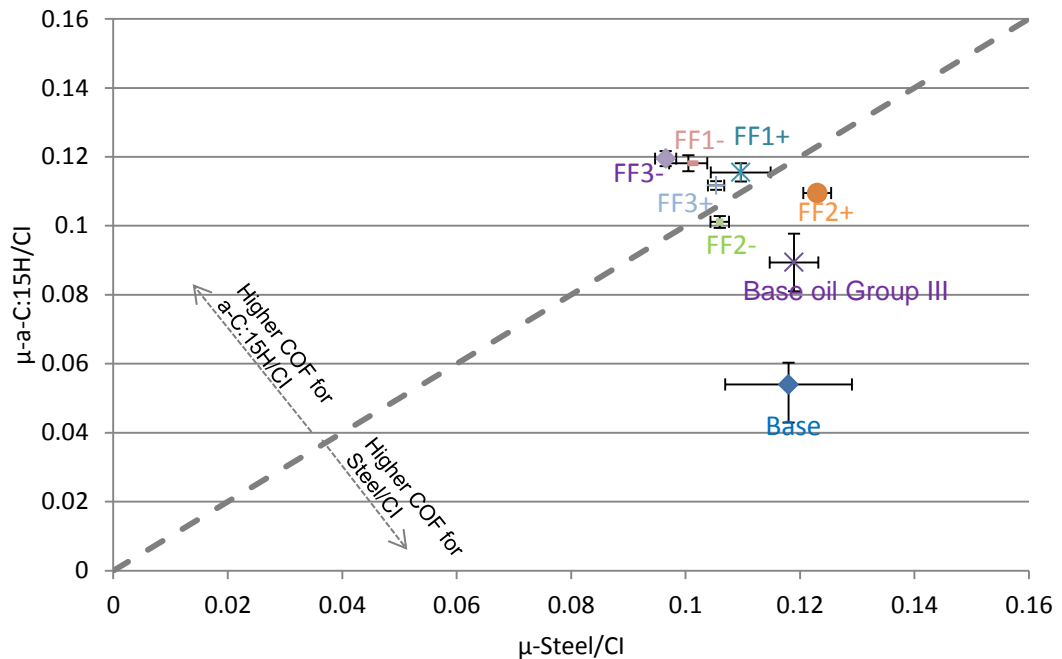


Figure 5-11 Steady state friction coefficients as a function of lubricants for a-C:15H/CI system versus Steel/CI system.

Overall, friction behaviour was observed to be oil dependent for both systems. Base oils (PAO and Base group III) showed a better friction performance in the DLC system compared to the steel system. In addition, FM-free oils (i.e. FF2+ and FF2-) gave a lower friction than FM containing oils (i.e. FF1+/FF1- and FF3+/FF3-) in the a-C:15H/CI whereas it was opposite in the steel/CI system. In the steel/CI system, the presence of ZDDP in the fully formulated oils increased the friction in comparison to the ZDDP-free oils. In the DLC/CI system, however, the presence of ZDDP did not significantly affect the friction performance.

5.4.2. Pin Wear

The wear coefficients of the CI counterbodies for various oils are given in Figure 5-12. In general, using fully formulated oils, pin wear rates were lower for the steel/CI system compared to a-C:15H/CI system. Regardless of the tribological system, ZDDP-free oils protected the CI pins better compared to ZDDP-containing fully formulated oils. This suggests that ZDDP is less effective in wear protection of the counterbody when was used together with detergent, dispersant and antioxidant. PAO showed the highest pin wear in the steel/CI system, as expected. In the a-C:15H/CI system, however, PAO showed lower pin wear than additive containing fully formulated oils in the a-C:15H/CI system. That could be attributed to the high wear observed on the DLC plate when lubricated with PAO. The wear products from the high wear of the DLC plates which can have a graphitic nature [192] could protect the surface of the pin from further wear. The effect of this transfer layer and its formation on the tribological performance of a-C:15H/CI system will be explained in detail as in Chapter 7.

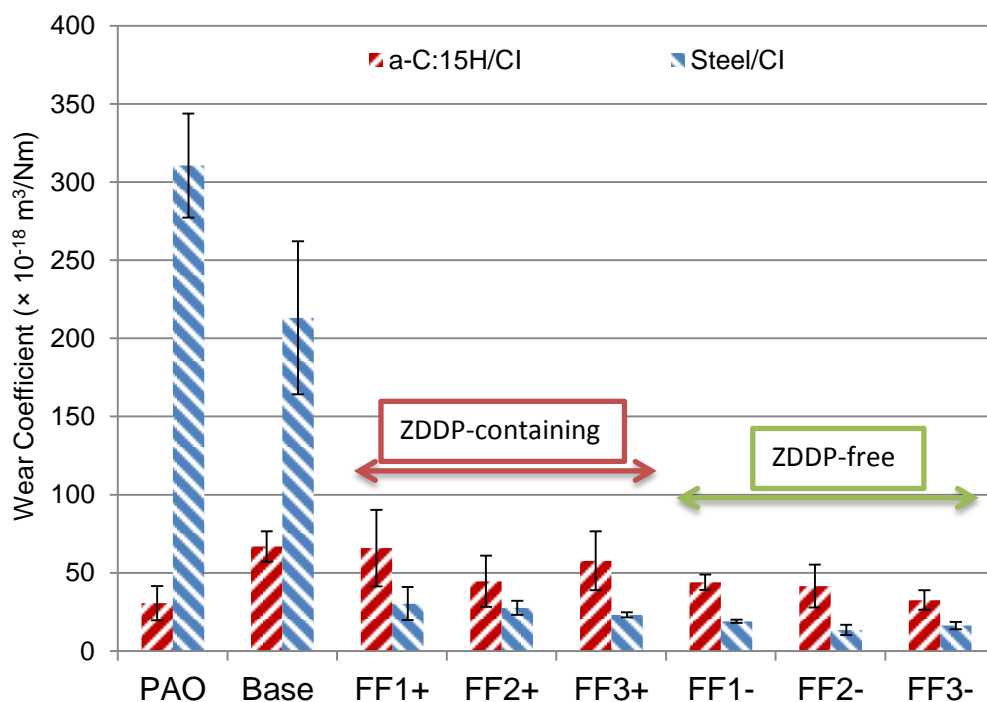


Figure 5-12. Dimensional wear coefficients as a function of lubricants for a-C:15H/CI system.

5.4.3. Effect of Transfer Layer

As explained in section 5-2, PAO and base oil group III showed a drop in friction in the a-C:15H system. In Figure 5-13, it is shown how wear products from a-C:15H are transferred to the counter body forming a layer on the pin when PAO and Base oil group III were used. The transfer material seems to accumulate around the edges of the wear scars on the pins.

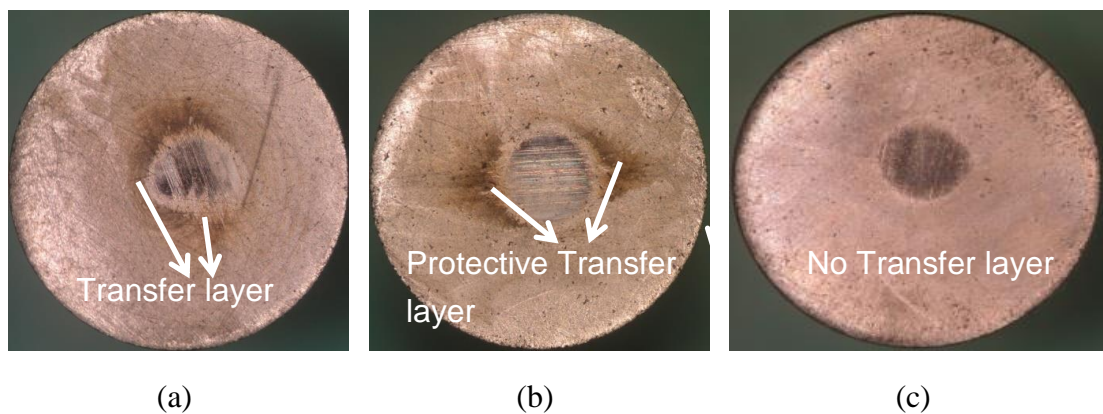


Figure 5-13 Transfer layer on the pin coming from the wear track of a-C:H coating when (a) PAO, (b) Base oil group III, (c) any of the fully formulated oils were used.

It should be noted that the transfer layer was not seen using any fully formulated oil (see Figure 5-13C). In order to investigate the possible effect of the transfer layer formed on friction reduction, the pin and the plate were cleaned by acetone every hour during the test to assure that no transfer material resided on the interface. The aim was to observe the effect of this layer on friction reduction and wear protection of the pin. In Figure 5-14, the friction response after the transfer material was removed every hour during the test, is shown. Resuming the tests after removing the formed transfer layer from the pin and the plate, friction dropped almost immediately. This suggests that the preconditioned a-C:15H surface facilitate regeneration of the transfer layer leading to low friction performance.

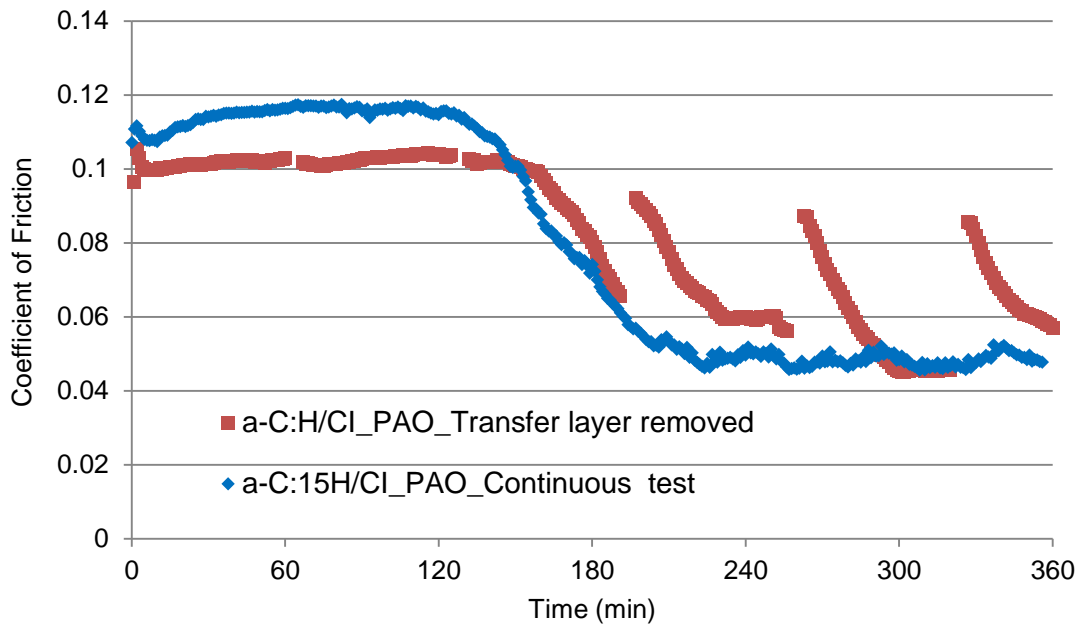


Figure 5-14 Friction response after cleaning transfer material every hour during the test.

In Figure 5-15 the steady state friction as a function of pin wear is shown. It can be seen that removing the formed transfer layer during the test not only hindered friction reduction but increased the pin wear.

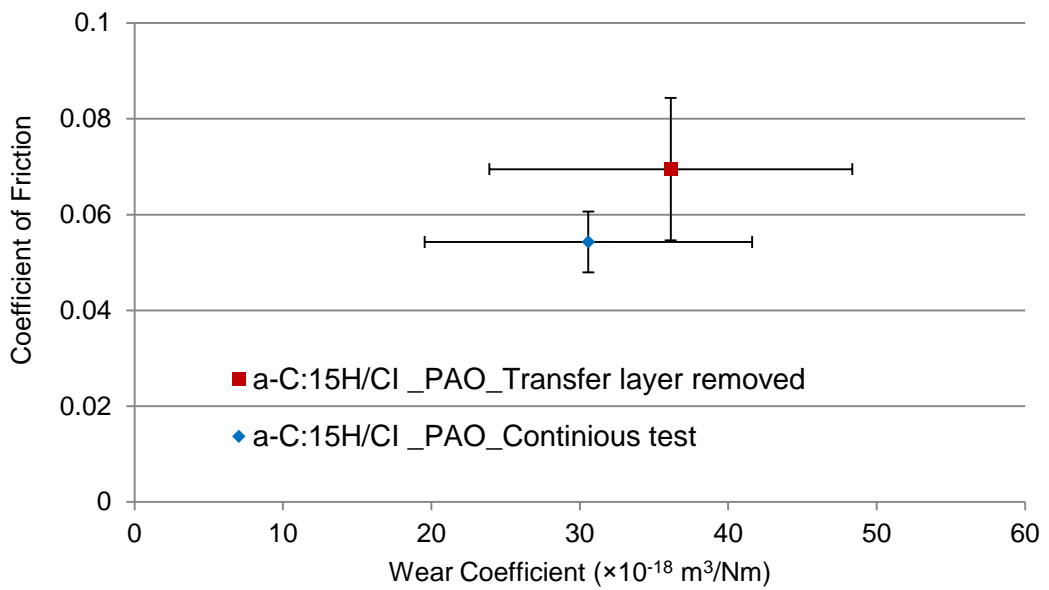


Figure 5-15 Effect of cleaning transfer layer on friction and wear.

Therefore, based on the results shown in Figure 5-14 and Figure 5-15, the positive effect of the formed transfer layer on friction reduction and reducing the wear of CI counterpart is evident. This could explain why using PAO the coefficient of friction and the wear rate is lower than those obtained by fully formulated oils. In order to understand the structural modifications of a-C:15H within the wear track and the nature of wear debris transferred to the CI counterbody from the worn a-C:15H coating, Raman spectroscopy analysis was performed in the wear scars of the a-C:15H coating and CI pin. Figure 5-16 shows Raman spectra obtained using PAO from: (a) outside of a-C:15H coating wear scar, (b) inside of a-C:15H coating wear scar, (c) transfer material on the pin and (d) out of wear scar of pin.

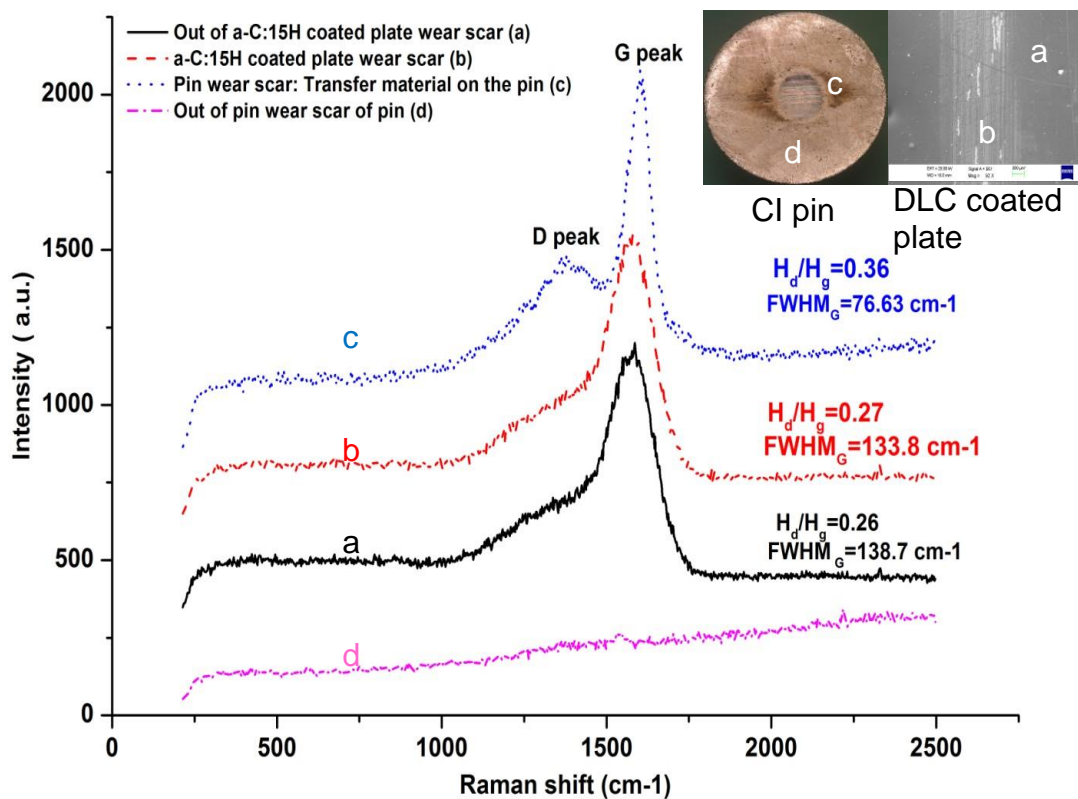


Figure 5-16 Raman spectroscopic analysis on the samples obtained using PAO. H_d and H_g are the intensity height of D and G peaks, respectively. The coloured boxes on the optical image of the CI pin and the SEM image of a-C:15H coating show the sites where the Raman analyses were carried out.

As shown in Figure 5-16, the value of the ratio H_d/H_g and the full-width at half-maximum (FWHM) of the G peak show insignificant difference within and outside the wear scar of the a-C:15H coating suggesting that no structural modifications of the a-C:15H coating due to the tribological test in the wear scar have occurred or that there was no detectable graphitic layer on the a-C:15H coating. However, distinct G and D peaks were detected in the wear scar on the CI pin, and no such peaks were observed outside the wear scar. The H_d/H_g ratio for the transfer material on the CI pin was found to be higher than a-C:15H coating and the FWHM of the G peak decreased, which indicates that the transfer of the material to the CI pin was more of graphitic nature material.

Furthermore, the D and G peaks were not found in the spectrum taken from outside the wear scar of the CI pin suggesting that the graphite flakes, which are normally present in the microstructure of the cast iron, did not participate in the formation of the transfer layer on the pins. It appears that the graphite present in the microstructure of CI was not sufficient to give a distinct G peak compared with the a-C:15H coating material [253].

5.4.4. Chemical Analysis of Tribofilms

Fully formulated oils contain different surface active engine oil additives, namely, friction modifier, anti-wear additives, detergents, dispersants, antioxidants, etc. Interaction between different additives could result in synergetic or antagonistic effects on the additive/surface interaction. This could make the tribochemistry of the system complex and difficult to understand [273].

Commonly-used friction modifiers and anti-wear additives are optimized to form tribofilms on ferrous surfaces. In ferrous surfaces, friction reduction is usually associated with the MoDTC activity. MoS₂ low friction sheets, derived from MoDTC decomposition, provide low friction at the tribological contacts [34-36]. ZDDP offers anti-wear properties by forming sulphide and phosphate containing tribofilms at the ferrous surfaces [35-37]. In addition,

MoDTC has been found to improve the wear resistance of the ferrous surfaces by forming N-containing species in the tribofilm [35].

Following the overall tribological performance of different FF oils, regardless of friction modifier being present in the formulation or not, friction reduction was not observed using any of the oils in both steel/CI and a-C:15H/CI system (i.e. FM was inefficient) while the wear performance of the a-C:15H coating was generally good.

In order to explain the observed tribochemical behaviour of different oils in both DLC and steel system, X-ray photoelectron spectroscopy (XPS) analyses were conducted on the wear scars formed on uncoated steel, and a-C:15H (DLC) coatings and their respective CI counterbodies to characterize the tribofilms where the X-ray penetrated several nanometers (~5nm) in the surface.

In this study, mainly due to time constraints, XPS analysis was only performed on FF2+, FF3+ and the corresponding ZDDP-free oils (i.e. FF2- and FF3-). Performing XPS analysis, the effect of FM on the tribofilm formulation could also be established as there was no FM blended in FF2+ and FF2- compared to FF3+ and FF3-. Argon etching was not performed in any of the cases as it is argued that the etched tribofilms may be damaged by irradiation, especially to sulphur species [36] which may result in misinterpretation of the low friction compound MoS₂, which is known to be responsible for friction reduction. XPS gives information of the outermost few nanometers of the tribofilm whereas MoDTC-derived MoS₂ can form clusters within the tribofilm which may not exist necessarily on the topmost surface. However, considering the friction response, MoDTC was not seen to take part in the film formation on both steel plates and CI pins using any of the MoDTC-containing oils. Figure 5-17 and Figure 5-18 show the survey scans on the tribofilms formed on the steel plates and CI pins, respectively.

In general, the tribofilm is mainly rich in oxygen. Based on the XPS quantification of the elements of the tribofilms formed both on steel and CI

pins by FF2+, FF3+, FF2- and FF3-, it can be seen that ZDDP derived elements (i.e. P and Zn) have been found on the steel plates and CI pins.

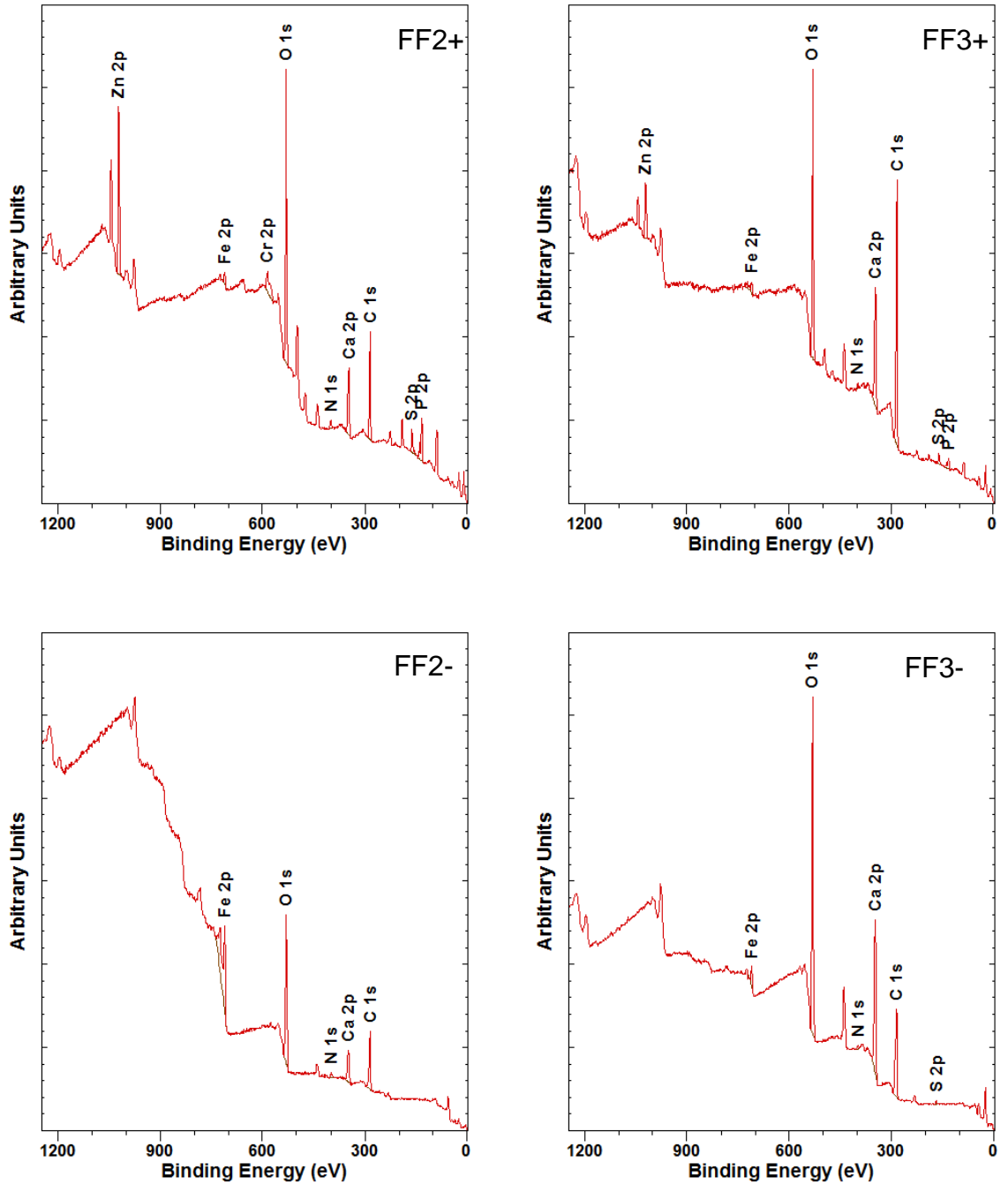


Figure 5-17 XPS survey scan for the tribofilms formed on the steel plates in steel/CI system.

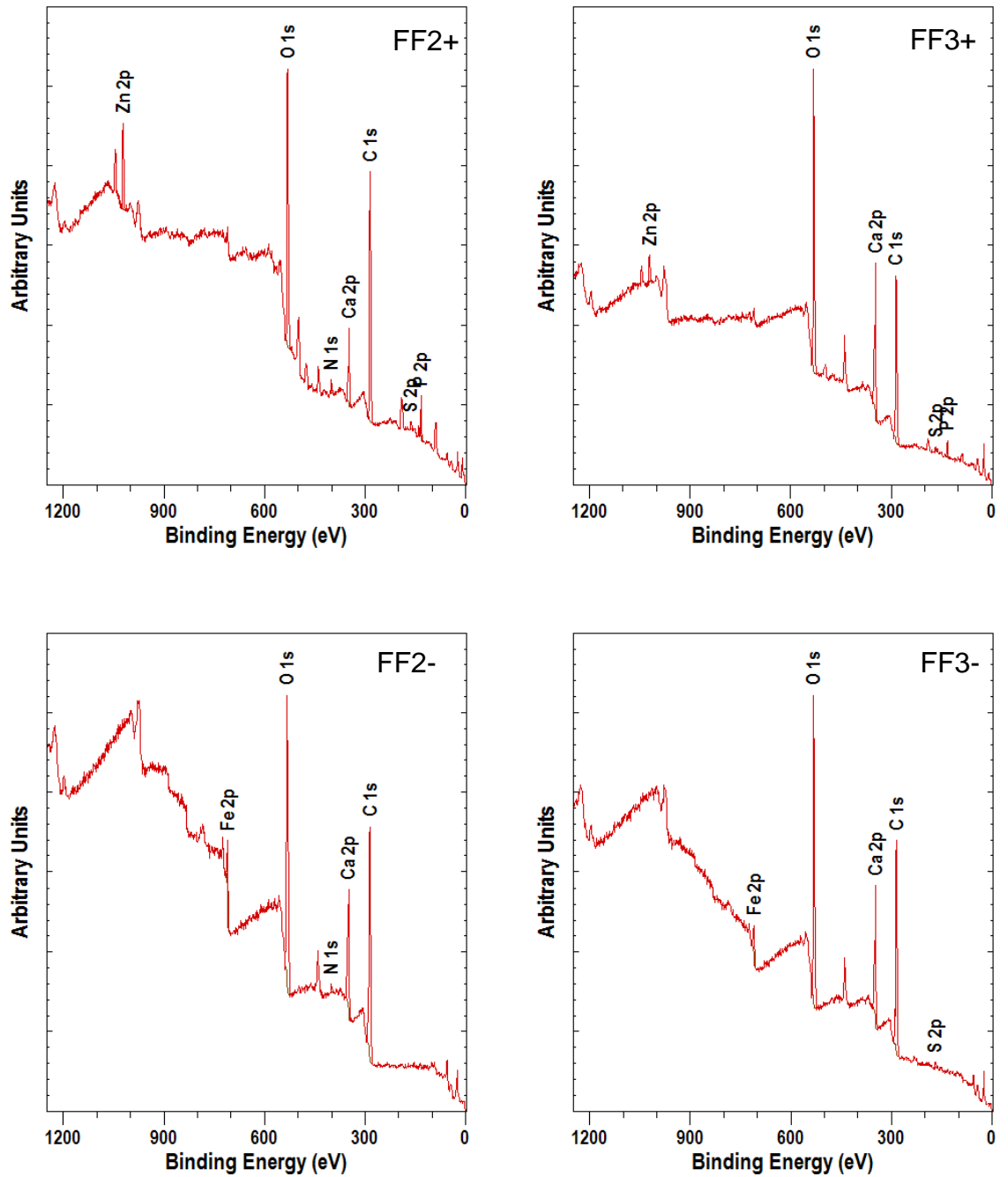


Figure 5-18 XPS survey scan for the tribofilms formed on the CI pins in steel/CI system.

In addition, detergent derived elements (N and Ca) were also found to contribute to the film formation on both steel plates and CI pins. In

Figure 5-19 and Figure 5-20, the survey scans on the tribofilms formed on the a-C:15H coated plates and the corresponding Cl pins, are given.

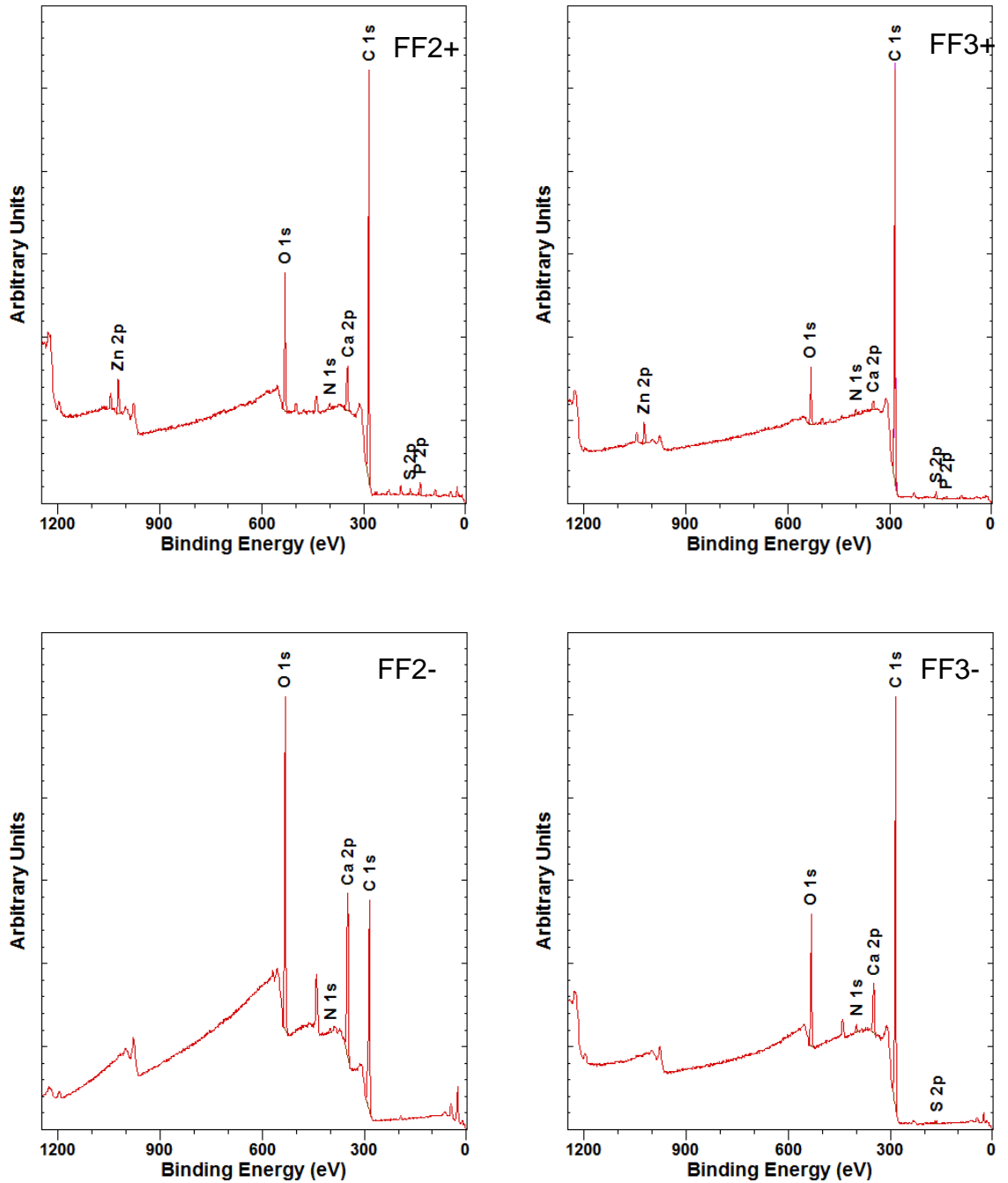


Figure 5-19 XPS survey scan for the tribofilms formed on the a-C:15H coated plates in a-C:15H/Cl system.

Based on the XPS quantification of the elements of the tribofilms formed both on a-C:15H coated plate and CI pins by FF2+, FF3+, FF2- and FF3-, the tribofilm is generally rich in carbon for the a-C:15H coated plates whereas Oxygen is more dominant on CI pins.

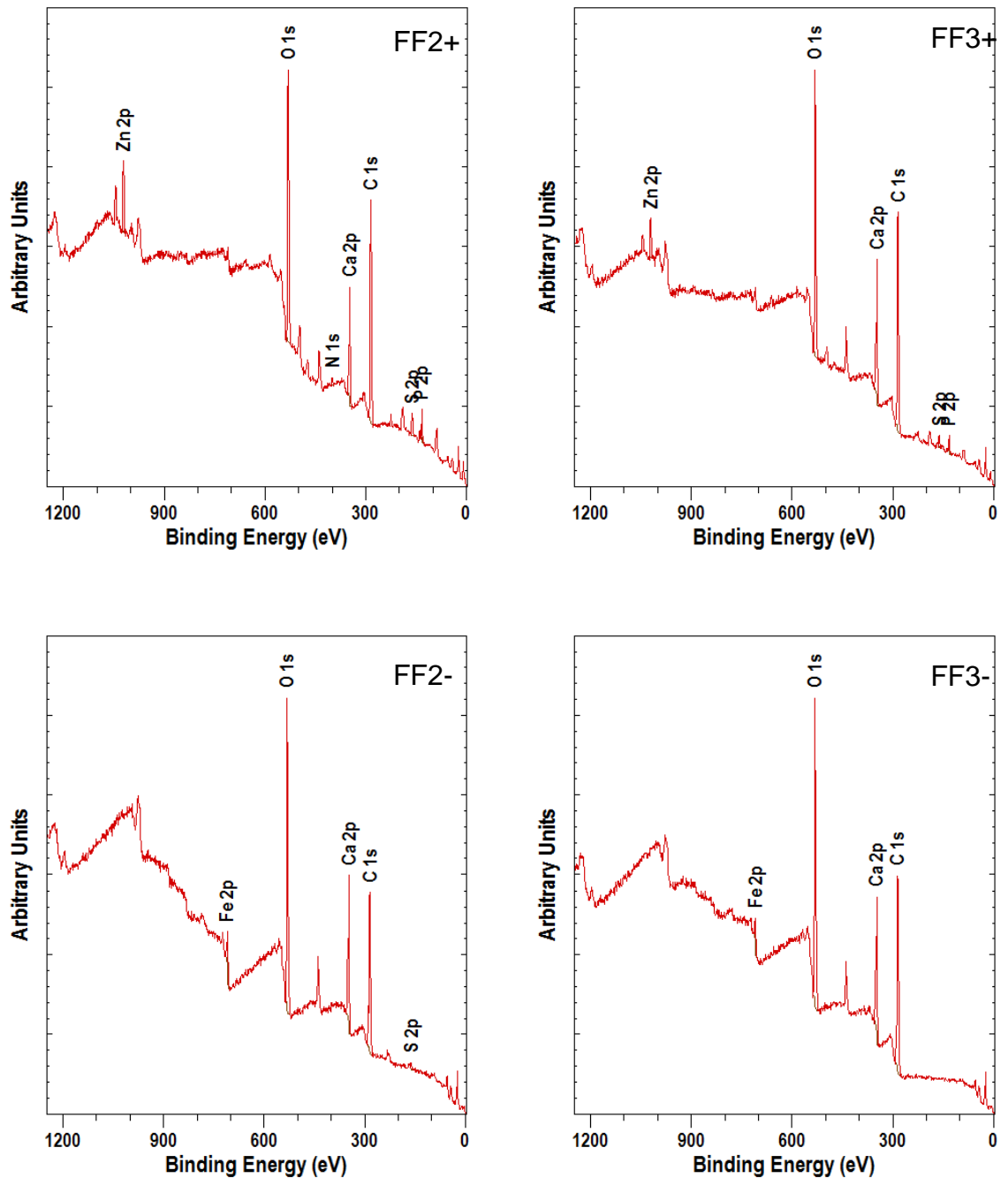


Figure 5-20 XPS survey scan for the tribofilms formed on the CI pins in a-C:15H/CI system.

In addition, other additive derived elements were also present in the tribofilm. In a similar manner to steel/CI system, P and Zn tribofilm has been formed on the a-C:15H coated plates and CI pins by ZDDP-containing oils while the absence of MoDTC-derived elements was evident on both a-C:15H coated plates and CI pins using any of the MoDTC-containing oils. Furthermore, detergent derived elements (N and Ca) contributed to the film formation on both a-C:15H plates and corresponding CI pins.

High resolution scans (long scans) of the elements are also carried out in order to provide a better picture of the species which are formed on the surface of the pins and plates. The binding energies of the main fitted peaks and corresponding chemical species for a-C:15H/CI and Steel/CI system are shown in table 5-1 to Table 5-4. It is evident that the amount of Mo 3d detected on the tribofilm formed from fully formulated oils is insignificant for both a-C:15H/CI and steel/CI systems.

Table 5-1 Binding energies, concentration of XPS and corresponding chemical in the tribofilms formed on steel plates in steel/CI system by oils FF2+, FF3+ and FF3-.

Oils	Binding Energies, chemical species and concentrations			
	S 2p	Mo 3d	P 2p	Zn 2p
steel plates				
FF2+	161.2 eV, Sulphide (100 %)	-	133.1 eV, pyrophosphate (100%)	1022.0 eV, ZnS/ZnO/Zn-phosphate (100%)
FF3+	160.8 eV, Sulphide (75.0 %) 167.5 eV, Sulphite (25.0 %)	Small to fit the curve	132.8 eV, pyrophosphate (100%)	1021.5 eV, ZnO/Zn-phosphate (100%)
FF3-	160.8 eV, Sulphide (10.9 %) 167.0 eV, Sulphite (59.3%) 168.9 eV, Sulphate (29.8%)	Small to fit the curve	-	-

Table 5-2 Binding energies, concentration of XPS and corresponding chemical in the tribofilms formed on CI pins in steel/CI system by oils FF2+, FF3+ and FF3-.

Oils	Binding Energies, chemical species and concentrations			
	S 2p	Mo 3d	P 2p	Zn 2p
CI pins				
FF2+	161.6 eV, Sulphide (100 %)	-	133.0 eV, pyrophosphate (100%)	1022.2 eV, ZnS/ZnO/Zn-phosphate (100%)
FF3+	161.1 eV, Sulphide (57.4 %) 167.9 eV, Sulphate (42.6 %)	Small to fit the curve	132.8 eV, pyrophosphate (100%)	1022.0 eV, ZnS/ZnO/Zn-phosphate (100%)
FF3-	160.9 eV, Sulphide (34.5 %) 168.0 eV, Sulphate (65.5%)	Small to fit the curve	-	-

Table 5-3 Binding energies, concentration of XPS and corresponding chemical in the tribofilms formed on a-C:15H coated plates in a-C:15H/CI system by oils FF2+, FF3+ and FF3-.

Oils	Binding Energies, chemical species and concentrations			
	S 2p	Mo 3d	P 2p	Zn 2p
a-C:15H coated plates				
FF2+	163.6 eV, Sulphide (21.6%) 162.1 eV, Sulphide (29%)	-	133.7 eV, metaphosphate (100%)	1022.5 eV, ZnS/ZnO/Zn-phosphate (100%)
FF3+	163.6 eV, Sulphide (68.7 %) 168.4 eV, Sulphate (15.2 %) 171.1 eV, Sulphate (16.1 %)	Small to fit the curve	133.8 eV, metaphosphate (100%)	1022.6 eV, ZnS/ZnO/Zn-phosphate (95%) 1024.4 eV, Zn-S-O (5%)
FF3-	163.6 eV, Sulphide (34.1%) 168.1 eV, Sulphate (49.9%) 169.8 eV, Sulphate (16.0%)	Small to fit the curve	-	-

Table 5-4 Binding energies, concentration of XPS and corresponding chemical in the tribofilms formed on CI pins in a-C:15H/CI system by oils FF2+, FF3+ and FF3-.

Oils	Binding Energies, chemical species and concentrations			
	S 2p	Mo 3d	P 2p	Zn 2p
CI pins				
FF2+	161.3 eV, Sulphide (100 %)	-	132.9 eV, pyrophosphate (100%)	1021.9 eV, ZnS/ZnO/Zn-phosphate (100%)
FF3+	161.2 eV, Sulphide (72.5 %) 168.3 eV, Sulphate (27.5 %)	Small to fit the curve	132.9 eV, pyrophosphate (100%)	1021.9 eV, ZnS/ZnO/Zn-phosphate (100%)
FF3-	-	Small to fit the curve	-	-

In addition, regardless of the tribo-system, a P peak was detected on all the ZDDP-containing fully formulated oils.

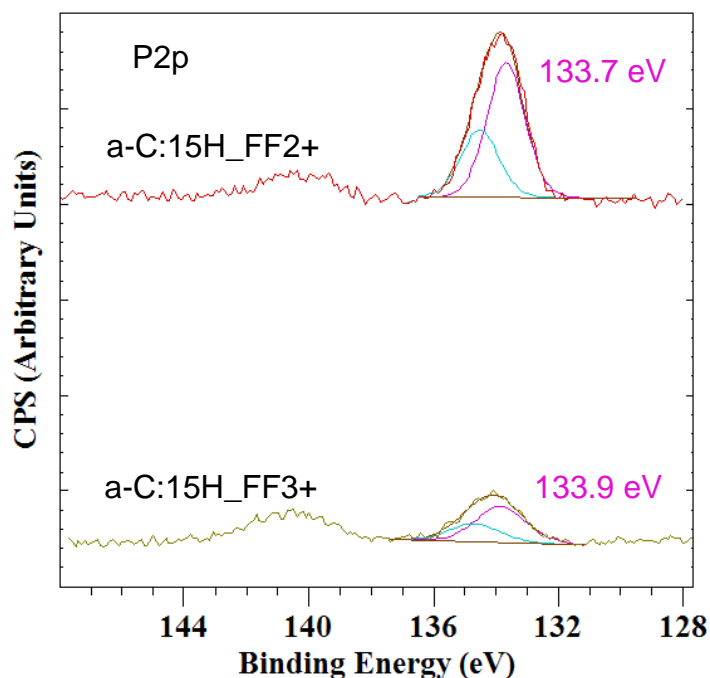


Figure 5-21 P 2p curve fitting for ZDDP-containing fully formulated oils on a-C:15H plates.

Zn 2p peaks were also found on both a-C:15H/CI and steel/CI systems for all the ZDDP-containing oils. The binding energies of the ZDDP-derived elements (shown in Table 5-1 to Table 5-4) suggest that, all fully formulated oils formed ZnS/ZnO/Zn-phosphate on both systems. Phosphate was also found in the tribofilm formed from FF3+ (ZDDP-containing fully formulated oils in combination with Mo-FM) in both a-C:15H/CI and steel/CI systems. In the a-C:15H/CI system, Fe 2p peaks were not detected in the tribofilms using any of the oils suggesting that the coating was not delaminated and that the iron coming from the pin worn particles did not take part in the tribofilm formation on the a-C:15H surface.

It is evident from Figure 5-22 that using fully formulated oils, detergent- and dispersant-derived elements were detected on both steel and a-C:15H surface. However, the nature of Ca and N species formed on a-C:15H were different from those on steel.

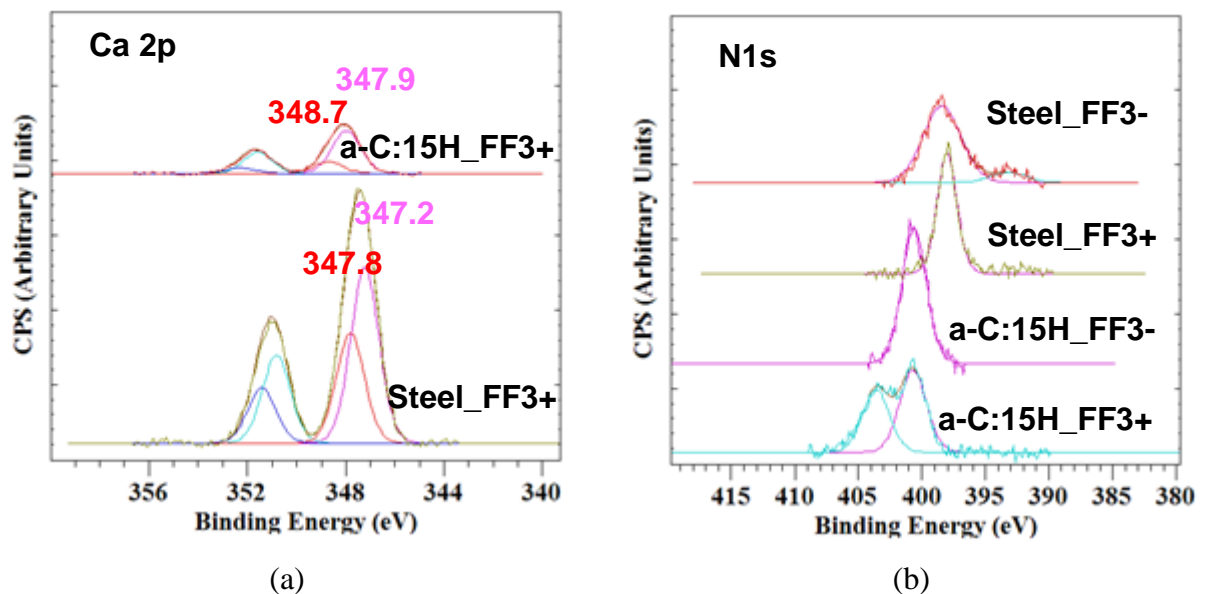


Figure 5-22 Detergent-derived Ca 2p peak (a) and dispersant-derived N 1s peak (b) using fully formulated oils.

Using FF3+ oil, the binding energy of Ca 2p main peak which was formed on the uncoated steel plate was 347.2 eV and 347.8 eV suggesting the formation of CaCO_3 and CaSO_4 compounds, respectively, whereas on the

DLC coated plate peaks were detected at 347.9 eV and 348.7 eV which corresponds to CaSO_4 and Ca-N-O compounds, respectively [267]. Nevertheless, investigations on the formation of Ca-based tribofilms in the literature are very restricted but in this study, the presence of Ca and N on the surface could affect the effectiveness of Mo-FM in low friction film formation on both a-C:15H and steel surfaces. This could be another explanation for comparatively high friction values observed from fully formulated oils in both of the systems.

Based on the tribo-test results and post chemical analysis of the surfaces, it was evident that using fully formulated oils, additive-derived tribofilms are formed on both DLC and steel surfaces. Oil additives could offer a beneficial wear performance to the DLC coatings by formation of lubricous tribochemical layer on the interface [211]. Formation of the tribofilm on the DLC surface could hinder graphitization of the coating which was observed using base oils. This will be discussed in detail in Chapter 7.

5.5. Summary

In phase I of this study, the friction and wear properties of a hydrogenated DLC coating under boundary lubrication conditions lubricated in fully formulated oils, have been investigated and the tribological performance compared with that of an uncoated steel system. Overall, this part of the study showed that the durability of the a-C:15H coating strongly depends on the type of lubricant used. Also, the effect of detergent, dispersant and antioxidants on the performance of the molybdenum-based friction modifier (Mo-FM) and ZDDP anti-wear additive should not be ignored. In summary, the following key points can be drawn from this part of the study:

- ZDDP decomposed under boundary lubrication condition and formed Zn-phosphate/ZnS/ZnO anti-wear species in the tribofilms formed on a-C:15H. In contrast, the amount of Mo 3p detected on the a-C:15H surface was very low using fully formulated oils which shows inefficiency of the Mo-FM additive in forming a low friction tribofilm on the interface.

- Friction reduction was not seen using any of the FM-containing lubricants suggesting that friction modifier in fully formulated oils were not effective in terms of friction reduction in both steel and DLC systems. This could be mainly due to low concentration of MoDTC with which the oils were blended. Furthermore, all the fully formulated oils contain detergent, dispersant, antioxidant which are the surface active additives and their interaction could affect Mo-FM-derived film formation. Detergent and dispersant derived tribofilms were detected on both uncoated steel and DLC surfaces.
- In general, all fully formulated oils demonstrated a good wear performance of the a-C:15H coatings. The main wear mechanism on the FM-free fully formulated oils was polishing wear while the presence of FM in the fully formulated oils with formulation carrying a 60 ppm of Mo-FM (i.e. FF3+ and FF30-), showed a positive effect on the wear of the a-C:15H coatings. Nevertheless, in phase I of this study, tribo-tests were carried out for 6 h and as such no significant difference in tribological behaviour of DLC and steel system was observed. Hence, longer tests can provide a better tribological comparison between different oils when lubricating DLC coatings.
- The a-C:15H coating durability is strongly lubricating oil dependant and the coating failure can be avoided using additive containing oils which form a protective tribofilm on the surfaces and suppress the a-C:15H coating structural modification. Base oil (group III) performed better wear performance than PAO suggesting the important role of selection of base oil in the lubricant.

Chapter 6 Results: Phase II - Effect of Mo-FM on the Tribological performance of a hydrogenated DLC coating.

6.1. Introduction

As shown in chapter 5, in phase I of the study, the friction reduction was not observed using any of the fully formulated oils while a-C:15H coating showed extremely low wear for 6 h tests using all fully formulated oils. The main objective of phase II, which is presented in this chapter, was to study the effect of a MoDTC-type friction modifier (Mo-FM) concentration on the friction and wear performance of 15 at.% hydrogenated DLC coating (a-C:15H) under boundary lubrication conditions using fully formulated oils. The tribological performance was compared to an uncoated steel system. It was intended to investigate whether increasing the Mo-FM level in the oil would result in an improvement of the performance of the system by reducing the friction without losing the durability observed and measured in the previous part (when lubricated with lower level (40 ppm and 60 ppm of MoDTC)). The test duration was also increased to investigate whether typical fully formulated oils would still perform well in terms of wear after 20 h of the tests. Initial tests revealed that 20 h is long enough for the comparison of the DLC coated plates in terms of friction and wear performance.

In phase II, ZDDP-containing and ZDDP-free fully formulated oils with 40, 300 and 600 ppm of Mo-FM with oxidation state of +4 friction modifier were used. The oils with 300 and 600 ppm are called FF300+, FF300-, FF600+ and FF600- (“+” refer to the presence of ZDDP in the oils and “-” refers to ZDDP-free oils). It should be noted that in this chapter, fully formulated oils with 40 ppm Mo-FM with oxidation state of +4 which were initially labelled as FF1+ and FF1- in previous chapter, are now annotated FF40+ and FF40- , respectively (“+” refer to the presence of ZDDP in the oils and “-” refers to ZDDP-free oils). In Figure 6-1, a map of the study in this chapter is presented.

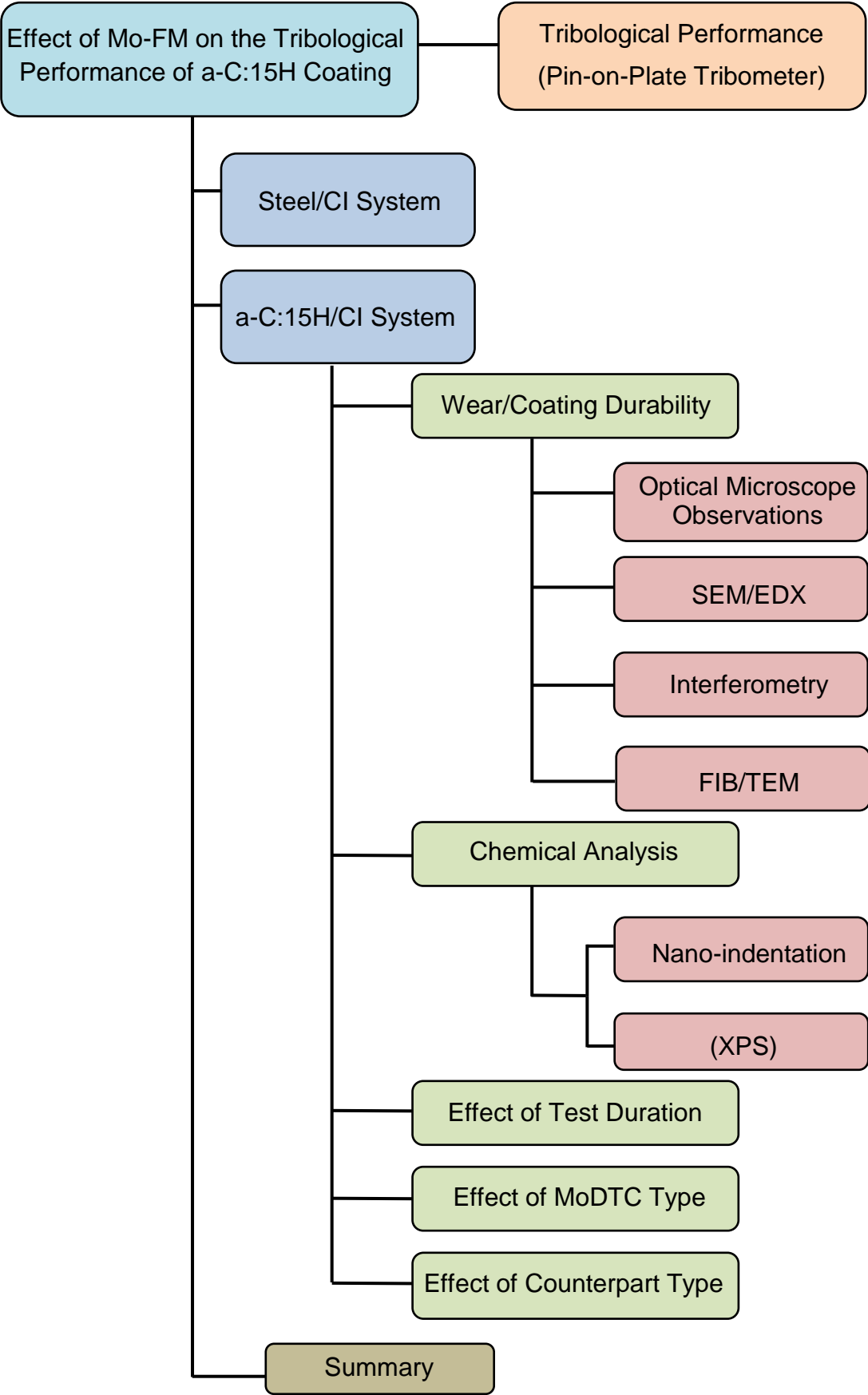


Figure 6-1 Map of the study which is presented in this chapter.

6.2. Tribological Performance of the Steel/CI System

6.2.1. Friction Results

Given in Figure 6-2 is the friction coefficient as a function of time for the steel/CI combination using six different oils. All tribo-tests were repeated no less than three times. It is evident that oils with low level of Mo-FM showed a high coefficient of friction after 20 h tests likewise reported for 6 h tests in chapter 5. Therefore, it is apparent that time duration does not affect the friction performance for low concentration Mo-FM containing fully formulated oils. In contrast, increasing the Mo-FM concentration to 300 ppm and 600 ppm in the oils formulation resulted in friction reduction. Although, the time requires for the friction to drop depends on the level of FM in the oil. In addition, higher Mo-FM concentration in the oils resulted in a faster friction drop in the induction phase of friction/time graph.

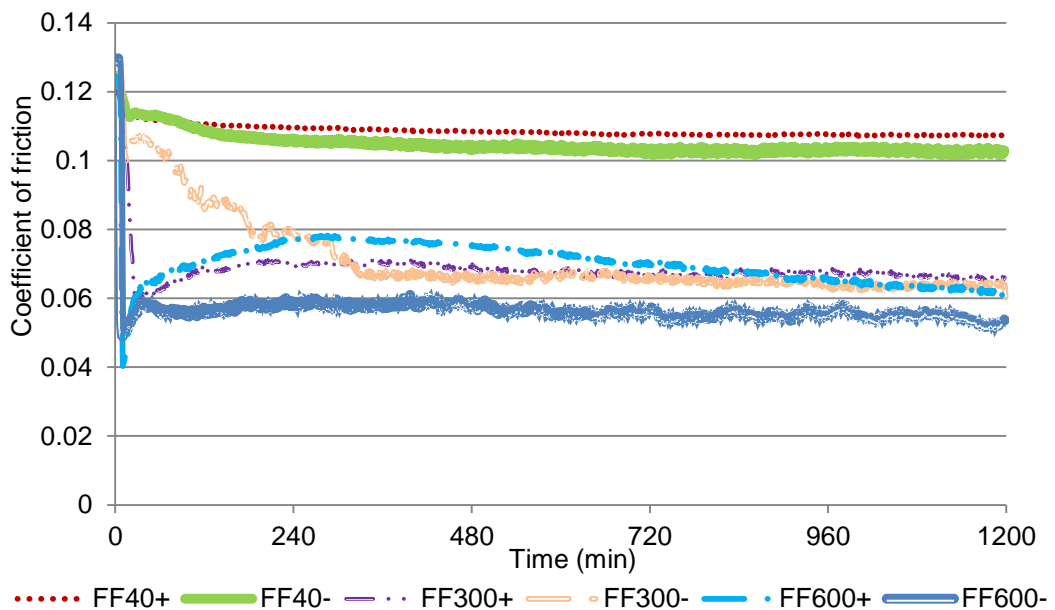


Figure 6-2 Friction traces as a function of time for the steel/CI system for FF40+, FF40-, FF300+, FF300-, FF600+ and FF600-.

The average friction coefficients of the last hour of the tests as a function of Mo-FM concentration for steel/CI system are shown in Figure 6-3. Generally, friction was observed to be proportional to Mo-FM concentration (i.e. the higher the Mo-FM the lower the friction). Based on the friction results for

steel/CI system, it was also seen that, except for the fully formulated oils with low Mo-FM concentration, the presence of ZDDP in the formulated oils increased friction values in comparison to the ZDDP-free oils, as has been extensively reported for steel systems [48, 55-58].

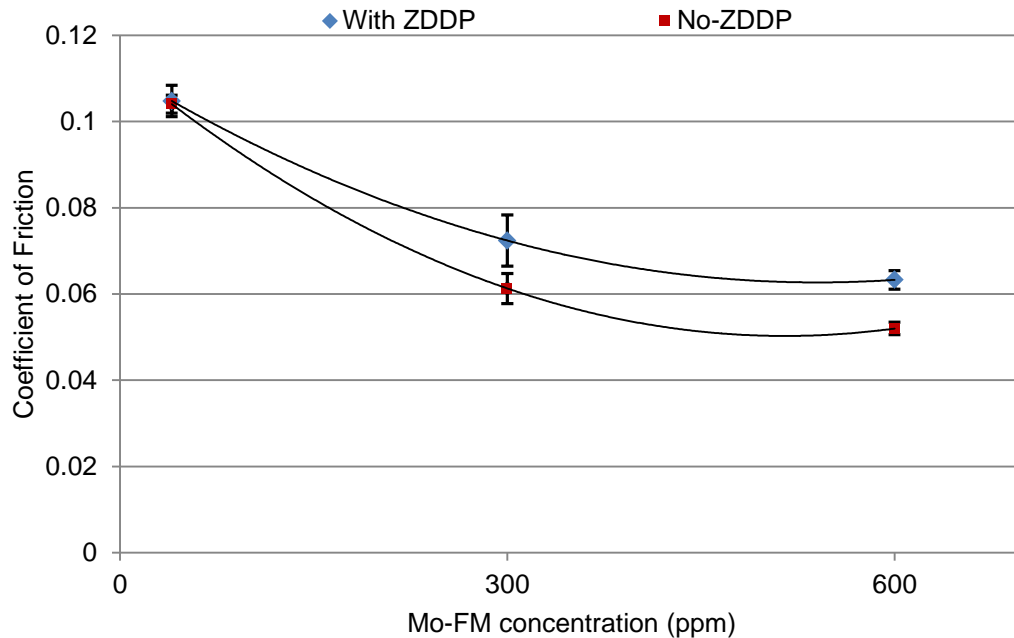


Figure 6-3 Steady state friction coefficients as a function of Mo-FM concentration for steel/CI system.

6.2.2. Wear Results

Wear measurement of the a-C:15H coated plates and uncoated steel plates were conducted using a Veeco WYKO optical white light interferometer. The loss volume of the plates were obtained by multiplying the average value of the cross sectional area by the stroke length. The wear coefficients as a function of Mo-FM concentration calculated using Equation 2-2 for steel plates are given in Figure 6-4. In general and considering the error bars, wear provided by all the lubricants and regardless of the level of FM in the oils are insignificant and the wear rates are comparable for all oils. However, it is evident that in the presence of ZDDP there was a slight improvement, if any, in the wear performance for oils with high level of Mo-FM (FF600+).

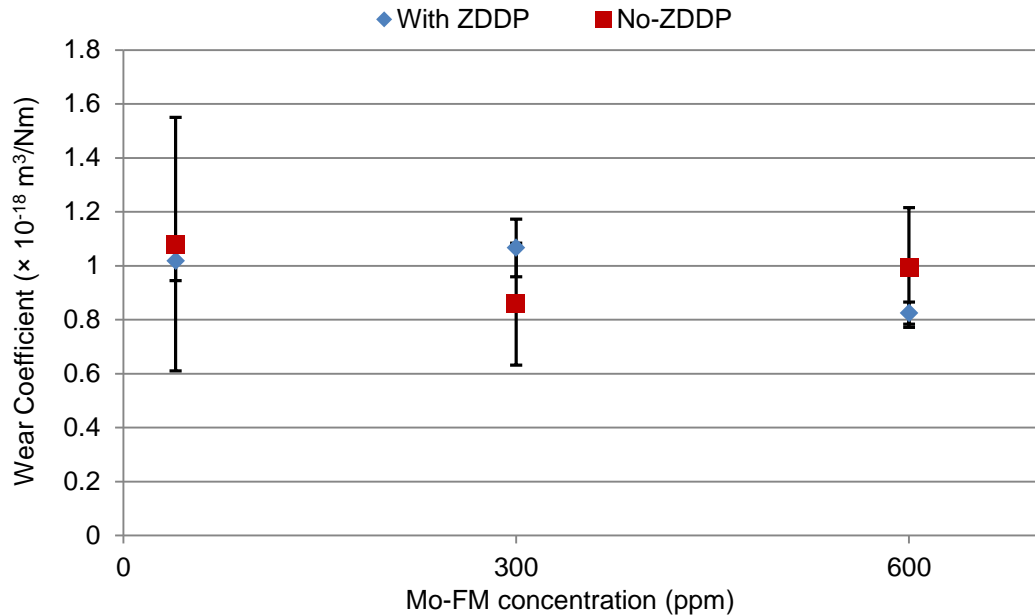


Figure 6-4 Wear coefficient versus Mo-FM concentration for the steel/CI system.

6.3. Tribological Performance of the a-C:15H/CI System

6.3.1. Friction Results

The friction coefficient as a function of time for the a-C:15H/CI combination using six different oils is given in Figure 6-5. Based on the friction traces, it can be seen that both the induction phase and the steady state friction was observed to be dependent on the Mo-FM level in the oils. The rate of friction drop was observed to rise with increase in Mo-FM level in fully formulated oils. The average friction coefficients of the last hour of the tests as a function of Mo-FM concentration for a-C:15H/CI system are presented in Figure 6-6. Overall, friction was observed to be oil dependant and reduced with increase in Mo-FM concentration as expected. Based on the friction results, it can be seen that Mo-FM was not effective in friction reduction when its concentration was low in the oil (40 ppm) while increasing the Mo-FM concentration in the oils resulted in lower values for friction. In general, the presence of ZDDP in the formulated oils (Oil300+ and Oil600+) increased friction in comparison to the ZDDP-free oils (Oil300- and Oil600-). However, in high level Mo-FM-containing fully formulated oils ZDDP did not significantly affect friction and the Mo-FM dominated the friction performance.

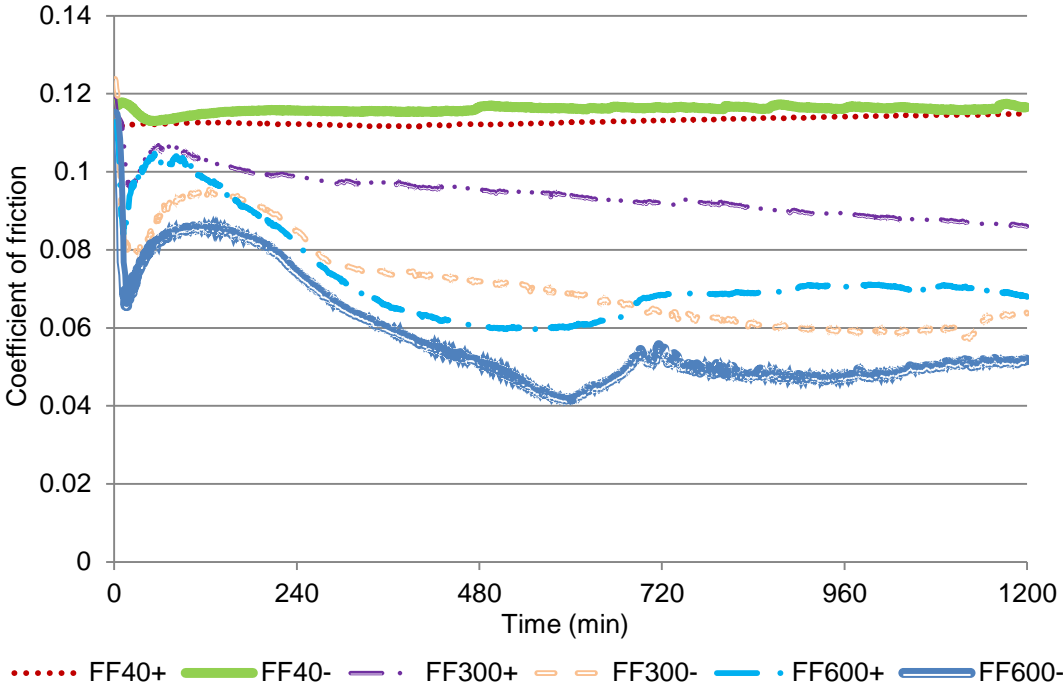


Figure 6-5 Friction traces as a function of time for the a-C:15H/Cl system for FF40+, FF40-, FF300+, FF300-, FF600+ and FF600-.

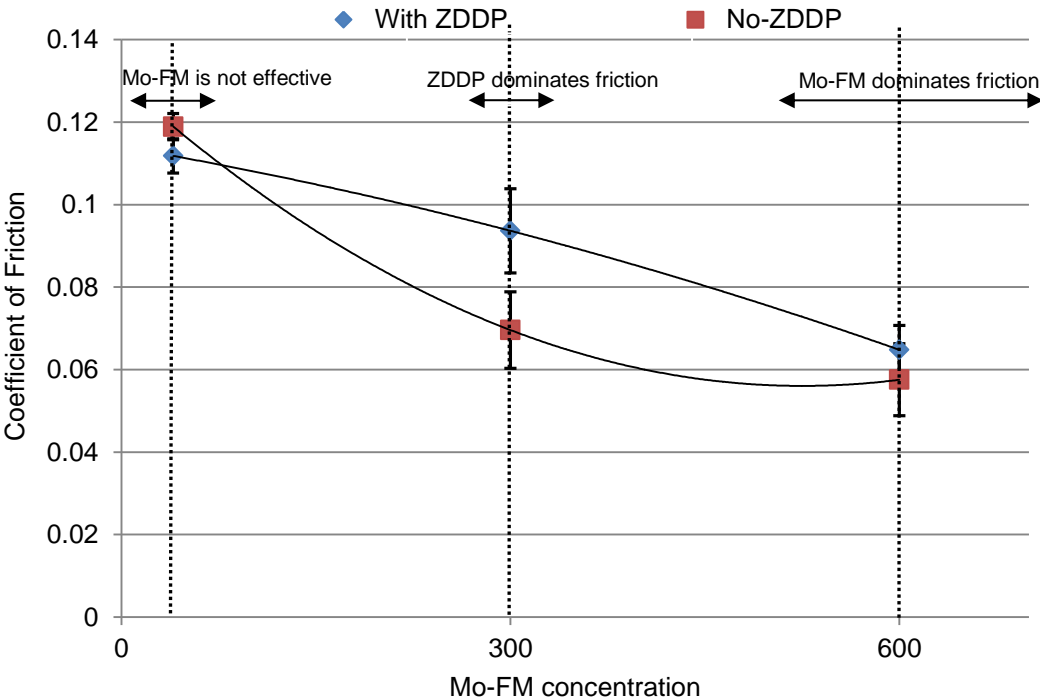


Figure 6-6 Steady state friction coefficients as a function of Mo-FM concentration for a-C:15H/Cl system.

6.3.2. Coating Durability and Wear Results

Similar to wear measurements of the steel plates, using a Veeco WYKO optical white light interferometer, the wear coefficients as a function of Mo-FM concentration calculated using Equation 2-2 for a-C:15H coating are given in Figure 6-7. It is evident that the higher the Mo-FM, the higher the wear. The wear provided by the lowest Mo-FM concentration-containing fully formulated oils (FF40+ and FF40-) on a-C:15H/CI system were observed to be very low while increasing Mo-FM concentration significantly increased the wear. It is interesting to note that the addition of ZDDP significantly improved the wear performance; this is clear by comparing FF300+ with FF300- and FF600+ with that of FF600-. However, ZDDP effectiveness in counteracting the adverse effect of Mo-FM is dominant for low and medium levels of Mo-FM. It is not as effective for high concentrations of Mo-FM. Overall, it is evident that reduction in friction comes at the price of the DLC coating high wear. From Figure 6-7, it is evident that FF300-, FF600+ and FF600- illustrated a high wear on the hydrogenated DLC coating.

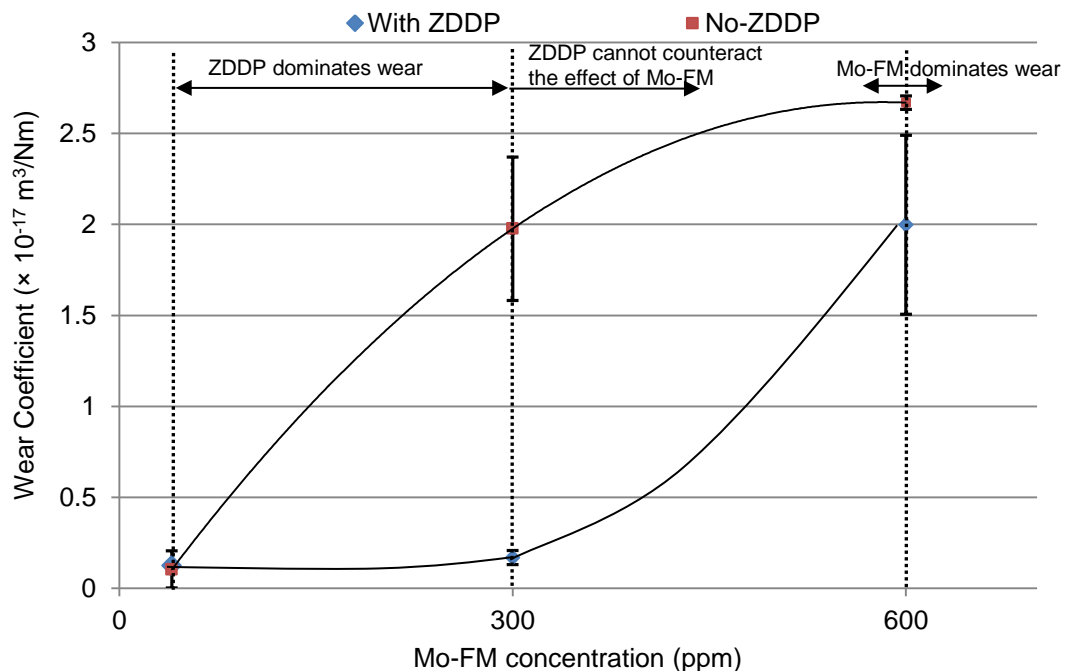


Figure 6-7 Wear coefficient versus Mo-FM concentration for the a-C:15H/CI system.

A typical 2D wear depth profile of high wearing a-C:15H coatings is given in Figure 6-8-Figure 6-10; a wear characteristic observed in high wearing oils (i.e. FF300-, FF600+ and FF600-). In general, it can be appreciated that as test duration increases, the risk of penetration through the coating increases leading to removal of the coating from the substrate. In addition, the width of wear in Y direction (cross section) of all high wearing oils was in the range of 1.3-1.4 mm which could be an indication of similar wear rates of the counterparts (CI pins).

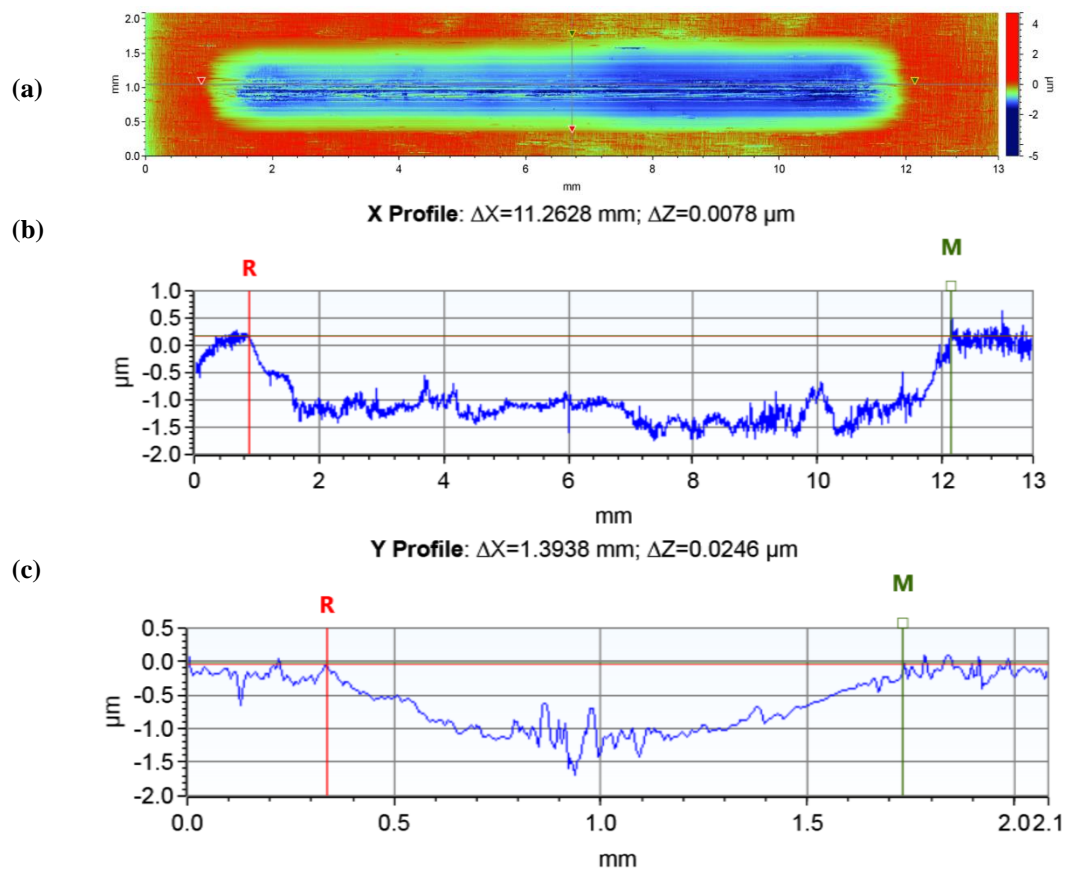


Figure 6-8 A typical profile of the wear scar formed on (a): a sample of a-C:15H coating for FF300- fully formulated oil along (b): X direction and (c): Y direction measured by WYKO.

It is evident from Figure 6-8 that the wear depth given by FF300- oil was seen to be uneven along the wear track in both directions for one measured point of a typical sample. The average wear depth was less than a micrometre in both directions.

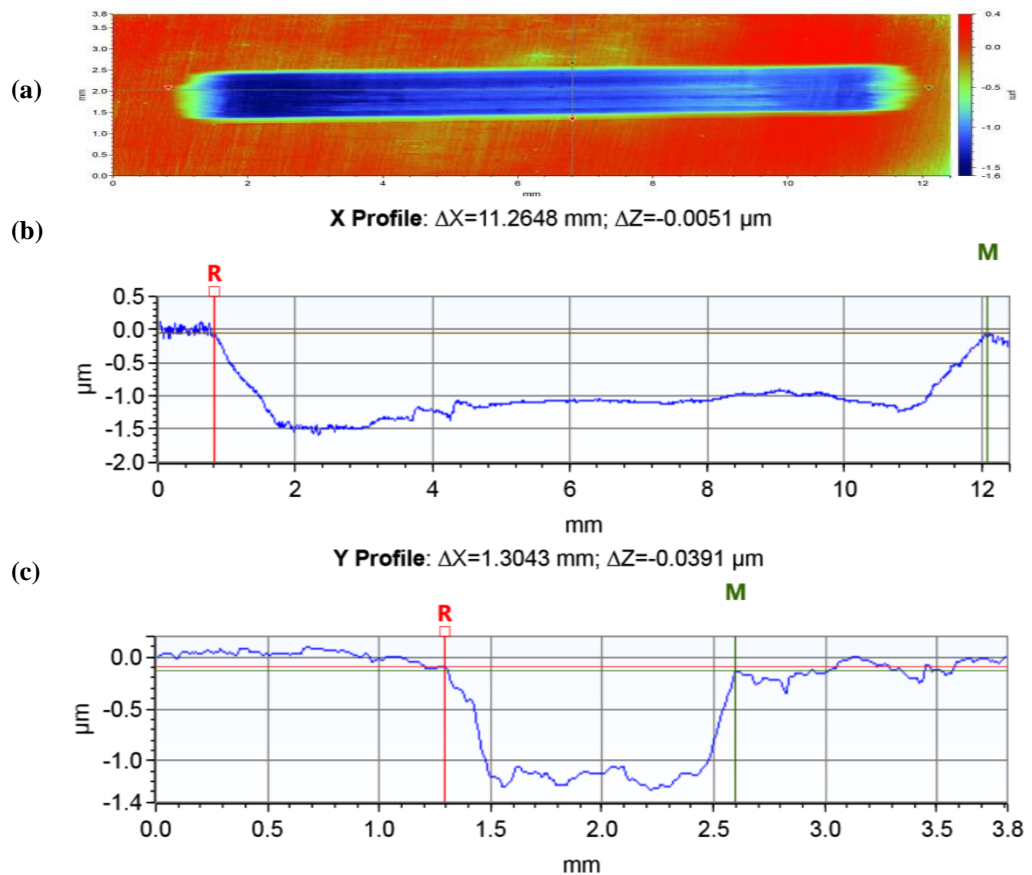


Figure 6-9 A typical profile of the wear scar formed on (a): a sample of a-C:15H coating for FF600+ fully formulated oil along (b): X direction and (c): Y direction measured by WYKO..

The wear depth given by FF600+ was relatively uniform along the wear scar in both directions as illustrated in Figure 6-9. The average wear depth was less than 1.2 μm in both directions for one measured point of a typical sample. However, the maximum wear depth was in the range of 1.5 μm at some regions along the X direction.

From Figure 6-10, a clear wear through the DLC coating is evident for FF600- oil. For this particular sample, the wear was seen to be almost uniform along the wear scar and the highest wear depth was seen to be 1.20-1.25 μm. It should be borne in mind that the wear rate values used for calculating the wear rates (Figure 6-7) was the average cross sectional areas of the wear scars at different positions of the wear scar for no less than three different samples.

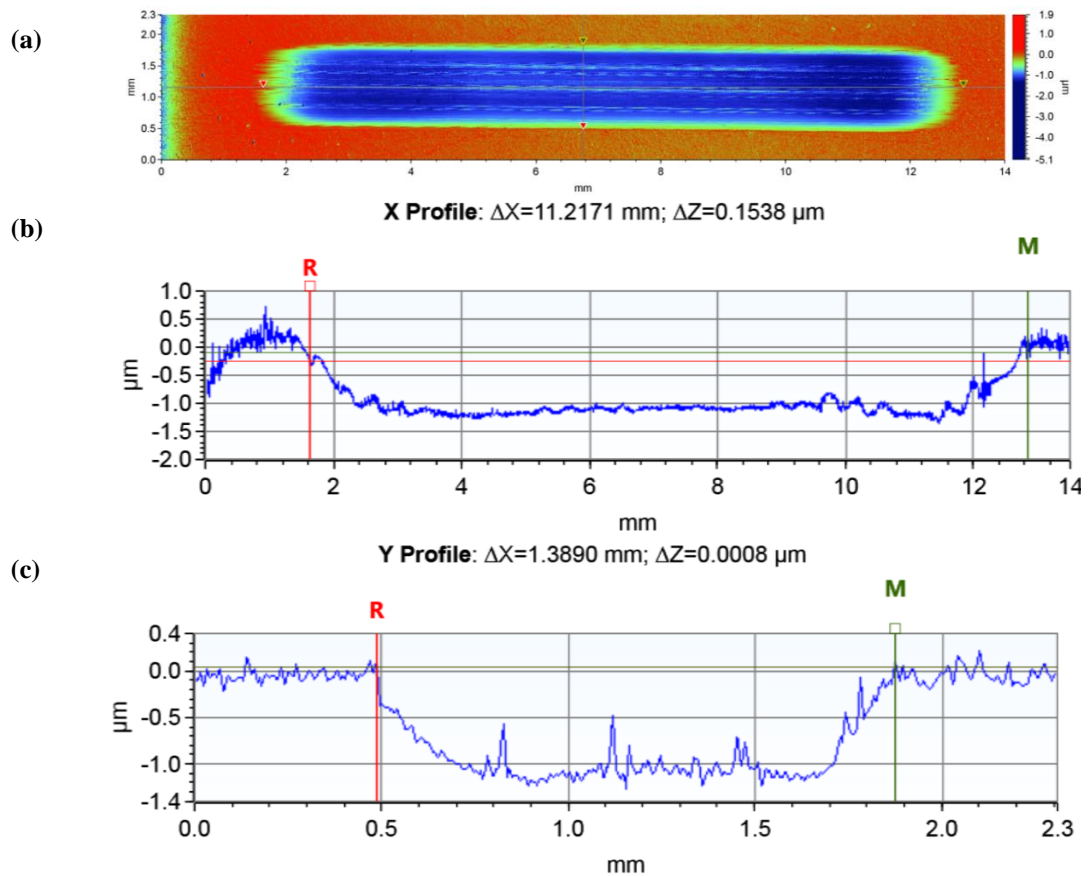


Figure 6-10 A typical profile of the wear scar formed on (a): a sample of a-C:15H coating for FF600- fully formulated oil along (b): X direction and (c): Y direction measured by WYKO.

Figure 6-11 shows typical images of wear scar. It is evident that the extent and mechanisms of wear is dependent on the additive package used in the lubricant. Based on the optical images, the colour of the wear tracks were brighter than outside of the wear tracks suggesting the relation of underlying Cr/CrN layers, as a result of the loss of coatings.

Delamination of the coatings was not observed using FF40+, FF40- and FF300+ (Figure 6-11a-c); rather, the wear of the coatings was dominated by gradual polishing wear. Additionally, the average depth of the wear tracks of a-C:15H coating for the highest obtained wear, provided by FF600-, was approximately 1.06 μm over the duration of the test when compared to the best wear performance by FF40- which was only 0.03 μm.

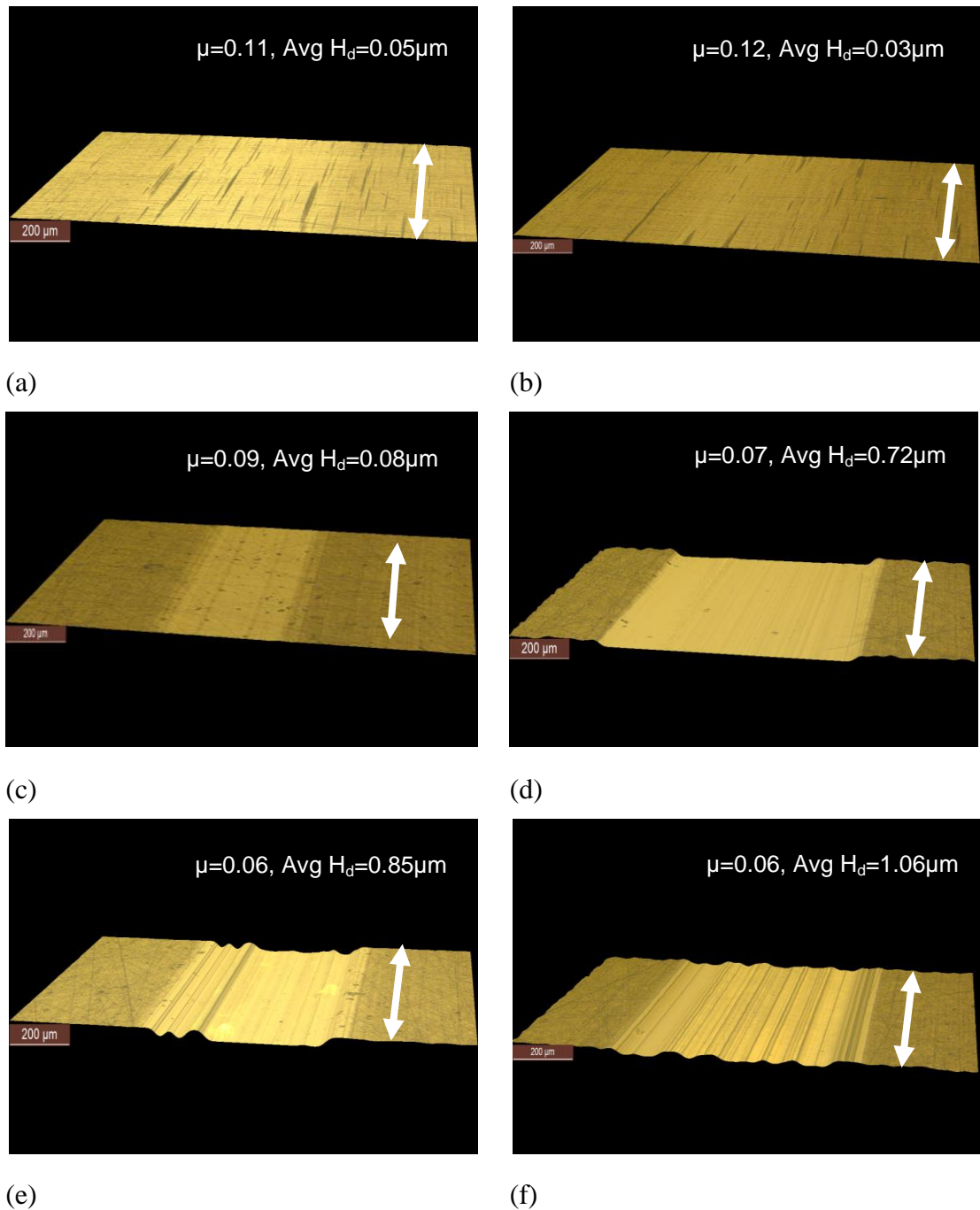


Figure 6-11 Optical images of the wear scars formed on the a-C:15H coated plates using (a) FF40+, (b) FF40-, (c) FF300+, (d) FF300-, (e) FF600+- and (f) Oil600-. The arrows on the images show sliding directions and μ and H_d are the coefficient of friction and the average depth of the wear track, respectively.

To verify the observations from wear results and optical microscope images, EDX was carried out in the wear scar. It is important to note that, the SEM/EDX analysis in this study was performed to check the durability of

coating, not to characterize tribofilms. The EDX measured the level of Cr from the Cr interlayer as a measure of coating thickness loss. The tribofilm on the plates was removed using acetone prior to the SEM/EDX analysis. Figure 6-12 shows a typical secondary electron (SE) image of a section of a-C:15H coating wear scar along with EDX mapping of C, Cr and Fe after the pin-on-plate tests. It is obvious that EDX mapping of a sample with higher wear provides lower carbon, higher chromium and some iron (in some cases) in the wear scar. Based on the mapping images, fully formulated oils with low level of Mo-FM showed very little difference in concentration of C and Cr comparing inside and outside of the wear scar implying very low gradual wear on the coated plates.

It is also clear that with increasing the level of Mo-FM, Cr was richer in the middle of the wear scar than outside (higher wear). Removal of dark coating exposed the underlying bright Cr interlayer as observed by optical images and confirmed by EDX analysis. Comparing EDX mapping of C, Cr and Fe atoms of a-C:15H coating after the tests, in general, ZDDP-containing oils showed lower wear compared to ZDDP-free oils. It should be noted that, Fe was seen to be dominant at some regions inside the wear scar for FF300- and FF600- while iron transfer from the pin is excluded as wear of the pin was comparable from all the tests (which will be discussed in the following paragraph) showing that either the substrate is exposed (delamination) or the coating became very thin in the wear scar region (severe wear).

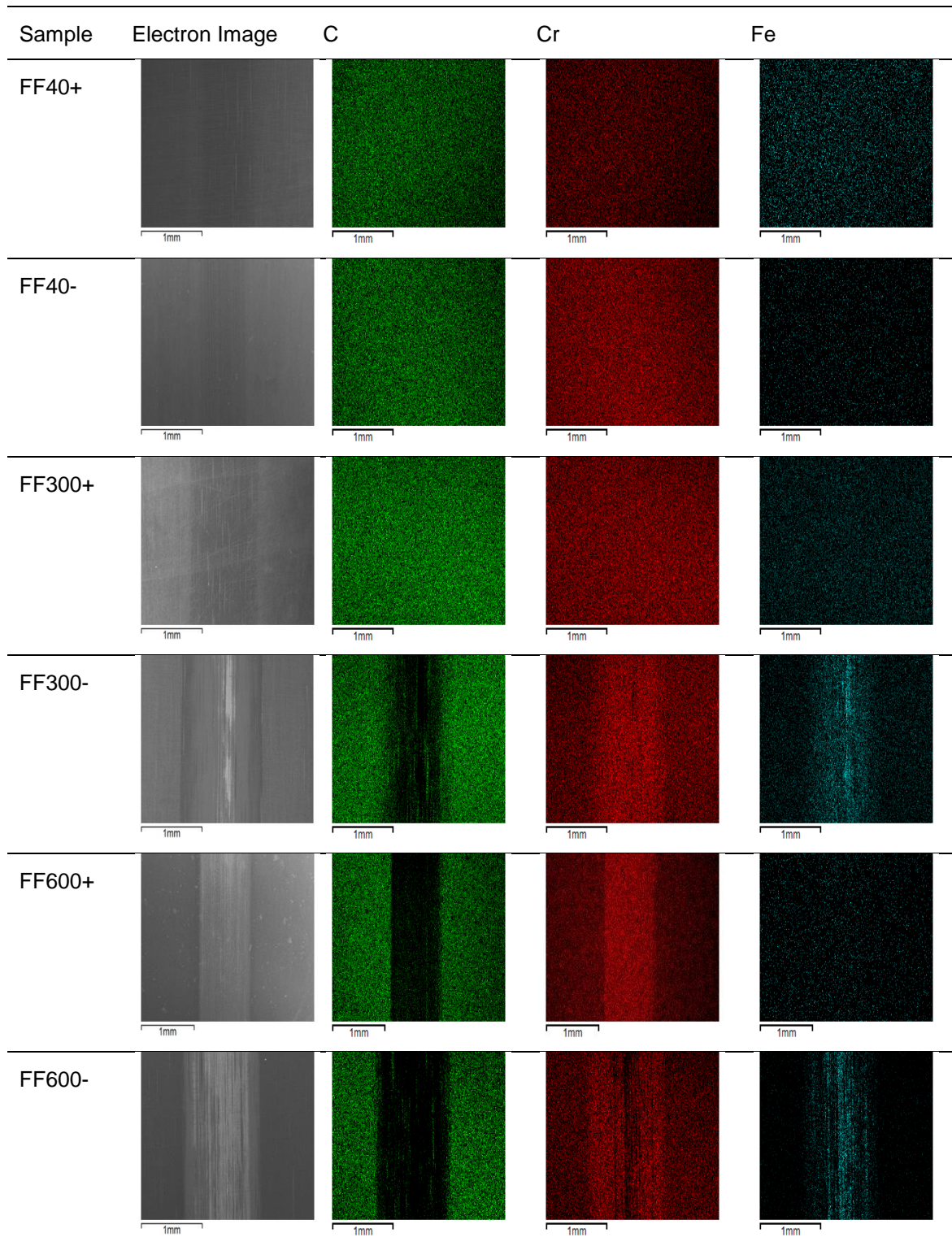


Figure 6-12 SEM image of a-C:15H coating along with EDX mapping of the C, Cr and Fe atoms for 20 h tests.

In order to provide a better picture of wear in a-C:15H coatings, FIB slides prepared from the wear scar of the coatings worn by high Mo-FM-containing

oils (FF600+ and FF600-) are compared with that of unworn coating. Figure 6-13-Figure 6-15 are the TEM images of the slides from a bare a-C:15H coating (Figure 6-13), worn a-C:15H coating by FF600+ (Figure 6-14) and worn a-C:15H coating by FF600- (Figure 6-15). The top layer of the bare coating (carbon) showed to have about 0.79 μm thickness whereas the thickness of the coating including the interlayers was seen to be 2.5 μm .

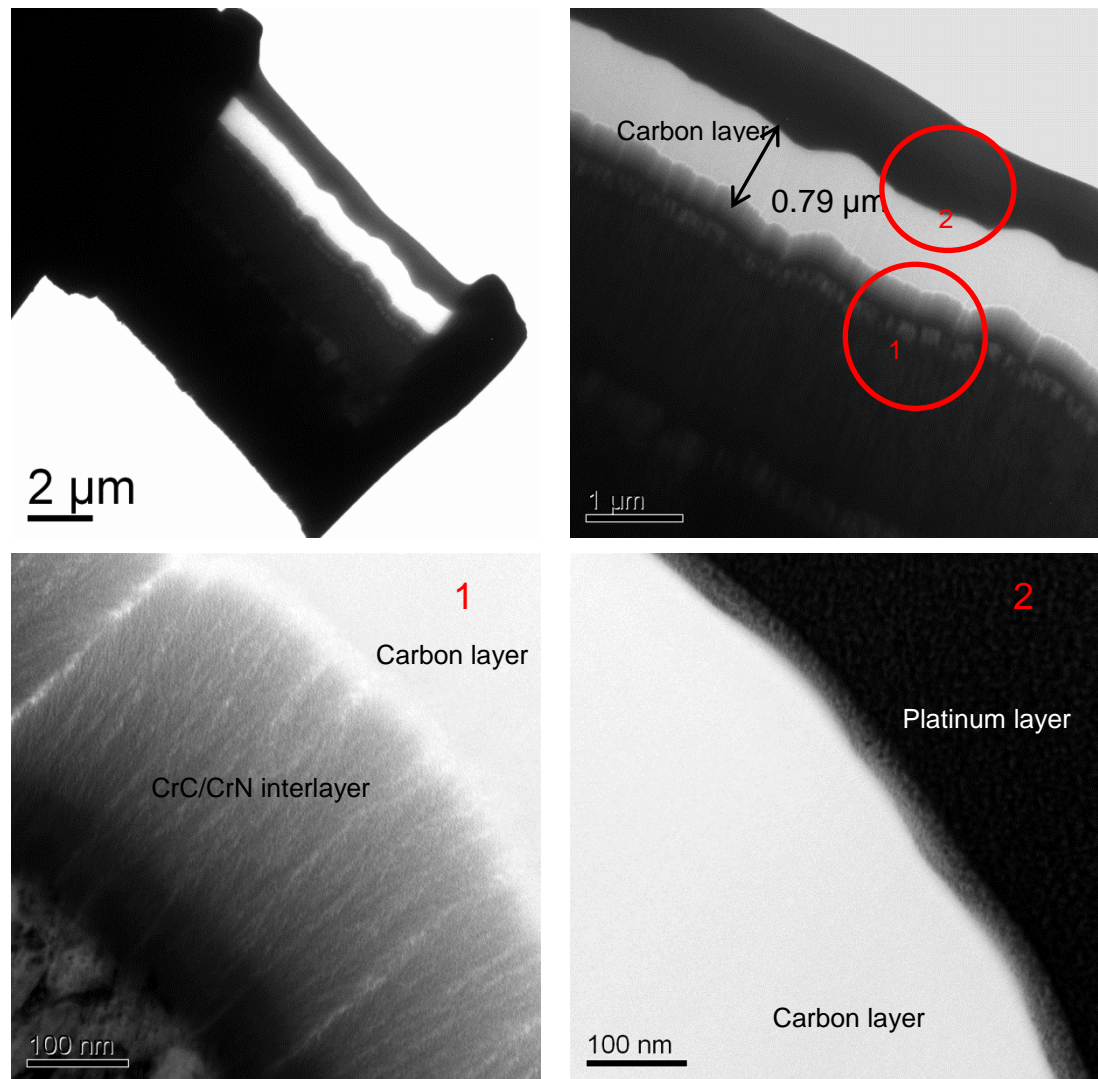


Figure 6-13 TEM image of the unworn a-C:15H coating. The areas circled in red are also presented in higher magnification.

Using FF600+, it is clear that carbon layer has become very thin at some regions inside the wear scar due to the high wear (see Figure 6-14). The area circled in red are also presented in higher magnification (see Figure 6-14 area 1 and 2). In the area where the carbon layer still exists (the

area annotated as 2), more than half of the top layer is removed due to the wear whereas in area 1, the a-C:15H coating top layer is worn severely and a deposit layer is visible which was not detected by EDX mapping (EDX mapping of the slides are presented later in this chapter). This deposit layer could be accumulation of worn DLC coating or a transformed carbon phase. The nature of this layer, however, is not verified.

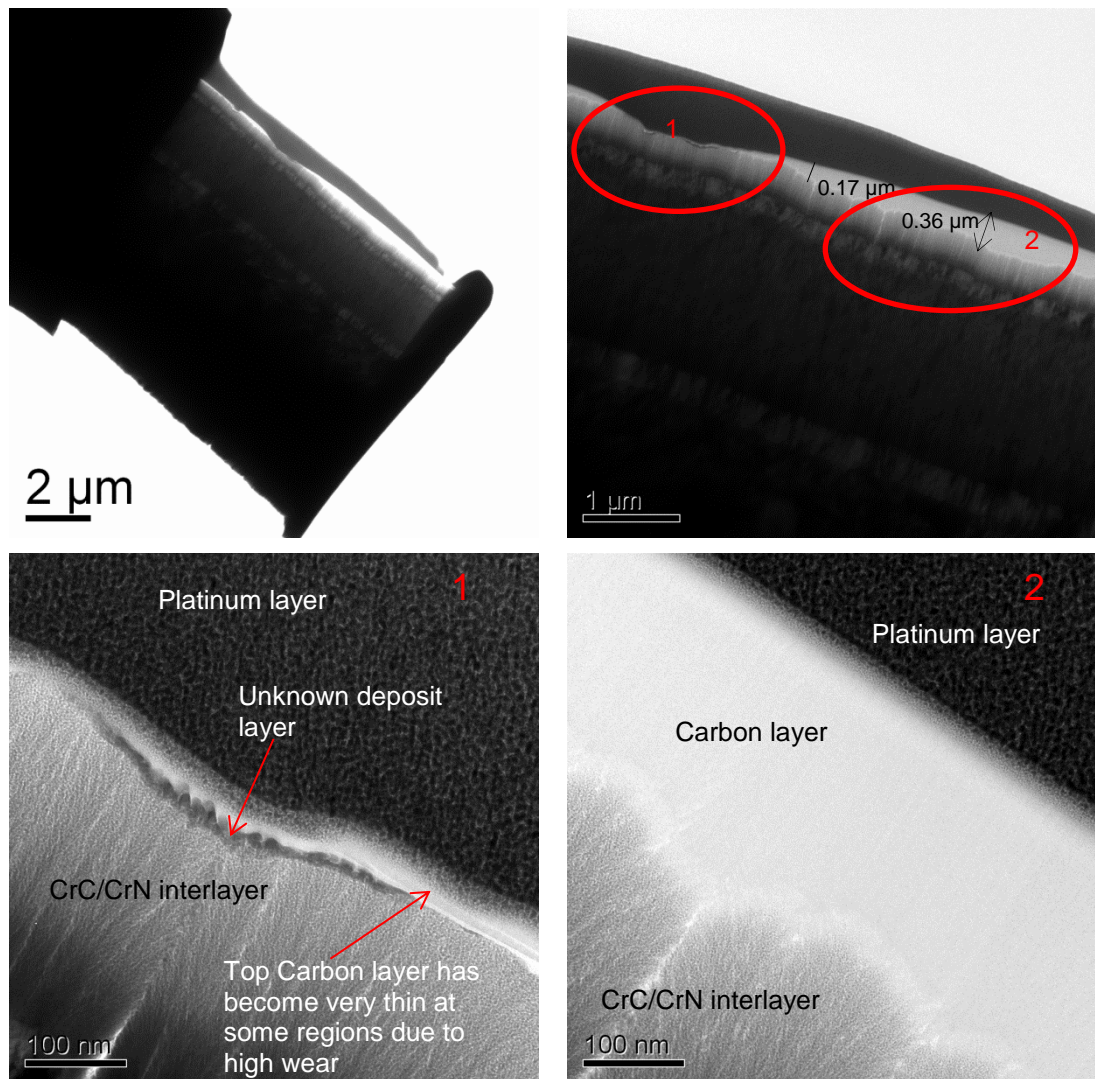


Figure 6-14 TEM image of the worn a-C:15H coating provided by FF600+. The areas circled in red are also presented in higher magnification.

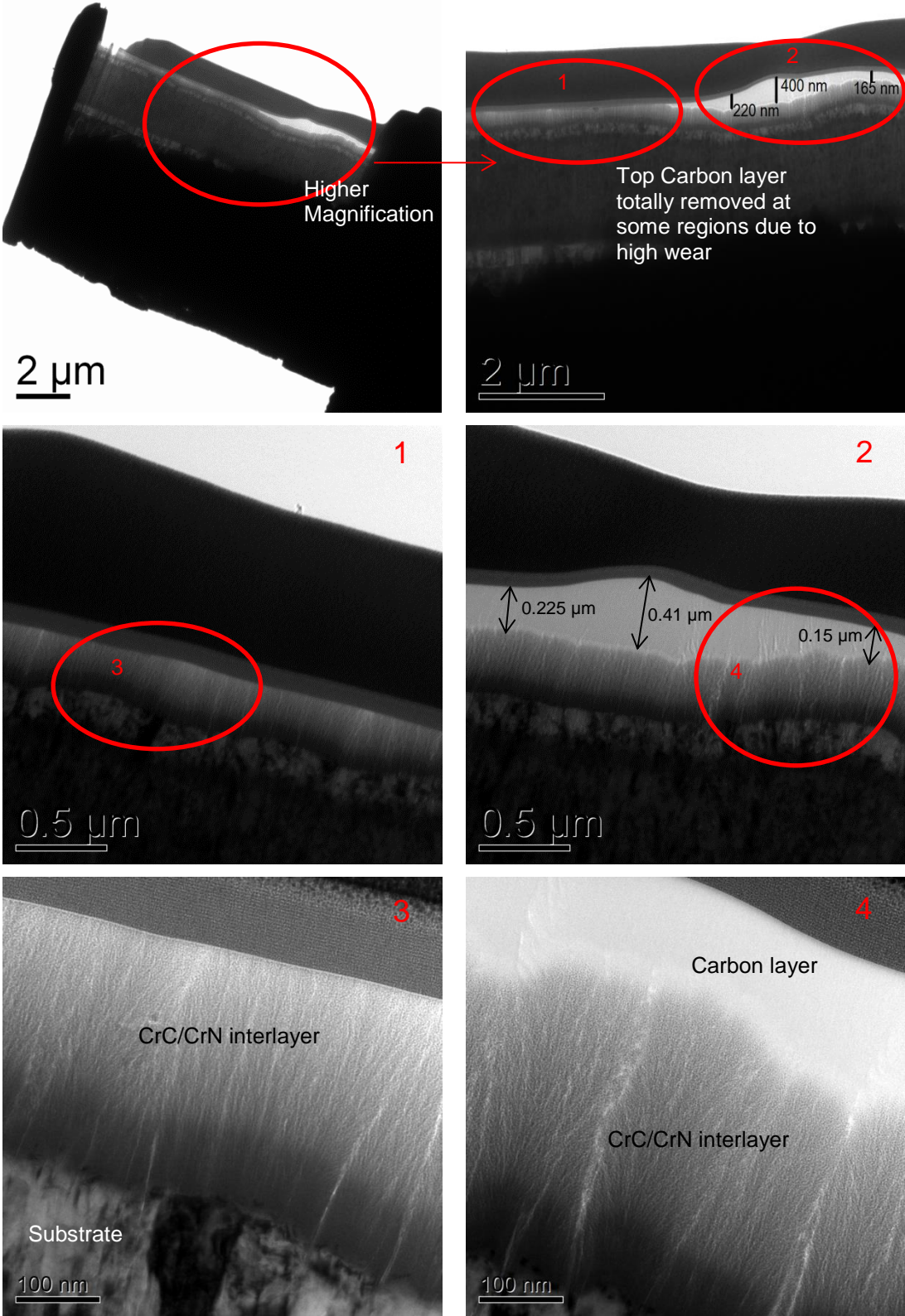


Figure 6-15 TEM image of the worn a-C:15H coating provided by FF600-. The areas circled in red are also presented in higher magnification.

For the highest wearing oil (FF600-), the coating is observed to become thinner in some regions ($\approx 165\text{nm}$ to 220 nm) whereas the top carbon layer is totally gone at limited regions (see Figure 6-15). This is in agreement with the observations obtained from optical microscope, interferometer and EDX mapping which showed that a-C:15H coated plates showed severe wear using FF600-.

In Figure 6-16- Figure 6-18, the EDX mapping of the slides prepared by FIB is shown. These were obtained to provide a better view of the coating layers before and after the tribo-test using high wearing oils (FF600+ and FF600-).

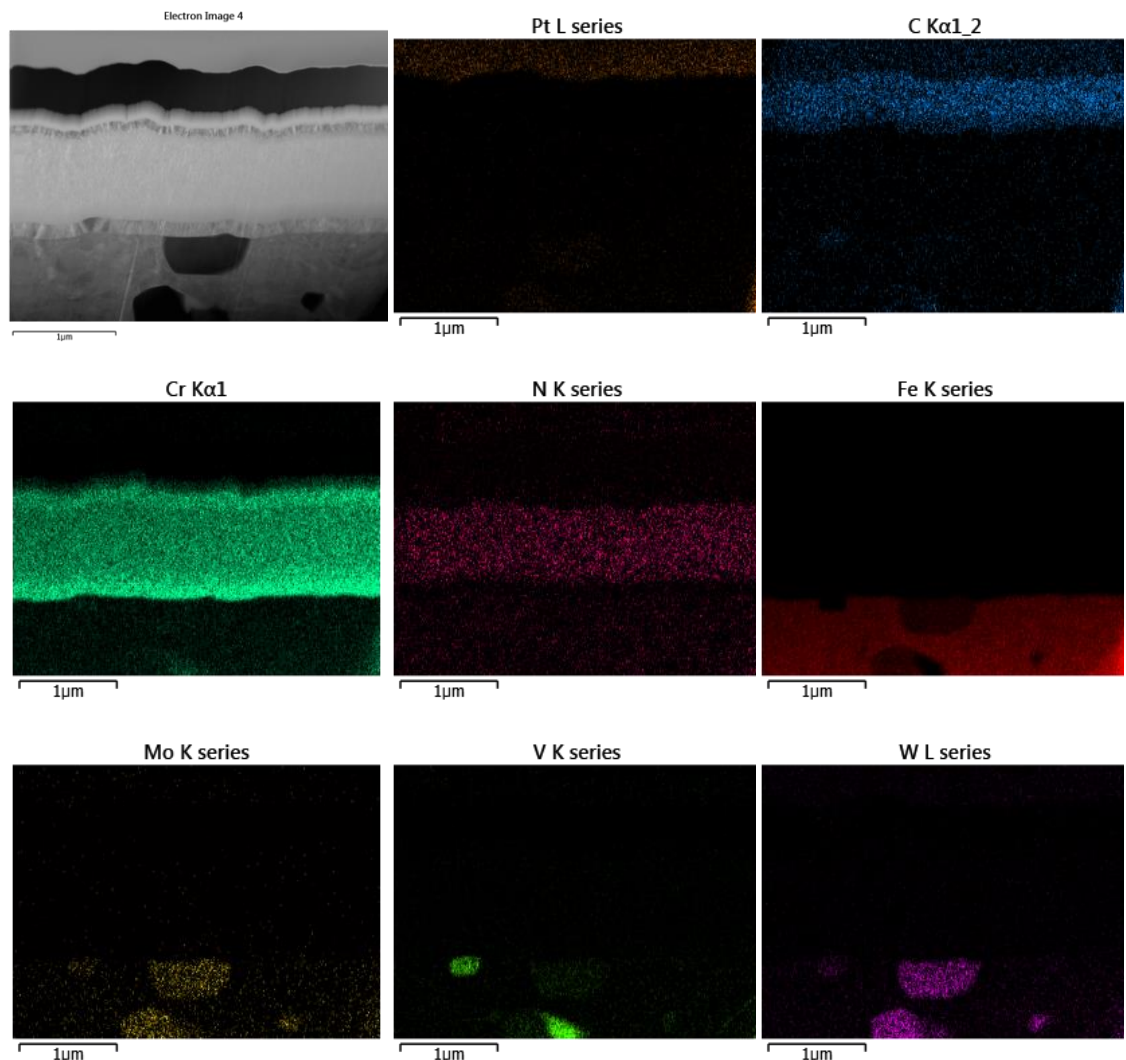


Figure 6-16 EDX mapping of the unworn a-C:15H coating.

Different elements were detected using EDX mapping from as-deposited DLC coating (see Figure 6-16) and worn a-C:15H coatings (see Figure 6-17- Figure 6-18). Platinum was detected on top of the layers as a protective platinum layer was deposited on the slide during sample preparation by FIB. The coating layers from top to bottom were detected to be carbon, chromium and Iron (substrate), respectively. It is clear, depending on the extent of wear, how layers differ (see Figure 6-17 and Figure 6-18) from an unworn a-C:15H coating (see Figure 6-16). Molybdenum, vanadium and tungsten were also detected and were related to the substrate (HSS steel). Detection of nitrogen was due to the nitrogen which was trapped in the DLC structure during the coating deposition procedure.

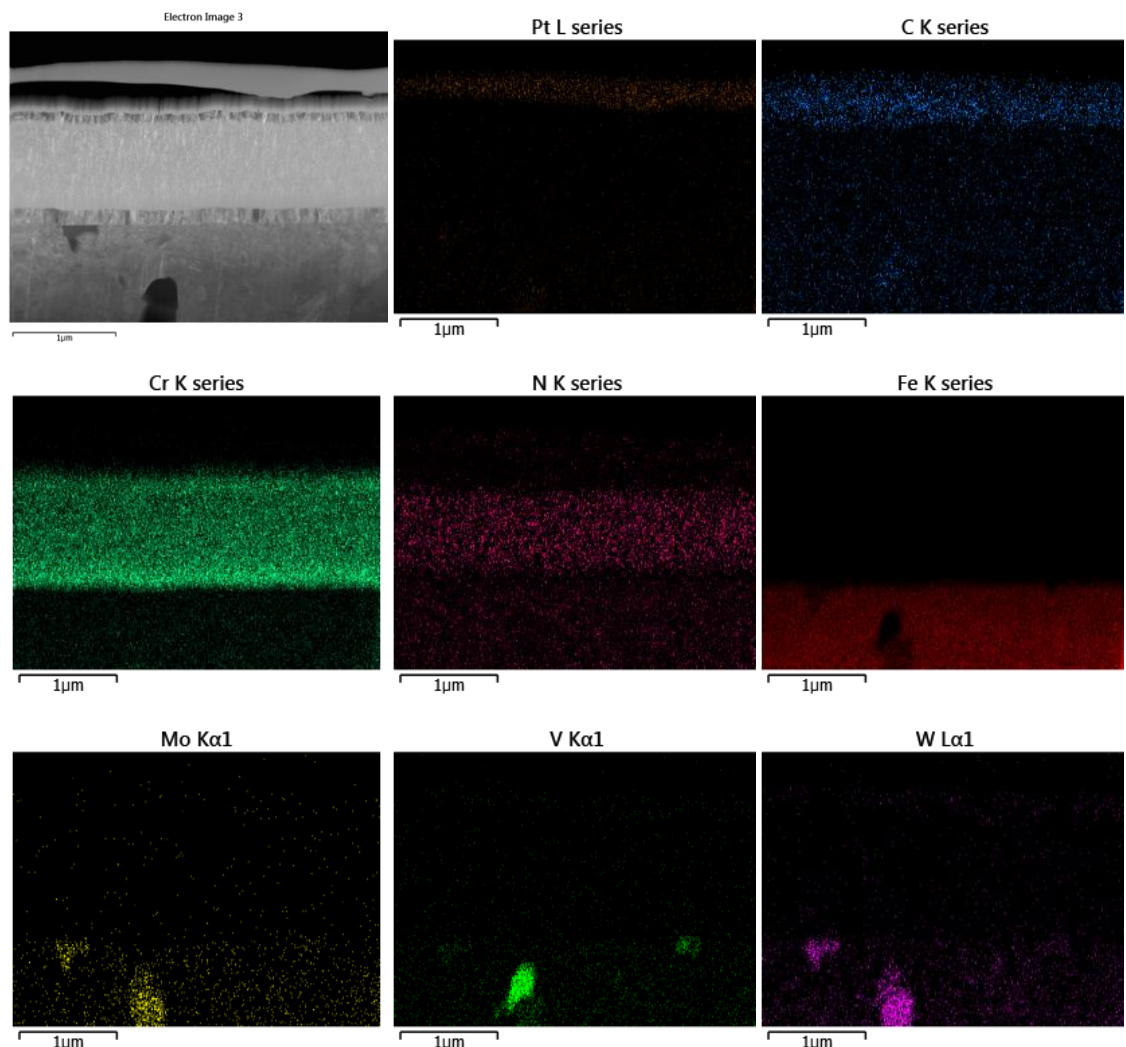


Figure 6-17 EDX mapping of the worn a-C:15H coating provided by FF600+.

From Figure 6-18, the increased intensity of the chromium signal at the bottom of the chromium interlayer (close to the iron substrate) was due to an increase in thickness of the specimen and not due to increased amount of chromium.

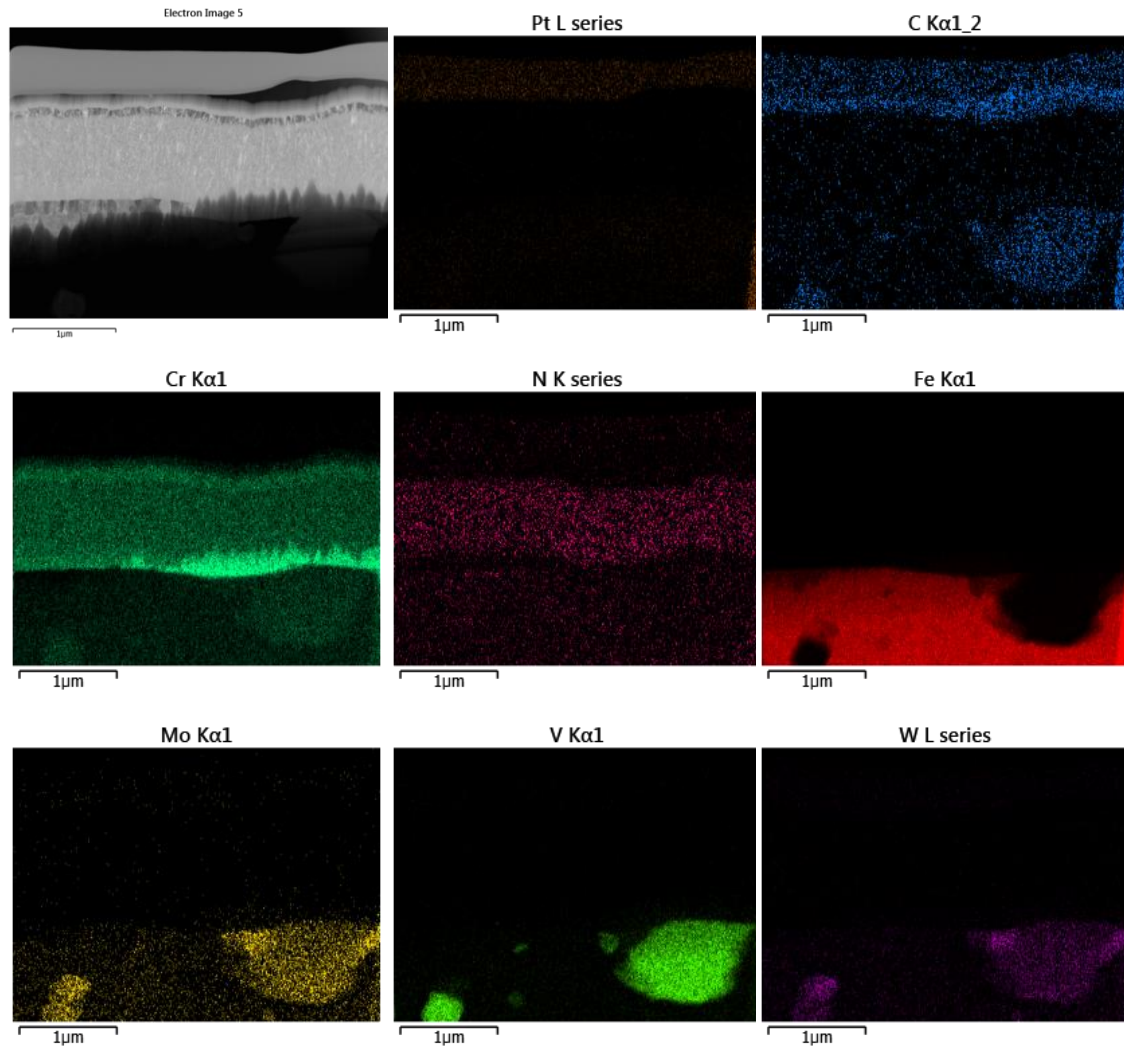


Figure 6-18 EDX mapping of the worn a-C:15H coating provided by FF600-.

The wear coefficients of the CI counterbodies for various oils are given in Figure 6-19. For lubricants with low Mo-FM concentration, surprisingly, the wear on the pin from ZDDP-free oil (FF40-) was less than that of the same oil but containing ZDDP (FF40+). It implies that the presence of ZDDP in the oil (with 40 ppm Mo-FM) did not provide a beneficial effect on wear reduction of the CI pin counterparts compared to the same oil without ZDDP. In general, considering the error bars, there was not much difference between

the wear rates for oils with medium (i.e. 300 ppm) and high (i.e. 600 ppm) level of Mo-FM and the values for all the oils were comparable and within the scatter of the results. Therefore, it can be argued that the different wear rates for the a-C:15H plates was not primarily due to the difference in the wear performance of the CI pin counterface. This is in line with the typical 2D profiles obtained from the a-C:15H coating wear scar where the width of wear in Y direction (cross section) of all high wearing oils was almost in the same range.

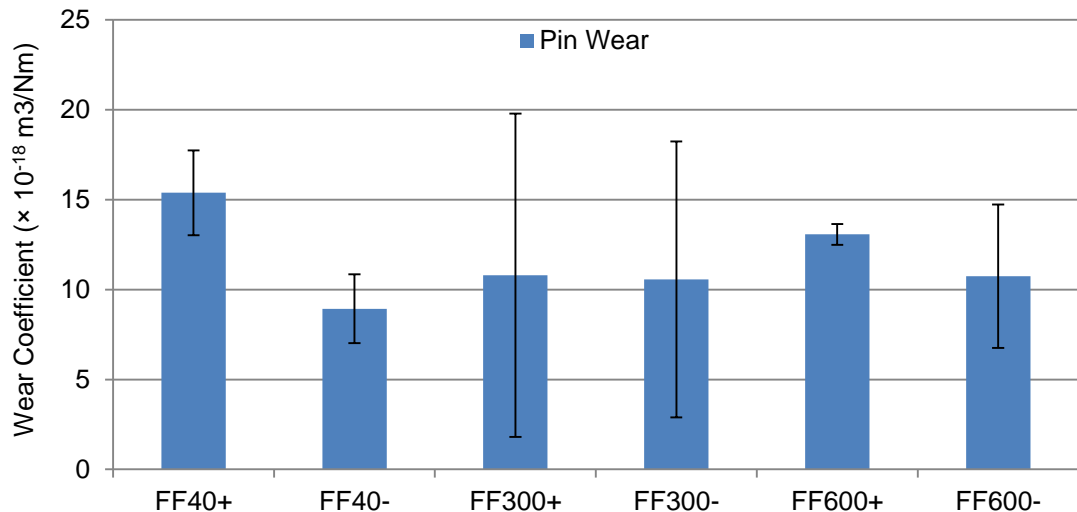


Figure 6-19 Dimensional pin wear coefficients as a function of lubricants for a-C:15H/CI systems.

Taking into account the observations for the wear data provided by interferometer, optical microscope and EDX mapping, it looks quite obvious that for high giving wear oils (i.e. FF300-, FF600+ and FF600-), the coating was worn through at some regions and the Cr interlayer was exposed. This could result in a different interface and the tribological behaviour could relate to the Cr/CI interface rather than DLC/CI. For FF600+ and FF600-, during the wearing period of the coating, i.e., in the initial stages of the sliding, the friction was dropping (see Figure 6-5). The friction values were then became stable after 8-10 h of the tribo-tests but again increased to a higher value. This behaviour could relate to the change in the interface and/or formation/depletion of the tribofilm on the interface. A reduction in steady state friction as a consequence of W-DLC coating removal and sliding of steel ball over the Cr interlayer in a DLC/steel system lubricated by EP additive was reported by authors [204]. Therefore, further surface analysis

of the tribofilms and shorter tests could clarify the tribological behaviour of the oils with different Mo-FM concentration which will be addressed in the following sections.

6.3.3. Chemical Analysis of Tribofilms

6.3.3.1. Elemental quantification

The chemical quantification of the surface tribofilms for the a-C:15H/CI tribocouple is shown in Table 6-1. The presence of the additive-derived elements on both the a-C:15H and the CI pin counterbody imply that the additives were decomposed under boundary lubrication and significantly influenced the tribological performance of the a-C:15H/system and particularly durability of the coating. Fe 2p peak was detected only in the tribofilm formed from FF600- suggesting that delamination of the a-C:15H coating occurred at some regions or/and that the iron coming from the pin worn particles took part in the tribofilm formation on the a-C:15H surface. This is in agreement with our observation from EDX analysis where iron was detected at some regions inside the wear track.

Table 6-1 XPS quantification of tribofilms for a a-C:15H/CI system after 20 h tests.

Sample	Surface	Elemental composition of Tribofilms (at.%)								
		Fe	O	P	Zn	C	Ca	Mo	N	S
FF40+	Pin	1.3	21.3	1.5	0.2	68.1	3.9	1.9	0.9	0.9
	Plate	0.0	4.3	0.3	0.2	91.9	0.8	1.1	0.9	0.6
FF40-	Pin	3.8	32.4	0.0	0.0	60.7	1.1	2.0	0.0	0.0
	Plate	0.0	4.3	0.0	0.0	90.7	1.2	1.1	2.0	0.7
FF300+	Pin	1.2	35.7	1.1	0.2	54.9	1.8	2.6	1.8	0.7
	Plate	0.0	3.7	0.4	0.1	92.0	0.6	1.4	1.1	0.8
FF300-	Pin	1.6	34.9	0.0	0.0	42.7	1.3	12.3	6.4	0.8
	Plate	0.0	2.8	0.0	0.0	93.5	0.6	0.9	1.8	0.4
FF600+	Pin	0.8	34.7	3.2	0.9	48.6	2.7	5.3	2.6	1.1
	Plate	0.0	3.0	0.4	0.1	91.4	0.7	2.3	1.3	0.8
FF600-	Pin	0.9	21.0	0.0	0.0	63.2	2.0	7.8	4.0	1.1
	Plate	0.3	9.1	0.0	0.0	76.5	1.6	6.9	4.1	1.4

6.3.3.2. Low friction film formation

From Table 6-1, it is also evident that the amount of Mo 3d detected in the tribofilm formed from oils with low level of Mo-FM is negligible compared to the oils with high Mo-FM concentration which made it almost impossible to fit

the obtained Mo 3d peaks. That could explain relatively high friction obtained by these oils (i.e. FF40+ and FF40-). Furthermore, oils with medium level of Mo-FM showed to provide negligible amount of Mo 3d on the tribofilm formed on the DLC plates using both FF300+ and FF300- whereas the amount of Mo 3d detected on the pins was comparatively higher for FF300- compared to FF300+ which could validate the lower friction values obtained by this oils. In addition, Mo was detected in the tribofilm formed from oils with high Mo-FM concentration both on the a-C:15H coated plates and the CI pins. However, the amount of Mo detected on the DLC plate provided by FF600+ was comparatively low and therefore, the Mo 3d peak was difficult to be fitted. The fitted Mo 3d peaks obtained from the FF600- tribofilm formed on both pin and a-C:15H coating are shown in Figure 6-20. Taking into account the binding energies of S 2p peaks, it is evident that both additives tribofilms contained abrasive Mo-oxide species (possible cause of DLC brittleness [41]) as well as the low shear strength MoS₂. That could explain the highest wear and lowest friction obtained by the oils with high level of Mo-FM (600 ppm).

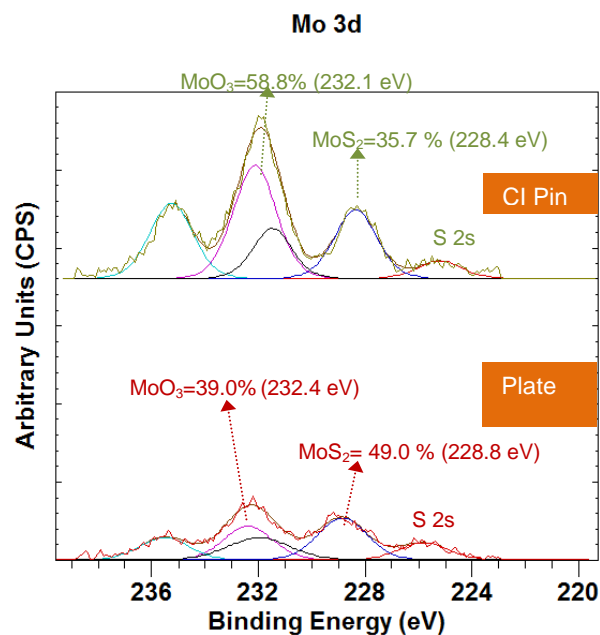


Figure 6-20 Curve fitting of Mo 3d peaks obtained from tribofilm formed from FF600- on both pin and a-C:15H coating.

The fitted carbon peaks for the highest wearing oil (FF600-) in the tribofilm formed on both CI pin and a-C:15H plate are shown in Figure 6-21. It can be

seen that only a minor portion of carbon on the a-C:15H coating was oil-derived oxygen-containing hydrocarbon species while a major part was detected to be pure carbon (graphitic) [267] which would derive from transfer from the coating. High wear provided by high Mo-FM concentration fully formulated oils resulted in transferring a-C:15H wear debris from the a-C:15H coating to the pin counterface which is confirmed by the presence of graphitic carbon in the tribofilms formed on the CI pin. Furthermore, the higher detected oil-derived hydrocarbon species on the CI pin could be due to the higher reactivity of ferrous counterbody with the lubricant components compared to the a-C:15H coating. Therefore, it is evident that DLC wear debris could also contribute to the friction reduction along with the additive derived low friction MoS₂ sheets [253].

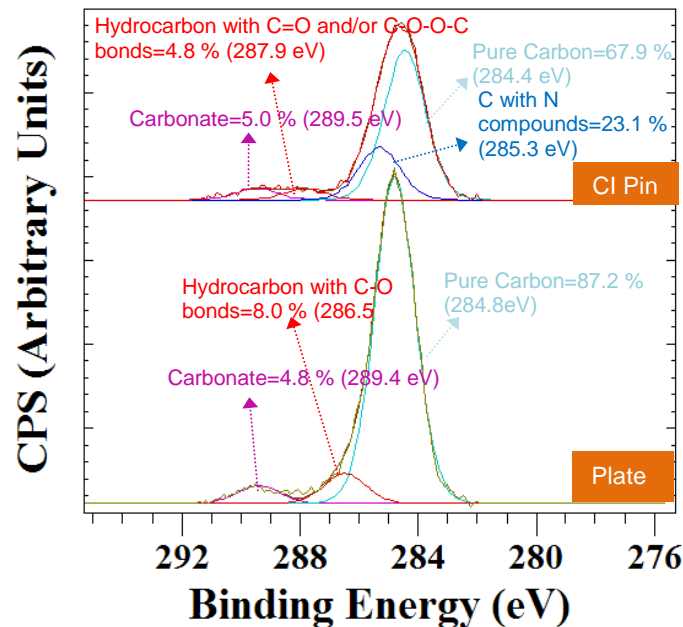


Figure 6-21 Carbon species on the wear scar of a-C:15H coating and CI pins for the highest wear giving lubricants (FF600-).

6.3.3.3. Antiwear film formation

Zn-phosphate and ZnS/ZnO species were formed in the tribofilms using all ZDDP-containing fully formulated oils which is in agreement with the presence of zinc phosphates on the low hydrogen-containing DLC (a-C:15H) coating as reported elsewhere [216]. It is also clear that the presence of Mo-

FM in the oil did not affect phosphate film formation on the surface. In addition, ZDDP increased friction when added to the lubricant which is in agreement with the literature where formation of pad-like tribofilm was identified as the reason for such higher friction [29]. The fitted Zn 2p and P 2p peaks are shown in Figure 6-22. The obtained results clearly show the critical role of ZDDP on the wear performance/durability of a-C:15H coating.

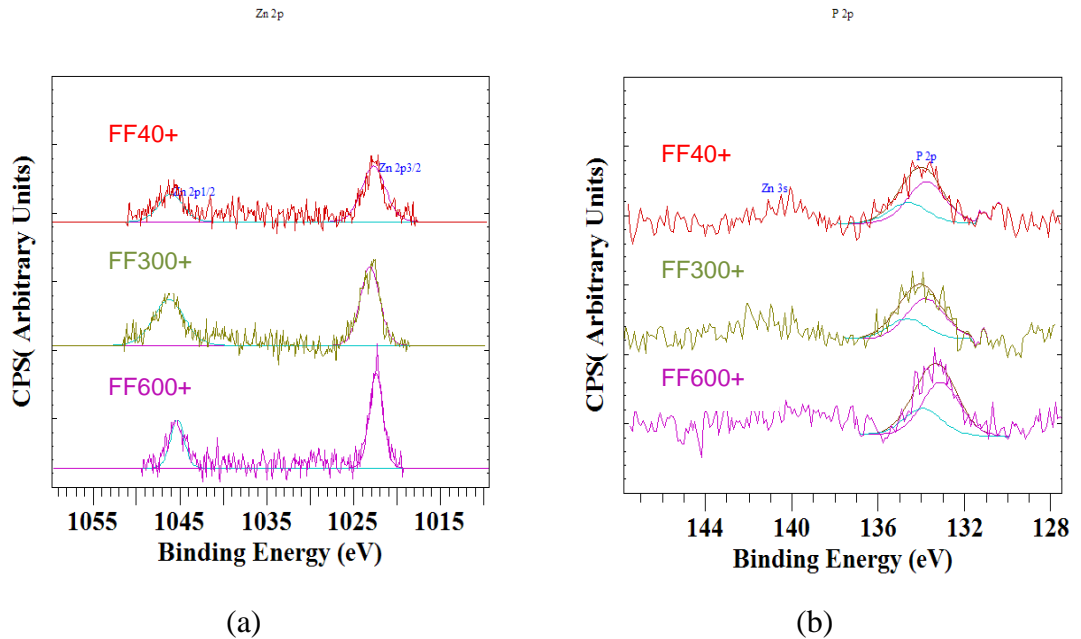


Figure 6-22 XPS spectra of ZDDP derived species (a) Zn 2p, (b) P2p formed on the a-C:15H coated plate using different fully formulated oils.

6.3.4. Mechanical Properties of the Coatings

Nano-indentation tests were conducted around the centre of worn a-C:15H coating surfaces as well as outside of the wear scar for each sample. In Table 6-2, the hardness and reduced elastic modulus (E_r) values for the coated samples after 20 h pin-on-plate test are given. Reduced modulus indicates the compliance of a sample with the indenter. It is calculated by combining the elastic modulus and Poisson's ratio of the indenter and the sample being indented. Comparing these values with properties of the as-deposited coating ($H > 20$ GPa and E_r 180 GPa), it can be observed that the coatings which experienced higher wear, generally showed decreased coating hardness and modulus of elasticity. Although the standard deviation from the average values were quite high specially when the measurements

were conducted outside of the wear scar. The high error for the obtained values outside of the wear scar probably originated from the specific surface morphology of the DLC coatings. In addition, the obtained values, outside of the wear scar differ from one sample to another which could be due to inevitable differences in sample preparation (e.g. different coating quality). Nevertheless, taking into account the standard deviation, the obtained results suggests that the mechanism of a-C:15H coating wear could be related to the change in the mechanical properties of the coating, which in turn is a function of tribochemistry of additive components on the a-C:15H coating surface.

Table 6-2 Nano-scale mechanical properties of DLC coating after 20 h tests.

Sample	Measurement position	Maximum depth (nm)	Standard deviation (\pm)	Hardness (GPa)	Standard deviation (\pm)	Reduced elastic modulus (GPa)	Standard deviation (\pm)
FF40+	Inside Wear Track	116.2	5.5	17.2	1.8	159.1	11.5
	Outside Wear Track	104.3	10.7	21.1	4.3	191.7	28.1
FF40-	Inside Wear Track	111.5	4.7	18.2	1.7	170.6	11.3
	Outside Wear Track	115.6	11.6	17.1	3.2	165.8	24.5
FF300+	Inside Wear Track	120.3	5.5	15.8	1.6	154.0	10.7
	Outside Wear Track	110.3	16.5	19.1	5.4	184.0	43.1
FF300-	Inside Wear Track	70.1	12.3	14.0	1.9	148.2	11.9
	Outside Wear Track	115.5	18.8	18.4	7.4	171.4	43.9
FF600+	Inside Wear Track	80.9	14.4	10.7	2.2	129.6	11.1
	Outside Wear Track	100.6	10.9	23.3	5.2	198.4	33.4
FF600-	Inside Wear Track	77.4	16.0	10.9	1.6	140.3	9.3
	Outside Wear Track	105.1	9.4	20.9	4.9	186.4	26.1

Due to the fact that FF600- showed delamination of the a-C:15H coating at some regions, the analysis was carried out in chosen areas where coating was still remained on the substrate. However, the obtained hardness and reduced elastic modulus values could have been affected by the Cr/CrN interlayer or/and substrate because of the high wear seen using this

particular oil. Therefore, The obtained results for analysis of the wear scar of the a-C:15H coating using FF600- is presented in red (Table 6-2) to highlight the possible “substrate effect”.

Moreover, the obtained nanoindentation average values from outside of the wear scar (see Table 6-2), and considering the standard deviation, were found to be comparatively close to that of as-deposited coating indicating that the wear mechanisms of the a-C:15H coatings are more likely to be tribochemical effect rather than pure chemical reaction of the oils with the a-C:15 coatings.

In addition, in order to find out whether the obtained results for mechanical properties of the DLC coatings, when the wear was high, have been potentially influenced by CrC/CrN interlayer or/and substrate, nanoindentation analysis was also performed on the CrN coatings (see Table 6-3) which were provided by the commercial provider of the DLC coatings. In addition nano-scale mechanical properties of the steel substrate were also conducted and are shown in Table 6-3. The CrN coating was a good replica of what could be found with regards to the interlayer in a a-C:15H DLC coating. The measurements are based on three different samples of each material and typical results are presented in Table 6-3.

Table 6-3 Nano-scale mechanical properties of CrN coating interlayer and steel substrate.

Sample	Maximum depth (nm)	Standard deviation (\pm)	Hardness (GPa)	Standard deviation (\pm)	Reduced elastic modulus (GPa)	Standard deviation (\pm)
CrN (Interlayer)	92.8	10.1	16.1	3.3	254.4	34.1
Steel (Substrate)	987.5	58.2	10.5	1.4	211.3	14.7

It should be noted that depth of penetration for nanoindentation analysis of coatings which experienced comparatively higher wear (i.e. FF300-, FF600+ and FF600-) was maintained to be less than 10% of the coatings thicknesses inside the wear scar to minimise the possible “substrate effect” on the obtained results. Obviously, FF600- showed severe

wear/delamination of the coating at some regions which might have affected the nanoindentation measurements of the coating lubricated with this particular oil.

Therefore, considering the depth of penetration for nanoindentation analysis and the mechanical properties of the CrN interlayer and the steel substrate, the tribochemistry of additive components dominates the surface modification of the a-C:15H coating surfaces rather than the “substrate effect” on the obtained values of hardness and Young’s modulus. DLC coating might have undergone graphitisation and showed lower values of lower Young’s modulus (E) and hardness (H) compared to bare coating [199]. However, nanoindentation analysis of the DLC coatings which were experienced shorter tribo-tests and subsequent lower wear, could further elucidate possible effect of CrC/CN interlayer or and substrate. This will be presented later in this chapter.

6.3.5. Effect of Test Duration

Following the results obtained using oils with different Mo-FM level, it was seen that the friction decreased with increase in Mo-FM concentration in the oils. MoDTC derived MoS₂ sheets, which are known to be responsible for friction reduction, were observed on the a-C:15H coated plates using oils with high level of Mo-FM. In addition wear values showed an inverse correlation with friction (i.e. the higher the friction the lower the wear values).

In order to provide a better picture of low friction film formation and wear mechanism, shorter tests were also performed (i.e. 6 and 12 h) and the tribological comparison were made with those obtained after 20 h tests. The aim was to provide an insight into DLC-MoDTC interaction by investigating whether a-C:15H coating first undergoes high wear due to the interaction with MoDTC and that is where the drop in friction starts occurring or it is the case that MoDTC decomposition products initially form a tribofilm on the surface offering low friction followed by high wear on the a-C:15H coated plates. The results for 20 h tests have been reported in previous section and are represented here for comparison purposes.

6.3.5.1. Friction Results

The steady state friction coefficients (i.e. the average of the last hour) as a function of test duration for the a-C:15H/Cl combination using six different oils are presented in Figure 6-23. Overall, regardless of the test duration, friction was seen to be oil dependant and a drop in friction was seen with increase in Mo-FM level (i.e. 300 ppm and 600 ppm) even 6 h after the start of the tests. In general, friction behaviour for FF40+, FF40- and FF300+ was seen to be independent of the test duration while in the case of FF300-, FF600+ and FF600- the friction values were observed to be on average lower after 12 h compared to 20 h. Based on the friction results, ZDDP in high level Mo-FM-containing fully formulated oils (600 ppm), when the test was running over 12 h, did not significantly affect friction and the presence of Mo-FM was the dominating factor on the observed friction response (i.e. the obtained friction values for 12 and 20 h tests for high Mo-FM-containing oils (FF600+ and FF600-) were comparable and within the scatter of the results).

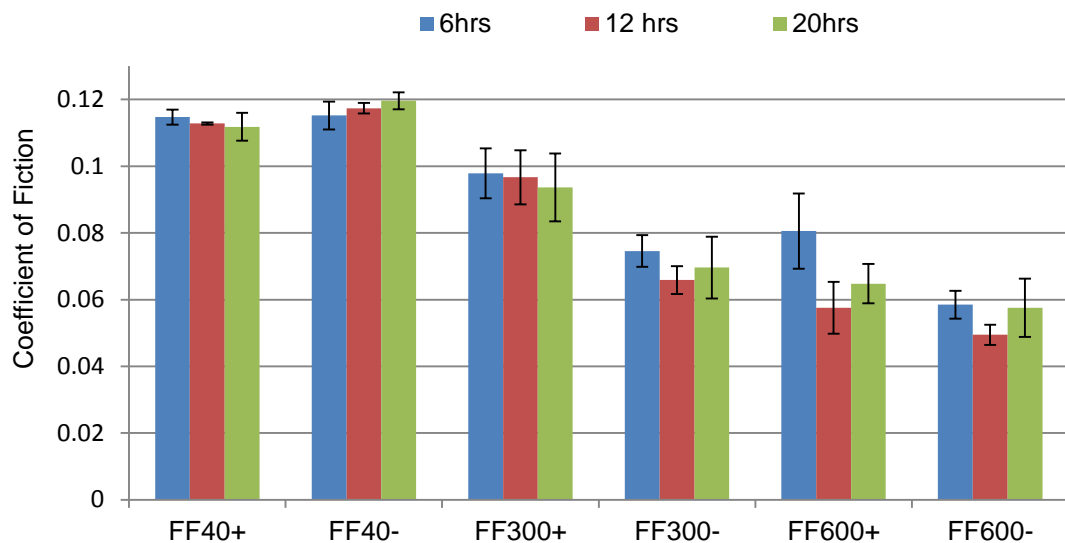


Figure 6-23 Steady state friction coefficients as a function of oils with different Mo-FM concentration at different time intervals for a-C:15H/Cl system.

6.3.5.2. Wear Results

The wear coefficients as a function of test duration for the a-C:15H/Cl combination using six different oils are given in Figure 6-24. The wear values for low Mo-FM concentration (i.e. FF40+ and FF40-) was found to be

extremely low for 6 h tests and therefore was almost impossible to be measured. That is why no wear values are present for 6 h tests using these oils (See Figure 6-24). By increasing the duration of the test to 12 and 20 h, the wear rates provided by low Mo-FM concentration-containing fully formulated oils (FF40+ and FF40-) on a-C:15H/CI system were still observed to be comparatively low. In addition FF300+ wear rates were also seen to be relatively low and comparable for all the time intervals. However, in the case of FF300-, FF600+ and FF600-, wear rates were generally higher compared to other oils and significantly increased with increase in the test duration.

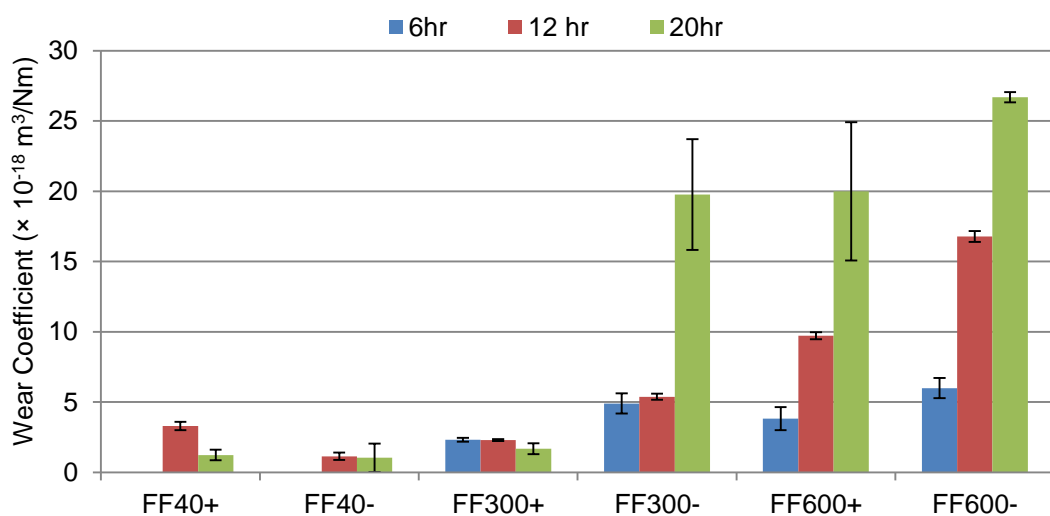


Figure 6-24 Wear coefficient as a function of oils with different Mo-FM level.

It is interesting to note that for 6 h tests and considering the error bars, the wear rates are similar for FF300-, FF600+ and FF600- while increasing the test duration made a significant difference in the wear rates of the a-C:15H coated plates. It is also evident that ZDDP did not offer any positive effect in wear protection for low concentration Mo-FM oils (FF40+ and FF40-) while for oils with medium and high Mo-FM level (i.e. FF300+, FF300-, FF600+ and FF600-), irrespective of the test duration, the wear performance was improved in the presence of ZDDP; this is clear by comparing FF300+ with FF300- and FF600+ with that of FF600-. However, it should be noted that for 20 h tests, ZDDP is not as effective in counteracting the adverse effect of Mo-FM on high wear of a-C:15H coating for high concentrations of Mo-FM (i.e. FF600+ compared to FF600-). Figure 6-25 shows typical images of wear track on the a-C:15H coating after 6,12 and 20 h, respectively.

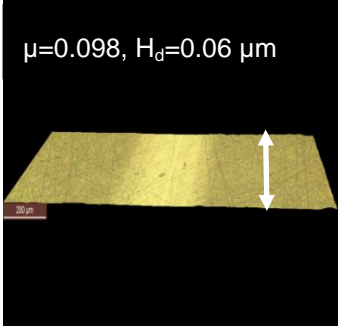
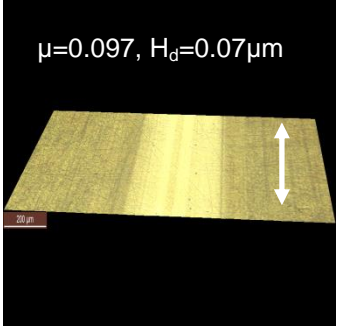
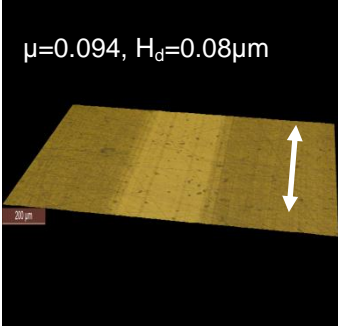
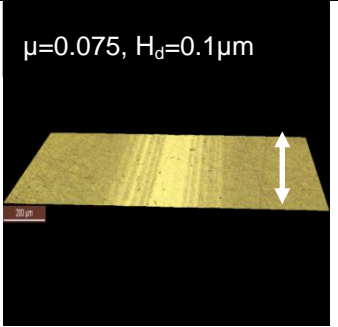
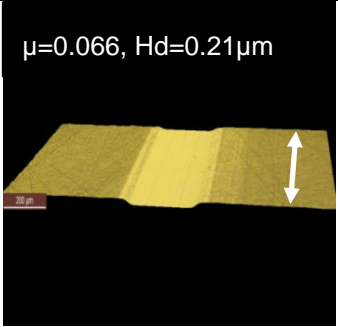
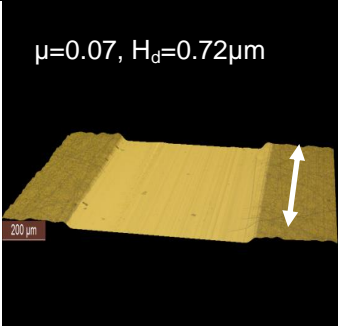
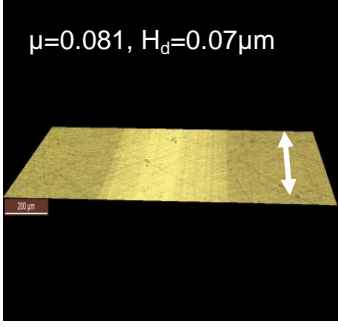
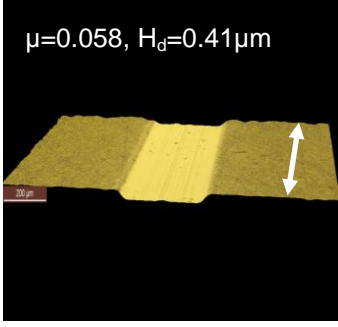
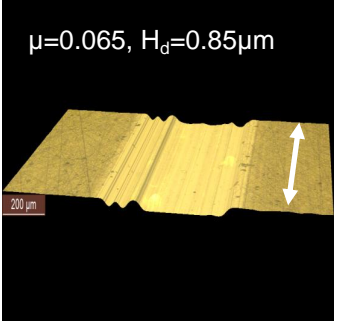
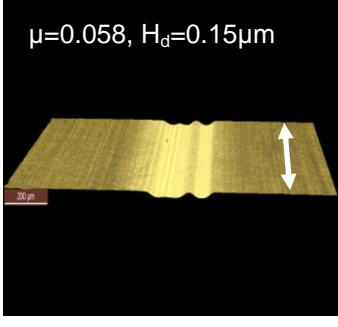
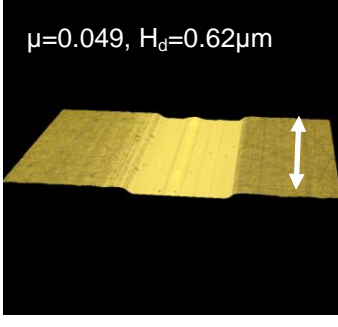
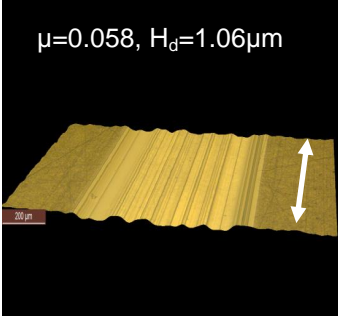
Oil	Test Duration (h)		
	6	12	20
a	$\mu=0.098, H_d=0.06 \mu\text{m}$ 	$\mu=0.097, H_d=0.07 \mu\text{m}$ 	$\mu=0.094, H_d=0.08 \mu\text{m}$ 
b	$\mu=0.075, H_d=0.1 \mu\text{m}$ 	$\mu=0.066, H_d=0.21 \mu\text{m}$ 	$\mu=0.07, H_d=0.72 \mu\text{m}$ 
c	$\mu=0.081, H_d=0.07 \mu\text{m}$ 	$\mu=0.058, H_d=0.41 \mu\text{m}$ 	$\mu=0.065, H_d=0.85 \mu\text{m}$ 
d	$\mu=0.058, H_d=0.15 \mu\text{m}$ 	$\mu=0.049, H_d=0.62 \mu\text{m}$ 	$\mu=0.058, H_d=1.06 \mu\text{m}$ 

Figure 6-25 Optical images of the wear scars formed on the a-C:15H coated plates using (a) FF300+, (b) FF300-, (c) FF600+ and (d) Oil600-. The arrows on the images show sliding directions and μ and H_d are the coefficient of friction and the average depth of the wear track, respectively.

Images of the wear track provided by low Mo concentration (Figure 6-25) are not presented here as they showed insignificant wear. Based on the provided images, it is evident that the extent and mechanisms of the wear is not only dependent on the additive package used in the lubricant but also affected by the test duration. The brighter colour of the wear track (see Figure 6-25), is due to the underlying Cr/CrN interlayers which is exposed as a result of the loss of top carbon layer of the DLC coating. To verify the observations from wear results and optical microscope images, EDX was carried out in the wear scar. The typical secondary electron (SE) image of a section of a-C:15H coating wear scar along with EDX mapping of C, Cr and Fe after 6 h tribo-tests using oils with medium (300 ppm) and high (600 ppm) MoDTC concentration are shown in Figure 6-26.

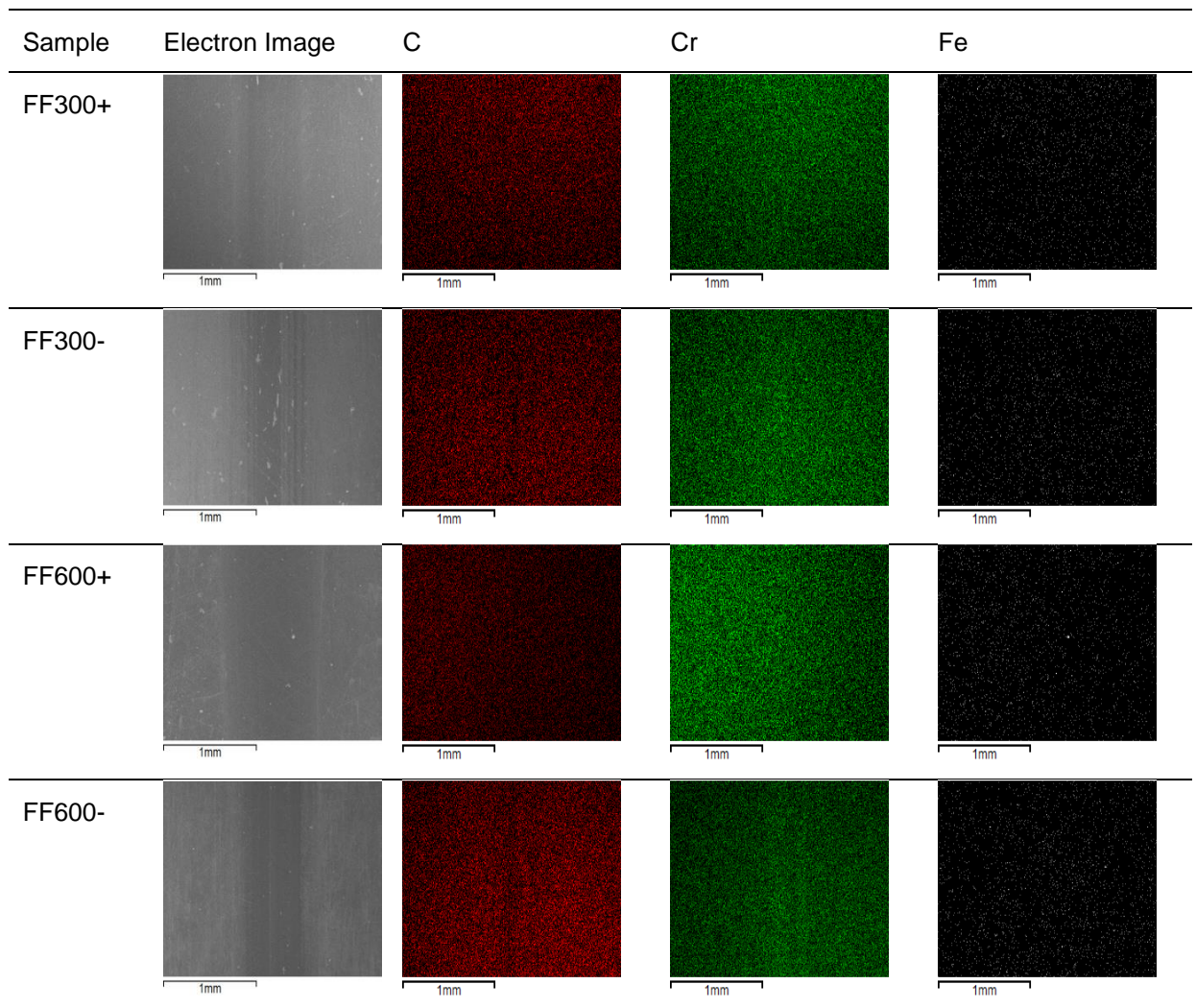


Figure 6-26 SEM image of a-C:15H coating along with EDX mapping of the C, Cr and Fe atoms for 6 h tests.

Based on the images (see Figure 6-26), no significant difference was observed by different oils after 6 h tests. For all the oils, except for FF600-, no sign of carbon removal or Cr-interlayer exposure was seen. Only in the case of FF600-, a trace of carbon removal was seen and the chromium was richer inside the wear track. This implies that the wear, given by these oils, was insignificant 6 h after the start of the tests which is in agreement with our wear data and optical microscope observation. Fe was not detected using any of the oils which elucidate any possible delamination of the coatings. In addition, the EDX mapping was carried out for medium and high Mo-FM concentration after 12 h tribo-tests (see Figure 6-27).

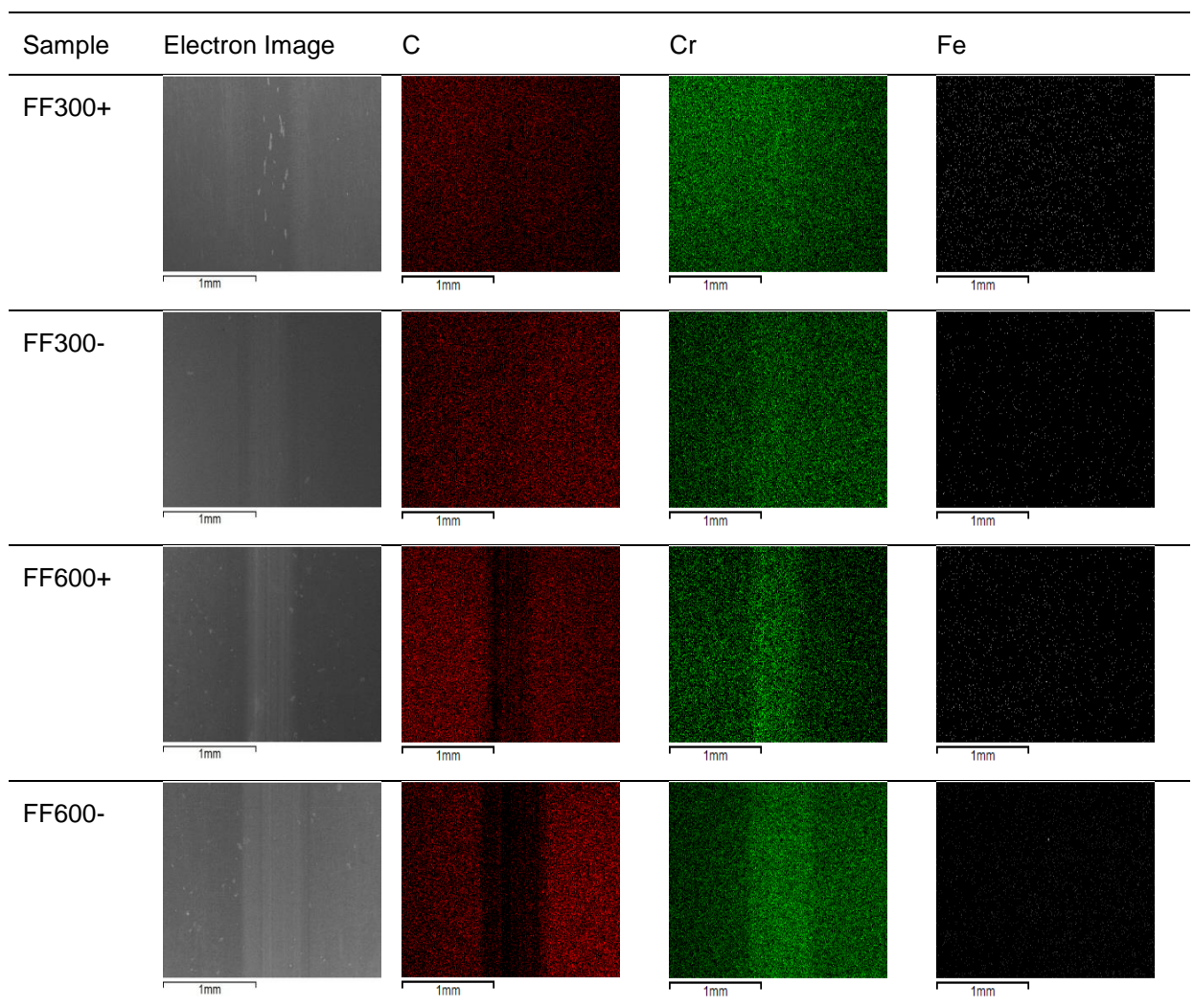


Figure 6-27 SEM image of a-C:15H coating along with EDX mapping of the C, Cr and Fe atoms for 12 h tests.

For oils with high MoDTC formulation (600 ppm), it is evident that by increasing the test duration, C was being removed and Cr was becoming richer in the middle of the wear scar than outside (higher wear). In general, this was more pronounced for ZDDP-free oil (FF600-). No significant difference in C, Cr and Fe content was seen for FF300+ whereas eliminating ZDDP from the oil formulation ((FF300-) resulted in slightly lower C and higher Cr inside the wear track. Comparing EDX mapping of C, Cr and Fe atoms of a-C:15H coating after the tests, in general, ZDDP-containing oils showed lower wear compared to ZDDP-free oils. Fe was absent at any regions inside the wear scar indicating that no delamination of the coatings or/and iron transfer from the CI pin to the DLC coating has occurred after 12 h of the tests using any of the oils.

Regardless of the test duration, FF300+ (Figure 6-25a) did not give high wear and/or delamination of the coating; rather, the wear of the coating was dominated by gradual polishing wear. Furthermore, the average depth of the wear track (h_d) of a-C:15H coating for the highest obtained wear, given by FF600-, was approximately 0.15 μm over 6 h test while it has increased dramatically to 1.06 μm when the test continued for 20 h.

6.3.5.3. Chemical Analysis of the Tribofilms

6.3.5.3.1. Elemental Composition

In order to compare the formed tribofilm on the a-C:15H plates and their corresponding counterparts as a function of the test duration XPS analysis was conducted on the samples. The chemical quantification of the tribofilms formed on the a-C:15H/CI tribocouple lubricated in oils with different MoDTC concentration for 6 and 12 h tests are shown in Table 6-4 and Table 6-5, respectfully. As expected, it is evident that oil additives were decomposed and formed on both the a-C:15H and the CI pin counterpart which in turn could generally dominates the tribological performance of the a-C:15H/system and durability/wear performance of the coatings in particular.

In addition, the absence of Fe 2p peak in the tribofilm formed from all oils on the a-C:15H coatings implies that no delamination of the a-C:15H coating occurred or/and that no iron coming from the pin worn particles participated

in the tribofilm formation on the a-C:15H surface. It should also be noted that based on the XPS analysis, Cr 2p peak was not detected in the tribofilm formed on the a-C:15H coating using Mo-FM-containing oils for both 6 and 12 h tests proposing that, despite the severe wear of the coatings which was observed using FF300-, FF600+ and FF600- oils, in any of the cases, the chromium internal layer was not exposed even after 12 h tribo-tests and that the tribofilms were formed on the top carbon layer of the DLC coatings.

Table 6-4 XPS quantification of tribofilms for a a-C:15H/CI system after 6 h tests.

Sample (6 h)	Surface	Elemental composition of Tribofilms (at.%)								
		Fe	O	P	Zn	C	Ca	Mo	N	S
FF300+	Pin	0.3	18.7	0.9	0.4	70.0	2.3	4.4	1.2	1.7
	Plate	0.0	5.7	0.2	0.1	90.2	0.2	1.9	0.9	0.7
FF600+	Pin	0.4	14.0	0.3	0.2	76.7	0.8	4.1	1.6	1.9
	Plate	0.0	7.4	0.2	0.1	86.7	0.5	3.2	0.9	0.8
FF300-	Pin	0.5	17.6	0.0	0.0	73.2	1.6	4.9	1.4	0.9
	Plate	0.0	5.5	0.0	0.0	90.8	0.5	1.6	1.1	0.5
FF600-	Pin	0.2	13.7	0.0	0.0	69.2	1.6	11.9	2.3	1.2
	Plate	0.0	6.3	0.0	0.0	89.5	0.5	2.0	1.0	0.7

Table 6-5 XPS quantification of tribofilms for a a-C:15H/CI system after 12 h tests.

Sample (12 h)	Surface	Elemental composition of Tribofilms (at.%)								
		Fe	O	P	Zn	C	Ca	Mo	N	S
FF300+	Pin	0.1	17.4	0.6	0.2	74.6	2.2	1.6	2.2	1.0
	Plate	0.0	2.1	0.1	0.2	94.9	0.3	1.1	0.7	0.6
FF600+	Pin	0.4	16.6	0.7	0.3	62.1	0.9	11.4	5.9	1.7
	Plate	0.0	2.4	0.2	0.1	93.9	0.0	1.4	1.3	0.7
FF300-	Pin	0.5	22.7	0.0	0.0	62.3	2.2	6.7	4.6	1.0
	Plate	0.0	1.9	0.0	0.0	95.8	0.3	0.8	0.9	0.3
FF600-	Pin	0.5	18.2	0.0	0.0	52.9	1.5	17.0	7.9	1.8
	Plate	0.0	2.9	0.0	0.0	93.8	0.3	1.4	1.1	0.5

6.3.5.3.2. Low Friction Film Formation

In terms of low friction film formation, as shown in Table 6-4 and Table 6-5, it is interesting to note that the amount Mo which was detected in the tribofilm formed on the pins was generally higher for 12 h compared to 6 h tests

which could justify relatively lower friction obtained after 12 h compared to 6 h tests. However, the amount of Mo which was formed on the a-C:15H coating plates was insignificant irrespective of the test duration. On the other hand, the amount of Mo which was seen on the CI tribofilm in the a-C:15H/CI system after 20 h test (see Table 6-1) was lower compared to 12 h test which is in line with the obtained friction results comparing 12 h tests with those of 20 h.

As mentioned earlier, the amount of Mo detected on the a-C:15H coated plates were insignificant and therefore fitting the obtained Mo 3d curves was a challenge and almost impossible. However, comparing the formed Mo 3d peaks on the counterparts could be a good tool to understand the tribochemistry of a-C:15H/CI system. The fitted Mo 3d peaks obtained from the oils with different MoDTC concentration formed on the pins after 6 h and 12 h are shown in Figure 6-28. Considering the binding energies of S 2p peaks, it is evident that abrasive Mo-oxide species as well as the low shear strength MoS₂ have been identified in the tribofilms formed on the CI pins regardless of the duration of the tests. However, in general, MoS₂ contributed more to the film formation.

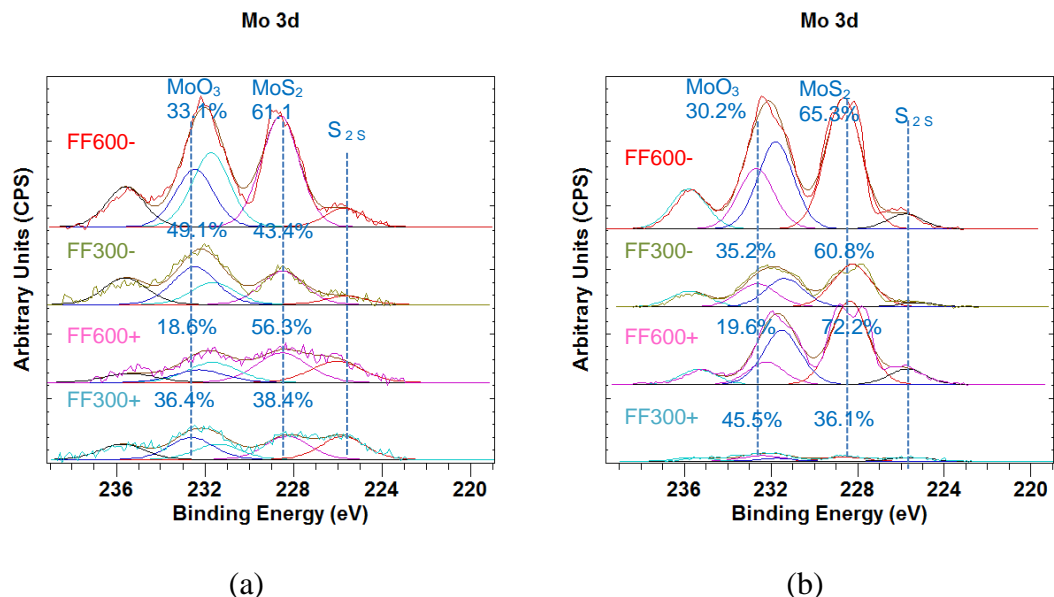


Figure 6-28 Curve fitting of Mo 3d peaks obtained from tribofilm formed from oils with different level of MoDTC on the CI pins after (a) 6 h and (b) 12 h.

As illustrated in Figure 6-28, it is also evident that FF600- oil formed a sharper peak with higher intensity than other oils which can be correlated to the richer low friction film on the CI pins justifying the lower obtained friction with this oil. Furthermore, in order to compare the low friction film formation with regards to the duration of the tests, the fitted Mo 3d peaks formed on the CI pins from oils with different level of Mo-FM as a function of test duration is shown in Figure 6-29.

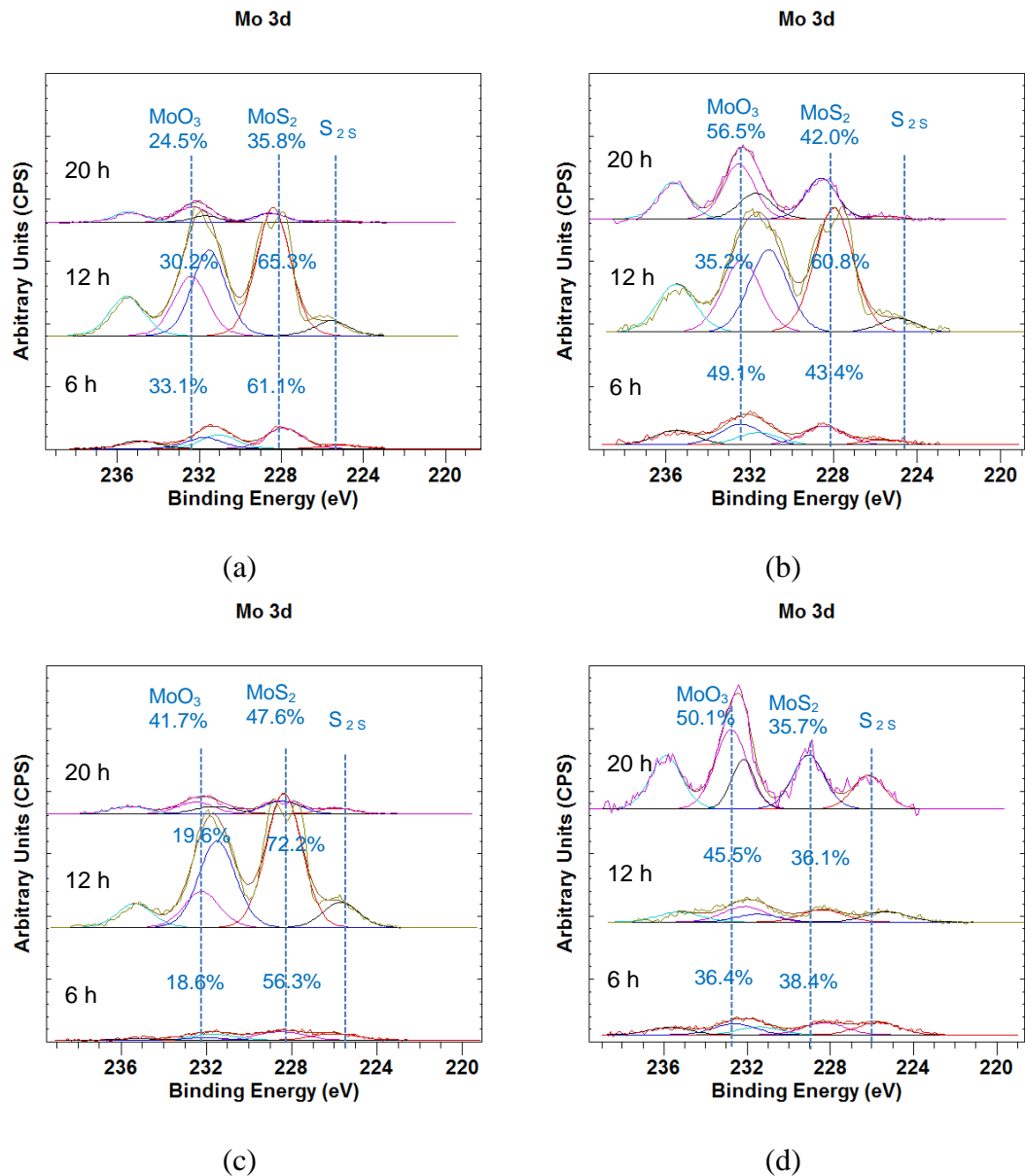


Figure 6-29 The fitted Mo 3d peaks formed on the CI pins from (a): FF600-, (b):FF300-, (c): FF600+ and (d):FF300+ as a function of test duration

It can be seen that for FF600-, FF600+ and FF300- oils (see Figure 6-29 a, b and C), the intensity of the Mo 3d peaks were higher after 12 h compared to 6 and 20 h tests. It implies that the tribofilm formed from these oils were richer in Mo, mainly consisted of MoS₂, after 12 h but that the Mo started to become depleted in the tribofilm when the tribo-tests continued for 20 h. This is in agreement with our friction results (see Figure 6-23) as using FF600-, FF600+ and FF300- oils, the lowest friction values were obtained after 12 h compared to 6 and 20 h tests.

In addition, the intensity of Mo 3d peak which is detected on the tribofilm formed from FF300+ is higher after 20 h of the tests compared to 6 and 12 h experiments. That could explain the friction values which were decreased with increase in the test duration using this oil. However, it is worth mentioning that the Mo tribofilm formed from FF300+ was mainly consisted of MoO₃ which has an abrasive nature and could increase the friction.

6.3.5.3.3. Anti-wear Film Formation

The XPS spectra of ZDDP derived species (Zn 2p and P 2p) formed on the a-C:15H plate (Figure 6-30-a and Figure 6-30-b) and on the CI pin (Figure 6-30-c and Figure 6-30-d) using FF600+ oil as a function of test duration is shown in Figure 6-30. It is clear that using FF600+ oil, irrespective of the duration of the tests, Zn-phosphate and ZnS/ZnO species were formed on both the a-C:15H plates and CI pins. The only exception was the tribofilm which is formed on the CI pin after 6 h using FF600+ which was mainly Zn-S-O compounds (BE=1023.15 eV). It is therefore evident that despite high level of Mo-FM which was blended in the FF600+ oil, the phosphate film formation on the surface was not halted.

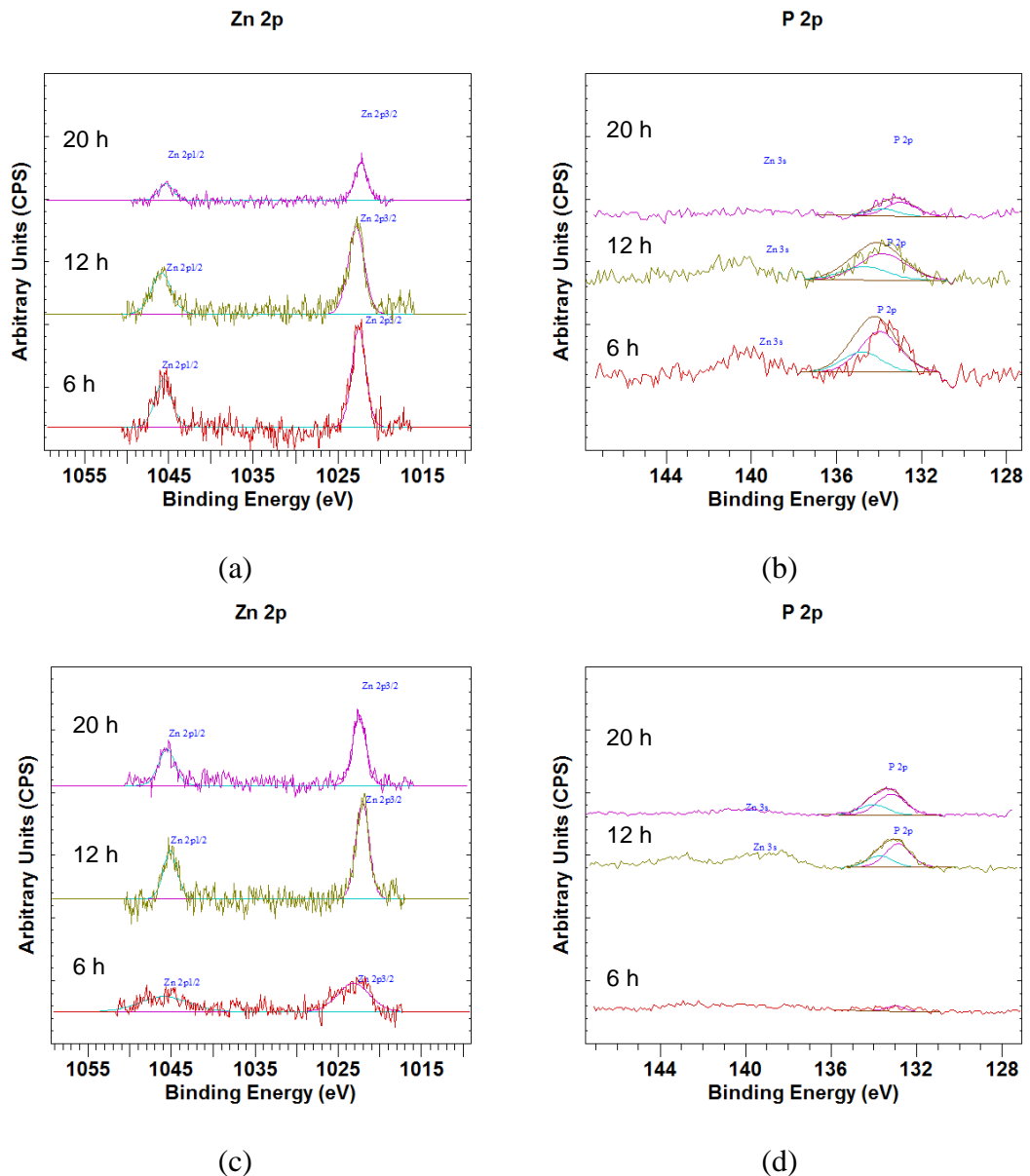


Figure 6-30 XPS spectra of ZDDP derived species (a) Zn 2p, (b) P2p formed on the a-C:15H coated plate and (c) Zn 2p and (d) P2p formed on the Cl pin using FF600+ as a function of test duration.

XPS spectra of Zn 2p and P 2p formed on the a-C:15H plate and on the Cl pin using FF300+ oil as a function of test duration was illustrated in Figure 6-31. It is evident that using FF300+ oil, and considering binding energies of the main peaks, the nature of the anti-wear tribofilm formed on surface of the a-C:15H coated plate was mainly Zn-S-O compound for 6 and 20 h tests whereas Zn-phosphate and ZnS/ZnO species were formed in the a-C:15H tribofilms after 12 h tests. In a similar manner, the surface of the Cl

pin counterparts were mainly rich in anti-wear ZDDP derived Zn-phosphate and ZnS/ZnO species.

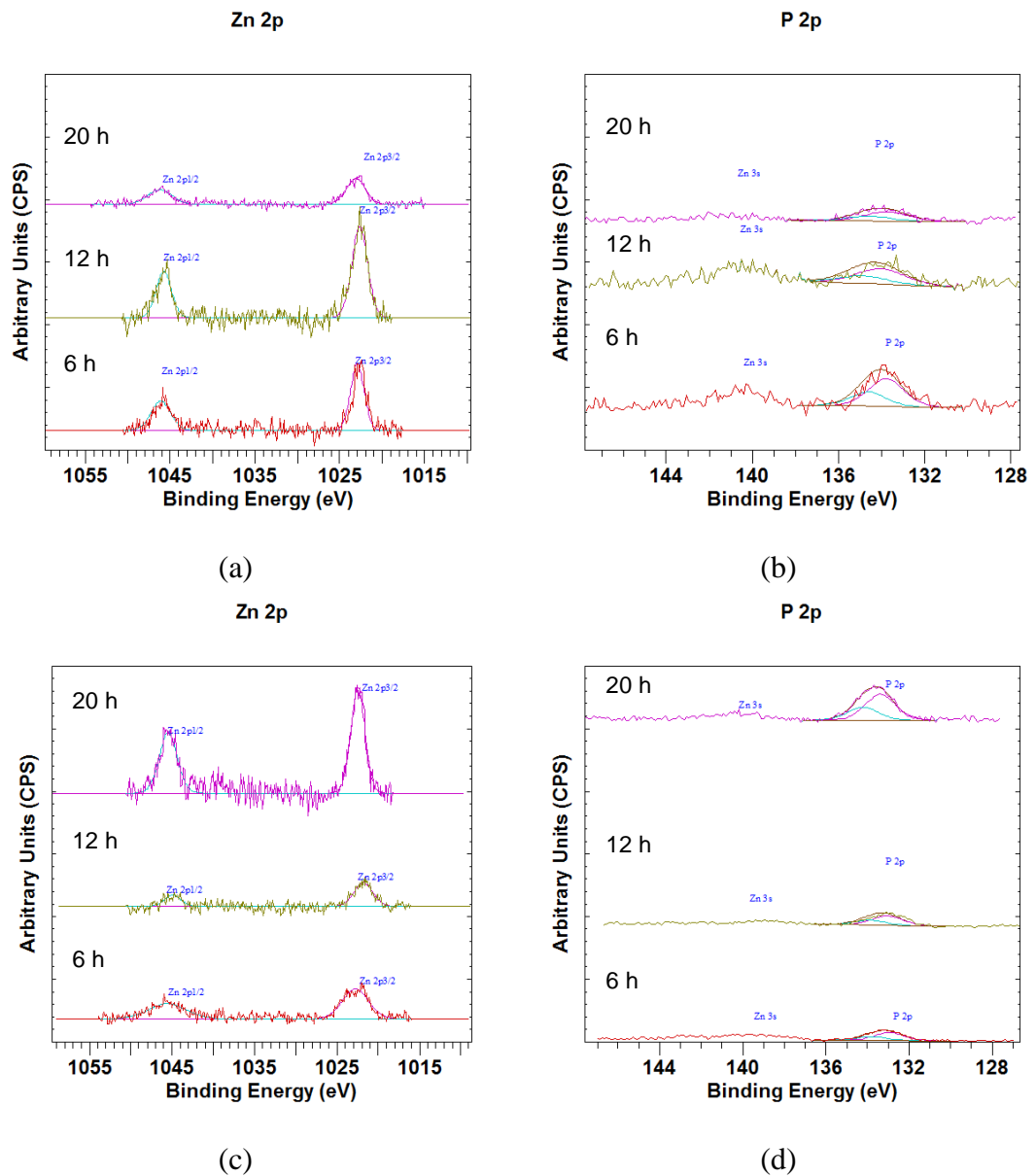


Figure 6-31 XPS spectra of ZDDP derived species (a) Zn 2p, (b) P2p formed on the a-C:15H coated plate using and (c) Zn 2p and (d) P2p formed on the CI pin using FF300+ as a function of test duration.

Nevertheless, using any of the ZDDP-containing fully formulated oils, and regardless of the test duration, the presence of ZDDP in the oil formulations raised the friction values compared to ZDDP-free fully formulated oils (see Figure 6-23), which could be due to the formation of pad-like tribofilm [29]. In

addition, as shown in Figure 6-24, irrespective of the test duration, ZDDP in the oil played an important role on the wear performance/durability of a-C:15H coating.

6.3.5.4. Mechanical properties of the coatings

In section 6.3.4, nano-indentation tests on the a-C:15H coatings which were undergone 20 h pin-on-plate experiments revealed that the tribochemistry of additive components is probably the dominating factor in hardness loss of the a-C:15H coating surfaces but that the “substrate effect” could also have had an impact on the obtained values of hardness and Young’s modulus. That was mainly due to the fact that using oils which were blended with high level of Mo-FM, the coatings became very thin at some regions inside the wear scar which in turn could have affected the measurements which were undertaken inside the wear scar of the coatings. Therefore, in order to have a better comparison between oils with different Mo-FM concentration, nano-indentation tests were carried out on the a-C:15H coatings which were undergone shorter tests (i.e. 6 and 12 h) and experienced lower wear, as a result. This could provide a better comparison and minimise the effect of substrate as the remaining coating inside the wear scar was reasonably better after 6 and 12 h tests.

In a similar manner to what was carried out in section 6.3.4, indentations were performed on the worn regions of a-C:15H coating surfaces as well as outside of the wear scar for each sample. The obtained results are shown in Table 6-6 and Table 6-7 for 6 and 12 h pin-on-plate experiments, respectively. The measured hardness and reduced elastic modulus (E_r) values for the coated samples are presented. For 6 h tests as shown in Table 6-6, it is evident that regardless of the extent of wear on the coatings and considering the standard deviation, hardness and modulus of elasticity values were comparable with those of as-deposited coating ($H > 20$ GPa and E_r 180 GPa). Comparing different DLC samples, It is also clear that the values obtained outside of the wear scar has large standard deviation from the average values which is probably due to the specific surface morphology of the DLC coatings. In addition, the obtained values, outside of the wear scar differ from one sample to another which could be due to inevitable differences in sample preparation (e.g. different coating quality). Similarly,

the obtained result for 12 h tests (see Table 6-7) shows that apart from FF600- (i.e. the lowest giving friction and highest wearing oil), there was no significant difference with regards to the hardness loss or/and Young's modulus compared to as-deposited coating. For FF600- oil, however, the hardness and elasticity modulus, which were almost unchanged after 6 h reciprocating experiments, decreased when the test duration continued for 12 h suggesting that the tribochemical effect of FF600- oil on surface modification of a-C:15H coating occurred after 6 h which is in agreement with our chemical analysis of the tribofilms where MoS₂ and MoO₃, which are the decomposition products from MODTC, were dominant on the a-C:15H coating after 12 h but not 6 h.

As shown in Figure 6-25, the average wear depth on a-C:15H coating wear track given by FF600-, was seen to be $H_d=0.62 \mu\text{m}$. In addition, the depth of penetration for nano-indentation analysis ($96.7 \pm 6.2 \text{ nm}$) which was chosen to be well below the 10% of the remaining coating thickness inside the wear scar implying that the tribochemistry of additive components initiated the surface modification of the a-C:15H coating and the obtained measurements were not mainly influenced by the "substrate effect".

Table 6-6 Nano-scale mechanical properties of DLC coating after 6 h tests.

Sample	Measurement position	Maximum depth (nm)	Standard deviation (\pm)	Hardness (GPa)	Standard deviation (\pm)	Reduced elastic modulus (GPa)	Standard deviation (\pm)
FF300+	Inside Wear Track	102.8	7.0	18.1	3.7	163.6	13.4
	Outside Wear Track	100.8	13.8	18.3	4.9	171.7	39.4
FF300-	Inside Wear Track	97.2	7.5	18.7	2	167.9	10.9
	Outside Wear Track	116.1	23.4	18.9	7.4	178.2	53.4
FF600+	Inside Wear Track	107.0	6.3	16.5	1.9	140.8	8.2
	Outside Wear Track	115.9	12.5	18.4	4.6	167.4	28.9
FF600-	Inside Wear Track	96.4	7.0	19.0	2.6	176.0	15.4
	Outside Wear Track	97.8	13.1	19.4	5.4	177.7	39.8

Table 6-7 Nano-scale mechanical properties of DLC coating after 12 h tests.

Sample	Measurement position	Maximum depth (nm)	Standard deviation (\pm)	Hardness (GPa)	Standard deviation (\pm)	Reduced elastic modulus (GPa)	Standard deviation (\pm)
FF300+	Inside Wear Track	98.8	8.9	19.5	2.4	165.2	18.8
	Outside Wear Track	98.1	11.1	19.9	4.5	174.7	37.3
FF300-	Inside Wear Track	100.6	4.9	17.7	1.6	166.7	7.3
	Outside Wear Track	97.9	14.1	18.7	5.5	185.2	37.9
FF600+	Inside Wear Track	93.3	6.1	20.7	2.0	180.8	8.8
	Outside Wear Track	94.2	15.8	22.3	8.0	192.1	50.5
FF600-	Inside Wear Track	96.7	6.2	12.4	2.7	150.4	9.8
	Outside Wear Track	103.9	13.31	16.4	4.9	165.3	37.9

6.3.6. Effect of Mo-FM Source

In previous sections of this chapter, the effect of Mo-FM in giving high wear to the a-C:15H coating was shown. It was seen that the higher the Mo-FM level in the oil, the higher the wear. It should be borne in mind that the Mo-FM which was used in previous sections was molybdenum dithiocarbamates with oxidation state of +4. In order to investigate the potential effect of Mo-FM source on the wear performance of the DLC coating, molybdenum dithiocarbamates with a different oxidation state (+5) was blended in the oil. Fully formulated oil with 300 ppm Mo-FM (oxidation state of +5) was used and the obtained results were compared with those observed earlier (section 6.3) using the same oil but formulated with Mo-FM with oxidation state of +4.

6.3.6.1. Friction Results

Friction traces as a function of time for the a-C:15H/CI combination using oils with different moly source is given in Figure 6-32. Based on the friction traces, regardless of presence or absence of ZDDP, using Mo-FM with oxidation state of +5, friction reduction was not observed over the duration of

the test. In contrast, a drop in friction was observed when ZDDP-free Mo-FM-containing fully formulated oil with oxidation state of +4 was used.

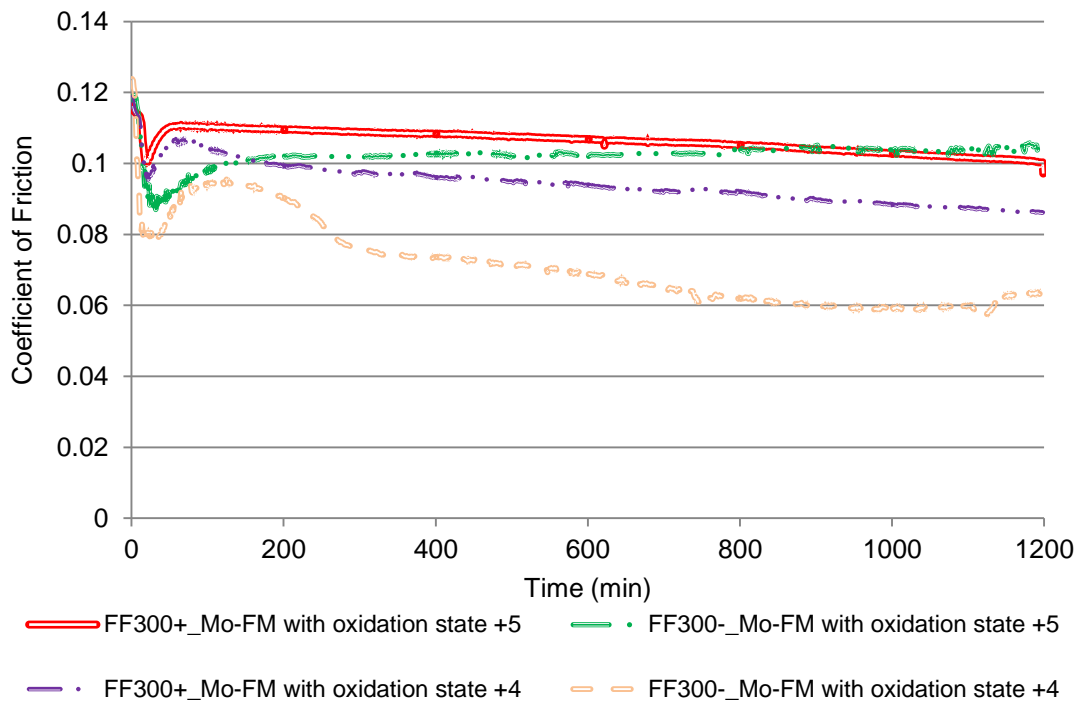


Figure 6-32 Friction traces as a function of time for the a-C:15H/Cl combination using oils with different Mo-FM source.

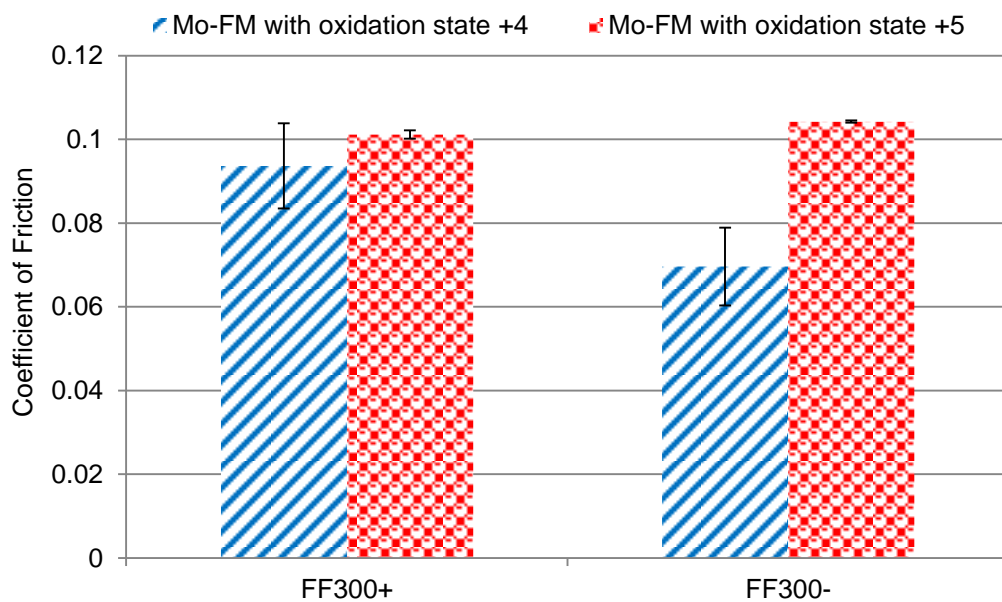


Figure 6-33 Steady state friction coefficients as a function of oils with different Mo-FM concentration at different time intervals for a-C:15H/Cl system.

The average steady state friction (i.e. the last hour of the tests) as a function of different oils for a-C:15H/CI system are presented in Figure 6-33. Overall, it is evident that friction behaviour was seen to be comparable for both Mo-FM with oxidation state of +5 and Mo-FM with oxidation state of +4 when ZDDP is present in the oil (FF300+). In contrast, Mo-FM with oxidation state of +4 provided a lower friction compared to Mo-FM with oxidation state of +5 when ZDDP is absent in the oils formulation (i.e. FF300-).

6.3.6.2. Wear Results

The wear coefficients as a function of Mo-FM source for a-C:15H coating are given in Figure 6-34. Based on the wear results, it is evident that, regardless of ZDDP being present in the oils or not, Mo-FM with oxidation state of +5-containing oils gave lower wear rate compared to Mo-FM with oxidation state of +4 after 20 h tests. In the case of the oils formulated with Mo-FM with oxidation state of +4, the wear rate was almost 12 times higher when ZDDP was not present in the oils (i.e. the addition of ZDDP to Mo-FM with oxidation state of +4-containing oils, significantly improved the wear performance).

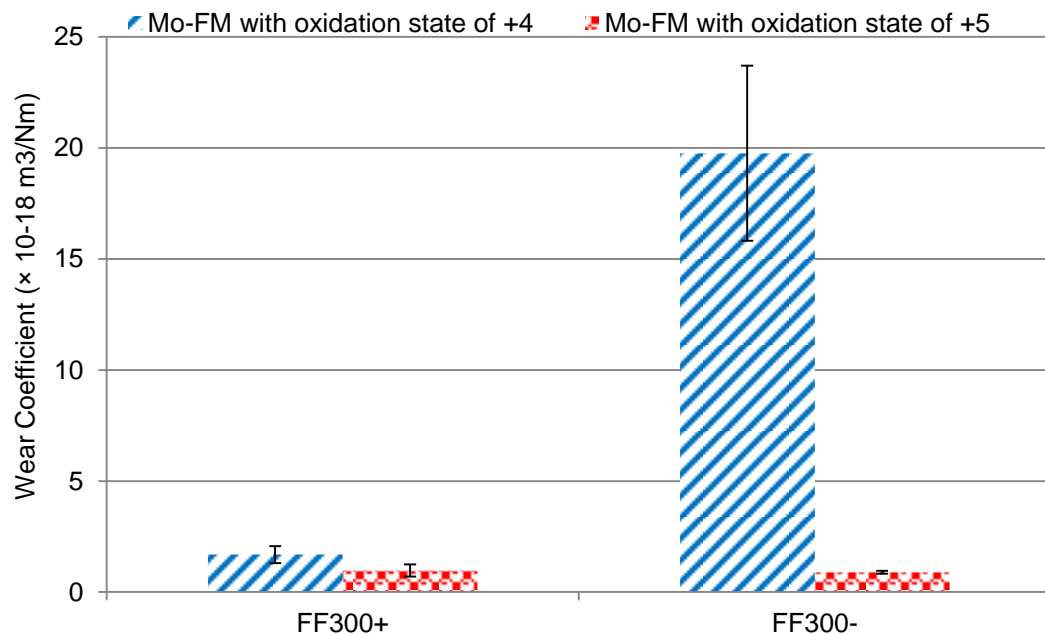


Figure 6-34 Wear coefficient as a function of oils with different Mo-FM concentration at different time intervals for a-C:15H/CI system.

In order to provide a better and comparative picture of the wear performance of oils with different type of MoDTC, typical images of wear track on the a-C:15H coating for oils with different Mo-FM source are shown in Figure 6-35. It is evident that the type of Mo-FM source used played an important role on the wear performance of the a-C:15h coating. In general, Mo-FM with oxidation state of +5-containing oils provided a lower wear compared to Mo-FM with oxidation state of +4-containing oils while, in the absence of ZDDP, the high wear given by Mo-FM with oxidation state of +4-containing oils exposed the underlying Cr/CrN interlayers. Comparing the μ and H_d values, it is clear that, in general, the higher the wear the lower the friction and vice versa.

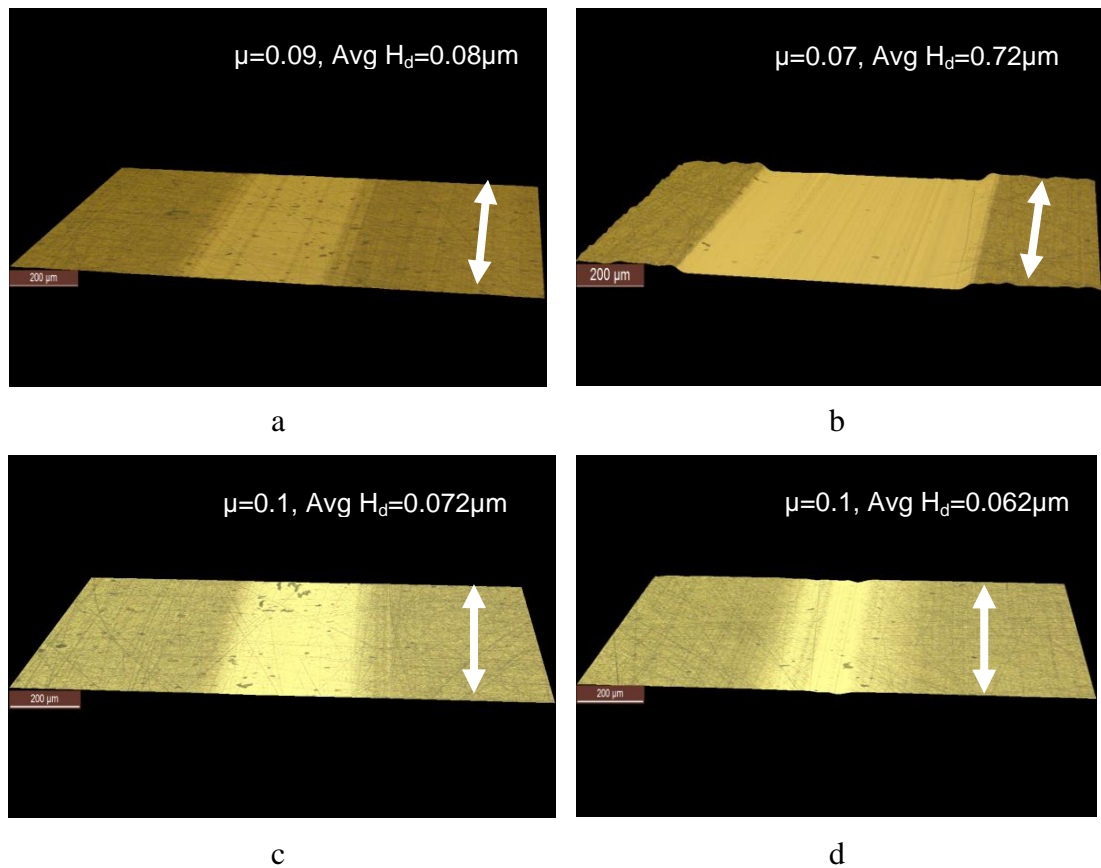


Figure 6-35 Optical images of the wear scars formed on the a-C:15H coated plates using (a) FF300+ (Mo-FM with oxidation state of +4), (b) FF300- (Mo-FM with oxidation state of +4), (c) FF300+ (Mo-FM with oxidation state of +5) and (d) FF300- (Mo-FM with oxidation state of +5). The arrows on the images show sliding directions and μ and H_d are the coefficient of friction and the average depth of the wear track, respectively.

In a similar manner to what was carried out in previous sections and to verify the observations from wear results and optical microscope images, EDX was carried out inside the wear scar. The tribofilm on the plates was removed by leaving the samples in an ultrasonic acetone bath (15 min) prior to the SEM/EDX analysis. Figure 6-36, illustrates the typical secondary electron (SE) image of a section of a-C:15H coating wear scar along with EDX mapping of C, Cr and Fe after the pin-on-plate tests. It is obvious that EDX mapping of a sample with higher wear provides lower carbon, higher chromium and some iron inside the wear scar.

From Figure 6-36, it is evident that only in the case of FF300- oil formulated with Mo-FM with oxidation state of +4, the top carbon layer was almost removed while Cr was richer inside the wear track. In addition, Fe was detected at some regions inside the wear scar of a-C:15H coating indicating that either the substrate is exposed (delamination) or the coating became very thin in the wear scar region (severe wear). This is in agreement with our previous observations using optical microscope and light interferometer which showed a high wear obtained by FF300- (Mo-FM with oxidation state of +4).

In spite of the fact that light interferometer showed a lower gradual wear using Mo-FM with oxidation state of +5, based on the EDX mapping presented in Figure 6-36, it is clear that wear scar given by Mo-FM with oxidation state of +5-containing fully formulated oils exhibited carbon removal at some points inside the wear scar. However, the amount of this removal was limited to the top carbon layer and was not extended to the interlayer or/ and the substrate.

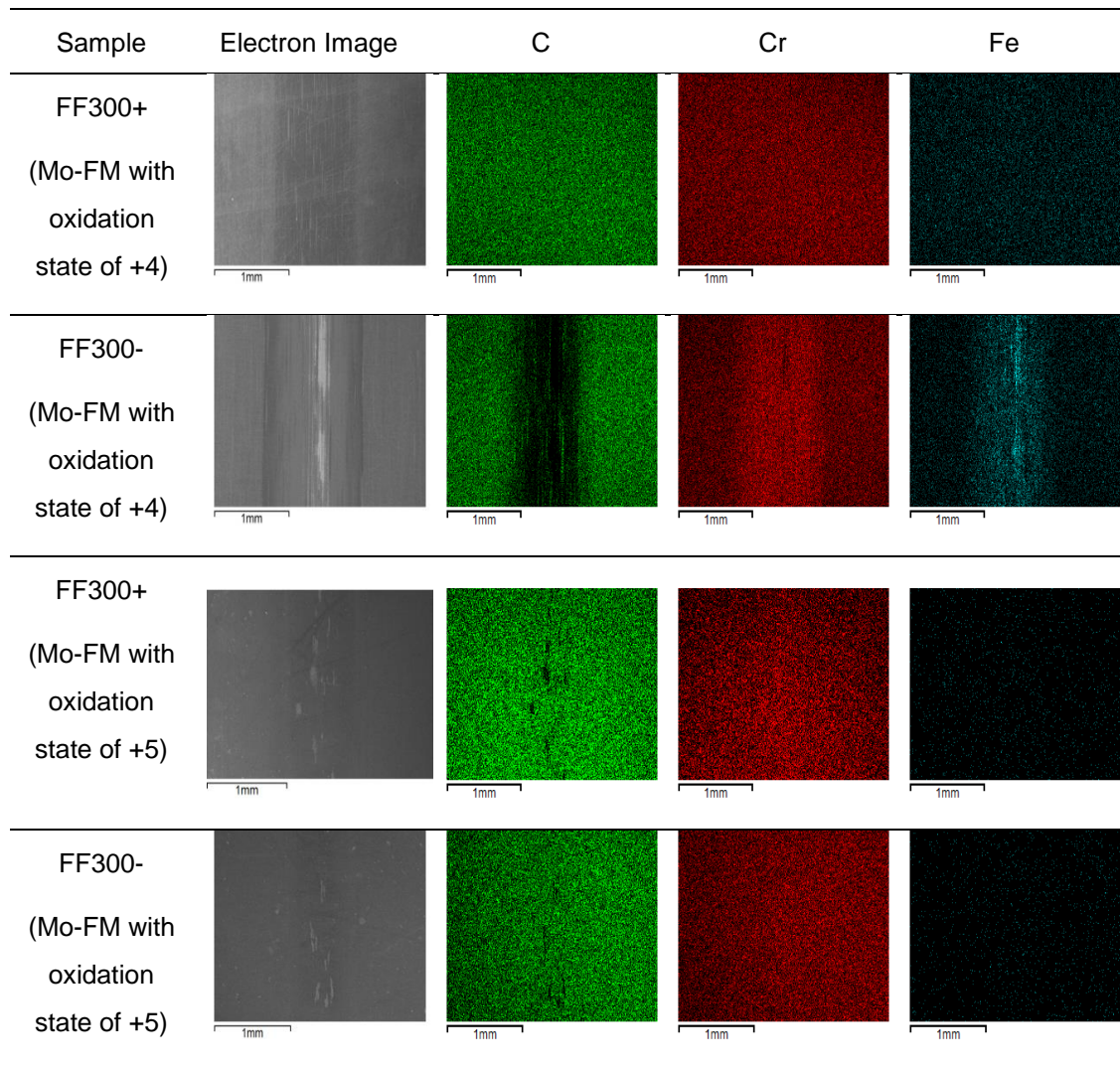


Figure 6-36 SEM image of a-C:15H coating along with EDX mapping of the C, Cr and Fe atoms.

6.3.6.3. Chemical Analysis of the Tribofilms

6.3.6.3.1. Elemental Composition

Following the tribo-tests using oils blended with different MoDTC source, XPS analysis was performed on the samples. The chemical quantification of the surface tribofilms for the a-C:15H/CI tribocouple lubricated in oils with different MoDTC source is shown in Table 6-8. XPS quantification obtained from Mo-FM with oxidation state of +4-containing oils is represented in the table for comparison purposes. Additive-derived elements were present on the tribofilm formed on both the a-C:15H and the CI pin counterbody

suggesting that the additives were decomposed under boundary lubrication. This could probably affect the tribological performance of the a-C:15H/system and particularly durability/wear performance of the coatings. Fe 2p peak was not detected in the tribofilm formed from any of the oils on the a-C:15H coatings signifying that delamination of the a-C:15H coating did not occur or/and that the iron coming from the pin worn particles did not participate in the tribofilm formed on the a-C:15H surface. In addition, Cr 2p peak was not found in the tribofilm formed on the a-C:15H coating using Mo-FM with oxidation state of +5-containing oils suggesting that wear of the coatings was not severe (enough) to make chromium internal layer exposed. This is in agreement with our physical observation where wear rates of a-C:15H coatings were measured to be fairly low using Mo-FM with oxidation state of +5 oils.

Table 6-8 XPS quantification of tribofilms for a a-C:15H/CI system lubricated in oils with different source of MoDTC.

Sample	Surface	Elemental composition of Tribofilms (at.%)								
		Fe	O	P	Zn	C	Ca	Mo	N	S
FF300+ (Mo-FM with oxidation state of +5)	Pin	0.2	19.3	0.7	0.1	73.0	2.6	2.0	0.8	1.3
	Plate	0.0	2.4	0.1	0.2	94.2	0.3	1.1	1.0	0.7
FF300- (Mo-FM with oxidation state of +5)	Pin	0.4	20.5	0.0	0.0	71.6	2.6	3.1	1.1	0.7
	Plate	0.0	5.9	0.0	0.0	90.4	0.9	0.9	1.6	0.4
FF300+ (Mo-FM with oxidation state of +4)	Pin	1.2	35.7	1.1	0.2	54.9	1.8	2.6	1.8	0.7
	Plate	0.0	3.7	0.4	0.1	92.0	0.6	1.4	1.1	0.8
FF300- (Mo-FM with oxidation state of +4)	Pin	1.6	34.9	0.0	0.0	42.7	1.3	12.3	6.4	0.8
	Plate	0.0	2.8	0.0	0.0	93.5	0.6	0.9	1.8	0.4

6.3.6.3.2. Low Friction Film Formation

Based on the elemental composition which is shown in Table 6-8, it is clear that regardless of the type of MoDTC which was blended in the oil, for ZDDP-containing oils with medium level of Mo-FM, the amount of Mo 3d detected on the tribofilm on both the a-C:15H coated plates and the pin counterparts was negligible. This made curve-fitting of the obtained Mo 3d high resolution peaks, from both the pin and the plate, almost impossible.

For ZDDP-free oils the amount of Mo 3d detected on the a-C:15H coated plates from oils with medium level of Mo-FM (FF300-) was insignificant whereas more Mo 3d was generally identified on the pins. Therefore, Mo 3d peaks obtained from tribofilm formed on the pins were used to compare ZDDP-free oils formulated with different Mo-oxidation state.

Figure 6-37 shows the long scan of Mo 3d peak obtained from tribofilm formed on the pin from ZDDP-free oils. It can be seen that both oils formed MoS_2 and MoO_3 on the tribofilm of the pins. However, in the case of FF300- (Mo-FM with oxidation state of +4) where the friction values were comparatively lower, more Mo 3d was detected on the tribofilm of the pin compared to FF300- treated with Mo-FM with oxidation state of +5. This could explain the lower obtained friction using this oil.

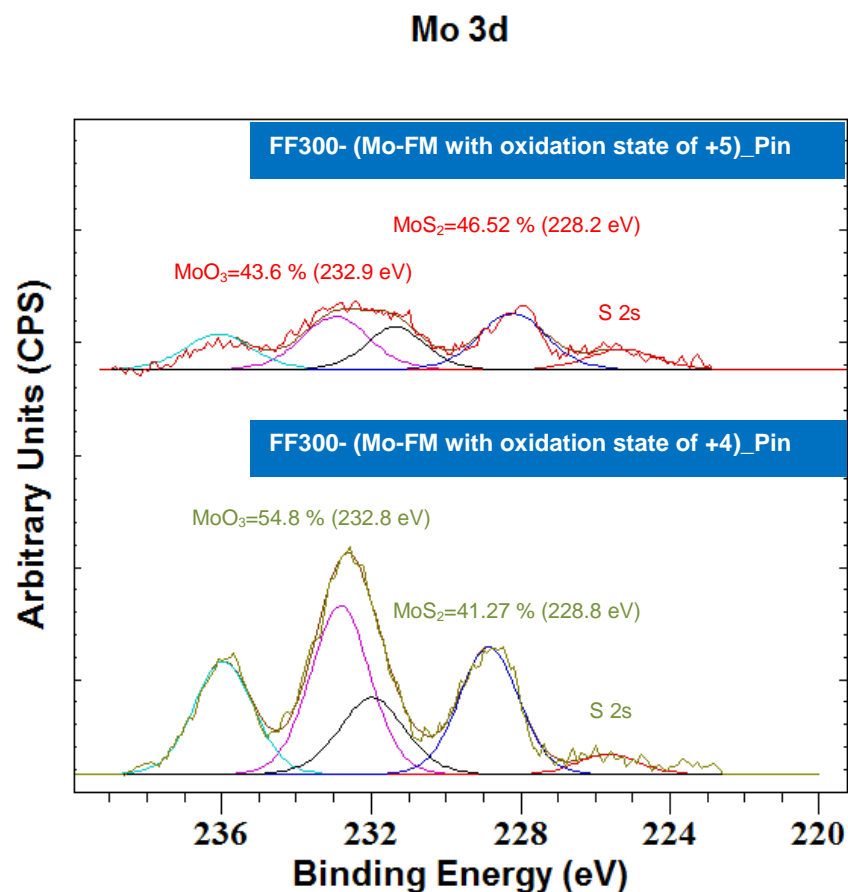


Figure 6-37 Curve fitting of Mo 3d peaks obtained from tribofilm formed from FF300- (Mo-FM with oxidation state of +5) and FF300- (Mo-FM with oxidation state of +4) on the pin.

6.3.6.3.3. Anti-wear Film Formation

Zn-phosphate and ZnS/ZnO species were formed in the tribofilms of the pins using FF300+ (Mo-FM with oxidation state of +5) which is in a similar manner to what was reported using FF300+ (Mo-FM with oxidation state of +4) whereas Zn-S-O compound was mainly formed on the a-C:15H coated plate.

It appears that phosphate film formation on the surface was not affected by the presence of Mo-FM with oxidation state of +5 in the oil (see Figure 6-38). The fitted Zn 2p and P 2p peaks are shown in Figure 6-38. The obtained results could explain high friction and good wear performance/durability of a-C:15H coating and reconfirms the important role of ZDDP on the wear protection of the DLC surface.

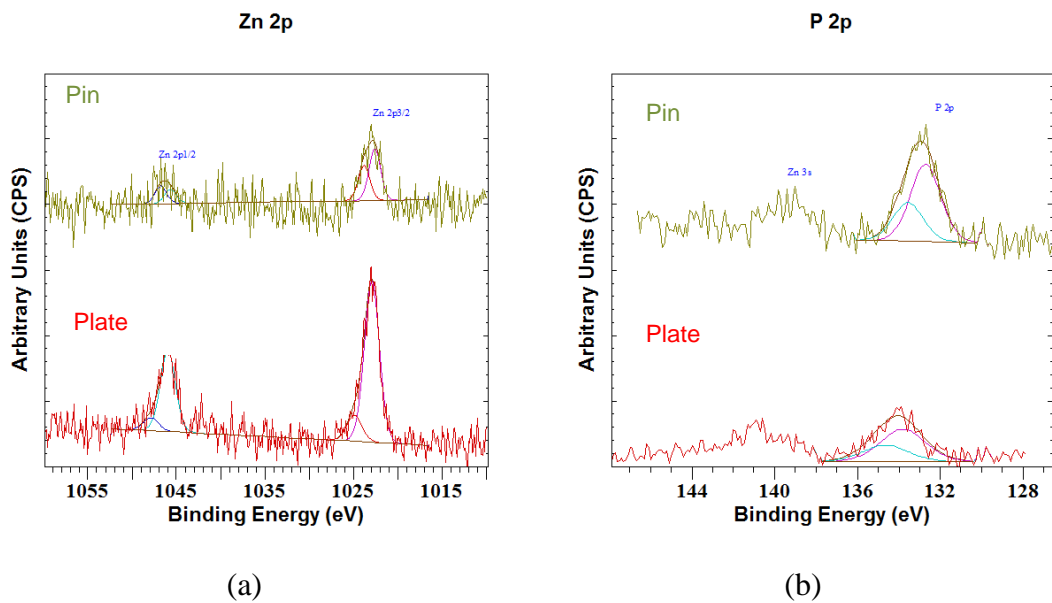


Figure 6-38 XPS spectra of ZDDP derived species (a) Zn 2p, (b) P2p formed on the a-C:15H coated plate using Mo-FM with oxidation state of +5-containing fully formulated oils.

6.3.6.3.4. Effect of Other Additives

Figure 6-39 demonstrates the high resolution scan of detergent-derived Ca 2p obtained from the tribofilm formed on both a-C:15H coated plate and the CI pin when lubricated in oils with different MoDTC type friction modifier. It is evident that irrespective of the formulation of the oils using different MoDTC,

Ca film was formed on both the pin and the plate. The binding energies of the Ca 2p peaks on the DLC plates using different oils was in the range of 348.5-348.9 eV (see Figure 6-29 (a)) which corresponds to $\text{Ca}(\text{NO}_3)_2$ whereas on the Cl pin surface Ca was in the form of CaCO_3 using FF300+ (Mo-FM with oxidation state of +5) and in the form of CaSO_4 by all other oils [267].

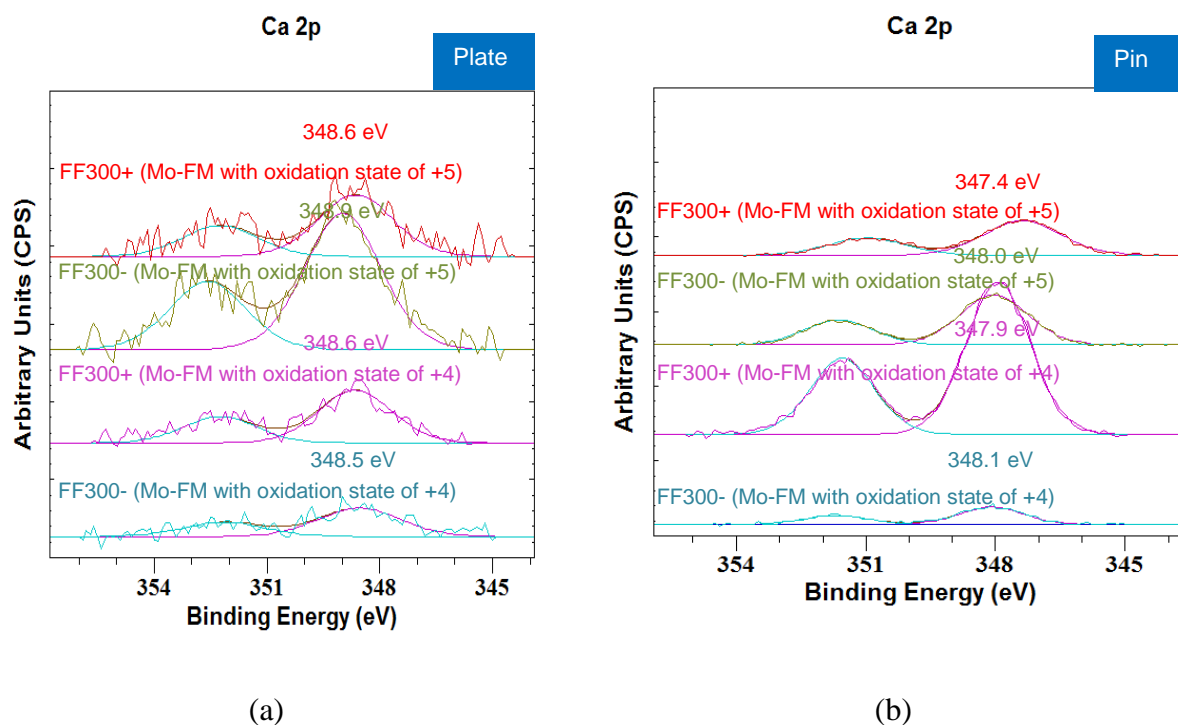


Figure 6-39 Detergent-derived Ca 2p peak formed on a-C:15H plate (a) and Cl pin (b) using oils with different MoDTC.

Nitrogen species are generally a decomposition product of dispersant which is blended in the oil. Figure 6-40 shows the long scan of N 1s from the tribofilm which is formed on the a-C:15H coatings and their corresponding pins using oils with different type of MoDTC. Nevertheless, the nature of Nitrogen species and the mechanisms by which they could potentially affect the film formation is beyond the scope of this study and requires further investigation.

Mo 3p peak has a line position of around 394 eV and therefore has an overlap with N 1s. It is clear that irrespective of the type of Mo-FM blended in

the oils used, no Mo 3p was detected on the a-C:15H tribofilm. In contrast, Mo3p peaks are evident in the tribofilm formed on the pin from Mo-FM with oxidation state of +4-containing oils which reconfirms the formation of MoDTC-derived compounds on the counterparts when oil was formulated using Mo-FM with oxidation state of +4 as a friction modifier .

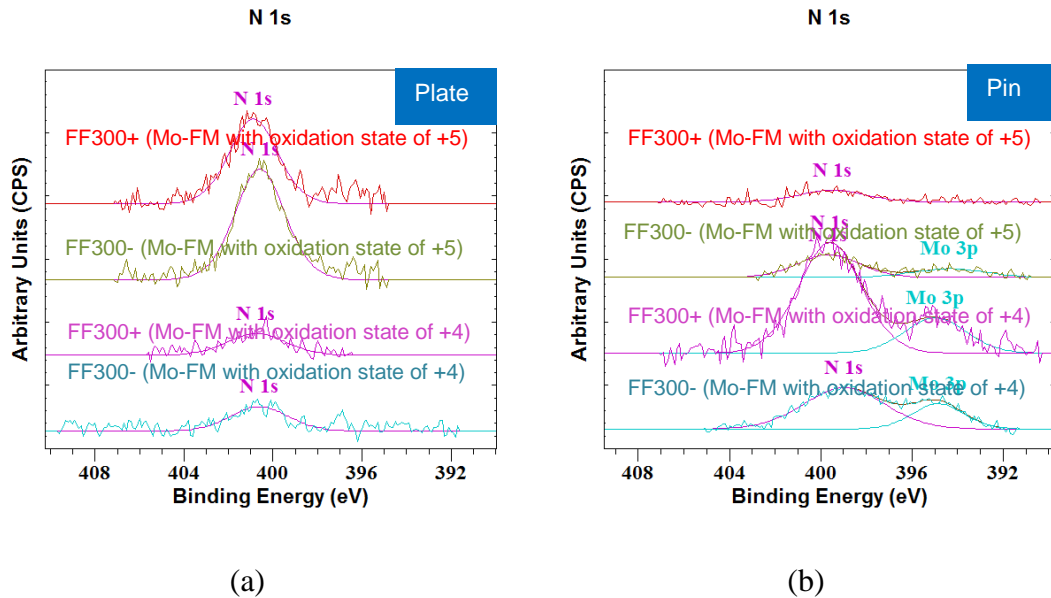


Figure 6-40 Dispersant-derived N 1s peak formed on a-C:15H plate (a) and CI pin (b) using oils with different MoDTC.

6.3.7. Effect of Counterpart Type

In another attempt and in order to find out the potential role of the counterpart substance, in general, and iron in particular, in giving high wear to the a-C:15H coating, 20 h tests were carried out using ceramic balls (Si_3N_4) while keeping the rest of the test parameters consistent (i.e. same temperature, contact pressure, etc.). In order to have a similar pressure to the DLC/CI system, the actual load on the silicon nitride ball in the DLC/ceramic was 13 N which gave a pressure of 700-800 MPa. The lubricating oil was chosen to be the lowest friction/highest wear giving oil (FF600-) and the obtained results were compared with those of CI pins. The obtained results for a-C:15H/CI system are represented here for comparison purposes.

6.3.7.1. Friction Results

Given in Figure 6-41 are the friction traces produced by the lowest friction/highest wearing oil (i.e. FF600-) using two different counterparts when rubbed against a-C:15H coated plate. Interestingly, using the same test parameters, no drop in friction was observed when the counterpart was ceramic while a significant friction reduction was evident using the CI pins.

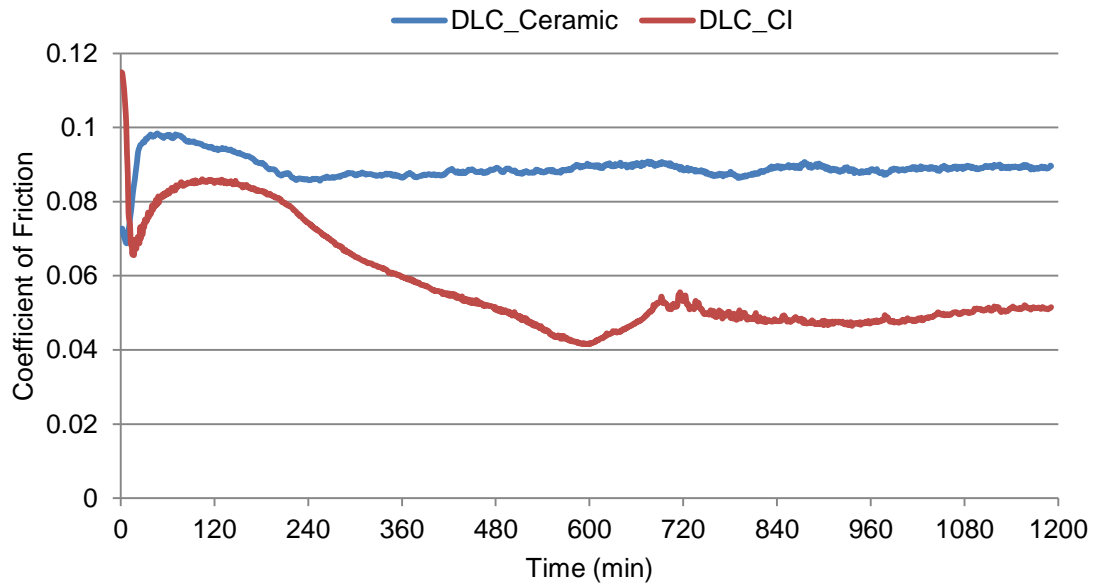


Figure 6-41 Friction traces as a function of time using different counterpart on a-C:15H coated plate lubricated in FF600-.

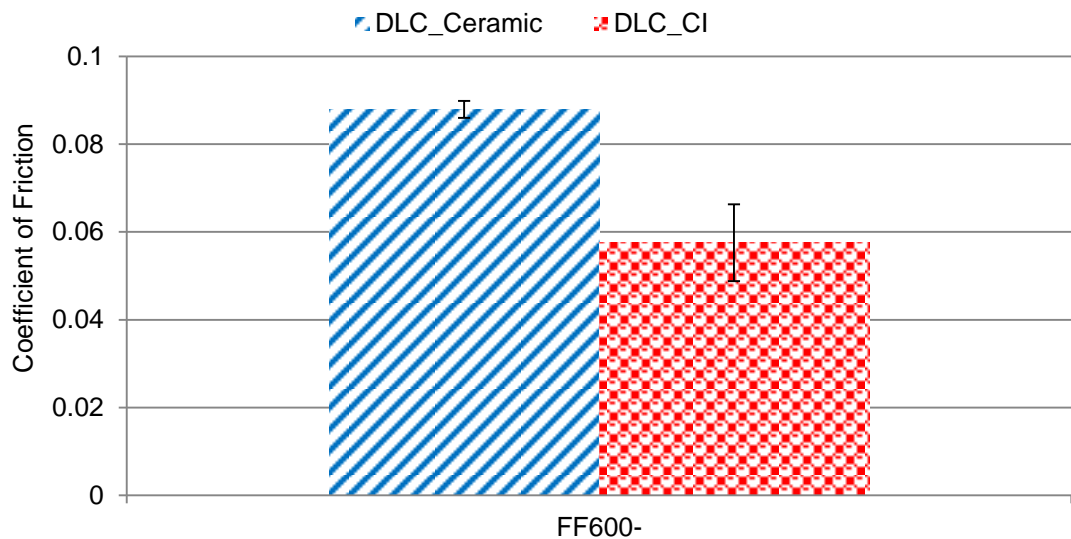


Figure 6-42 Steady state friction coefficients as a function of FF600- using different counterpart on a-C:15H coated plate.

In addition, steady state friction coefficient (i.e. average of the last hour of the tests) for two different counterparts are shown in Figure 6-42. It is clear that the friction was almost 1.5 times lower when CI pin was used compared to ceramic ball.

6.3.7.2. Wear Results

Typical images of the wear scar on the a-C:15H coating plate imposed by the ceramic ball (Figure 6-43a) and the cast iron pin (Figure 6-43b) using the highest wear/lowest friction giving oil (i.e. FF600-) are presented. It is clear that using ceramic as the counterpart, there was barely any evidence of significant wear on the plate after 20 h tests while high wear was observed using the same oil but with the cast iron counterpart.

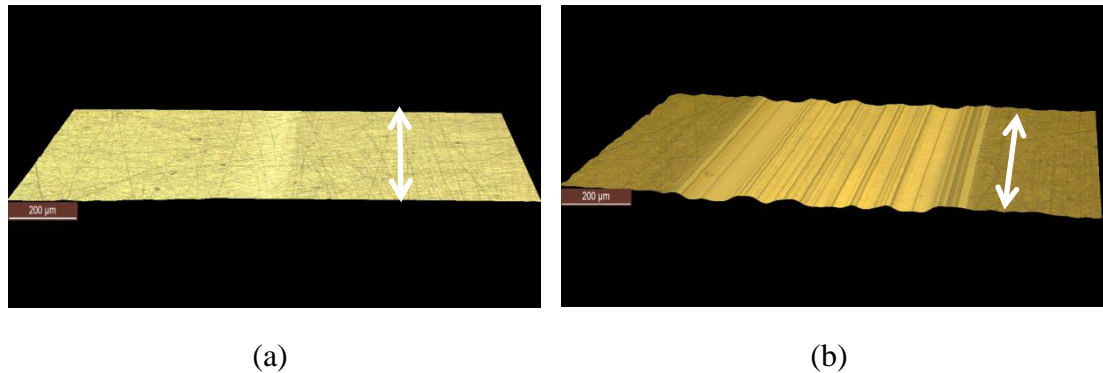


Figure 6-43 Optical images of the wear scars formed on the a-C:15H coated plates using (a) FF600- (ceramic ball) and (b) FF600- (CI pin). The arrows on the images show sliding directions and μ and H_d are the coefficient of friction and the average depth of the wear track, respectively.

In addition, EDX mapping of the a-C:15H coating using two different counterpart are shown in Figure 6-44. Based on the EDX mapping results, It is clear that using the ceramic ball, no difference in C and Cr concentration was seen comparing inside and outside of the wear scar implying almost no gradual wear of the coated plates. Using the CI pin, Fe was detected at some regions inside the wear scar for FF600- showing that the coating became very thin in the wear scar region (severe wear). It should be noted that, iron transfer from the CI pin is excluded due to the fact that wear of the pin was comparable from all the tests (see Figure 6-19).

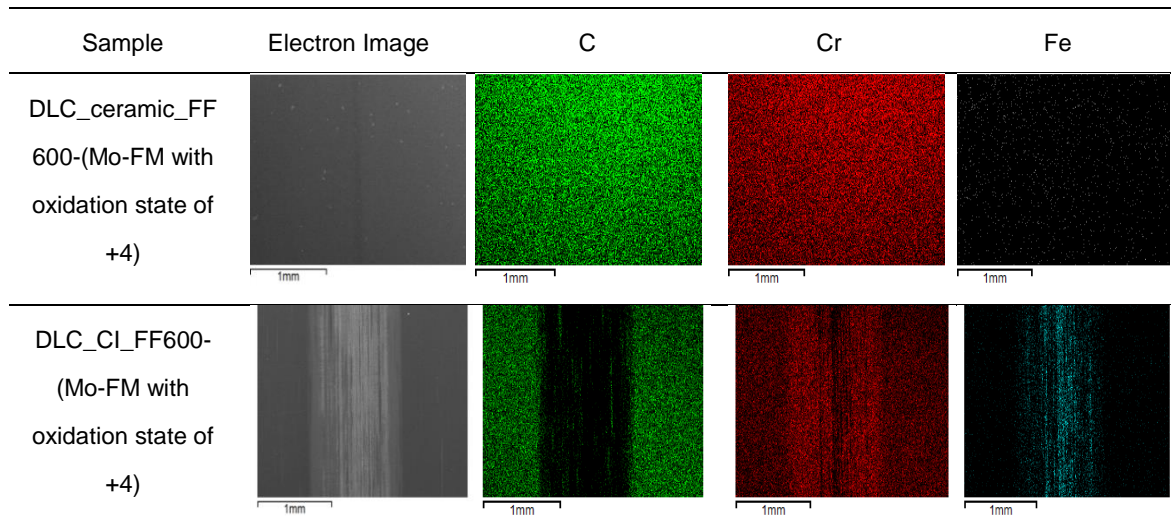


Figure 6-44 SEM image of a-C:15H coating along with EDX mapping of the C, Cr and Fe atoms.

6.3.7.3. Chemical Analysis of the Tribofilm

6.3.7.3.1. Chemical Quantification

In order to investigate the effect of using different counterparts on the tribological performance of DLC coatings, XPS analysis was performed on the tribofilm formed on the a-C:15H coated plates when rubbed against the cast iron pin compared to the ceramic ball using the highest wearing oil (FF600-). Figure 6-45 illustrates the survey scans on the tribofilms formed on the DLC coated plates using the CI pin and the ceramic ball, respectively. It is evident that regardless of the type of the counterpart, additive-derived elements were present in the tribofilm formed on a-C:15H. Fe 2p and Cr 2p peaks were only detected in the tribofilm when rubbed against the CI pin indicating that severe wear/delamination of the a-C:15H coating only occurred when the counterpart was cast iron. This suggests that the presence of iron is crucial in the wear process by which FF600- oil gave high wear to the DLC coating in the a-C:15/CI system. This is in agreement with our physical observation where iron was detected at some regions inside the wear track only when the counterpart was cast iron.

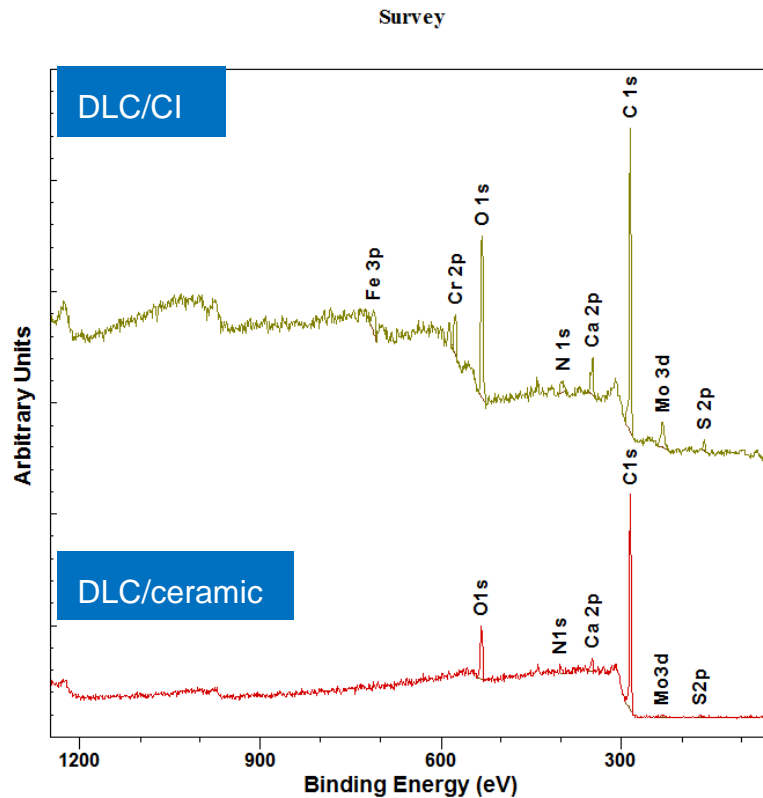


Figure 6-45 Survey scan obtained from inside a-C:15H coating wear scar when rubbed against CI (top) and ceramic (bottom).

The XPS quantification of the elements of the tribofilms formed on a-C:15H plates when rubbed against the ceramic ball and the CI pin are given in Table 6-9. It is clear that the tribofilm formed on the a-C:15H plate in both DLC/ceramic and DLC/CI was rich in carbon whereas minor portion of the tribofilm was the contribution of other additives. Nevertheless, more additive-derived elements was detected in the tribofilm formed on the a-C:15H in the DLC/CI system compared to DLC/ceramic.

Table 6-9 XPS quantification of tribofilms on the a-C:15H coating for a-C:15H/CI and a-C:15H/ceramic systems.

Sample	Elemental composition of Tribofilms (at.%)						
	O	C	Ca	Mo	N	S	Fe
DLC/ceramic	4.9	89.0	0.8	3.1	1.7	0.5	0.0
DLC/CI	9.1	76.5	1.6	6.9	4.1	1.4	0.3

6.3.7.3.2. Low Friction Film Formation

As shown in Table 6-9, although MoDTC decomposed and took part in the film formation on the a-C:15H coating using both the CI pin and the ceramic ball, Mo 3p was more dominant in the tribofilm formed on the a-C:15H coating when rubbed against CI.

In Figure 6-46, the high resolution scan of Mo 3d peak obtained from tribofilm formed on a-C:15H coated plate using the CI pin (top) and the ceramic ball (bottom) is given. It is evident that, for a-C:15H/CI, MoS₂ and MoO₃ which are the decomposition products of MoDTC formed on the a-C:15H coating. In the case of a-C:15H/ceramic system, binding energy of 229.6 eV corresponds to either MoO₂ or MoS₂ and binding energy of 233.2 eV corresponds to MoO₃. Nevertheless, the amount of Mo3d detected on the tribofilm of the DLC in the a-C:15H/CI formed from FF600- is higher compared to the a-C:15H/ceramic system which could be the potential cause of lower friction and higher wear observed in a-C:15H/CI.

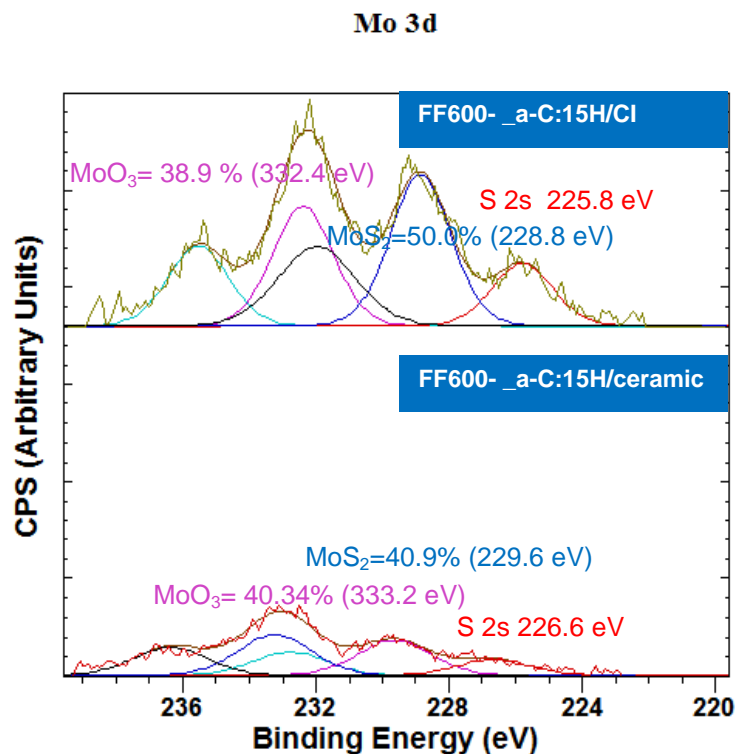


Figure 6-46 Curve fitting of Mo 3d peaks obtained from tribofilm formed from FF600- on the a-C:15H coating using the CI pin (top) and the ceramic ball (bottom).

6.3.7.3.3. Effect of Other Additives

Figure 6-47 shows the long scan of Ca 2p and N 1s peaks. It is clear that regardless of the type of counterpart, using FF600-, detergent- and dispersant-derived elements were detected on a-C:15H surface. It should be noted that calcium in the tribofilm formed on the a-C:15H coating in the a-C:15H/CI system was in the form of CaCO_3 which could potentially increase the friction [274] whereas in the a-C:15H/ceramic system Ca turned out to be $\text{CaSO}_4/\text{Ca}(\text{NO}_3)_2$. It is worth mentioning that Mo 3p peak (see Figure 6-35 b) which has an overlap with N 1s is clearly identified on the a-C:15H tribofilm using both counterparts which reconfirms the formation of MoDTC-derived compounds. However, the Mo 3p peak was more evident and sharp in the DLC/CI system.

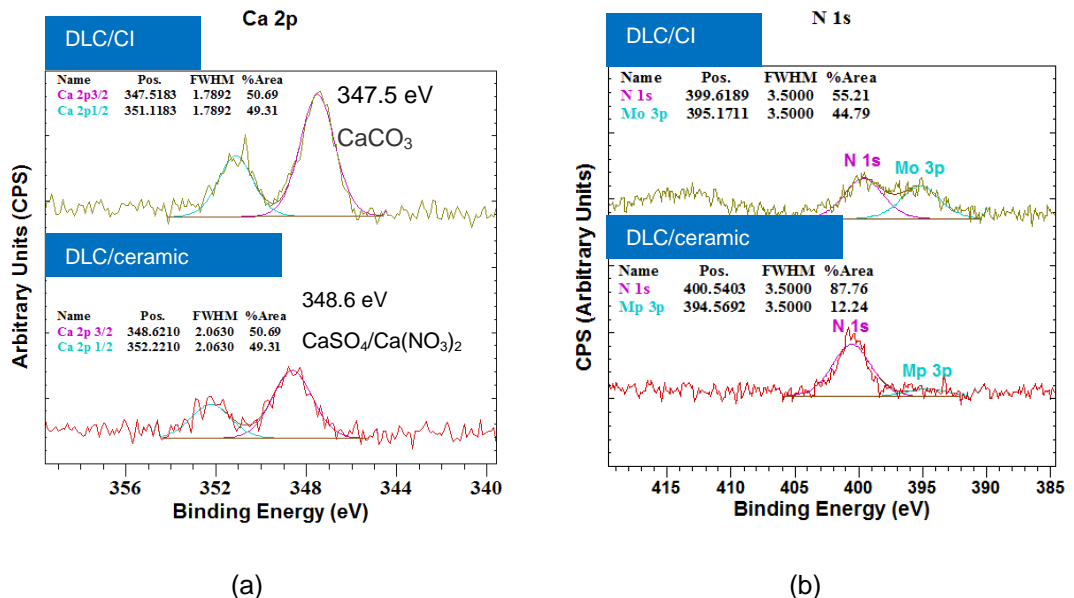


Figure 6-47 Detergent-derived Ca 2p peak (a) and dispersant-derived N 2p peak (b) using FF600- oil using the CI pin(top) and the ceramic ball (bottom).

6.4. Summary

In this part of the study (phase II), the effect of increasing Mo-FM concentration in one type of fully formulated oil on the tribological performance of both steel/CI and DLC/CI system was investigated in detail. In addition, test duration was increased to 20 h to discriminate between

different oils in terms of tribological performance of the a-C:15H coating. Initial tests suggested that 20 h was long enough for the highest wearing oil (FF600-) to give severe wear of the DLC coating, and as a result removal of the a-C:15H coating and reaching to the CrN/CrC interlayer. Following long 20 h tests, friction response of the oils (see Figure 6-5), was seen to vary with time. In particular, for FF600+ and FF600- oils, the friction coefficients which were initially dropped, started to rise again in the region of 10-12 h after the start of the tests. Thus, 12 h test were conducted to provide a better understanding of friction behaviour and wear mechanisms of the oils on the DLC coatings as a function of time. In addition, 6 h tests were conducted in the region where friction was still decreasing and the coating was not suffering from severe wear. Furthermore, the effect of Mo-FM type which was blended in the oils was investigated. In summary, the following key points can be drawn from this part of the study:

- High concentration of Mo-FM with oxidation state of +4 can promote wear of a-C:15H coating in oils without ZDDP and this wear can be mitigated by the addition of ZDDP. Unlike ZDDP, the presence of other additives (antioxidants, detergents and dispersants) in a fully formulated did not provide similar wear protection.
- The presence of ZDDP in the oil increased the friction for steel/Cl. This was also true for DLC/Cl when lubricated in oil formulated with medium (i.e. 300 ppm) and high level (i.e. 600 ppm) of Mo-FM.
- The mechanical properties of the a-C:15H coating can be modified by the addition of the Mo-FM with oxidation state of +4 in a fully formulated oil. Furthermore, considering the standard deviation of the obtained nanoindentation measurements of the coatings outside of the wear scar, no significant difference was observed as compared to as-deposited coating. This suggests that the antagonism effect of Mo-FM to a-C:15H in terms of wear was more of tribochemistry of the rubbing surfaces rather than chemical reaction of the oils with the a-C:15H coating.

- The tribochemical effect of oils with higher concentration of Mo-FM on surface modification of a-C:15H coating required more than 6 h to occur which was also in agreement with our chemical analysis of the tribofilms where MoDTC derived MoS₂ and MoO₃, which are reported to be the potential cause of surface modification/graphitisation of DLC [41, 254], were dominant on the a-C:15H coating after 12 h but not 6 h.
- Tribological tests and surface analysis of the DLC coatings over the time intervals suggests that MoDTC decomposition products initially form a tribofilm on the surface offering low friction followed by high wear on the a-C:15H coated plates. In addition, for high wearing oils, wearing through the coating and reaching to CrC/CrN interlayer may also be responsible for a reduced steady state friction [204].
- The high wear observed by ZDDP-free oils with medium level of Mo-FM with oxidation state of +4 on the a-C:15H coating was not seen by the same oil but blended with Mo-FM with oxidation state of +5. This suggests the important role of MoDTC type in promoting high wear to DLC coatings.
- The MoDTC-induced high wear of a-C:15H coated plates was only seen in the a-C:15H/CI combination but the same effect was not observed when DLC rubbed against the ceramic counterpart. This indicates that the presence of the steel plays an important role on wear mechanisms by which MoDTC is causing a high wear on the hydrogenated DLC coating.

Chapter 7 Discussion

7.1. Introduction

In phase I of the study, fully formulated oils were used to evaluate the overall tribological performance of 15% hydrogenated DLC under boundary lubrication conditions and the tribological performance compared with that of an uncoated steel system. The obtained results suggest that fully formulated oils (with 40/60 ppm or no Mo-FM) provide no friction reduction in both the steel/CI and a-C:15H/CI systems. In addition, using these oils, DLC coating showed extremely low wear making the wear measurements almost impossible. Following the overall tribological evaluation of the DLC coating using fully formulated, the effect of MoDTC concentration on tribological performance of DLC system has been assessed in phase II and the obtained results are presented in chapter 6 in detail. The observations which are key to this study along with the possible hypotheses and potential wear mechanisms will be the focus of this chapter. In addition, the obtained results will be assessed and compared with other published literature.

7.2. Effect of Lubricant Additives on Tribological Performance of the DLC/CI and the Steel/CI System.

7.2.1. Low Friction Film Formation

The DLC/lubricant interaction strongly depends on the type of DLC as well as lubricant composition, particularly when these coatings are rubbed against uncoated steel surfaces [170]. In the literature, direct interaction of MoDTC and ZDDP with some hydrogenated DLCs has been evidenced and the formed tribofilms on the coating surface have been reported to improve the friction and wear performance of these contacts [206, 217].

In this study, oils with low concentration of Mo-FM did not provide any friction reduction. The coefficient of friction obtained using these oils, was relatively high in both DLC and steel systems. In addition, XPS analyses revealed that the amount of Mo, detected in the tribofilm formed on both

surfaces, was insignificant. Since the friction coefficient in both systems was in the same range, the different contact type could not be responsible for such high friction values.

The friction behaviour of the fully formulated oils on both of the DLC/CI and the steel/CI systems can be correlated to the increased shear strength at the interface due to the surface/additive interaction, as widely reported for different lubricated systems [29, 210, 257, 275] as well as DLC [209, 276]. The interaction between different additives which are present in the oils' formulation could play a great role in the functionality of Mo-FM and friction reduction which will be discussed in detail later in this chapter. That could also explain relatively high friction obtained by conventional fully formulated oils (with 40/60 ppm Mo-FM) used in phase I of this study.

In addition, high friction obtained using fully formulated oils with low level of Mo-FM (40/60 ppm) could be also due to the low concentration of friction modifier in the formulations. In other words, certain amount of Mo-containing source is paramount for the reduction in friction. The MoDTC effectiveness in giving low friction depends on different factors including its concentration in the oil [97, 100, 101, 113]. The level of MoDTC in the oil was suggested to be at least 500 ppm [113] and 180 ppm [101] for an efficient friction reduction.

In this study, formation of MoS_2 which could be partly responsible for providing low friction, was only dominant in the tribofilm formed from fully formulated oils with the increased Mo-FM concentration (300 ppm and 600 ppm) in the DLC/CI tribocouple. In addition, Yamamoto and Gando [97] reported that the concentration of MoDTC in the solution only affects the induction phase of the friction response and the steady state friction values were independent of the MoDTC concentration used. In this study, however; both the induction phase and the steady state friction was observed to be dependent on the Mo-FM level in the oils.

Coefficients of friction as a function of Mo-sulphide/Mo-oxide ratio for a-C:15H/CI using oils with different concentration of Mo-FM are given in

Figure 7-1. It is evident that the higher the Mo-sulphide/ Mo-oxide ratio, the lower were the friction coefficients. In addition, It is also clear that Mo-sulphide/ Mo-oxide was increased with increase in Mo-FM concentrations in the oil formulation. Hence, the results presented in Figure 7-1 clearly demonstrate that the friction behaviour of a-C:15H coating is influenced by the formation of low friction MoS₂ species.

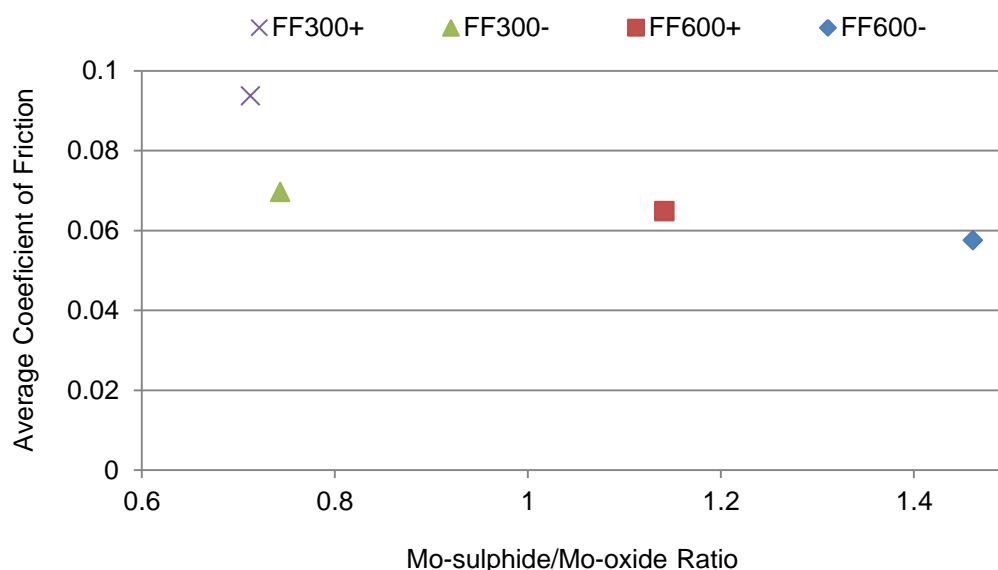


Figure 7-1 Average coefficient of friction as a function of Mo-sulphide/Mo-oxide ratio for a-C:15H/Cl system using oils with different concentration of Mo-FM after 20 h tests.

Figure 7-2 illustrates Mo-sulphide/Mo-oxide ratio for a-C:15H coating as a function of test duration using oils with different level of Mo-FM. It is evident that the tribofilm formed from these oils were richer in MoS₂ after 12 h compared to 6 and 20 h tests. However, Mo-sulphide/Mo-oxide ratio decreased with increase in test duration for low friction giving oils (i.e. FF300-,FF600+ and FF600-). This is in agreement with our friction results (see Figure 6-23) where the friction coefficients obtained using these oils were lower after 12 h compared to 6 and 20 h tests. It should be noted that although the Mo-sulphide/Mo-oxide ratio is higher for FF600+ oil, the XPS high resolution scan of Mo obtained from tribofilm formed on the cast iron pin using FF600- showed a higher Mo intensity compared to FF600+. This could be an indication of the higher amount of MoS₂/MoO₃ formed on the cast iron counterpart when rubbed against a-C:15H coating lubricated in FF600-. This

could also justify the lower friction values obtained in the DLC/CI system using FF600- oil compared to other oils.

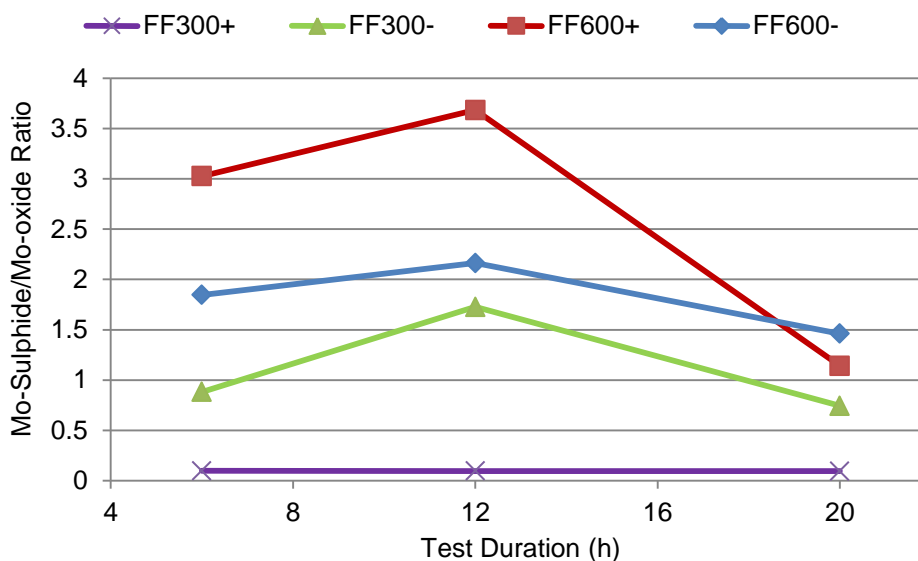


Figure 7-2 Mo-sulphide/Mo-oxide ratio for a-C:15H coating as a function of test duration using oils with different level of Mo-FM.

Reduction in friction in the DLC/CI system, comes at the price of significant wear of hydrogenated DLC. In addition, high wear of the a-C:15H coating which was seen by fully formulated oils treated with medium (300 ppm) and high (600 ppm) level of MoDTC, resulted in transfer of DLC worn material to the CI pin. The presence of sp^2 carbon bonds in the DLC coating matrix provides them with inherent low friction properties and so the transfer layer of the a-C:15H coating, as evidenced by the XPS analysis, may consist of the low shear strength sp^2 -dominated graphitic carbon. Therefore, it is clear that a combination of MoDTC derived MoS_2 species along with DLC wear debris facilitated friction reduction in the a-C:15H/CI tribocouple. This is also in agreement with a similar study [229] which was conducted on the a-C:15H/steel system using fully formulated oils where a mixture of additive- and a-C:15H-derived products was found to be responsible for tribological behaviour of a-C:15H/steel system. In Figure 7-3, mechanism of low friction film formation on the a-C:15H coating is schematically compared with that on the uncoated steel surface. Figure 7-3 shows that the friction reduction on the DLC surface is influenced by both low friction MoS_2 and low friction DLC

wear debris whereas on the steel surfaces low friction MoS₂ species were dominating friction [253].

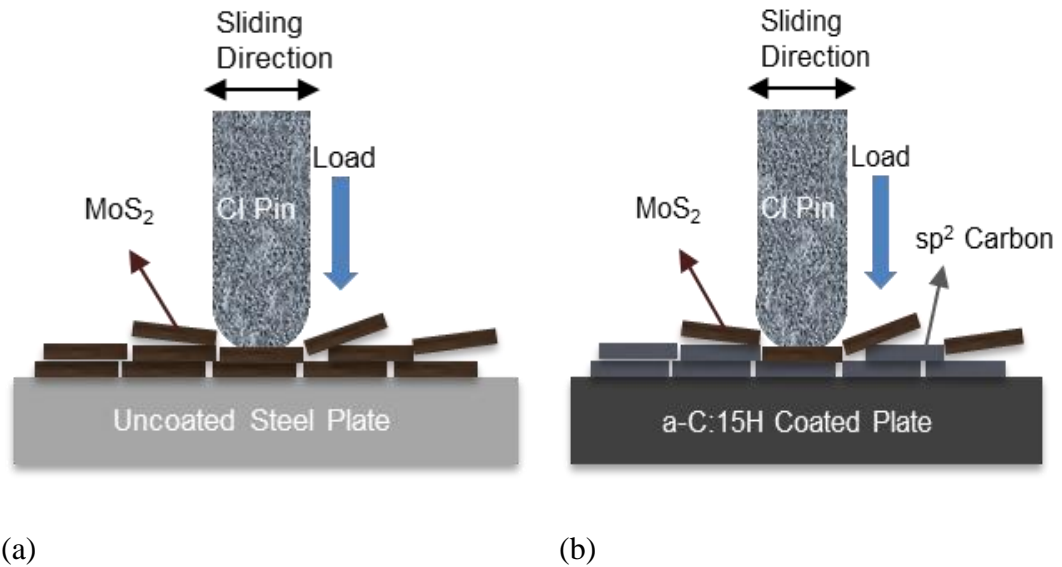


Figure 7-3 Schematic diagram of low friction film present at the interface in (a):steel/CI [253] and (b): a-C:15H/CI systems.

7.2.2. Anti-wear Film Formation

The obtained results clearly showed the critical role of selected additives in the oils on the durability of the coating which is in agreement with previous findings [214, 253].

Zn-phosphate and ZnS/ZnO species were formed in the tribofilms using fully formulated oils. That could explain the good wear performance which was observed using all typical fully formulated oils (FM-free for with 40/60 ppm Mo-FM) in both the DLC/CI and steel/CI system. This is in agreement with published literature where formation of ZDDP-derived compounds on the DLC coating provided better wear performance of the DLC coating under boundary lubrication conditions [4, 206, 216-220]. Furthermore, the presence of Mo-FM in the oil did not affect phosphate film formation on the surface.

In the steel/CI system, different MoDTC concentration did not affect the performance of ZDDP and the steel plate wear rates were comparable for all the oils. The wear given for all the oils were insignificant and in the same range ($\approx 1 \times 10^{-18} \text{ m}^3/\text{Nm}$) indicating the effectiveness of ZDDP in providing a good wear performance of the uncoated steel/CI system regardless of the level of MoDTC in the oil.

This study also showed that ZDDP offered a significant improvement in wear protection; however, its anti-wear performance depends significantly on the concentration of Mo-FM in the lubricant. However, XPS analysis showed that all ZDDP-containing fully formulated oils form ZDDP derived tribofilm on DLC surface as well as CI counterpart. Zn-phosphate and ZnS/ZnO species were formed in the tribofilms using all ZDDP-containing fully formulated oils.

For low level of Mo-FM (40 ppm) the wear was not very much dependant on the presence or absence of ZDDP. In both cases (i.e. FF40+ and FF40-) the wear was extremely low after 20 h tribo-tests.

Based on the obtained results in this study, ZDDP effectiveness in providing a good wear performance of a hydrogenated DLC was more pronounced when it was used with medium level of Mo-FM (300ppm). For medium level of Mo-FM, the presence of ZDDP in the oil prevents the high wear given by MoDTC to the DLC coating (i.e. comparing FF300+ and FF300-). Similarly, Haque *et al.* [220] reported that addition of the anti-wear additive ZDDP to MoDTC-containing base oil could suppress the adverse effect of MoDTC in giving high wear to DLC coating in a DLC/steel system [220]. In addition, Tung *et al.* [232] showed that MoDTC could reduce the wear of a DLC coating lubricated in fully formulated engine oil but with the aid of ZDDP which was present in the tested oil. It has been shown that DLC high wear was not seen with DLC/DLC contact and therefore, the presence of steel counterface was thought to be crucial in promoting the formation of MoO_3 [255], or iron oxide particles may produce higher local temperatures [214] which could then results in modification/graphitization of the DLC coating, and thus high wear. ZDDP derived glassy phosphate species which were formed on the surface of the coating could protect the surface from excessive wear or/and the formation of iron oxide particles. ZDDP could also

act as an oxidation inhibitor [29, 38, 39] and hinder the formation of MoO_3 which is the potential cause of high DLC wear (possible cause of DLC brittleness) [41] in MoDTC-containing oils..

Although, XPS analysis showed the presence of ZDDP derived elements on the tribofilm formed on both DLC coated plates and CI pins using oils formulated with high level of Mo-FM, the given wear was high for both ZDDP-containing and ZDDP-free oils. It could be argued that the large amount of MoDTC supply in the oil formulation had a detrimental effect on the structure of ZDDP tribofilm. It was shown that a thick patchy pad-like tribofilm which was formed by ZDDP alone became much thinner and the patchy structure was vanished [123]. In addition, the larger amount of MoO_3 formed in the tribofilm could enhance removal of tribofilms from DLC coating due to its abrasive nature resulting in high wear losses [246]. Nevertheless further study is required to establish the exact link between Mo-containing friction modifiers and the wear of DLC and the mechanisms by which ZDDP could stop this effect.

7.2.3. Effect of ZDDP on Friction Reduction

In this study, ZDDP in combination with Mo-FM showed friction reduction in the a-C:15H/CI system when comparing FF3+ with FF3-. Although, no such relation was observed comparing FF1+ with FF1- which could be due to the lower Mo concentration in FF1+ and FF1- (40 ppm) compared to FF3+ and FF3- (60 ppm). In the literature several reports showed that in steel systems MoDTC in combination with ZDDP was more effective in friction reduction [117-119]. For Mo-FM free oils, the presence of ZDDP increased the friction (i.e. FF2+ compared to FF2-) which has been widely reported for ferrous systems [48, 55-58]. In addition, for oils with medium and high level of Mo-FM, addition of ZDDP to the oil formulation resulted in an increase in friction values of the a-C:15H/CI system.

In the steel/CI system, in general, ZDDP increased friction when added to the lubricant which is in agreement with the literature where formation of pad-like tribofilm was identified as the reason for such higher friction [29].

The results obtained in this study was is in agreement with the published literature where the presence of ZDDP in the lubricants was shown to increase the friction [48, 55-58]. The increase in friction by ZDDP was correlated to the anti-wear film formation [56]. Increase in roughness due to the formation of ZDDP film could promote boundary lubrication and a higher friction as a result [58]. In contrast, in some other literature, addition of ZDDP to the lubricant found to have either neutral effect [62] or friction drop [63].

7.2.4. Effect of Other Additives Interaction on Tribofilm Formation

Fully formulated oils contain different additives including detergent and dispersant. They are blended in a fully formulated engine oil to form a film on the part surface preventing deposition of sludge and varnish and to keep oil insoluble contaminants and degradation products in suspension, at elevated temperature for detergents and at low temperatures for the dispersant additives. However, interaction between different additives when used together in formulated oils could result either in synergetic or antagonistic effects modifying the characteristics of the protective surface tribofilms which in turn affects the oil performance regarding anti-wear and frictional responses [93].

Using fully formulated oils, detergent and dispersant-derived elements were detected on both steel and a-C:15H surface. However, the nature of Ca and N species formed on the a-C:15H were different from those on the steel surfaces. It was shown that in a ZDDP/detergent/dispersant mixture, dispersant did not make a significant contribution to the film formation and formed a thin layer of nitrogen-containing material on the outer surface [132]. The presence of Ca and N on the surface could influence the formation of FM-derived tribofilms on both a-C:15H and steel surfaces. Interaction between ZDDP and Ca-based detergent could reduce the amount of S, P and Zn on the tribofilm and increase friction due to less rich film and formation of CaCO_3 [274]. That could explain comparatively high friction values observed when fully formulated oils with low level of Mo-FM was used (40/60 ppm). In contrast, the interaction between MoDTC, ZDDP and overbased calcium borate detergent in a ternary oil solution was shown to provide 25% better friction (coefficient of 0.05 compared to 0.07) than the binary ZnDTP/MoDTC mixture. However, the anti-wear efficiency of the

ZnDTP/MoDTC system was found to be independent of the presence of the calcium borate [277].

Detergents have been shown to provide anti-wear properties by forming carbonates in the wear scar [115, 124, 125]. Metallic detergents, however, were seen to have an antagonistic effect on the wear performance of ZDDP [124, 126, 127]. On the other hand, succinimide dispersants were found to increase wear when added to ZDDP solutions [115, 129]. However, this adverse effect was diminished by borating the succinimide. Formation of a borate component in the anti-wear film was responsible for this improvement [130]. The antagonistic effect of dispersants on wear reduction was attributed to the reduction in the amount of ZDDP available for film formation by forming a complex.

In this study, however, the direct effect of detergent and dispersant interactions in the formulation cannot be established as all lubricants were fully formulated oils containing detergent, dispersant, antioxidants as well as other surface active additives. However, undoubtedly the competition for surface sites between the wider range of surface-active additives present in the formulation could result in a different behaviour than what has been already published in the literature mostly using binary and ternary oil solutions. Based on the obtained results in phase I of this study, all fully formulated oils showed an excellent wear performance as well as relatively high friction for both DLC/CI and steel/CI system. The presence of detergents, dispersants and antioxidants in the blend did not seem to provide similar surface protection of the coating against “Mo-FM induced wear” when ZDDP was absent in the formulation (i.e. comparing FF300+ to FF300-).

7.2.5. Effect of Oil Chemistry on Coating Wear/Delamination

7.2.5.1. Graphitisation of Hydrogenated DLC Coating

Having a graphite-like structure through transferring worn materials from the a-C:15H coating to the interface could significantly reduce friction in dry conditions [185, 190, 191]. Graphitisation could be initiated by high temperature (400°C) causing the hydrogen to be diffused out of the a-C:15H

matrix which in turn results in collapse of the random covalent structure of a-C:15H and provide a graphitic layer. Based on a simple model, asperity temperature rise due to friction (friction-induced temperature) can be calculated by Equation 7-1 [16, 185].

$$\Delta T = \frac{1}{4} \frac{\mu P u}{(K_{DLC} + K_{CI}) a} \quad \text{Equation 7-1}$$

where $a = \left(\frac{P}{\pi H}\right)^{\frac{1}{2}}$, ΔT is the induced temperature rise, μ the friction coefficient, P is the applied normal load (Pa), u the sliding speed (m/s), K_{DLC} and K_{CI} are the thermal conductivities of the a-C:15H coating and CI counterbody ($\text{Wm}^{-1}\text{K}^{-1}$), respectively, a the contact radius of the real contact area, and H is the measured hardness of the a-C:15H coating (Pa).

Considering the highest obtained coefficient of friction and the experimental parameters of this study, the rise of the temperature at the contact was not significant ($\approx 20^\circ\text{C}$). Therefore, the friction-induced temperature was too low to be responsible for the phase transformation of the a-C:15H coating.

The phase transformation temperature of DLC coating is a function of contact pressure which can be expressed by Equation 7-2 [278].

$$T = T_c \exp \left[\frac{-|\Delta v|}{L} \Delta p \right] \quad \text{Equation 7-2}$$

Where T_c is the critical phase transformation temperature ($= \sim 350^\circ\text{C}$), L is the phase transition energy of diamond ($15.6 \times 10^4 \text{ Jkg}^{-1}$), Δv is the difference between the specific volume of hydrogen-free ($0.284 \times 10^{-3} \text{ m}^3 \text{ kg}^{-1}$) and hydrogenated coating ($0.294 \times 10^{-3} \text{ m}^3 \text{ kg}^{-1}$ to $0.416 \times 10^{-3} \text{ m}^3 \text{ kg}^{-1}$), Δp is the difference between Hertzian contact pressure and atmospheric pressure.

Using Equation 7-2 and taking into account the experimental parameters of this study, the phase transformation temperature of a-C:15H coating is much

higher than the operating temperature of the experiments (100°C). Therefore, the Hertzian contact pressure exerted by the counterbody on the a-C:15H coating is not likely to be responsible for DLC graphitisation. However, according to Clapeyron law (Equation 7-2) transformation of a-C:15H could occur at a much lower temperature when subjected to high pressure (stressed-induced graphitisation) [190]. The phase transformation temperature of DLC coating as a function of contact pressure is plotted in Figure 7-4. Depending on different assumptions with regards to the specific volume of the hydrogenated coating ($0.294 \times 10^{-3} \text{m}^3 \text{kg}^{-1}$ to $0.416 \times 10^{-3} \text{m}^3 \text{kg}^{-1}$), three different curves are obtained. Green, blue and red curves represent the upper limit, average and higher limit of these values, respectively. Generation of ferrous wear particles from the worn CI counterbody along with the scratches with positive edges on the surface, decrease the contact area and increase the contact pressure significantly, thus, subsequently reduces the temperature required for initiation of graphitisation and accelerate the graphitisation process [279, 280]. Estimation of the phase transformation temperature for DLC coating has also been reported elsewhere [198, 214] showing the important role of contact pressure on structural changes of a-C:15H.

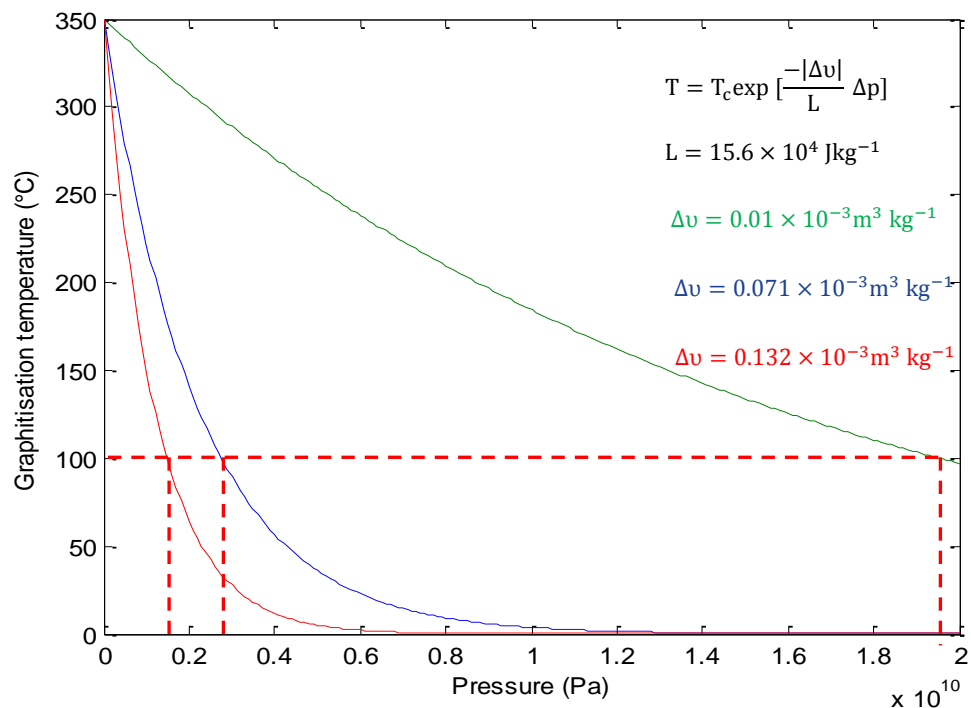


Figure 7-4 The phase transformation temperature of DLC coating as a function of contact pressure [278].

7.2.5.2. Wear Mechanism/DLC Coating Failure

Additive-free PAO used in this study provided comparatively lower friction while showing severe delamination of the a-C:15H surface as well as high gradual wear. The high contact pressure exerted by positive edges of the scratches [279] and “micro-size” iron particles coming from the counterbody [214] could be responsible for graphitisation of the a-C:15H surface which consequently could lead to severe delamination of the a-C:15H coating (Figure 7-5). It is interesting that the pin wear provided by PAO was less than those of fully formulated oils. It could be argued, wear products from DLC, which can have a graphitic nature [192], can be transferred to the counterbody forming a transfer layer on the softer surface. The softer surface (i.e. pin surface) will then be protected from being worn off while the DLC slides over the transfer layer (Figure 5-13). The wear rate of DLC will also be extremely low after the transfer layer is formed. In addition the transfer layer also behaves as a solid lubricant [185, 193]. It should be noted that transfer layer has low shear strength and is progressively removed from the surface [190]. The formation and adhesion properties of this transfer layer depend strongly on the tribological and environmental conditions as well as the chemical properties of the counterpart [194].

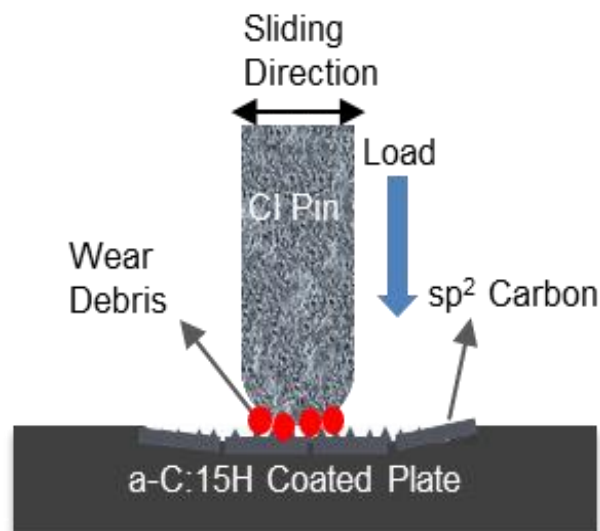


Figure 7-5 Schematic of the effect of iron particles and positive edges of the scratches on pressure induced graphitisation of DLC coating when lubricated in base oils.

Increasing graphitisation and removal and transfer of materials to the counterbody with time will lead to gradual thinning of the a-C:15H coating which in turn will decrease the load bearing capability of the a-C:15H coating. With the poor load bearing capability of the coating, the high shear stress is transmitted to the substrate causing plastic deformation to the substrate/intermediate layer which leads to debonding of the Cr interlayer from the substrate and to the coating failure accordingly [281].

A similar low friction and high gradual abrasive/polishing wear was observed when base oil group III was used but mild delamination was seen after 6 h of the tests. Nevertheless both base oils showed higher wear of the a-C:15H coating and lower friction compared to fully formulated oils. On the other hand the pin wear in the a-C:15H/CI system using base oil group III was higher than all other oils. Considering mild delamination/graphitization on the coating and the fact that there was no additive blended in the base oil to form any possible protective tribofilm on the pin surface, it can be argued that less transfer materials have been transferred to the pin surface, and thus resulted in less wear protection.

Based on the tribo-test results and post chemical analysis of the surfaces, it was evident that using fully formulated oils, the additive-derived tribofilm has been formed on both DLC and steel surfaces. Additives in fully formulated oils could suppress graphitization by providing a “tribochemical protective layer” on the interface. Oil additives could offer a beneficial wear performance to the DLC coatings by formation of lubricous tribochemical layer on the interface [211]. Additive-derived anti-wear compounds could inhibit the formation of wear particles which in turn could avoid pressure induced graphitization. In addition, the formed tribofilm can reduce the peak-stresses and provide a more uniform stress distribution at the interface [282-284]. This reduces the interfacial strain which is a recognized mechanism for the graphitization of DLC. That is well in agreement with our observations where graphitization of DLC coating occurred using base oils but not with additive-containing fully formulated oils (Figure 7-6). The ability of additives to suppress graphitization was also reported by Kalin *et al.* [200] and Vengudusamy *et al.* [229]. The formed tribofilm could also prevent the counterbody from excessive wear which could explain why less wear was

observed on the pins when additive-containing oils were used compared to the base oil in the a-C:15H/CI system.

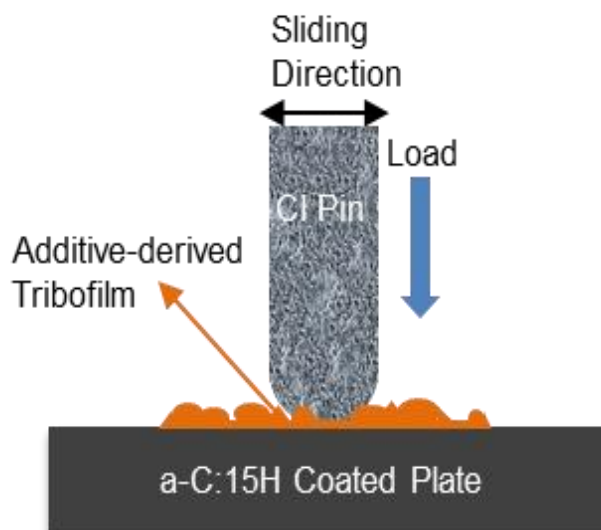


Figure 7-6 Schematic of the effect of tribochemical protective layer in suppressing graphitisation of DLC coating when lubricated in conventional fully formulated oils (low concentration of Mo-FM).

The main wear mechanisms on the FM-free fully formulated oils appeared to be polishing wear while the presence of 60 ppm FM in the oil formulation (i.e. FF300+ and FF300-) showed a slight positive effect on the wear of the a-C:15H coatings. In the a-C:15H coating, Haque *et al.* [220] reported the negative effect of the friction modifier on the anti-wear performance of ZDDP in the a-C:15H/CI system. However, they have used model oils (i.e. ZDDP and ZDDP/MoDTC) rather than fully formulated oils. In addition, concentration of MoDTC in their work was 500 ppm which was much higher than 60 ppm.

7.3. Effect of Mo-FM on a-C:15H Coating Durability/Wear

In phase II, the focus of the study was on the effect of MoDTC concentration on the tribological performance of the a-C:15H coating. In light of the physical observations and tribochemical analysis of the wear scar, friction and wear behaviour of hydrogenated DLC (a-C:15H) coating was found to depend on the concentration of the Mo based friction modifier and the wear performance was much better when ZDDP is present in the oil. The

tribochemical mechanisms, which contribute to this behaviour, are discussed in the following section.

7.3.1. Mechanisms of MoDTC-induced High Wear on DLC

The effect of MoDTC in increasing wear of DLC coatings has been reported in the literature [41, 224, 253]. However, they mainly used single additive solutions rather than more realistic fully formulated oils. Using fully formulated oils, this study has shown that the wear of the a-C:15H coating in the boundary lubrication regime is largely affected by the presence of Mo-FM and that its effect strongly depends on the level of Mo-FM in the lubricant.

XPS study confirmed that MoS_2 and MoO_3 which are known to be decomposition products from MoDTC [34, 35, 259] are formed, particularly from high concentration Mo-FM-containing fully formulated oils, on the wear scar. Nano-indentation study suggested that, depending on the level of Mo-FM in the oil, the mechanical properties of the a-C:15H coatings were modified and that the wear scar became softer than as-received coating with increasing the Mo-FM level. The mechanisms by which MoDTC gives high wear on DLC could be explained by different hypotheses.

Shinyoshi *et al.* [41] suggested that flash heat by friction and mechanical energy during sliding resulted in resolution of C-H bonds and formation of dangling bonds. MoDTC decomposes on the sliding surfaces generating MoO_3 . The reaction of generated MoO_3 with the active sites of DLC (C-H bonds and dangling bonds) could eventually result in high wear, and thus brittleness of the DLC coating [41]. They evidenced the reaction of MoO_3 with DLC coating by performing a TG-DTA reaction analysis. The analyses were conducted in an N_2 atmosphere on various Mo compounds which were thought to be part of MoDTC decomposition products along with carbon powder of different structure which is believed to be present in the DLC matrix. They showed that the carbon powder which was heated to 800°C with MoO_3 indicated a reaction and elimination of the D-band when analysed by Raman spectroscopy.

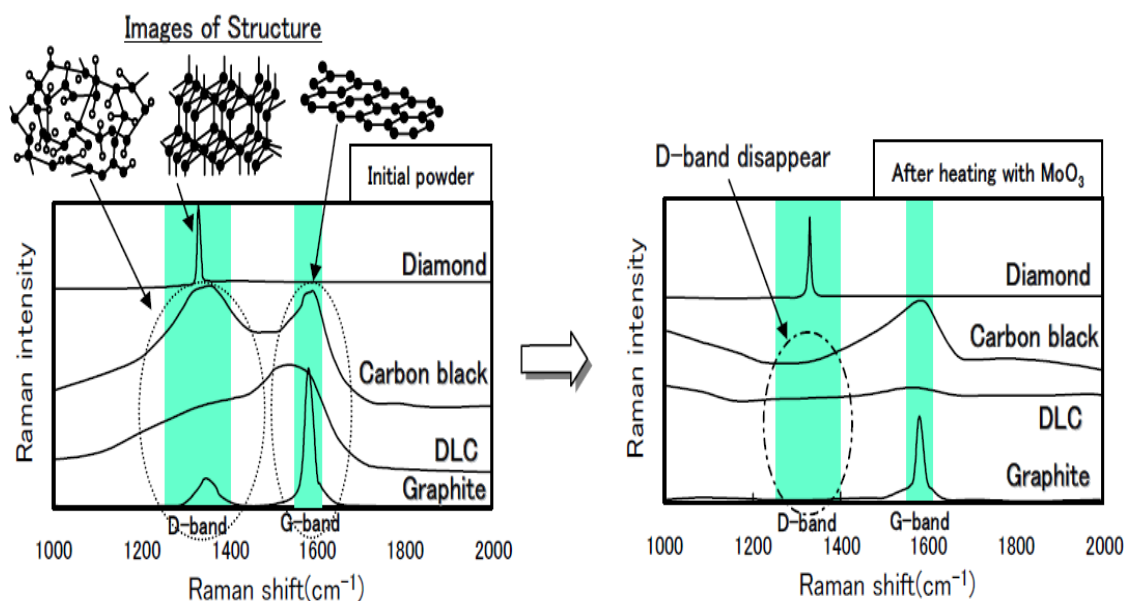
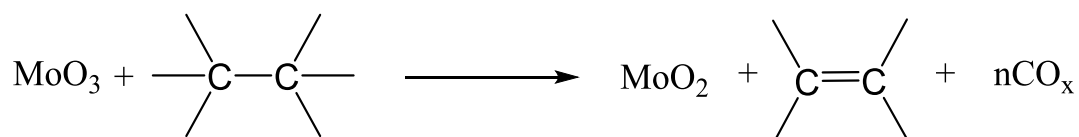


Figure 7-7 Raman spectra of carbon powder after heating with MoO_3 [41].

Based on this hypothesis, it can be proposed that MoO_3 can easily reduce to MoO_2 by the following chemical reaction:



Reaction of MoO_3 with the C-C bonds could promote graphitisation of DLC. In addition, temperature and/or stress-induced graphitisation of DLC coating have been reported by different authors [185, 190, 198]. Graphitisation of DLC could then be followed by wearing through the DLC coating.

In contrast, Sugimoto *et al.* [254] investigated the connection between graphitisation and MoO_3 and suggested that DLC wear mechanism in oils containing MoDTC is independent of the presence of MoO_3 . They suggested the following mechanism for MoDTC-induced high wear on DLC:

1. During sliding, the surface of DLC undergoes friction/temperature induced graphitization which will change the DLC to a brittle structure and wear develops from these sheared areas.
2. Formation of hard Mo compounds on the steel counterpart will promote wear by assisting the shearing of the DLC surface.

In the proposed mechanism, however, the process by which Mo hard compounds could accelerate the shearing of graphitised DLC areas was not verified. Based on the proposed hypothesis [254], the presence of steel counterpart which is hardened by Mo compounds ($H_{\text{average}}=17.6$ GPa), is essential for shearing of the DLC surface after the initial graphitisation of the coating. In agreement, Vengudusamy *et al.* [224] did not observe a high wear in a DLC/DLC system compared to DLC/steel combination using MoDTC-containing lubricant. They suggested that the wear mechanisms by which MoDTC is causing high wear to DLC involves the presence of the steel counterpart.

As shown in section 6.3.7, in order to elucidate the effect of steel counterpart in promoting MoDTC-induced high wear, the CI pin was replaced with a silicon nitride ceramic ball. Ceramic balls are considered to be inert and much harder than the CI pin. Therefore, formation of Mo compounds on the ceramic ball would be mitigated due to the inertness of the counterpart. On the other hand, the high hardness of the ceramic ball (15-20 GPa) could replicate the situation where Mo compounds hardened the steel counterpart which was believed [254] to play a significant role in imposing high wear to the DLC coating.

In this study, the friction and wear behaviour of DLC coating, when the counterpart was a ceramic ball was compared with that of the CI pin. The lubricant which gave the highest wear to the DLC/CI combination was chosen (i.e. high level of MoDTC and free of ZDDP) for a better comparison of the tribological behaviour when CI was replaced with ceramic. Running 20 h tribo-tests, friction was observed to be lower and wear was much higher using the CI pin compared to the ceramic ball. In fact, no significant wear was seen on the DLC plate when rubbed against the hard ceramic ball. XPS

analysis showed clear evidence of Mo compounds formation (both sulphides and oxides) on the DLC wear track using both the CI pin and the ceramic ball. However, the presence of Mo compounds was much more pronounced when rubbed against the CI pin (Figure 6-45 and Figure 6-46). In addition, Mo compounds were also present on the CI counterpart. That could explain lower friction/higher wear observed in the DLC/CI system compared to the DLC/ceramic system. In addition, steel may promote formation of Mo compounds. According to HSAB principle [76], in the presence of Iron, since S^{2-} and metal atoms are known to be soft base and acid, respectively, FeS is formed which acts as a protective layer and facilitates formation of Mo compounds on the steel counterpart [35].

Figure 7-8 shows the coefficient of wear and hardness variation with time for the DLC/CI and the DLC/ceramic combinations. It is clear that using CI pins, the wear showed an inverse relationship with hardness of the coating, i.e. the higher the coating wear, the lower the hardness, and vice versa. However, the hardness value of DLC coating was not changed when rubbed against the ceramic ball and was observed to be in the range of hardness of as-deposited coating. The obtained results do not contradict the finding by Sugimoto *et al.* [254] but suggest that graphitization/surface modification of DLC did not occur when the counterpart was ceramic. It appears that hardened steel counterpart independently, could not accelerate wear in MoDTC-induced wear observed in DLC/steel combination. It could be argued that using CI pins, as mentioned in section 7.2.1, iron wear debris can be generated during sliding. These iron particles could exert a very high local pressure and lowers down the graphitisation temperature of DLC coating. Unlike CI pins, the ceramic ball is a harder counterpart and does not generate significant third body particles and that could explain why graphitisation of DLC was not observed using the ceramic ball.

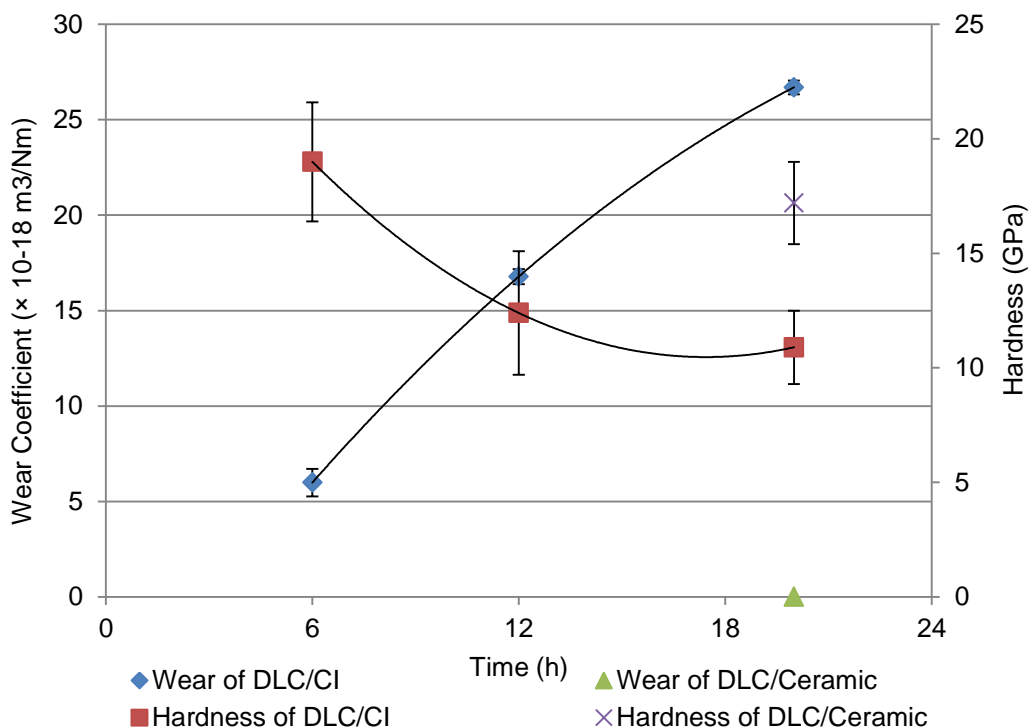


Figure 7-8 Wear and harness variation with time using DLC/CI and DLC/ceramic systems.

Whether MoO_3 reacts with DLC and promotes graphitisation or Mo compounds are hardening the ferrous counterpart leading to acceleration of the wear processes, it is reasonable to assume that MoDTC decomposition products are playing a great role in giving this high wear to hydrogenated DLC and that the presence of steel counterpart is essential for such high wear. However, it is not verified whether the wear process is catalysed by Mo compounds or mainly abrasive by MoO_3 . It has been reported that MoO_3 /dithiocarbamate ligands combinations act as oxidation catalysts for hydrocarbons [285].

Based on the observations, and the proposed mechanisms for MoDTC-induced high wear by authors [41, 224, 254], the mechanisms leading to low friction and high wear, induced by MoDTC in a DLC/CI system are proposed (schematically shown in Figure 7-9) as follows:

1. During sliding, wear debris formed from cast iron pins increase the contact pressure and promotes pressure induced graphitisation.

2. MoDTC forms low friction MoS_2 species on the CI pin, offering low friction of the a-C:15H/CI system. Formation of hard Mo compounds on the DLC/CI interface assist the shearing of the DLC surface and accelerate wear (MoO_3 has an abrasive nature).
3. Tribochemical reaction of the MoDTC-derived tribofilm with DLC surface promoting a high wear on a-C:15H coating.

This hypothesis is further supported by observations seen when the ceramic counterbody was used. Ceramic balls are hard ($H=15\text{-}20$ GPa) and would not provide much wear debris. This will terminate the first stage of the wear mechanism (pressure induced graphitisation of DLC).

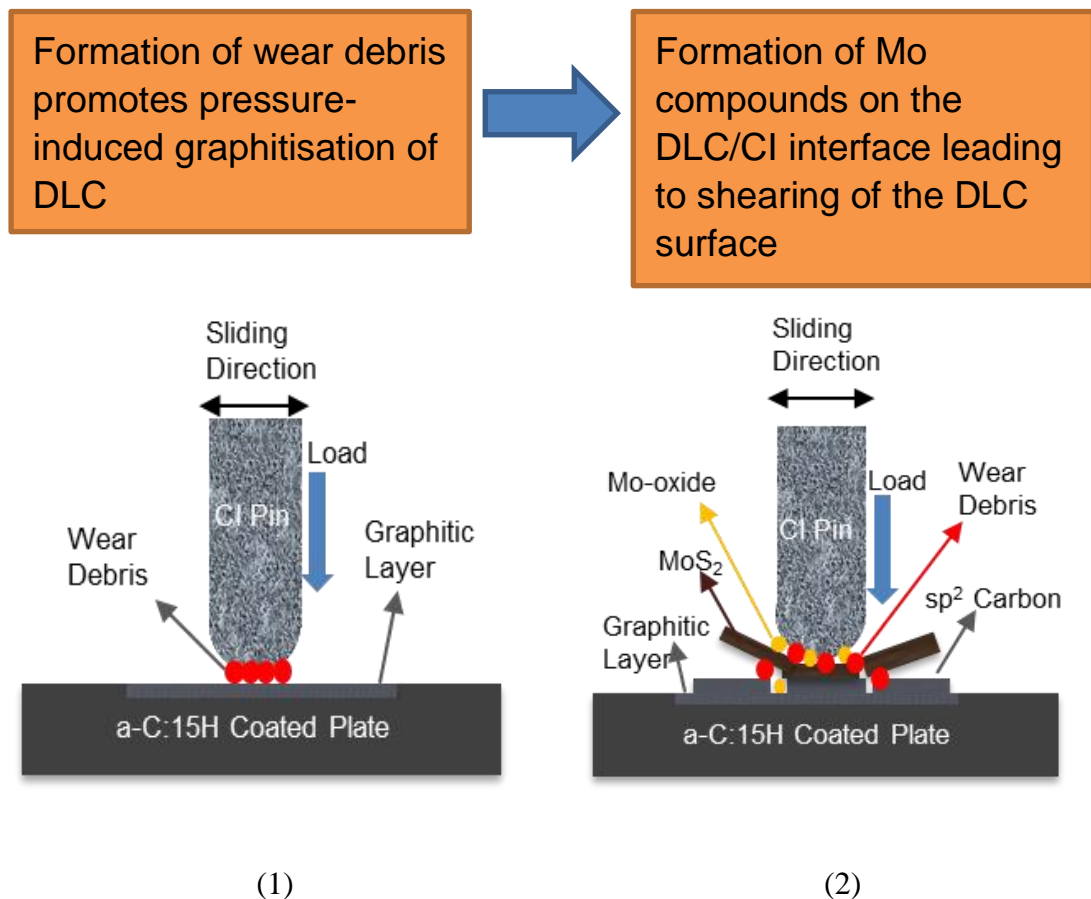


Figure 7-9 Schematic diagram showing the MoDTC-induced wear mechanisms. (1) and (2) represent the first and the second stage of the proposed wear mechanisms.

As discussed earlier in section 7.2.2, this high wear was mitigated in the presence of ZDDP for medium level of Mo-FM (FF300+). It could be argued that ZDDP could protect the pin surface from wear and generation of third body wear debris. ZDDP-derived zinc polyphosphate could react with MoO_3 and iron oxides leading to their elimination. ZDDP could also prevent pure MoS_2 from oxidation and further formation of abrasive MoO_3 [37]. Barros' Bouchet *et al.* [206] reported the positive effect of ZDDP when used in combination with MoDTC in the a-C:15H/steel system. They claimed that ZDDP could facilitate the formation of low friction MoS_2 by supplying more sulphur.

However, ZDDP was not effective in mitigating the adverse effect of MoDTC in giving high wear to DLC when the Mo-FM level was high in the oil (i.e. FF600+). This could be primarily due to high supply of MoDTC in the oil formulation which detrimentally affected ZDDP film structure leading to a much thinner tribofilm [123]. In addition, larger amount of MoDTC in the oil could facilitate MoO_3 formation in the tribofilm. MoO_3 is thought to be abrasive which could potentially enhance removal of protective tribofilms from DLC coatings [246]. This could lead to the formation of cast iron wear debris which is essential for initiation of graphitisation followed by high wear (as proposed earlier).

7.3.2. Effect of Mo-FM Source on MoDTC-induced Wear

As part of this study, the possible effect of MoDTC source on the “MoDTC induce wear” was investigated. Based on the obtained results, when ZDDP was present in the oils formulation, friction and wear behaviour was seen to be comparable for both Mo-FM with oxidation state of +5 and Mo-FM with oxidation state of +4 (i.e. FF300+). In contrast, removing ZDDP from the oil, Mo-FM with oxidation state of +4 provided a lower friction and much higher wear than Mo-FM with oxidation state of +5 (i.e. FF300-). That indicates the critical role of MoDTC source in giving high wear to DLC by MoDTC-containing fully formulated oils.

Mo-FM with the oxidation state of +4 can facilitate the formation of MoS_2 whereas Mo-FM with the oxidation state of +5 first needs reduction to +4 to

be able to form MoS_2 . Besides, the presence of oxygen in the Mo-FM with oxidation state of +5 structure accelerate the formation of molybdenum oxides which could bring detrimental effects on friction performance and was thought to be responsible for MoDTC-induced wear to DLC coatings [41]. However, XPS analyses revealed that the amount of Mo3d detected on the tribofilm of the pin formed from FF300- (Mo-FM with oxidation state of +4) was higher than FF300- (Mo-FM with oxidation state of +5) and as a result, more MoO_3 was present in the tribofilm formed from FF300- (Mo-FM with oxidation state of +4). That could explain the higher friction and lower wear obtained by ZDDP-free oil formulated with the Mo-FM with oxidation state of +5. Sugimoto *et al.* [254], however, reported that “MoDTC-induced high wear” is independent of the presence or absence of MoO_3 .

In contrast with findings of this study, the effect of MoDTC in giving high wear to DLC has been reported for multiple Mo-FM sources [220, 253]. However, the difference in concentration of MoDTC and the tests parameters with the ones which were conducted in this study, could result in contradictory results.

7.4. Practical Tribochemistry of DLC

7.4.1. Lubrication Comparison of the a-C:15H/CI and the Steel/CI systems

Based on this study, friction and wear results obtained from steel/CI system were generally different from those of a-C:15H/CI system. ZDDP usually decomposes on the ferrous surfaces and then it reacts with Fe_2O_3 from either wear debris/ ferrous surface and form strongly bonded Zn-phosphate anti-wear compounds [85, 88, 121]. Comparing the XPS atomic concentration of ZDDP-derived elements formed on the surface, it can be seen that the amount of Zn and P elements are higher on the steel compared to the a-C:15H surface. This suggests that a thicker film is obtained when the surface was ferrous.

Comparing the pin wear results, a-C:15H greatly reduces the wear of the counterbody when additive-free base oils were used. All other oils showed higher wear of the pins in the a-C:15H/CI system. It can be explained by the fact that the wear rate on the a-C:15H plates was extremely low and based on the physical observations; transfer layer is not believed to be formed on the pins using fully formulated oils. Thus, under tribological conditions, usually, the softer of the two materials which in this study is cast iron will be worn. In the case of a-C:15H/CI system, using additive free base oils, the formed transfer layer on the pins would protect the pin surface from further wear providing a lower wear on the pins leading to higher wear on the a-C:15H plate. In addition the transfer layer could also behave as a solid lubricant justifying the low friction obtained by the base oils in the a-C:15H/CI system which was discussed in detail in section 7.2.1.

The obtained results in this study are in agreement with a similar study on a-C:15H coating by Haque *et al.* [144] where FF oils showed higher pin wear in the a-C:15H/CI system than in the steel/CI system. The wear rates of cast iron pins with fully formulated oils in this study were in the range of 33×10^{-18} - 66×10^{-18} depending on the type of oil used. Haque *et al.* [144] however, reported values in the range of about 10×10^{-18} - 70×10^{-18} with three different FF oils for a similar contact pressure. The observed variation in the wear rates could be mainly due to the difference in the oil formulations as other test parameters were similar.

In addition, the average wear depth of cast iron pins observed for different oils are plotted in Figure 7-10. The obtained results are also compared with the average wear depth seen in a chilled cast iron cam nose of a 2.3L 4D55T/C diesel engine [286]. In this study, the obtained wear for cast iron pins in the steel/CI system and in the a-C:15H/CI system are generally 4-6 times and 6-10 times, respectively, higher than the average wear values reported for the cam nose in a real engine. The observed discrepancy in wear values could primarily originate from different test parameters used (contact type, entrainment speed, temperature, pressure, oil type, etc.) [287]. In addition, the high hardness of a-C:15H coating in this study compared to the uncoated shim in a real diesel engine could also be involved in the observed variations in wear results.

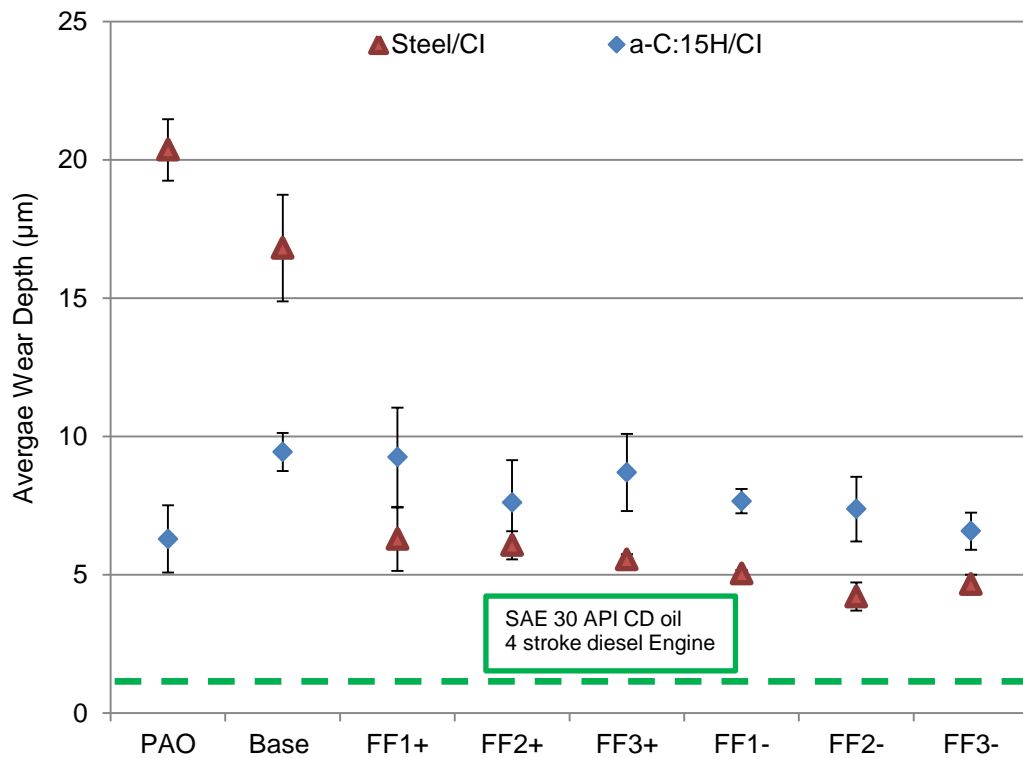


Figure 7-10 The comparison between the wear depth of the CI pins when rubbed against a-C:15H coating and uncoated steel plates with average cam nose wear in 4D55T/C diesel engine [286].

7.4.2. DLC Life Time/Optimum Performance

It was shown that conventional fully formulated oils which were free from friction modifiers (i.e. FF2+/FF2-) or contain low level of Mo-FM (40/60 ppm) provided comparatively high friction and low wear on a-C:15H coating. Increasing MoDTC concentration in the oils with the intention of obtaining lower friction resulted in a better friction response but with the cost of high wear of the a-C:15H coating. In Figure 7-11, the overall performance of the a-C:15H/CI system in terms of friction and wear is shown. It is apparent that the lower the friction, the higher the wear rates for the a-C:15H coating. Interestingly FF300+ showed comparatively lower friction compared to FF40+ and FF40- while, owing to the presence of ZDDP, maintained a good wear performance. This suggest that an additive solution can be tailored for the mitigation of DLC wear with formulation carrying a 300 ppm of Mo-FM. Thus, among all the oils, FF300+ provided an optimum friction/wear performance.

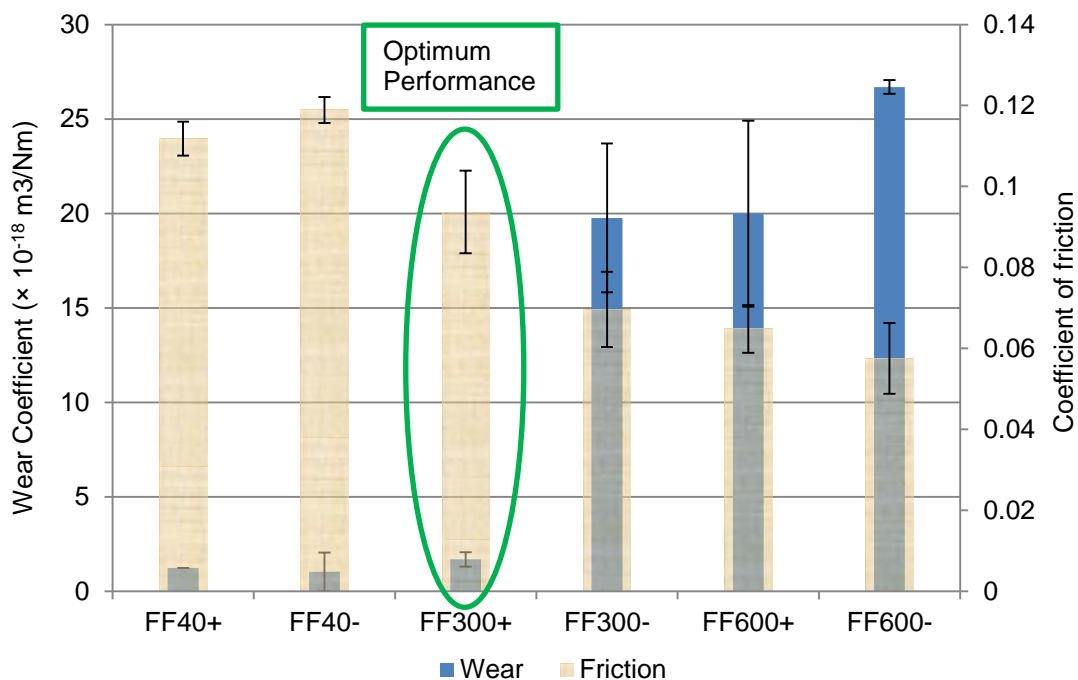


Figure 7-11 Friction and wear response of a-C:15H coating in the a-C:15H/CI system lubricated with oils formulated with different Mo-FM level (20 h tests).

This study revealed that graphitisation of a-C:15H coating occurred with base oils whereas fully formulated oils without Mo-FM or with low level of Mo-FM suppressed graphitisation by forming protective additive-derived tribofilms. The high wear on the a-C:15H coating was also observed by increasing the Mo-FM level in the FF oils, and as a result the mechanical properties of a-C:15H coating were modified. Despite superior friction reduction by formation of DLC-derived low friction graphitic carbon, graphitisation is detrimental as it increases the wear of the DLC coating. Thus, as test duration increases, the high wear of the DLC coating would eventually result in entire removal of the coating from the substrate. In Figure 7-12, the average wear depth of a-C:15H coating lubricated in fully formulated oils with different level of Mo-FM as a function of test duration is given. It appears that the DLC coating will eventually be worn through the CrC/CrN interlayer using oils with medium and high level of Mo-FM (with one exception being FF300+). However, depending on the level of Mo-FM in the oils, the penetration rate (Table 7-1) is different (i.e. the higher the Mo-FM concentration, the higher the penetration rate).

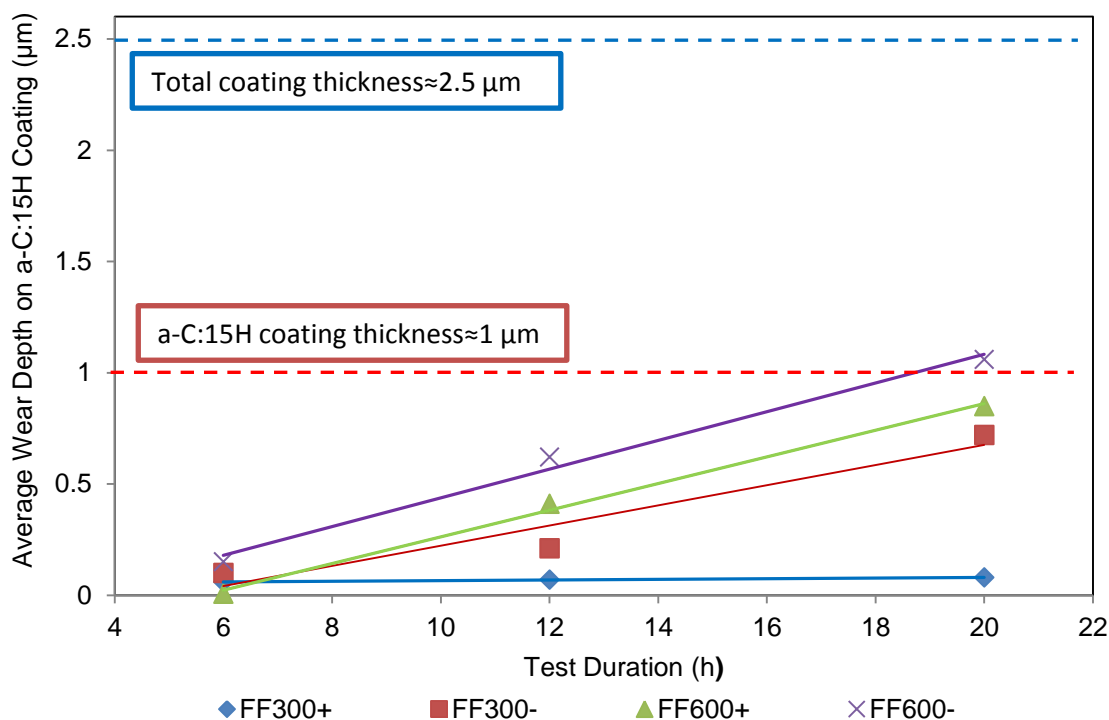


Figure 7-12 Average wear depth on a-C:15H coating as a function of FF oils formulated with different Mo-FM level.

Based on the obtained results, if the tests continue, FF300-, FF600+ and FF600- will result in the removal of the a-C:15H coating and reaching to the CrN/CrC interlayer in about 19, 22 and 27 h, respectively. Interestingly, using FF300+, DLC coating will last much longer (677 h) while giving almost 20% and 28% lower friction compared to FF40+ and FF40- (COF=0.12), respectively.

Table 7-1 a-C:15H coating thickness loss rate ($\mu\text{m}/\text{h}$) and DLC coating life (h)

Oils	Penetration Rate ($\mu\text{m}/\text{h}$)	a-C:15H coating life (h)
FF300+	0.001	677.1
FF300-	0.045	27.2
FF600+	0.060	22.3
FF600-	0.065	18.7

Lubricant optimisation by means of applying new additives or/and additives with developed chemistry is one approach towards obtaining an optimum

DLC/lubricant system. However, tailoring DLC to be more compatible with the current additive technology should also be considered. Recently, applying CrC/a-C:H coatings with different Cr content, it was reported that CrC/a-C:H coatings with Cr:C ratios in the range of 1, but having a significant amount of an amorphous a-C:H phase, provided an optimum solution for metal free a-C:15H/MoDTC-containing lubricant interaction as they exhibit both low friction and extremely low wear rates [288]. Nevertheless, engine components in a real engine should operate for hundreds of thousands of cycles before being replaced implying that coating the parts with DLC requires careful optimisation of DLC/lubricant to avoid early failure of the coated parts in use.

Chapter 8 Conclusions and Future Work

8.1. Concluding Remarks

This study provided some insights into the DLC lubrication. The obtained results revealed the possibility of the tribofilm formation on a a-C:15H coating and the effectiveness in reducing boundary friction and wear in a-C:15H/CI systems under FF-lubricated condition. The a-C:15H coating durability was found to be strongly oil dependant. Coating failure can be avoided using additive-containing oils by forming a protective tribofilm on the surfaces, and thus suppressing the a-C:15H coating structural modification.

The friction and wear properties of the a-C:15H coating/commercial in fully formulated oils under boundary lubrication conditions have been investigated in detail and the tribological performance compared with that of an uncoated steel system. In general, the durability of the a-C:15H coating was seen to be strongly dependant on the type of lubricant. Furthermore, the effect of detergent, dispersant and antioxidants on the performance of the molybdenum-based friction modifier (Mo-FM) and ZDDP anti-wear additive have been considered. The XPS analysis revealed the formation of detergent- and dispersant-derived species in the tribofilm.

In addition, the effect of Mo-FM concentration in one type of fully formulated oil on the tribological performance DLC/CI system was investigated and the obtained results were compared with those of the steel/CI system. To investigate the above, the test duration was set to 6, 12 and 20 h. Conducting tests in different time intervals provided a better understanding of the mechanisms by which MoDTC produces high wear on the a-C:15H coating. Furthermore, the effect of Mo-FM type and counterpart type on MoDTC-induced wear was studied.

In summary, the key conclusions made from this work are presented:

- In general, friction reduction was observed using base oils but at the price of severe delamination of the a-C:15H surface in some regions inside the wear scar as well as high gradual wear. It appears that graphitization of DLC coating was responsible for such high wear. Potentially, the high contact pressure exerted by positive edges of the scratches and generation of “micro-size” iron particles from the counterbody could promote pressure-induced graphitization of the a-C:15H surface leading to high gradual wear of the a-C:15H coating.
- Based on the provided SEM and optical microscope images, base oil (group III) gave slightly better wear performance than PAO suggesting the important role of base oil type in the lubricant.
- Formation of ZDDP-derived Zn-phosphate/ZnS/ZnO anti-wear species under boundary lubrication condition was evident in the tribofilms formed on both the a-C:15H coating and coating the counterpart (CI pin). This could reduce the peak-stresses by offering a more uniform stress distribution at the interface providing superior wear performance to DLC. In addition, the formation of an anti-wear “tribochemical protective layer” on the interface could suppress/inhibit the formation of wear particles, and as a result pressure-induced graphitization of DLC.
- Using conventional fully formulated oils with low levels of Mo-FM (40/60 ppm), the amount of Mo detected Mo 3d peak on both the a-C:15H/uncoated steel surface and cast iron pins was very low. This implies ineffectiveness of the Mo-FM additive in forming a low friction tribofilm on the interface. Furthermore, this could justify comparatively high friction obtained using these oils on both the a-C:15H/CI and the steel/CI systems.
- Ineffectiveness of friction modifier on friction reduction in both the steel and the DLC systems was mainly attributed to the low concentration of MoDTC in the lubricants. In addition, in the presence of ZDDP, phosphate formation on the surface can influence MoDTC film formation. Furthermore, several surface active additives, such as;

detergents, dispersants and antioxidants are present in the fully formulated oils which could synergistically or antagonistically affect low friction film formation on the surface. The friction behaviour of the fully formulated oils on both the DLC/CI and the steel/CI can also be correlated to the increased shear strength at the interface due to the surface/additive interaction.

- Conventional fully formulated oils showed a good wear performance of the a-C:15H coatings (phase I). The main wear mechanisms on the FM-free fully formulated oils were polishing wear while the presence of 60 ppm FM showed a slight positive effect on the wear of the a-C:15H coatings. However, increasing concentration of Mo-FM (with oxidation state of +4) in the oils promoted wear of a-C:15H coating in the oils without ZDDP (phase II) and, for certain level of Mo-FM (300 ppm), this wear was mitigated by the addition of ZDDP. This implies the critical role of MoDTC concentration in the oil and its effect on the tribological performance of a-C:15H coating.
- This study indicated that the presence of ZDDP in fully formulated oils can promote some level of confidence that an additive solution can be tailored for the mitigation of DLC wear with formulation having 300 ppm of Mo-FM (FF300+).
- Unlike ZDDP, the presence of other surface active additives (antioxidants, detergents and dispersants) in fully formulated oils did not offer protection of the a-C:15H coating against MoDTC-induced high wear.
- Apparently, using FF oils with medium and high level of Mo-FM, the mechanical properties of the a-C:15H coating were modified. Furthermore, the MoDTC-induced high wear seen for a-C:15H coating was more of tribochemistry of the rubbing surfaces rather than chemical reaction of the oils with the a-C:15H coating. This was evident by comparing the hardness values of the outside of the wear tracks with as-deposited coating, which, considering the standard deviation, were almost the same.

- XPS analysis of the tribofilms formed from oils with medium and high level of MoDTC showed that MoS₂ and MoO₃ species, which are the potential cause of surface modification/graphitisation of DLC, were dominant on the a-C:15H coating after 12 h. Thus, it is apparent that the tribochemical effect of MoDTC-containing oils on surface modification of a-C:15H coating requires certain amount of time to occur.
- Tribological tests and surface analysis of the DLC coatings over the time intervals suggested that MoDTC decomposition products initially form a tribofilm on the surface offering low friction followed by high wear on the a-C:15H coated plates. In addition, for high wearing oils, wearing through the coating and reaching to CrC/CrN interlayer may change the interface from the a-C:15H/CI to the interlayer/CI system.
- The MoDTC type was also found to be important in promoting MoDTC-induced wear. This study revealed that the high wear on the a-C:15H coating observed using ZDDP-free oils with medium level of Mo-FM was only seen when the oxidation state of Mo-FM was +4. However, the same effect was not observed with the same formulation but carrying Mo-FM with oxidation state of +5.
- This study revealed that the presence of the steel counterpart is involved in the wear mechanisms by which the MoDTC is causing high wear on a-C:15H coating. It was shown that MoDTC-induced high wear on DLC plates was only seen when rubbed against CI pins. This phenomenon was diminished when the CI counterpart was replaced with silicon nitride ceramic counterpart.

8.2. Suggestions for Future Work

Undoubtedly, formulations can be optimised for DLC surfaces; much remains to be done in this area but good progress has been made. There are different aspects of DLC lubrication which could be investigated and are

not accomplished in the current work mainly due to time constraints. Few suggestions are proposed to continue research in this direction:

- Nanoscratch tests could be conducted on the worn DLC coated plates to investigate the potential brittleness of the DLC coating caused by MoDTC-derived species. This could further support the results obtained from nanoindentation analysis performed in this study and provide a better picture of wear mechanisms involved in this phenomenon.
- Conducting some simple static tests by heating the DLC coated samples with oils containing different additives. This will be followed by Fourier Transform Infrared spectroscopy (FTIR) analysis of the samples. This will elucidate possible thermal effects on chemical reaction of the additives, MoDTC in particular, with the DLC coatings.
- Optimising Mo and other FMs to produce low friction and manageable wear. This includes developing new friction modifiers and applying organic friction modifiers to replace with Mo-FM.
- The obtained results in this study are only valid for a-C:15H coating. Changing DLC coatings to be more compatible with current Mo additive technology could be a potential approach to take. In addition, applying different coatings with varying degrees of hydrogenation and metal doping on a commercial basis could lead to a DLC coated system with an optimum tribological performance. Some preliminary suggestions for doping will be W, Cr and Mo. Mo chosen to specifically replace Mo from the friction modifier additive MoDTC.
- To verify the test data obtained from the current study by using the same blends in the valve train test rig. This would provide a more realistic system and validate the assumptions made regarding simple tribometer testing.

List of References

1. Holmberg, K., P. Andersson, and A. Erdemir, *Global energy consumption due to friction in passenger cars*. Tribology International, 2012. **47**(0): p. 221-234.
2. Jost, H.P. and J. Schofield, *Energy Saving through Tribology: A Techno-Economic Study*. Proceedings of the Institution of Mechanical Engineers, 1981. **195**(1): p. 151-173.
3. Fontaras, G. and Z. Samaras, *On the way to 130 g CO₂/km: estimating the future characteristics of the average European passenger car*. Energy Policy, 2010. **38**(4): p. 1826-1833.
4. Taylor, R.I. and R.C. Coy, *Improved fuel efficiency by lubricant design: A review*. Proceedings of the Institution of Mechanical Engineers, Part J: Journal of Engineering Tribology, 2000. **214**(1): p. 1-15.
5. Herdan, J.M., *Lubricating oil additives and the environment - An overview*. Lubrication Science, 1997. **9**(2): p. 161-172.
6. Bartz, W.J., *Lubricants and the environment*. Tribology International, 1998. **31**(1-3): p. 35-47.
7. International Energy Agency, O.f.E.C.-o. and Development, *Energy technology perspectives 2010 : scenarios & strategies to 2050*. 2010, Paris: OECD/IEA.
8. Fessler, R.R. and G.R. Fenske, *Multiyear Program Plan: Reducing Friction and Wear in Heavy Vehicles*, in *Other Information: PBD: 13 Dec 1999; PBD: 13 Dec 1999*. 1999. p. Medium: ED; Size: 60 pages.
9. Tung, S.C. and M.L. McMillan, *Automotive tribology overview of current advances and challenges for the future*. Tribology International, 2004. **37**(7): p. 517-536.
10. Stachowiak, G.W. and A.W. Batchelor, *Engineering tribology / G.W. Stachowiak, A.W. Batchelor*. Third Edition ed. Tribology series ; 24. 2005, Amsterdam ; New York :: Elsevier. 832.
11. Williams, J., *Engineering Tribology*. 2005: University of Cambridge 508.
12. Dowson, D., *History of tribology*. 2nd ed. 1998: John Wiley & Sons.
13. Sarkar, A.D., *Friction and wear*. 1980, New York: Academic Press.
14. Priest, M., *Introduction to Tribology lecture notes*. 2009, University of Leeds.
15. Neville, A., Morina, A., *Wear and chemistry of lubricants*. In: Stachowiak, G. (ed.) in *Wear-Materials, Mechanisms and Practice*. 2005, Wiley & Sons.: London. p. 71-94.
16. Rabinowicz, E., *Friction and wear of materials*. 1965, New York: Wiley.
17. Bhushan, B., *Modern tribology handbook*. Mechanics and materials science series. 2001, Boca Raton, FL: CRC Press.
18. Archard, J.F., *Single Contacts and Multiple Encounters*. Journal of Applied Physics, 1961. **32**(8): p. 1420-1425.

19. Hertz, H., *Über die Berührung fester elastische Körper and über die Harts (On the contact of rigid elastic solids and on hardness)*. Verhandlungen des Vereins zur Beförderung des Gewerbefleißes, Leipzig, 1882.
20. Hertz, H., *Miscellaneous papers, translated from first German edition (1895) by DE Jones and JA Schott*. 1896, London: MacMillan.
21. Hamrock, B.J. and D. Dowson, *Ball bearing lubrication : the elastohydrodynamics of elliptical contacts*. 1981, New York: Wiley.
22. Stachowiak, G.W. and A.W. Batchelor, *Elastohydrodynamic Lubrication*, in *Engineering Tribology (Third Edition)*. 2006, Butterworth-Heinemann: Burlington. p. 287-362.
23. Srivastava, S.P.T.S.o.I., *Advances in lubricant additives and tribology*. 2009, New Delhi: Tech Books International in association with Tribology Society of India.
24. Mang, T.D.W., *Lubricants and lubrications*. 2001, Weinheim; New York; Chichester: Wiley-VCH.
25. Harris, T.A. and M.N. Kotzalas. *Essential concepts of bearing technology*. 2006.
26. Wells, H.M.S.J.E.S.o.C.I., *The theory and practice of lubrication : the "germ" process*. 1920, London: Central House.
27. Kerley, R.V., *A History of Aircraft Piston Engine Lubricants*. 1981, SAE International.
28. Beeck, O., J. Givens, and E. Williams, *On the mechanism of boundary lubrication. II. Wear prevention by addition agents*. Proceedings of the Royal Society of London. Series A. Mathematical and Physical Sciences, 1940. **177**(968): p. 103-118.
29. Spikes, H., *The History and Mechanisms of ZDDP*. Tribology Letters, 2004. **17**(3): p. 469-489.
30. Rudnick, L.R. *Lubricant Additives Chemistry and Applications, Second Edition*. 2009.
31. Mattox, D.M., *Handbook of Physical Vapor Deposition (PVD) Processing*. 1998, William Andrew Publishing/Noyes.
32. Pierson, H.O.P.H.O., *Handbook of chemical vapor deposition*. 1999, Norwich, NY: Noyes Publications.
33. Rosnagel, S.M., J.J. Cuomo, and W.D. Westwood, *Handbook of Plasma Processing Technology - Fundamentals, Etching, Deposition, and Surface Interactions*. 1990, William Andrew Publishing/Noyes.
34. Grossiord, C., K. Varlot, J.M. Martin, T. Le Mogne, C. Esnouf, and K. Inoue, *MoS₂ single sheet lubrication by molybdenum dithiocarbamate*. Tribology International, 1998. **31**(12): p. 737-743.
35. Morina, A., A. Neville, M. Priest, and J.H. Green, *ZDDP and MoDTC interactions and their effect on tribological performance – tribofilm characteristics and its evolution*. Tribology Letters, 2006. **24**(3): p. 243-256.
36. De Barros, M.I., J. Bouchet, I. Raoult, T. Le Mogne, J.M. Martin, M. Kasrai, and Y. Yamada, *Friction reduction by metal sulfides in boundary lubrication studied by XPS and XANES analyses*. Wear, 2003. **254**(9): p. 863-870.

37. Martin, J.-M., C. Grossiord, T. Le Mogne, and J. Igarashi, *Transfer films and friction under boundary lubrication*. *Wear*, 2000. **245**(1-2): p. 107-115.
38. Bovington, C. and R. Castle, *Lubricant chemistry including the impact of legislation*, in *Tribology Series*, M.P.G.D. D. Dowson and A.A. Lubrecht, Editors. 2002, Elsevier. p. 141-146.
39. Gellman, A.J. and N.D. Spencer, *Surface chemistry in tribology*. Proceedings of the Institution of Mechanical Engineers, Part J: Journal of Engineering Tribology, 2002. **216**(6): p. 443-461.
40. Barnes, A.M., K.D. Bartle, and V.R.A. Thibon, *A review of zinc dialkyldithiophosphates (ZDDPS): characterisation and role in the lubricating oil*. *Tribology International*, 2001. **34**(6): p. 389-395.
41. Shinyoshi, T., Y. Fuwa, and Y. Ozaki, *Wear Analysis of DLC Coating in Oil Containing Mo-DTC*. 2007.
42. Khorramian, B.A., G.R. Iyer, S. Kodali, P. Natarajan, and R. Tupil, *Review of antiwear additives for crankcase oils*. *Wear*, 1993. **169**(1): p. 87-95.
43. Sheasby, J.S., T.A. Caughlin, and J.J. Habeeb, *Observation of the antiwear activity of zinc dialkyldithiophosphate additives*. *Wear*, 1991. **150**(1-2): p. 247-257.
44. Bovington, C.H. and A. Hubbard, *Lubricant additive effects on valve train friction and wear*. 1989: p. IMechE 1989-9.
45. Sheasby, J.S., T.A. Caughlin, and W.A. Mackwood, *The effect of steel hardness on the performance of antiwear additives*. *Wear*, 1996. **201**(1-2): p. 209-216.
46. Lin, Y.C. and H. So, *Limitations on use of ZDDP as an antiwear additive in boundary lubrication*. *Tribology International*, 2004. **37**(1): p. 25-33.
47. So, H. and R.C. Lin, *The combined effects of ZDDP, surface texture and hardness on the running-in of ferrous metals*. *Tribology International*, 1999. **32**(5): p. 243-253.
48. Jahanmir, S., *Wear reduction and surface layer formation by a ZDDP additive*. *Journal of tribology*, 1987. **109**(4): p. 577-586.
49. Sieber, I., K. Meyer, H. Kloss, and A. Schöpke, *Characterization of boundary layers formed by different metal dithiophosphates in a four-ball machine*. *Wear*, 1983. **85**(1): p. 43-56.
50. Wu, Y.L. and B. Dacre, *Effects of lubricant-additives on the kinetics and mechanisms of ZDDP adsorption on steel surfaces*. *Tribology International*, 1997. **30**(6): p. 445-453.
51. So, H., Y.C. Lin, G.G.S. Huang, and T.S.T. Chang, *Antiwear mechanism of zinc dialkyl dithiophosphates added to a paraffinic oil in the boundary lubrication condition*. *Wear*, 1993. **166**(1): p. 17-26.
52. Cann, P., G. Johnston, and H. Spikes, *The formation of thick films by phosphorus-based anti-wear additives*. *Tribology-Friction, Lubrication and Wear. Fifty Years On.*, 1987. **1**: p. 543-554.
53. Choa, S.-H., K.C. Ludema, G.E. Potter, B.M. Dekoven, T.A. Morgan, and K.K. Kar, *A model of the dynamics of boundary film formation*. *Wear*, 1994. **177**(1): p. 33-45.

54. Taylor, L., A. Dratva, and H. Spikes, *Friction and wear behavior of zinc dialkyldithiophosphate additive*. Tribology transactions, 2000. **43**(3): p. 469-479.
55. Holinski, R., *The influence of boundary layers on friction*. Wear, 1979. **56**(1): p. 147-154.
56. Kennedy, S. and L. Moore, *Additive effects on lubricant fuel economy*. 1987, Society of Automotive Engineers, Warrendale, PA.
57. Kubo, K., M. Kibukawa, and Y. Shimakawa. *EFFECT ON FRICTION OF LUBRICANTS CONTAINING ZINC DITHIOPHOSPHATE AND ORGANO-MOLYBDENUM COMPOUND*. 1985. London, Engl: r Inst of Mechanical Engineers, London by Mechanical Engineering Publ Ltd.
58. Taylor, L., H. SPIKES, and H. CAMENZIND, *Film-forming properties of zinc-based and ashless antiwear additives*. SAE transactions, 2000. **109**(4): p. 2095-2105.
59. Tripaldi, G., A. Vettor, and H. Spikes, *Friction behavior of ZDDP films in the mixed, boundary/EHD regime*. SAE transactions, 1996. **105**(4): p. 1819-1830.
60. Taylor, L. and H. Spikes, *Friction-enhancing properties of ZDDP antiwear additive: part I—friction and morphology of ZDDP reaction films*. Tribology transactions, 2003. **46**(3): p. 303-309.
61. Taylor, L.J. and H.A. Spikes, *Friction-enhancing properties of ZDDP antiwear additive: part II—influence of ZDDP reaction films on EHD lubrication*. Tribology transactions, 2003. **46**(3): p. 310-314.
62. Sheasby, J., T. Caughlin, A. Blahey, and K. Laycock, *A reciprocating wear test for evaluating boundary lubrication*. Tribology International, 1990. **23**(5): p. 301-307.
63. Cann, P. and A. Cameron, *Studies of thick boundary lubrication— influence of zddp and oxidized hexadecane*. Tribology international, 1984. **17**(4): p. 205-208.
64. Watkins, R.C., *The antiwear mechanism of zddp's. Part II*. Tribology International, 1982. **15**(1): p. 13-15.
65. Spedding, H. and R.C. Watkins, *The antiwear mechanism of zddp's. Part I*. Tribology International, 1982. **15**(1): p. 9-12.
66. Bird, R.J. and G.D. Galvin, *The application of photoelectron spectroscopy to the study of e. p. films on lubricated surfaces*. Wear, 1976. **37**(1): p. 143-167.
67. Dacre, B. and C.H. Bovington, *ADSORPTION AND DESORPTION OF ZINC DI-ISOPROPYLDITHIOPHOSPHATE ON STEEL*. ASLE TRANS, 1982. **V 25**(N 4): p. 546-554.
68. Bovington, C. and B. Dacre, *The adsorption and reaction of decomposition products of zinc di-isopropyldiophosphate on steel*. ASLE transactions, 1984. **27**(3): p. 252-258.
69. Coy, R. and R. Jones, *The thermal degradation and EP performance of zinc dialkyldithiophosphate additives in white oil*. ASLE transactions, 1981. **24**(1): p. 77-90.
70. Jones, R. and R. Coy, *The chemistry of the thermal degradation of zinc dialkyldithiophosphate additives*. Asle Transactions, 1981. **24**(1): p. 91-97.

71. Bell, J., K. Delargy, and A. Seeney, *Paper IX (ii) The Removal of Substrate Material through Thick Zinc Dithiophosphate Anti-Wear Films*. Tribology series, 1992. **21**: p. 387-396.
72. Yin, Z., M. Kasrai, M. Fuller, G.M. Bancroft, K. Fyfe, and K.H. Tan, *Application of soft X-ray absorption spectroscopy in chemical characterization of antiwear films generated by ZDDP Part I: the effects of physical parameters*. Wear, 1997. **202**(2): p. 172-191.
73. Martin, J.M., C. Grossiord, T. Le Mogne, S. Bec, and A. Tonck, *The two-layer structure of Zndtp tribofilms: Part I: AES, XPS and XANES analyses*. Tribology International, 2001. **34**(8): p. 523-530.
74. Martin, J.M., T. Onodera, C. Minfray, F. Dassenoy, and A. Miyamoto, *The origin of anti-wear chemistry of ZDDP*. Faraday Discussions, 2012. **156**: p. 311-323.
75. Onodera, T., J.M. Martin, C. Minfray, F. Dassenoy, and A. Miyamoto, *Antiwear chemistry of ZDDP: coupling classical MD and tight-binding quantum chemical MD methods (TB-QCMD)*. Tribology Letters, 2012: p. 1-9.
76. Pearson, R.G., *Chemical hardness*. 1997, Weinheim, Germany; New York: Wiley-VCH.
77. Martin, J.M., *Antiwear mechanisms of zinc dithiophosphate: A chemical hardness approach*. Tribology Letters, 1999. **6**(1): p. 1-8.
78. Minfray, C., T. Le Mogne, J.-M. Martin, T. Onodera, S. Nara, S. Takahashi, H. Tsuboi, M. Koyama, A. Endou, H. Takaba, M. Kubo, C.A. Del Carpio, and A. Miyamoto, *Experimental and Molecular Dynamics Simulations of Tribochemical Reactions with ZDDP: Zinc Phosphate–Iron Oxide Reaction*. Tribology Transactions, 2008. **51**(5): p. 589-601.
79. Onodera, T., Y. Morita, A. Suzuki, R. Sahnoun, M. Koyama, H. Tsuboi, N. Hatakeyama, A. Endou, H. Takaba, M. Kubo, C.A. Del Carpio, C. Minfray, J.M. Martin, and A. Miyamoto, *A theoretical investigation on the abrasive wear prevention mechanism of ZDDP and ZP tribofilms*. Applied Surface Science, 2008. **254**(23): p. 7976-7979.
80. Fuller, M.L.S., M. Kasrai, G.M. Bancroft, K. Fyfe, and K.H. Tan, *Solution decomposition of zinc dialkyl dithiophosphate and its effect on antiwear and thermal film formation studied by X-ray absorption spectroscopy*. Tribology International, 1998. **31**(10): p. 627-644.
81. Martin, J., *Lubricant additives and the chemistry of rubbing surfaces: metal dithiophosphates tribochemical films revisited*. Japanese Journal of Tribology, 1997. **42**(9): p. 1095.
82. Williams, J.A., *The Behaviour of Sliding Contacts Between Non-Conformal Rough Surfaces Protected by 'Smart' Films*. Tribology Letters, 2004. **17**(4): p. 765-778.
83. Georges, J.M., A. Tonck, S. Poletti, E.S. Yamaguchi, and P.R. Ryason, *Film Thickness and Mechanical Properties of Adsorbed Neutral and Basic Zinc Diisobutyl Dithiophosphates*. Tribology Transactions, 1998. **41**(4): p. 543-553.
84. Bec, S. and A. Tonck, *Nanometer Scale Mechanical Properties of Tribochemical Films*, in *Tribology Series*,

- C.M.T.T.H.C.C.G.D.Y.B.L.F.J.M.G. D. Dowson and A.A. Lubrecht, Editors. 1996, Elsevier. p. 173-184.
85. Pidduck, A.J. and G.C. Smith, *Scanning probe microscopy of automotive anti-wear films*. *Wear*, 1997. **212**(2): p. 254-264.
 86. Warren, O.L., J.F. Graham, P.R. Norton, J.E. Houston, and T.A. Michalske, *Nanomechanical properties of films derived from zinc dialkyldithiophosphate*. *Tribology Letters*, 1998. **4**(2): p. 189-198.
 87. Graham, J.F., C. McCague, and P.R. Norton, *Topography and nanomechanical properties of tribochemical films derived from zinc dialkyl and diaryl dithiophosphates*. *Tribology Letters*, 1999. **6**(3-4): p. 149-157.
 88. Aktary, M., M.T. McDermott, and J. Torkelson, *Morphological evolution of films formed from thermooxidative decomposition of ZDDP*. *Wear*, 2001. **247**(2): p. 172-179.
 89. Bec, S., A. Tonck, J.-M. Georges, R.C. Coy, J.C. Bell, and G.W. Roper, *Relationship between mechanical properties and structures of zinc dithiophosphate anti-wear films*. *Proceedings of the Royal Society of London. Series A: Mathematical, Physical and Engineering Sciences*, 1999. **455**(1992): p. 4181-4203.
 90. Nicholls, M., P. Norton, G. Bancroft, M. Kasrai, T. Do, B. Frazer, and G. De Stasio, *Nanometer scale chemomechanical characterization of antiwear films*. *Tribology Letters*, 2004. **17**(2): p. 205-216.
 91. Nicholls, M.A., G.M. Bancroft, P.R. Norton, M. Kasrai, G. De Stasio, B.H. Frazer, and L.M. Wiese, *Chemomechanical properties of antiwear films using X-ray absorption microscopy and nanoindentation techniques*. *Tribology Letters*, 2004. **17**(2): p. 245-259.
 92. Ye, J., M. Kano, and Y. Yasuda, *Evaluation of Local Mechanical Properties in Depth in MoDTC/ZDDP and ZDDP Tribochemical Reacted Films Using Nanoindentation*. *Tribology Letters*, 2002. **13**(1): p. 41-47.
 93. Bec, S., A. Tonck, J.M. Georges, and G.W. Roper, *Synergistic Effects of MoDTC and ZDTP on Frictional Behaviour of Tribofilms at the Nanometer Scale*. *Tribology Letters*, 2004. **17**(4): p. 797-809.
 94. Morina, A., J.H. Green, A. Neville, and M. Priest, *Surface and Tribological Characteristics of Tribofilms Formed in the Boundary Lubrication Regime with Application to Internal Combustion Engines*. *Tribology Letters*, 2003. **15**(4): p. 443-452.
 95. Nicholls, M., T. Do, P. Norton, G.M. Bancroft, M. Kasrai, T.W. Capehart, Y.-T. Cheng, and T. Perry, *Chemical and Mechanical Properties of ZDDP Antiwear Films on Steel and Thermal Spray Coatings Studied by XANES Spectroscopy and Nanoindentation Techniques*. *Tribology Letters*, 2003. **15**(3): p. 241-248.
 96. Lansdown, A., *Molybdenum disulphide lubrication*. Vol. 35. 1999: Access Online via Elsevier.
 97. Yamamoto, Y. and S. Gondo, *Friction and wear characteristics of molybdenum dithiocarbamate and molybdenum dithiophosphate*. *Tribology Transactions*, 1989. **32**(2): p. 251-257.

98. Davis, F. and T. Eyre, *The effect of a friction modifier on piston ring and cylinder bore friction and wear*. Tribology International, 1990. **23**(3): p. 163-171.
99. Martin, J., T. Le Mogne, C. Grossiord, and T. Palermo, *Tribochemistry of ZDDP and MoDDP chemisorbed films*. Tribology Letters, 1996. **2**(3): p. 313-326.
100. Graham, J., H. Spikes, and S. Korcek, *The friction reducing properties of molybdenum dialkyldithiocarbamate additives: part I—factors influencing friction reduction*. Tribology transactions, 2001. **44**(4): p. 626-636.
101. Graham, J., H. Spikes, and R. Jensen, *The friction reducing properties of molybdenum dialkyldithiocarbamate additives: Part II—Durability of friction reducing capability*. Tribology transactions, 2001. **44**(4): p. 637-647.
102. Martin, J., T. Le Mogne, M. Boehm, and C. Grossiord, *Tribochemistry in the analytical UHV tribometer*. Tribology international, 1999. **32**(11): p. 617-626.
103. Grossiord, C., J. Martin, T. Le Mogne, and T. Palermo, *In situ MoS₂ formation and selective transfer from MoDPT films*. Surface and coatings Technology, 1998. **108**: p. 352-359.
104. Grossiord, C., K. Varlot, J.-M. Martin, T. Le Mogne, C. Esnouf, and K. Inoue, *MoS₂ single sheet lubrication by molybdenum dithiocarbamate*. Tribology international, 1998. **31**(12): p. 737-743.
105. Miklozic, K.T., J. Graham, and H. Spikes, *Chemical and physical analysis of reaction films formed by molybdenum dialkyldithiocarbamate friction modifier additive using Raman and atomic force microscopy*. Tribology Letters, 2001. **11**(2): p. 71-81.
106. Singh, T., A. Bhattacharya, and V. Verma, *A study in EP activity evaluation of some new oil-soluble Mo-S complexes*. Tribology international, 1992. **25**(6): p. 381-385.
107. Tripathi, A., A. Bhattacharya, R. Singh, and V. Verma, *Tribological studies of 1-alkyl-2, 5-dithiohydrazodicarbonamides and their Mo–S complexes as EP and multifunctional additives*. Tribology international, 2000. **33**(1): p. 13-20.
108. Morina, A., *Lubricant additive interactions, surface reactions and the link to tribological performance in engines*. 2005, Heriot-Watt University.
109. Morita, Y., T. Onodera, A. Suzuki, R. Sahnoun, M. Koyama, H. Tsuboi, N. Hatakeyama, A. Endou, H. Takaba, and M. Kubo, *Development of a new molecular dynamics method for tribochemical reaction and its application to formation dynamics of MoS₂ tribofilm*. Applied Surface Science, 2008. **254**(23): p. 7618-7621.
110. Onodera, T., R. Miura, A. Suzuki, H. Tsuboi, N. Hatakeyama, A. Endou, H. Takaba, M. Kubo, and A. Miyamoto, *Development of a quantum chemical molecular dynamics tribochemical simulator and its application to tribochemical reaction dynamics of lubricant additives*. Modelling and Simulation in Materials Science and Engineering, 2010. **18**(3): p. 034009.

111. Voong, M., *Optimisation of crankcase lubricant additive-material combinations for reduced friction and wear in internal combustion engines*. 2005.
112. Spikes, H., *Film-forming additives-direct and indirect ways to reduce friction*. Lubrication Science, 2002. **14**(2): p. 147-167.
113. Sorab, J., Korcek, S., and Bovington, C., , *Friction Reduction in Lubricated Components Through Engine Oil Formulation* 1998.
114. Yamamoto, Y., and Gondo, S., *On properties of surface films formed with Molybdenum Dithiocarbamate (MoDTC) under different conditions*. Japanese Journal of Tribology, 1991. **36**(3): p. 309-321.
115. Rounds, F.G., *Additive interactions and their effect on the performance of a zinc dialkyl dithiophosphate*. ASLE TRANSACTIONS, 1978. **21**(2): p. 91-101.
116. Korcek, S., R. K Jensen, M. D Johnson, and J. Sorab, *Fuel efficient engine oils, additive interactions, boundary friction, and wear*. Tribology Series, 1999. **36**: p. 13-24.
117. Kasrai, M., J. Cutler, K. Gore, G. Canning, G. Bancroft, and K. Tan, *The chemistry of antiwear films generated by the combination of ZDDP and MoDTC examined by X-ray absorption spectroscopy*. Tribology transactions, 1998. **41**(1): p. 69-77.
118. Unnikrishnan, R., M. Jain, A. Harinarayan, and A. Mehta, *Additive-additive interaction: an XPS study of the effect of ZDDP on the AW/EP characteristics of molybdenum based additives*. Wear, 2002. **252**(3): p. 240-249.
119. Muraki, M., Y. Yanagi, and K. Sakaguchi, *Synergistic effect on frictional characteristics under rolling-sliding conditions due to a combination of molybdenum dialkyldithiocarbamate and zinc dialkyldithiophosphate*. Tribology international, 1997. **30**(1): p. 69-75.
120. Muraki, M. and H. Wada, *Influence of the alkyl group of zinc dialkyldithiophosphate on the frictional characteristics of molybdenum dialkyldithiocarbamate under sliding conditions*. Tribology International, 2002. **35**(12): p. 857-863.
121. Martin, J.-M., C. Grossiord, K. Varlot, B. Vacher, and J. Igarashi, *Synergistic effects in binary systems of lubricant additives: a chemical hardness approach*. Tribology Letters, 2000. **8**(4): p. 193-201.
122. Sogawa, Y., N. Yoshimura, and O. Iwasaki, *R&D on new friction modifier for lubricant for fuel economy improvement*. www.pecjorjp/gijutu-report/e-report/00E115epdf, 2000.
123. Yablon, D.G., P.H. Kalamaras, D.E. Deckman, and M.N. Webster, *Atomic force microscopy and raman spectroscopy investigation of additive interactions responsible for anti-wear film formation in a lubricated contact*. Tribology transactions, 2006. **49**(1): p. 108-116.
124. Wan, Y., M.L. Suominen Fuller, M. Kasrai, G.M. Bancroft, K. Fyfe, J.R. Torkelson, Y.F. Hu, and K.H. Tan, *Effects of detergent on the chemistry of tribofilms from ZDDP: studied by X-ray absorption spectroscopy and XPS*, in *Tribology Series*, M.P.G.D. D. Dowson and A.A. Lubrecht, Editors. 2002, Elsevier. p. 155-166.
125. Willermet, P.A., *Some engine oil additives and their effects on antiwear film formation*. Tribology Letters, 1998. **5**(1): p. 41-47.

126. Willermet, P.A., D.P. Dailey, R.O. Carter Iii, P.J. Schmitz, W. Zhu, J.C. Bell, and D. Park, *The composition of lubricant-derived surface layers formed in a lubricated cam/tappet contact II. Effects of adding overbased detergent and dispersant to a simple ZDTP solution*. Tribology International, 1995. **28**(3): p. 163-175.
127. Kasrai, M., M.S. Fuller, G.M. Bancroft, E.S. Yamaguchi, and P.R. Ryason, *X-Ray Absorption Study of the Effect of Calcium Sulfonate on Antiwear Film Formation Generated From Neutral and Basic ZDDPs: Part 2 — Sulfur Species*. Tribology Transactions, 2003. **46**(4): p. 543-549.
128. Kasrai, M., M.S. Fuller, G.M. Bancroft, and P.R. Ryason, *X-Ray Absorption Study of the Effect of Calcium Sulfonate on Antiwear Film Formation Generated From Neutral and Basic ZDDPs: Part 1— Phosphorus Species*. Tribology Transactions, 2003. **46**(4): p. 534-542.
129. Shiomi, M., J.i. Mitsui, K. Akiyama, K. Tasaka, M. Nakada, and H. Ohira, *Formulation Technology for Low Phosphorus Gasoline Engine Oils*. 1992, SAE International.
130. Shirahama, S. and M. Hirata, *The effects of engine oil additives on valve train wear*. Lubrication Science, 1989. **1**(4): p. 365-384.
131. Inoue, K. and H. Watanabe, *Interactions of Engine Oil Additives*. A S L E Transactions, 1983. **26**(2): p. 189-199.
132. Smith, G.C. and J.C. Bell, *Multi-technique surface analytical studies of automotive anti-wear films*. Applied Surface Science, 1999. **144–145**(0): p. 222-227.
133. Pereira, G., A. Lachenwitzer, M. Kasrai, G. Bancroft, P. Norton, M. Abrecht, P. Gilbert, T. Regier, R. Blyth, and J. Thompson, *Chemical and mechanical analysis of tribofilms from fully formulated oils Part 1— Films on 52100 steel*. Tribology-Materials, Surfaces & Interfaces, 2007. **1**(1): p. 48-61.
134. Priest, M. and C. Taylor, *Automobile engine tribology—approaching the surface*. Wear, 2000. **241**(2): p. 193-203.
135. Taylor, C.M., *Paper VI (i) Valve Train Lubrication Analysis*, in *Tribology Series*, C.M.T. D. Dowson and M. Godet, Editors. 1991, Elsevier. p. 119-131.
136. Taylor, C.M., *Fluid film lubrication in automobile valve trains*. Proceedings of the Institution of Mechanical Engineers, Part J: Journal of Engineering Tribology, 1994. **208**(4): p. 221-234.
137. Becker, E.P., *Trends in tribological materials and engine technology*. Tribology International, 2004. **37**(7): p. 569-575.
138. Enomoto, Y. and T. Yamamoto, *New materials in automotive tribology*. Tribology Letters, 1998. **5**(1): p. 13-24.
139. Nakamura, Y., Y. Egami, and K. Shimizu, *Development of an assembled camshaft by mechanical bonding*. SP-Society of Automotive Engineers, 1996(1138): p. 109-116.
140. Kano, M. and I. Tanimoto, *Wear mechanism of high wear-resistant materials for automotive valve trains*. Wear, 1991. **151**(2): p. 229-243.
141. McCune, R.C. and G.A. Weber, *Automotive Engine Materials*, in *Encyclopedia of Materials: Science and Technology (Second Edition)*,

- K.H.J.B. Editors-in-Chief: , et al., Editors. 2001, Elsevier: Oxford. p. 426-434.
142. Fukuoka, S., N. Hara, A. Mori, and K. Ohtsubo, *Friction loss reduction by new lighter valve train system*. JSAE Review, 1997. **18**(2): p. 107-111.
 143. Eyre, T. and B. Crawley, *Camshaft and cam follower materials*. Tribology International, 1980. **13**(4): p. 147-152.
 144. Haque, T., *Tribochemistry of Lubricant Additives on Non-Ferrous Coatings for Reduced Friction, Improved Durability and Wear in Internal Combustion Engines*. 2007, University of Leeds.
 145. Yasuda, Y., M. Kano, Y. Mabuchi, and S. Abou, *Research on Diamond-Like Carbon Coatings for Low-Friction Valve Lifters*. 2003, SAE International.
 146. Lawes, S., M. Fitzpatrick, and S.V. Hainsworth, *Evaluation of the tribological properties of DLC for engine applications*. Journal of Physics D: Applied Physics, 2007. **40**(18): p. 5427.
 147. Gangopadhyay, A., E. Soltis, and M. Johnson, *Valvetrain friction and wear: influence of surface engineering and lubricants*. Proceedings of the Institution of Mechanical Engineers, Part J: Journal of Engineering Tribology, 2004. **218**(3): p. 147-156.
 148. Johnston, S. and S.V. Hainsworth, *Effect of DLC coatings on wear in automotive applications*. Surface engineering, 2005. **21**(1): p. 67-71.
 149. NISSAN, *Nano-technology based ultra-low friction technology*. 2013.
 150. Ronkainen, H., *Tribological properties of hydrogenated and hydrogen-free diamond-like carbon coatings*. 2001.
 151. Ball, B., *Made to Measure: New Materials for the 21st Century*. 1997, New Jersey, USA: Princeton University Press. 447.
 152. Gardos, M.N.S., K.E. Dismukes, J.P.(Eds.), *Synthetic Diamond: Emerging CVD Science and Technology*. 1994, New York, USA.: John Eiley & Sons Inc.
 153. Lee, S.T., Z. Lin, and X. Jiang, *CVD diamond films: nucleation and growth*. Materials Science and Engineering: R: Reports, 1999. **25**(4): p. 123-154.
 154. Ronkainen, H., J. Likonen, and J. Koskinen, *Tribological properties of hard carbon films produced by the pulsed vacuum arc discharge method*. Surface and Coatings Technology, 1992. **54-55**(Part 2): p. 570-575.
 155. Robertson, J., *Diamond-like amorphous carbon*. Materials Science and Engineering: R: Reports, 2002. **37**(4-6): p. 129-281.
 156. Matthews, A. and S.S. Eskildsen, *Engineering applications for diamond-like carbon*. Diamond and Related Materials, 1994. **3**(4-6): p. 902-911.
 157. Bloyce, A., *Carbon PVD coatings wear it well*. Materials World, 2000. **8**(3): p. 13-15.
 158. Hershberger, J., O. oztürk, O.O. Ajayi, J.B. Woodford, A. Erdemir, R.A. Erck, and G.R. Fenske, *Evaluation of DLC coatings for spark-ignited, direct-injected fuel systems*. Surface and Coatings Technology, 2004. **179**(2-3): p. 237-244.

159. Lettington, A.H., *Applications of diamond-like carbon thin films*. Carbon, 1998. **36**(5-6): p. 555-560.
160. Talke, F.E., *Tribology in magnetic recording technology*. Industrial Lubrication and Tribology, 2000. **52**: p. 157-164.
161. Guy, A.G., *Essentials of Materials Science*. 1976, New York, USA: McGrawHill, Inc.
162. Bhushan, B., *Principles and Applications of Tribology*. 1999, New York, USA: John Wiley & Sons, Inc. 1020.
163. Donnet, C., *Tribology of solid lubricant coatings*. Condensed Matter News, 1995. **4**(6): p. 9-24.
164. Donnet, C. and A. Grill, *Friction control of diamond-like carbon coatings*. Surface and Coatings Technology, 1997. **94-95**: p. 456-462.
165. Robertson, J., *Mechanical properties and structure of diamond-like carbon*. Diamond and Related Materials, 1992. **1**(5-6): p. 397-406.
166. Ferrari, A.C., A. Libassi, B.K. Tanner, V. Stolojan, J. Yuan, L.M. Brown, S.E. Rodil, B. Kleinsorge, and J. Robertson, *Density, sp^3 fraction, and cross-sectional structure of amorphous carbon films determined by x-ray reflectivity and electron energy-loss spectroscopy*. Physical Review B, 2000. **62**(16): p. 11089.
167. Ferrari, A.C. and J. Robertson, *Interpretation of Raman spectra of disordered and amorphous carbon*. Physical Review B, 2000. **61**(20): p. 14095-14107.
168. Robertson, J., *Properties of diamond-like carbon*. Surface and Coatings Technology, 1992. **50**(3): p. 185-203.
169. Ruff, A.W., *Modern Tribology Handbook*. 2000: Boca Raton, FL: CRC Press.
170. Erdemir, A. and C. Donnet, *Tribology of diamond-like carbon films: recent progress and future prospects*. Journal of Physics D-Applied Physics, 2006. **39**(18): p. R311-R327.
171. Angus, J.C., J.E. Stultz, P.J. Shiller, J.R. Macdonald, M.J. Mirtich, and S. Domitz, *Composition and Properties of the So-Called Diamond-Like Amorphous-Carbon Films*. Thin Solid Films, 1984. **118**(3): p. 311-320.
172. Moon, M.W., H.M. Jensen, J.W. Hutchinson, K.H. Oh, and A.G. Evans, *The characterization of telephone cord buckling of compressed thin films on substrates*. Journal of the Mechanics and Physics of Solids, 2002. **50**(11): p. 2355-2377.
173. Neuville, S.a.M., A., *Hard Carbon Coatings: The Way Forward*. MRS Bulletin, 1997: p. 22-26.
174. Robertson, J., *Deposition and properties of diamond-like carbons*. Material Research Society Symposium Proceedings, 1999. **555**: p. 12.
175. Weissmantel, C., *Preparation, structure, and properties of hard coatings on the basis of i -C and i -BN*. In: K.J. Klabunde (ed.), in *Thin Films from Free Atoms and Particles*. 1985, Academic Press: Orlando, FL. p. 153-201.
176. Memming, R., H.J. Tolle, and P.E. Wierenga, *Properties of polymeric layers of hydrogenated amorphous carbon produced by a plasma-*

- activated chemical vapour deposition process II: Tribological and mechanical properties*. Thin Solid Films, 1986. **143**(1): p. 31-41.
177. Miyoshi, K., R.L.C. Wu, and A. Garscadden, *Friction and wear of diamond and diamondlike carbon coatings*. Surface and Coatings Technology, 1992. **54–55, Part 2**(0): p. 428-434.
178. Sugimoto, I. and S. Miyake, *Oriented hydrocarbons transferred from a high performance lubricative amorphous C:H:Si film during sliding in a vacuum*. Applied Physics Letters, 1990. **56**(19): p. 1868-1870.
179. Erdemir, A., F.A. Nichols, X.Z. Pan, R. Wei, and P. Wilbur, *Friction and wear performance of ion-beam-deposited diamond-like carbon films on steel substrates*. Diamond and Related Materials, 1994. **3**(1–2): p. 119-125.
180. Meletis, E.I., A. Erdemir, and G.R. Fenske, *Tribological characteristics of DLC films and duplex plasma nitriding/DLC coating treatments*. Surface and Coatings Technology, 1995. **73**(1–2): p. 39-45.
181. Donnet, C., A. Erdemir, and SpringerLink, *Tribology of diamond-like carbon films fundamentals and applications*. 2008, New York: Springer.
182. Donnet, C., M. Belin, J.C. Augé, J.M. Martin, A. Grill, and V. Patel, *Tribochemistry of diamond-like carbon coatings in various environments*. Surface and Coatings Technology, 1994. **68–69**(0): p. 626-631.
183. Tallant, D.R., J.E. Parmeter, M.P. Siegal, and R.L. Simpson, *The thermal stability of diamond-like carbon*. Diamond and Related Materials, 1995. **4**(3): p. 191-199.
184. Sánchez-López, J.C., A. Erdemir, C. Donnet, and T.C. Rojas, *Friction-induced structural transformations of diamondlike carbon coatings under various atmospheres*. Surface and Coatings Technology, 2003. **163–164**(0): p. 444-450.
185. Liu, Y., A. Erdemir, and E.I. Meletis, *A study of the wear mechanism of diamond-like carbon films*. Surface and Coatings Technology, 1996. **82**(1-2): p. 48-56.
186. Liu, Y., A. Erdemir, and E.I. Meletis, *An investigation of the relationship between graphitization and frictional behavior of DLC coatings*. Surface and Coatings Technology, 1996. **86–87, Part 2**(0): p. 564-568.
187. Ong, C.W., X.A. Zhao, J.T. Cheung, S.K. Lam, Y. Liu, C.L. Choy, and P.W. Chan, *Thermal stability of pulsed laser deposited diamond-like carbon films*. Thin Solid Films, 1995. **258**(1-2): p. 34-39.
188. Bremond, F., P. Fournier, and F. Platon, *Test temperature effect on the tribological behavior of DLC-coated 100C6-steel couples in dry friction*. Wear, 2003. **254**(7–8): p. 774-783.
189. Ogwu, A.A., R.W. Lamberton, S. Morley, P. Maguire, and J. McLaughlin, *Characterisation of thermally annealed diamond like carbon (DLC) and silicon modified DLC films by Raman spectroscopy*. Physica B: Condensed Matter, 1999. **269**(3–4): p. 335-344.
190. Voevodin, A.A., A.W. Phelps, J.S. Zabinski, and M.S. Donley, *Friction induced phase transformation of pulsed laser deposited diamond-like carbon*. Diamond and Related Materials, 1996. **5**(11): p. 1264-1269.

191. Sánchez-López, J.C., A. Erdemir, C. Donnet, and T.C. Rojas, *Friction-induced structural transformations of diamondlike carbon coatings under various atmospheres*. Surface and Coatings Technology, 2003. **163-164**: p. 444-450.
192. Güttler, J. and J. Reschke, *Metal-carbon layers for industrial application in the automotive industry*. Surface and Coatings Technology, 1993. **60**(1-3): p. 531-535.
193. Hirvonen, J.-P., R. Lappalainen, J. Koskinen, A. Anttila, T.R. Jervis, and M. Trkula, *Tribological characteristics of diamond-like films deposited with an arc-discharge method*. Journal of Materials Research, 1990. **5**(11): p. 2524-2530.
194. Liu, Y., A. Erdemir, and E.I. Meletis, *Influence of environmental parameters on the frictional behavior of DLC coatings*. Surface and Coatings Technology, 1997. **94-95**: p. 463-468.
195. Erdemir, A., C. Bindal, J. Pagan, and P. Wilbur, *Characterization of transfer layers on steel surfaces sliding against diamond-like hydrocarbon films in dry nitrogen*. Surface and Coatings Technology, 1995. **76-77, Part 2**(0): p. 559-563.
196. Li, K.Y., Z.F. Zhou, I. Bello, C.S. Lee, and S.T. Lee, *Study of tribological performance of ECR-CVD diamond-like carbon coatings on steel substrates: Part 1. The effect of processing parameters and operating conditions*. Wear, 2005. **258**(10): p. 1577-1588.
197. Liu, Y.A.N. and E.I. Meletis, *Evidence of graphitization of diamond-like carbon films during sliding wear*. Journal of Materials Science, 1997. **32**(13): p. 3491-3495.
198. Zhou, Z.F., K.Y. Li, I. Bello, C.S. Lee, and S.T. Lee, *Study of tribological performance of ECR-CVD diamond-like carbon coatings on steel substrates: Part 2. The analysis of wear mechanism*. Wear, 2005. **258**(10): p. 1589-1599.
199. Rabbani, F., *Phenomenological evidence for the wear-induced graphitization model of amorphous hydrogenated carbon coatings*. Surface and Coatings Technology, 2004. **184**(2-3): p. 194-207.
200. Kalin, M. and J. Vizintin, *Real contact temperatures as the criteria for the reactivity of diamond-like-carbon coatings with oil additives*. Thin Solid Films, 2010. **518**(8): p. 2029-2036.
201. Schulz, H., M. Leonhardt, H.J. Scheibe, and B. Schultrich, *Ultra hydrophobic wetting behaviour of amorphous carbon films*. Surface and Coatings Technology, 2005. **200**(1-4): p. 1123-1126.
202. Roy, R.K., H.-W. Choi, S.-J. Park, and K.-R. Lee, *Surface energy of the plasma treated Si incorporated diamond-like carbon films*. Diamond and Related Materials, 2007. **16**(9): p. 1732-1738.
203. Nakamura, T., T. Ohana, M. Suzuki, M. Ishihara, A. Tanaka, and Y. Koga, *Surface modification of diamond-like carbon films with perfluorooctyl functionalities and their surface properties*. Surface Science, 2005. **580**(1-3): p. 101-106.
204. Kalin, M. and J. Vizintin, *Differences in the tribological mechanisms when using non-doped, metal-doped (Ti, WC), and non-metal-doped (Si) diamond-like carbon against steel under boundary lubrication*,

- with and without oil additives*. Thin Solid Films, 2006. **515**(4): p. 2734-2747.
205. Yao, N., A.G. Evans, and C.V. Cooper, *Wear mechanism operating in W-DLC coatings in contact with machined steel surfaces*. Surface and Coatings Technology, 2004. **179**(2–3): p. 306-313.
 206. de Barros Bouchet, M.I., J.M. Martin, T. Le-Mogne, and B. Vacher, *Boundary lubrication mechanisms of carbon coatings by MoDTC and ZDDP additives*. Tribology International, 2005. **38**(3): p. 257-264.
 207. Kano, M., Y. Yasuda, Y. Okamoto, Y. Mabuchi, T. Hamada, T. Ueno, J. Ye, S. Konishi, S. Takeshima, J.M. Martin, M.I. De Barros Bouchet, and T.L. Mognée, *Ultralow friction of DLC in presence of glycerol mono-oleate (GNO)*. Tribology Letters, 2005. **18**(2): p. 245-251.
 208. Kalin, M. and J. Vižintin, *A comparison of the tribological behaviour of steel/steel, steel/DLC and DLC/DLC contacts when lubricated with mineral and biodegradable oils*. Wear, 2006. **261**(1): p. 22-31.
 209. Kalin, M., J. Vižintin, J. Barriga, K. Vercaemmen, K. van Acker, and A. Arnšek, *The effect of doping elements and oil additives on the tribological performance of boundary-lubricated DLC/DLC contacts*. Tribology Letters, 2004. **17**(4): p. 679-688.
 210. Mortier, R.M.F.M.F.O.S.T. *Chemistry and technology of lubricants*. 2010.
 211. Kalin, M., E. Roman, and J. Vizintin, *The effect of temperature on the tribological mechanisms and reactivity of hydrogenated, amorphous diamond-like carbon coatings under oil-lubricated conditions*. Thin Solid Films, 2007. **515**(7-8): p. 3644-3652.
 212. Topolovec-Miklozic, K., F. Lockwood, and H. Spikes, *Behaviour of boundary lubricating additives on DLC coatings*. Wear, 2008. **265**(11–12): p. 1893-1901.
 213. Equey, S., S. Roos, U. Mueller, R. Hauert, N.D. Spencer, and R. Crockett, *Tribofilm formation from ZnDTP on diamond-like carbon*. Wear, 2008. **264**(3-4): p. 316-321.
 214. Haque, T., A. Morina, A. Neville, R. Kapadia, and S. Arrowsmith, *Effect of oil additives on the durability of hydrogenated DLC coating under boundary lubrication conditions*. Wear, 2009. **266**(1-2): p. 147-157.
 215. Kano, M., Y. Yasuda, and J.P. Ye, *The effect of ZDDP and MoDTC additives in engine oil on the friction properties of DLC-coated and steel cam followers*. Lubrication Science, 2004. **17**(1): p. 95-103.
 216. Haque, T., A. Morina, A. Neville, R. Kapadia, and S. Arrowsmith, *Non-ferrous coating/lubricant interactions in tribological contacts: Assessment of tribofilms*. Tribology International, 2007. **40**(10-12): p. 1603-1612.
 217. Miyake, S., T. Saito, Y. Yasuda, Y. Okamoto, and M. Kano, *Improvement of boundary lubrication properties of diamond-like carbon (DLC) films due to metal addition*. Tribology International, 2004. **37**(9): p. 751-761.
 218. Haque, T., A. Morina, A. Neville, R. Kapadia, S. Arrowsmith, S. Tung, B. Kinker, M. Woydt, and S.W. Dean, *Study of the ZDDP Antiwear*

- Tribofilm Formed on the DLC Coating Using AFM and XPS Techniques*. J. ASTM Int. Journal of ASTM International, 2007. **4**(7).
219. de Barros'Bouchet, M.I., C. Matta, T. Le Mogne, J.M. Martin, T. Sagawa, S. Okuda, and M. Kano, *Improved mixed and boundary lubrication with glycerol-diamond technology*. Tribology - Materials, Surfaces & Interfaces, 2005. **1**: p. 28-32.
220. Haque, T., A. Morina, and A. Neville, *Influence of friction modifier and antiwear additives on the tribological performance of a non-hydrogenated DLC coating*. Surface and Coatings Technology, 2010. **204**(24): p. 4001-4011.
221. Vengudusamy, B., J.H. Green, G.D. Lamb, and H.A. Spikes, *Influence of hydrogen and tungsten concentration on the tribological properties of DLC/DLC contacts with ZDDP*. Wear, 2013. **298–299**(0): p. 109-119.
222. Vengudusamy, B., J.H. Green, G.D. Lamb, and H.A. Spikes, *Tribological properties of tribofilms formed from ZDDP in DLC/DLC and DLC/steel contacts*. Tribology International, 2011. **44**(2): p. 165-174.
223. Tasdemir, H.A., M. Wakayama, T. Tokoroyama, H. Kousaka, N. Umehara, Y. Mabuchi, and T. Higuchi, *Ultra-low friction of tetrahedral amorphous diamond-like carbon (ta-C DLC) under boundary lubrication in poly alpha-olefin (PAO) with additives*. Tribology International, 2013. **65**(0): p. 286-294.
224. Vengudusamy, B., J.H. Green, G.D. Lamb, and H.A. Spikes, *Behaviour of MoDTC in DLC/DLC and DLC/steel contacts*. Tribology International, 2012. **54**(0): p. 68-76.
225. Podgornik, B., S. Jacobson, and S. Hogmark, *Influence of EP additive concentration on the tribological behaviour of DLC-coated steel surfaces*. Surface and Coatings Technology, 2005. **191**(2-3): p. 357-366.
226. Podgornik, B., D. Hren, J. Vizintin, S. Jacobson, N. Stavlid, and S. Hogmark, *Combination of DLC coatings and EP additives for improved tribological behaviour of boundary lubricated surfaces*. Wear, 2006. **261**(1): p. 32-40.
227. Kalin, M., E. Roman, L. Ožbolt, and J. Vižintin, *Metal-doped (Ti, WC) diamond-like-carbon coatings: Reactions with extreme-pressure oil additives under tribological and static conditions*. Thin Solid Films, 2010. **518**(15): p. 4336-4344.
228. Mistry, K.K., A. Morina, A. Erdemir, and A. Neville, *Extreme Pressure Lubricant Additives Interacting on the Surface of Steel- and Tungsten Carbide–Doped Diamond-Like Carbon*. Tribology Transactions, 2013. **56**(4): p. 623-629.
229. Vengudusamy, B., A. Grafl, and K. Preinfalk, *Tribological properties of hydrogenated amorphous carbon under dry and lubricated conditions*. Diamond and Related Materials, 2014. **41**(0): p. 53-64.
230. Podgornik, B., M. Sedlaček, and J. Vižintin, *Compatibility of DLC coatings with formulated oils*. Tribology International, 2008. **41**(6): p. 564-570.

231. Forsberg, P., F. Gustavsson, V. Renman, A. Hieke, and S. Jacobson, *Performance of DLC coatings in heated commercial engine oils*. *Wear*, 2013. **304**(1–2): p. 211-222.
232. Tung, S.C. and H. Gao, *Tribological characteristics and surface interaction between piston ring coatings and a blend of energy-conserving oils and ethanol fuels*. *Wear*, 2003. **255**(7-12): p. 1276-1285.
233. Podgornik, B., J. Vizintin, S. Jacobson, and S. Hogmark, *Tribological behaviour of WC/C coatings operating under different lubrication regimes*. *Surface and Coatings Technology*, 2004. **177-178**: p. 558-565.
234. Ronkainen, H., S. Varjus, and K. Holmberg, *Friction and wear properties in dry, water- and oil-lubricated DLC against alumina and DLC against steel contacts*. *Wear*, 1998. **222**(2): p. 120-128.
235. Stallard, J. and D.G. Teer, *A study of the tribological behaviour of CrN, Graphit-iC and Dymon-iC coatings under oil lubrication*. *Surface and Coatings Technology*. **188-189**: p. 525-529.
236. de Barros'Bouchet, M.I., I. Raoult, T. Le Mogne, J.M. Martin, M. Kasrai, and Y. Yamada, *Friction reduction by metal sulfides in boundary lubrication studied by XPS and XANES analyses*. *Wear*, 2003. **254**(9): p. 863-870.
237. Equey, S., S. Roos, U. Mueller, R. Hauert, N.D. Spencer, and R. Crockett, *Reactions of zinc-free anti-wear additives in DLC/DLC and steel/steel contacts*. *Tribology International*, 2008. **41**(11): p. 1090-1096.
238. Podgornik, B. and J. Vižintin, *Tribological reactions between oil additives and DLC coatings for automotive applications*. *Surface and Coatings Technology*, 2005. **200**(5–6): p. 1982-1989.
239. Podgornik, B., S. Jacobson, and S. Hogmark, *DLC coating of boundary lubricated components—advantages of coating one of the contact surfaces rather than both or none*. *Tribology International*, 2003. **36**(11): p. 843-849.
240. Vercammen, K., K. Van Acker, A. Vanhulsel, J. Barriga, A. Arnsek, M. Kalin, and J. Meneve, *Tribological behaviour of DLC coatings in combination with biodegradable lubricants*. *Tribology international*, 2004. **37**(11): p. 983-989.
241. Ban, M., M. Ryoji, S. Fujii, and J. Fujioka, *Tribological characteristics of Si-containing diamond-like carbon films under oil-lubrication*. *Wear*, 2002. **253**(3-4): p. 331-338.
242. Podgornik, B., S. Jacobson, and S. Hogmark, *DLC coating of boundary lubricated components--advantages of coating one of the contact surfaces rather than both or none*. *Tribology International*, 2003. **36**(11): p. 843-849.
243. Podgornik, B., D. Hren, and J. Vižintin, *Low-friction behaviour of boundary-lubricated diamond-like carbon coatings containing tungsten*. *Thin Solid Films*, 2005. **476**(1): p. 92-100.
244. Yang, L., A. Neville, A. Brown, P. Ransom, and A. Morina, *Friction reduction mechanisms in boundary lubricated W-doped DLC coatings*. *Tribology International*, 2014. **70**(0): p. 26-33.

245. Fu, Z.-q., C.-b. Wang, W. Zhang, W. Wang, W. Yue, X. Yu, Z.-j. Peng, S.-s. Lin, and M.-j. Dai, *Influence of W content on tribological performance of W-doped diamond-like carbon coatings under dry friction and polyalpha olefin lubrication conditions*. *Materials & Design*, 2013. **51**(0): p. 775-779.
246. Yue, W., C. Liu, Z. Fu, C. Wang, H. Huang, and J. Liu, *Synergistic effects between sulfurized W-DLC coating and MoDTC lubricating additive for improvement of tribological performance*. *Tribology International*, 2013. **62**(0): p. 117-123.
247. Minami, I., T. Kubo, H. Nanao, S. Mori, T. Sagawa, and S. Okuda, *Investigation of Tribo-Chemistry by Means of Stable Isotopic Tracers, Part 2: Lubrication Mechanism of Friction Modifiers on Diamond-Like Carbon*. *Tribology Transactions*, 2007. **50**(4): p. 477-487.
248. Kržan, B., J. Vižintin, J. Vižintin, M. Kalin, K. Dohda, and S. Jahanmir, *Tribology of Mechanical Systems: A Guide to Present and Future Technologies*. ASME presss, New York, 2004: p. 107.
249. Grischke, M., A. Hieke, F. Morgenweck, and H. Dimigen, *Variation of the wettability of DLC-coatings by network modification using silicon and oxygen*. *Diamond and Related Materials*, 1998. **7**(2–5): p. 454-458.
250. Matthews, A., *Advanced Surface Coatings A Handbook of Surface Engineering*. 2013: Springer Verlag.
251. Kalin, M., I. Velkavrh, J. Vižintin, and L. Ožbolt, *Review of boundary lubrication mechanisms of DLC coatings used in mechanical applications*. *Meccanica*, 2008. **43**(6): p. 623-637.
252. Mabuchi, Y., T. Hamada, H. Izumi, Y. Yasuda, and M. Kano, *The Development of Hydrogen-free DLC-coated Valve-lifter*. 2007, SAE International.
253. Haque, T., A. Morina, and A. Neville, *Effect of Friction Modifiers and Antiwear Additives on the Tribological Performance of a Hydrogenated DLC Coating*. *Journal of Tribology-Transactions of the Asme*, 2010. **132**(3): p. 13.
254. Sugimoto, I., *Mechanism on Specific Wear of DLC Film in Engine Oil with Mo-DTC*. *TRANSACTIONS OF THE JAPAN SOCIETY OF MECHANICAL ENGINEERS Series A*, 2012. **78**(786): p. 213-222.
255. Vengudusamy, B., J.H. Green, G.D. Lamb, and H.A. Spikes, *Behaviour of MoDTC in DLC/DLC and DLC/Steel contacts*. *Tribology International*, (0).
256. Haque, T., A. Morina, and A. Neville, *Tribological performance evaluation of a hydrogenated diamond-like carbon coating in sliding/rolling contact – effect of lubricant additives*. *Proceedings of the Institution of Mechanical Engineers, Part J: Journal of Engineering Tribology*, 2011. **225**(6): p. 393-405.
257. Pawlak, Z. *Tribochemistry of lubricating oils*. 2003; Available from: <http://www.sciencedirect.com/science/book/9780444512963>.
258. Atkins, P.W., *Physical chemistry*. 1978, San Francisco: W.H. Freeman.
259. Morina, A., A. Neville, M. Priest, and J.H. Green, *ZDDP and MoDTC interactions in boundary lubrication – The effect of temperature and*

- ZDDP/MoDTC ratio. *Tribology International*, 2006. **39**(12): p. 1545-1557.
260. Neville, A., A. Morina, T. Haque, and M. Voong, *Compatibility between tribological surfaces and lubricant additives--How friction and wear reduction can be controlled by surface/lube synergies*. *Tribology International*, 2007. **40**(10-12): p. 1680-1695.
261. Kodali, P., K.C. Walter, and M. Nastasi, *Investigation of mechanical and tribological properties of amorphous diamond-like carbon coatings*. *Tribology International*, 1997. **30**(8): p. 591-598.
262. Hauert, R., *An overview on the tribological behavior of diamond-like carbon in technical and medical applications*. *Tribology International*, 2004. **37**(11-12): p. 991-1003.
263. Haque, T., A. Morina, A. Neville, R. Kapadia, S. Arrowsmith, S. Tung, B. Kinker, M. Woydt, and S.W. Dean, *Study of the ZDDP Antiwear Tribofilm Formed on the DLC Coating Using AFM and XPS Techniques*. *J. ASTM Int. Journal of ASTM International*, 2007. **4**(7): p. 92-102.
264. Kramer, D.E., A.A. Volinsky, N.R. Moody, and W.W. Gerberich, *Substrate effects on indentation plastic zone development in thin soft films*. *Journal of Materials Research*, 2001. **16**(11): p. 3150-3157.
265. Fischer-Cripps, A.C., *Review of analysis methods for sub-micron indentation testing*. *Vacuum*, 2000. **58**(4): p. 569-585.
266. Fairley, N., *CasaXPS version 2.3.15*. Casa Software Ltd.
267. Moulder, J.F., K.D. Bomben, P.E. Sobol, and W.F. Stickle, *Handbook of x-ray photoelectron spectroscopy. A reference book of standard spectra for identification and interpretation of xps data*. 1992, Eden Prairie, MN: Physical Electronics.
268. Zhang, H.S. and K. Komvopoulos, *Direct-current cathodic vacuum arc system with magnetic-field mechanism for plasma stabilization*. *Review of Scientific Instruments*, 2008. **79**(7): p. 073905-7.
269. Schwan, J., S. Ulrich, V. Batori, H. Ehrhardt, and S.R.P. Silva, *Raman spectroscopy on amorphous carbon films*. *Journal of Applied Physics*, 1996. **80**(1): p. 440-447.
270. Praver, S., K.W. Nugent, Y. Lifshitz, G.D. Lempert, E. Grossman, J. Kulik, I. Avigal, and R. Kalish, *Systematic variation of the Raman spectra of DLC films as a function of sp²:sp³ composition*. *Diamond and Related Materials*, 1996. **5**(3-5): p. 433-438.
271. Tay, B.K., X. Shi, H.S. Tan, H.S. Yang, and Z. Sun, *Raman studies of tetrahedral amorphous carbon films deposited by filtered cathodic vacuum arc*. *Surface and Coatings Technology*, 1998. **105**(1-2): p. 155-158.
272. Scheibe, H.J., D. Drescher, and P. Alers, *Raman characterization of amorphous carbon films*. *Fresenius' Journal of Analytical Chemistry*, 1995. **353**(5): p. 695-697.
273. ATC, *Lubricant additives and the environment*. 2007 The Technical Committee of Petroleum Additive Manufacturers in Europe.
274. Reyes, M. and A. Neville, *The effect of anti-wear additives, detergents and friction modifiers in boundary lubrication of traditional Fe-base*

- materials, in *Tribology series*, M.P.G.D. D. Dowson and A.A. Lubrecht, Editors. 2003, Elsevier. p. 57-65.
275. Waara, P., J. Hannu, T. Norrby, and Å. Byheden, *Additive influence on wear and friction performance of environmentally adapted lubricants*. Tribology International, 2001. **34**(8): p. 547-556.
276. Kalin, M., J. Vižintin, K. Vercammen, J. Barriga, and A. Arnšek, *The lubrication of DLC coatings with mineral and biodegradable oils having different polar and saturation characteristics*. Surface and Coatings Technology, 2006. **200**(14–15): p. 4515-4522.
277. Martin, J.-M., C. Grossiord, K. Varlot, B. Vacher, T. Le Mogne, and Y. Yamada, *Friction-induced two-dimensional solid films from lubricant additives*. Lubrication Science, 2003. **15**(2): p. 119-132.
278. Le Huu, T., H. Zaidi, D. Paulmier, and P. Voumard, *Transformation of sp³ to sp² sites of diamond like carbon coatings during friction in vacuum and under water vapour environment*. Thin Solid Films, 1996. **290-291**: p. 126-130.
279. Jaoul, C., O. Jarry, P. Tristant, T. Merle-Méjean, M. Colas, C. Dublanche-Tixier, and J.M. Jacquet, *Raman analysis of DLC coated engine components with complex shape: Understanding wear mechanisms*. Thin Solid Films, 2009. **518**(5): p. 1475-1479.
280. Abdollah, M.F.B., Y. Yamaguchi, T. Akao, N. Inayoshi, N. Umehara, and T. Tokoroyama, *Phase transformation studies on the a-C coating under repetitive impacts*. Surface and Coatings Technology, 2010. **205**(2): p. 625-631.
281. Villiger, P., C. Sprecher, and J.A. Peters, *Parameter optimisation of Ti-DLC coatings using statistically based methods*. Surface and Coatings Technology, 1999. **116-119**: p. 585-590.
282. Lazzarotto, L., L. Dubar, A. Dubois, P. Ravassard, and J. Oudin, *Three selection criteria for the cold metal forming lubricating oils containing extreme pressure agents*. Journal of Materials Processing Technology, 1998. **80-81**(0): p. 245-250.
283. Ravikiran, A. and S. Jahanmir, *Effect of interfacial layers on wear behavior of a dental glass-ceramic*. Journal of the American Ceramic Society, 2000. **83**(7): p. 1831-1833.
284. Kalin, M., S. Jahanmir, and G. Dražič, *Wear mechanisms of glass-infiltrated alumina sliding against alumina in water*. Journal of the American Ceramic Society, 2005. **88**(2): p. 346-352.
285. Afsharpour, M., A. Mahjoub, and M. Amini, *A Nano-Hybrid of Molybdenum Oxide Intercalated by Dithiocarbamate as an Oxidation Catalyst*. Journal of Inorganic and Organometallic Polymers and Materials, 2008. **18**(4): p. 472-476.
286. Nagai, I., H. Endo, H. Nakamura, and H. Yano, *Soot and Valve Train Wear in Passenger Car Diesel Engines*. 1983, SAE International.
287. Williamson B.P, G., I.R. and Benwell, S., *Measurement of Oilfilm thickness in the Elasto-Hydrodynamic contact between a cam and Bucket follower in a Motored Cylinder Head: Newtonian Oils int. Fuels and Lubricants Meeting and Exposition, Baltimore, Maryland, USA., SAE Int. J. Engines, 1989. 1: p. 11.*

288. Keunecke, M., K. Bewilogua, J. Becker, A. Gies, and M. Grischke, *CrC/a-C:H coatings for highly loaded, low friction applications under formulated oil lubrication*. *Surface and Coatings Technology*, 2012. **207**(0): p. 270-278.